Degradation of Biomass Pellets during Transport, Handling and Storage

An experimental and numerical study

Gilvari, H.

DOI
10.4233/uuid:aecd60c9-f7f9-416a-92ff-80261d7c954c

Publication date
2021

Document Version
Final published version

Citation (APA)
Gilvari, H. (2021). *Degradation of Biomass Pellets during Transport, Handling and Storage: An experimental and numerical study*. [Dissertation (TU Delft), Delft University of Technology].
https://doi.org/10.4233/uuid:aecd60c9-f7f9-416a-92ff-80261d7c954c

Degradation of Biomass Pellets during Transport, Handling and Storage

An experimental and numerical study

Hamid Gilvari

Delft University of Technology

Degradation of Biomass Pellets during Transport, Handling and Storage

An experimental and numerical study

Dissertation

for the purpose of obtaining the degree of doctor
at Delft University of Technology
by the authority of the Rector Magnificus, Prof.dr.ir. T.H.J.J. van der Hagen,
chair of the Board for Doctorates
to be defended publicly on
Wednesday 28, April 2021 at 12:30 o'clock

By

Hamid GILVARI

Master of Science in Chemical and Process Engineering,
Lappeenranta University of Technology, Finland
born in Tehran, Iran

This dissertation has been approved by the promotors:

Dr.ir. D. L. Schott and Prof.dr.ir. W. de Jong

Composition of the doctoral committee:

Rector Magnificus,	Chairperson
Dr.ir. D. L. Schott	Delft University of Technology, promotor
Prof.dr.ir. W. de Jong	Delft University of Technology, promotor
……..	
Independent members:	
Prof.dr.ir. J.T. Padding	Delft University of Technology
Prof.dr. P. Osseweijer	Delft University of Technology
Prof.dr.ir. H.J. Heeres	University of Groningen
Prof.dr. S. Larsson	Swedish University of Agricultural Sciences, Sweden
Dr. A. Ramirez Gomez	Universidad Politécnica de Madrid, Spain

Keywords: biomass pellets, transport and storage, mechanical strength, discrete element methods, breakage and degradation

ISBN: 978-94-6421-329-4

Printed in the Netherlands

In memories of my uncles,

Akbar and Reza

To my parents, Mahdi and Zinat

and my love, Hengameh

Summary

Presently, biomass pellets play a significant role in energy transition scenarios worldwide. Due to the lack of local supplies, many countries import their pellets from countries with enormous resources. For instance, in Europe, a big share of pellets is imported from the USA, Canada, and Asian countries. Pellets are normally transferred in bulk using ocean vessels with a capacity of up to 40,000 metric tons.

Due to mechanical forces and environmental changes throughout the transport and storage steps, pellets are prone to degradation. This may degrade pellets physically or chemically. As a result, fines and dust are generated. Moreover, as pellets absorb and adsorb moisture from the environment, the moisture content and the heating value of pellets may change, and this may also weaken the physical structure because of swelling. The presence of fines and dust may lead to self-ignition and dust explosion, material loss, equipment fouling, and environmental and health issues.

The goal of this dissertation is to investigate to what extent biomass pellets degrade during transport and storage. To achieve this, first, we conducted an extensive literature review to reveal the factors that affect the extent of degradation of pellets. Moreover, we studied the commonly used methods to assess the quality parameters and the degradation behavior of pellets in detail. Then, we carried out a series of experiments on physical and chemical degradations of pellets from laboratory to large-scale and analyzed them in the operational and environmental context. By conducting these experiments, we unveiled the relationship between the laboratory test results and the pilot or large-scale transport impact on the proportion of generated fines. Furthermore, a model in the discrete element method (DEM) was developed and used to simulate the breakage pattern of individual pellets under the compression test. The model shows high fidelity in simulating the breakage behavior of pellets under compressive forces in two directions.

Chapter 2 presents a literature review, conducted to discover what causes the pellets to degrade most, and to evaluate different methods to assess the quality parameters of pellets. This was the first step to obtain an overview of the state-of-the-art concerning pellet stability research and development. The systematic review showed that although different laboratory equipment was overwhelmingly used amongst researchers and industries to assess the quality parameters of pellets, no clear relationships have been established between the results from

the laboratory equipment and the large-scale transportation. Moreover, considering the literature, we divided the factors affecting the quality parameters of biomass pellets into four major groups: feedstock properties, pre-treatment condition specifications, pelletization process specifications, and storage conditions.

A series of experiments were performed from the laboratory to the large-scale to link the quality of pellets to the magnitude of pellet's fragmentation in a real-life situation. **Chapter 3** provides experimental research consisting of (small-scale) laboratory experiments. By using an image-processing tool, we measured the length distributions of pellets before and after durability experiments. This chapter shows how different pellet length distributions (PLD), test conditions, and torrefaction after pelletization may create a bias in mechanical durability results. Afterward, in **chapter 4**, we studied the fragmentation of pellets in a pilot-scale transportation system. A belt conveyor with a width of 0.4 m and a speed of up to 1.6 $m.s^{-1}$ was used to investigate the breakage behavior of commercially used pellets. In general, the increased drop height and the number of handling steps increased the proportion of fines in the system, however, the speed of the belt conveyor at a range between 0.5 and 1.5 $m.s^{-1}$ and the belt's load from 30 to 50% of the maximum capacity did not significantly affect the proportion of generated fines. In **chapter 5**, large-scale industrial experiments were performed on the entire transportation system of a pellet-fired power plant in the Netherlands with a capacity of 450 $ton.h^{-1}$. The change in the quality and properties of pellets was investigated concerning the effect of different transport equipment. It was observed that transport via a free fall of 7.8 m increases the proportion of fines from 4.8% to 9.0% for pellets with an initial mechanical durability of 97.6%.

Different environmental conditions in the pellet storage area were simulated by changing the temperature and the relative humidity; then, their effects on the pellet properties were studied. As given in **chapter 6,** depending on the storage conditions and time, we concluded that pellets may be susceptible to degradation. Amongst different storage scenarios from freezing temperature to high temperature and relative humidity conditions, frosting followed by defrosting at relatively high temperature (40ºC) and relative humidity (85%) degrade the pellets most. This degradation was observed in both physical and chemical properties by swelling of the pellets' structure, increased moisture content, decreased mechanical durability, and decreased heating values.

In practice, studying the interactions between the pellets and the equipment used to transport, handle, and store pellets are difficult because of the large variety in the type of equipment and properties of pellets. Computer-aided numerical simulations such as the discrete element method (DEM) could be used to study the breakage behavior of pellets under external forces during transport and handling. In **chapter 7**, we develop a DEM model, using the Timoshenko-Ehrenfest theory and calibrated to represent the breakage behavior of single pellets of different types, after which, the results were compared with the experimental results. The model shows a high potential to simulate the breakage behavior of pellets and shows high fidelity to represent the breakage properties of other types of pellets. The calibrated model can open up a huge world of opportunities for future investigations of the physical degradation of pellets by leading to new equipment design for transport and storage.

This study contributes to a better understanding of the materials' behavior during transport, handling, and storage. This is essential to design efficient and sustainable transport and storage equipment, which should not be overlooked in energy transition scenarios.

Samenvatting

Momenteel spelen biomassapellets wereldwijd een belangrijke rol in energietransitie scenario's. Door het gebrek aan lokale grondstoffen, importeren veel landen hun pellets uit landen met enorme grondstofvoorraden. In Europa wordt bijvoorbeeld een groot deel van de pellets geïmporteerd uit de VS, Canada en Aziatische landen. Pellets worden normaal gesproken in bulk overgeslagen door middel van zeeschepen met een capaciteit tot 40.000 ton.

Door mechanische krachten en omgevingsveranderingen tijdens de transport- en opslagstappen zijn pellets vatbaar voor zowel fysische als chemische degradatie. Als gevolg hiervan worden fijne deeltjes en stof gegenereerd. Aangezien pellets vocht uit de omgeving absorberen en adsorberen, kunnen bovendien het vochtgehalte en de verwarmingswaarde van pellets veranderen, waardoor de fysieke structuur kan verzwakken door zwelling. De aanwezigheid van fijne deeltjes en stof kan leiden tot zelfontbranding en stofexplosie, materiaalverlies, vervuiling van apparatuur en milieu- en gezondheidsproblemen.

Het doel van dit proefschrift is om te onderzoeken in hoeverre biomassapellets worden degraderen tijdens transport en opslag. Om dit te bereiken, hebben we eerst een uitgebreid literatuuronderzoek uitgevoerd om te identificeren welke factoren de mate van degradatie van pellets beïnvloeden. Bovendien hebben we een uitgebreide studie gedaan naar de veelgebruikte methoden om de kwaliteitsparameters en de degradatie van pellets te beoordelen. Vervolgens hebben we een reeks experimenten uitgevoerd met betrekking tot de fysische en chemische degradatie van pellets van het laboratorium tot op grote schaal en deze geanalyseerd in de operationele en omgevingscontext. Door deze experimenten uit te voeren, hebben we de relatie tussen de laboratoriumtestresultaten en de invloed van pilot- of grootschalige op de hoeveelheid gegenereerde fijne deeltjes blootgelegd. Verder werd een model in de discrete-element-methode (DEM) ontwikkeld en gebruikt om het breekpatroon van individuele pellets onder de compressietest te simuleren. Het model toont een hoge betrouwbaarheid bij het simuleren van het breukgedrag van pellets onder drukkrachten in twee richtingen.

Hoofdstuk 2 presenteert een literatuuronderzoek, uitgevoerd om te ontdekken waardoor de pellets het meest worden afgebroken en om te evalueren welke verschillende methoden worden gebruikt om de kwaliteitsparameters van pellets te beoordelen. Dit was de eerste stap

om een overzicht te krijgen van de stand van de techniek op het gebied van onderzoek en ontwikkeling van pellet stabiliteit. De systematische studie heeft uitgewezen dat, hoewel er door onderzoekers en in industrie overweldigend gebruik wordt gemaakt van verschillende laboratoriumapparatuur om de kwaliteitsparameters van pellets te beoordelen, er geen duidelijke relaties zijn vastgesteld tussen de resultaten van de laboratoriumapparatuur en het grootschalige transport. Bovendien hebben we, rekening houdend met de literatuur, de factoren die van invloed zijn op de kwaliteitsparameters van biomassapellets in vier hoofdgroepen onderverdeeld: grondstofeigenschappen, specificaties van voorbehandelingscondities, specificaties voor het pelletiseren en opslagomstandigheden.

Er is een reeks experimenten uitgevoerd van laboratoriumschaal tot op grote schaal om de kwaliteit van pellets te koppelen aan de omvang van de fragmentatie van pellets in een praktijksituatie. **Hoofdstuk 3** presenteert experimenteel onderzoek bestaande uit (kleinschalige) laboratoriumexperimenten. Met behulp van een beeldverwerkingstool hebben we de lengteverdelingen van pellets (Engels: pellet length distributions, PLD) gemeten voor en na slijtage-experimenten. Dit hoofdstuk laat zien hoe factoren zoals verschillende lengteverdelingen van pellets, testomstandigheden en torrefactie na het pelletiseren een vertekend beeld kunnen geven van de mechanische duurzaamheid. Vervolgens wordt in **hoofdstuk 4** de fragmentatie van pellets in een transportsysteem op pilot-scale bestudeerd. Het breekgedrag van commercieel gebruikte pellets wordt onderzocht met behulp van een bandtransporteur met een breedte van 0,4 m en een snelheid tot 1,6 m.s-1. Over het algemeen resulteren een grotere valhoogte en het aantal handlingstappen in een verhoogd aandeel fijne deeltjes in het systeem, maar wanneer de snelheid van de bandtransporteur in een bereik tussen 0,5 en 1,5 $m.s^{-1}$ ligt en de belasting van de band een waarde tussen 30-50% van de maximale capaciteit heeft, dan is er geen significante invloed op het aandeel gegenereerde deeltjes. In **hoofdstuk 5** zijn grootschalige industriële experimenten uitgevoerd op het gehele transportsysteem van een pellet-gestookte elektriciteitscentrale in Nederland met een capaciteit van 450 ton.h-1. Er is onderzoek gedaan naar het effect van verschillende transportmiddelen op de verandering in de kwaliteit en de eigenschappen van pellets. Het is gebleken dat transport via een vrije val van 7,8 m het aandeel fijne deeltjes verhoogt van 4,8% naar 9,0% voor pellets met een initiële mechanische duurzaamheid van 97,6%.

Verschillende omgevingscondities in de opslagruimte voor pellets werden gesimuleerd door de temperatuur en de relatieve vochtigheid te veranderen; vervolgens werden hun effecten op de eigenschappen van de pellets bestudeerd. Zoals vermeld in **hoofdstuk 6** hebben we

geconcludeerd dat, afhankelijk van de opslagomstandigheden en -tijd, pellets gevoelig kunnen zijn voor degradatie. Van de verschillende opslagscenario's van vriestemperatuur tot hoge temperatuur en relatieve vochtigheid, laat vriezen gevolgd door ontdooien bij relatief hoge temperatuur (40ºC) en relatieve vochtigheid (85%) de pellets het meest afbreken. Deze achteruitgang werd waargenomen in zowel fysische als chemische eigenschappen door zwelling van de structuur van de pellets, verhoogd vochtgehalte, verminderde mechanische duurzaamheid en verlaagde verwarmingswaarden.

In de praktijk is het moeilijk om de interacties tussen de pellets en de apparatuur die wordt gebruikt om pellets te transporteren, te behandelen en op te slaan, te bestuderen vanwege de grote verscheidenheid in het type apparatuur en de eigenschappen van pellets. Computerondersteunde numerieke simulaties zoals de discrete-element-methode (DEM) zouden kunnen worden gebruikt om het breukgedrag van pellets onder externe krachten tijdens transport en gebruik te bestuderen. In **hoofdstuk 7** ontwikkelen we een DEM-model, welke gebruik maakt van de Timoshenko-Ehrenfest-theorie en gekalibreerd is om het breekgedrag van afzonderlijke pellets van verschillende typen weer te geven, waarna de resultaten worden vergeleken met de experimentele resultaten. Het model toont hoge potentie om het breekgedrag van pellets te simuleren en toont een hoge betrouwbaarheid om de breekeigenschappen van andere soorten pellets weer te geven. Het gekalibreerde model kan een wereld aan mogelijkheden openen voor toekomstig onderzoek naar de fysieke afbraak van pellets door te leiden tot nieuw ontwerp van transport- en opslagapparatuur. Deze studie draagt bij aan een beter begrip van het gedrag van materialen tijdens transport, gebruik en opslag. Dit is essentieel voor het ontwerpen van efficiënte en duurzame transport- en opslagapparatuur, aspecten die niet over het hoofd mogen worden gezien in energietransitie scenario's.

List of abbreviations

ANOVA	Analysis of variances
ASABE	American society of agricultural and biological engineers
ASAE	American society of association executives
ASTM	American society for testing and materials
B	Binder
BD	Bulk density
BPM	Bonded particle model
CEN	European committee for standardization
CPU	Central processing unit
CRM	Contact radius multiplier
CTI	*Comitato termotecnica Italiano*
CTS	*Clima temperatur systeme GmbH*
DEM	Discrete element methods
DIN	*Deutsches institut für normung*
DoD	Degree of densification
EBPM	Edinburgh bonded particle model
EMC	Equilibrium moisture content
EN	European norm
Ex	Excluding
FC	Fixed carbon
FEM	Finite element methods
GHG	Greenhouse gas emissions
HHV	High heating value
HSE	Health, safety, and environment
HT	Holding time
HTC	Hydrothermal carbonization
IRI	Impact resistance index
ISO	International standard organization
KPI	Key performance indicator
LHV	Low heating value
MC	Moisture content
MF	Mesocarp fiber
NA	Not available
NS	Not specified
OVAT	One variable at a time
PD	Pellet density
PDI	Pellet durability index
PFI	Pellet fuel institute (USA)
PKS	Palm kernel shell
PLD	Pellet length distribution
PRM	Particle replacement method

PSD	Particle size distribution
PVC	Polyvinyl chloride
RCC	Roller compacted concrete
RD	Relaxed density
Ref	Reference
RH	Relative humidity
RSM	Response surface model
TA250	Torrefied Ash wood at 250 degrees Celsius
TA265	Torrefied Ash wood at 265 degrees Celsius
TD	True density
TGA	Thermogravimetric analysis
Torr	Torrefaction
TS	Tensile strength
UK	The United Kingdom
USA	The United States of America
VM	Volatile matter
W	Water
WRI	Water-resistance index

List of symbols

A	Ash content
D	Diameter
DU	Mechanical durability
GP	Giga Pascal
L	Length
MJ	Mega joule
MP	Mega Pascal
Mton	Million tons
P	Pressure
T	Temperature
ºC	Degree Celsius

Table of Contents

1 Introduction

1.1 Background

The excessive use of fossil fuels in the past up to the present century has led to a sharp increase in greenhouse gas (GHG) emissions to the atmosphere. With an increase in GHG emissions into the atmosphere on the one hand and increased global energy demand, on the other hand, there is an emerging need for novel solutions to mitigate GHG emissions. Recently, new regional and global regulations have been set to tackle this problem. For instance, the Paris agreement on climate change [1] aims to keep global warming to well below 2ºC by 2100 and efforts to keep it even well below 1.5ºC. However, this foresight requires crucial alternatives for energy sources.

Biomass is one of the main alternative energy sources considered as a renewable fuel that can be applied to cope with climate changes and meet the GHG reduction targets. Although a big debate is still going on the use of biomass species for the production of renewable energies, currently, about 10% of the total worldwide energy demand is supplied by biomass [2] and efforts are being made to accelerate the use of biomass in the following decades. Biomass, according to CEN TS 14588 standard [3], refers to the material of biological origin excluding material embedded in geological formations and transformed to fossil. Wood, agricultural residues, food, and forest residues are some examples of biomass species. Biomass can be used as a solid energy source, or can be converted to liquid or gas fuels.

Solid biomass may undergo thermal pretreatment and densification processes to decrease its inherent high moisture content and to increase its low bulk density, before use. These processes result in a higher energy content per unit mass and diminish some challenges when dealing with biomass; for example, they improve transportation volume and cost, ease of storage, and combustion characteristics. In a thermal pretreatment process, as the name implies, biomass is treated thermally in order to reduce the moisture content and often also volatile matters. Drying, Torrefaction, hydrothermal carbonization, steam-explosion, and pyrolysis are the most common thermal pretreatment processes for biomass. In a densification process, biomass is densified using high pressure (typically up to 150 MPa and higher) and elevated temperature (typically up to 100+ºC) [4] to compress the structure of biomass feedstock so that small particles adhere to one another and form the final shape, which is usually a pellet or a briquette.

According to CEN TS 14588 standard [3], biofuel pellets are usually in cylindrical form with a length typically 5 to 30 mm, and broken ends. Table 1.1 shows the elevated properties of typical wood pellets and torrefied pellets in comparison to wood chips and compares these properties

with those of coal. It is seen that the moisture content of wood chips decreases and its bulk density increases notably after pelletization and torrefaction processes so that these properties almost reach out to those of coal. The energy content per unit volume (normally in $MJ.m^{-3}$) also increases up to three folds, which makes the torrefied pellets a good competitor to coal.

Table 1.1: Typical properties of wood chips, wood pellets, torrefied pellets, and coal adapted from [5].

Property	Wood chips	Wood pellets	Torrefied pellets	Coal
				
Moisture content (wt. %)	30–55	7–10	1–5	10–15
Volatile matter (wt. %)	75–84	75–84	55–65	15–30
Heating value($MJ.kg^{-1}$)	7–12	15–17	18–24	23–28
Bulk density ($kg.m^{-3}$)	200–300	550–650	650–800	800–850

The use of densified solid biomass has grown significantly in recent years. The worldwide consumption of wood pellets alone, increased from about 10 million metric tons in 2007 to more than 37 million metric tons in 2019 [6]. Although there are various types of feedstock, pretreatment, and pelletization processes, for simplicity, all types of untreated and treated biomass-based pellets are hereafter referred to as biomass pellets.

Even though biomass pellets show great potential to be applied as a renewable source of energy and many governments encourage industries and investors to use pellets, not every country can supply the local demands due to the shortage of feedstock. For example, many European countries, therefore, import a big share of pellets from countries with high supply sources. The USA and Canada are the biggest global pellet exporters with around 8.5 million metric tons of pellets being exported to the EU in 2019 (Figure 1.1). Besides, the EU imported up to 2.6 million metric tons of pellets from other European countries such as Russia in that year [6].

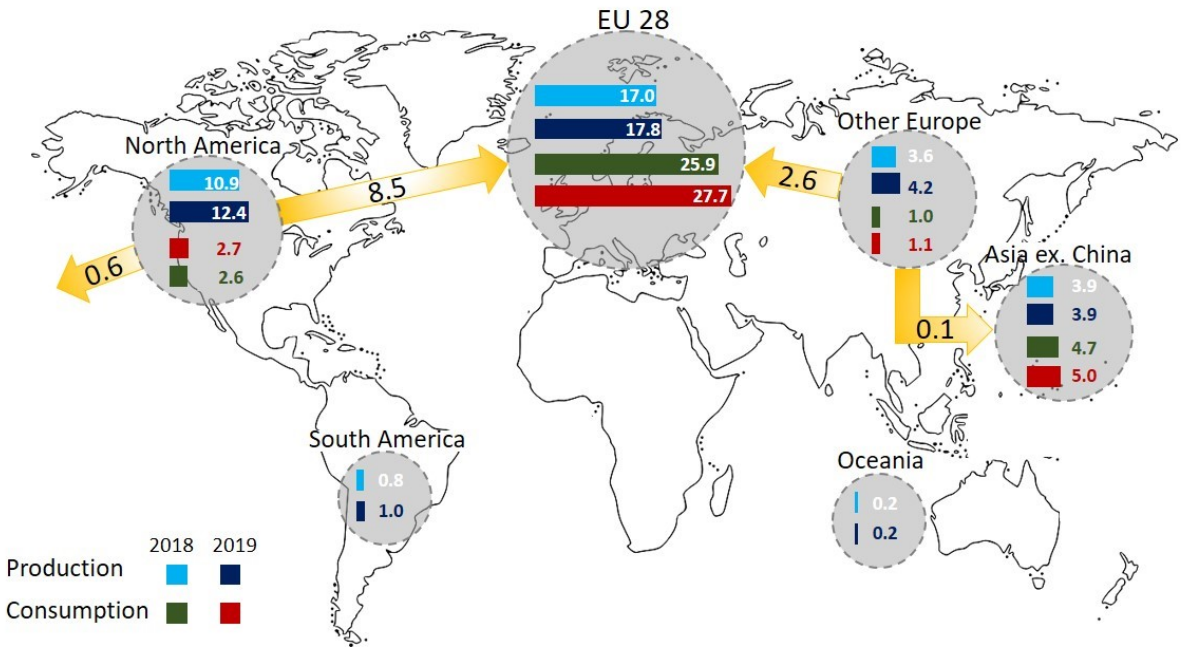

Figure 1.1: Worldwide production, consumption, and trade flow of wood pellets in 2018–2019 in Mtons. Data from [6].

1.2 Problem Statement

During the journey from the production site to the end user's location, pellets are transported in bulk, which may damage them before the final use. Presently, a big proportion of pellets are normally exported internationally by vessels with a typical capacity of 20,000–40,000 metric tons. Due to the fragile and hydrophilic nature of pellets, they are susceptible to degradation during transport, handling, and storage. Apart from vessels, equipment such as grabs, pneumatic conveyors, hoppers, belt conveyors, transfer chutes, silos, and domes, are being applied to transfer pellets in the journey. During the journey, several forces such as compressive, impact, and attrition forces act on pellets causing breakage and fragmentation. Moreover, a change in environmental conditions such as temperature, relative humidity, and direct rain exposures may degrade the physical structure and energy content of pellets.

Degradations of pellets in their physical structure or energy contents may cause several problems during transport and final use. The breakage of pellets can increase the generation of fines and dust, which are reported to cause problems associated with loss of materials, increased risk of fire or explosions, equipment fouling, health issues for the people working nearby, and air pollutions. Several fatal problems have been reported regarding self-ignition and dust explosions of pellets e.g. [7], [8]. Chemical changes in the pellets can cause decreased calorific values due to the increased oxidation and moisture content [9].

There is a limited number of experimental and modeling studies on the degradation and breakage behavior of biomass pellets either experimentally or via simulations. So far, research reports dealing with biomass pellets are mainly focused on three main domains: research on the effect of feedstock on the pellet properties, research on the pretreatment or densification specifications and efficiencies, and research on the techno-economical aspects of using biomass pellets [4], [10]–[12]. The existing reports on the breakage behavior of pellets are mainly based on pilot-scale or laboratory tests, and up to now, there is no literature considering the physical degradation of pellets during large-scale transport and storage systems.

Studying the mechanical degradation of pellets during pellet-pellet and pellet-equipment interactions can also be performed using modeling and simulation. Due to the heterogeneous nature of biomass pellets and the difficulties of experiments, comparing the physical degradation of pellets in various conditions is hard. Using numerical methods, one can create a calibrated model of pellets to be tested in various conditions to examine the effect of equipment design on the degradation of pellets. Once such a model is established, it allows design optimization of the equipment used in the transport sector. So far, only one research article modeled the breakage function of biomass pellets in a virtual environment, which used finite element methods (FEM) [13]. Although FEM has been proven as a beneficial method to study the material's behavior under forces, due to its nature, it can not track individual particles inside a pellet and therefore, the breakage patterns and the fines generated throughout the transportation system cannot be predicted. Thus, a model able to track the discrete elements inside a pellet may give better insights into the breakage behavior of pellets. The discrete element method (DEM) also known as discrete element models enable us to follow the behavior of microparticles resulting in the opportunity of modeling the macro behavior of systems. Hence, it can be used to predict the degradation and breakage behavior of biomass pellets.

1.3 Research Question

Although the production and use of biomass pellets are rapidly growing, research on the degradation of pellets is far less considered. In this thesis, however, the goal is to identify and bridge the gap in science considering the effect of material-equipment interactions and environmental effects on the degradation of pellets. Thus, this thesis investigates the degradation of biomass pellets due to handling, transport, and storage. Thus, an overall research question is formulated as follows:

"How do biomass pellets degrade during transport and storage?"

In order to answer the research question, first, the following sub-questions should be answered:

1. What are the existing methods to assess the degradation behavior of biomass pellets? In addition, which factors affect the quality parameters of pellets prior to and post pelletization process?
2. What are the effects of pellet length, test conditions, and torrefaction on the degradation of pellets?
3. To what extent does the physical degradation of pellets in pilot-scale transportation correlate with the durability results?
4. To what extent do pellets degrade during large-scale transport, handling, and storage, and what is the relationship between their physical degradation and durability results?
5. What is the effect of temperature and humidity variation on the degradation behavior of pellets during storage?
6. To what extent can the degradation behavior of biomass pellets be simulated using DEM?

1.4 Methodologies

Based on the literature survey that maps the cutting edge research and technology, we can systematically assess the affecting factors on biomass pellet degradation. The research gaps following from the literature review can elucidate the research plans. In this dissertation, three main methodologies were used to answer the research question and the sub-questions.: literature survey, experimental, and numerical methods.

An extensive literature review is carried out to discover the most crucial factors influencing the quality parameters of pellets before, during, and post pelletization. This includes the specifications of the feedstock and its components, pretreatment conditions, pelletization specifications, and post pelletization circumstances. In addition, the diversity of methods to assess the quality parameters of pellets is investigated and the effect of their specifications on the quality determination is elucidated.

The experimental investigations studying the degradation behavior of biomass pellets are twofold: mechanical or chemical. In both cases, however, reports are usually limited to laboratory measurements using less than 10 kg of pellets in each test. In this dissertation, nonetheless, the focus is to quantify the degradation behavior of pellets in different scales, i.e.

from laboratory to large-scale. To achieve this goal, first, the validity of the most commonly used methods in the literature is assessed through some experimental studies. Then, to study the mechanical degradation, the breakage behavior and fines generation of pellets is quantified through transportation by performing both pilot and large-scale experiments. For pilot-scale studies, design of experiments (DoE) methodology is applied to study the fines generation of pellets when transported by a belt conveyor. For large-scale experiments, a pellet-fired power plant is chosen as a case study, and fines generation through the whole transport system is studied. To fill the gap between scales, the results of the laboratory, pilot, and large-scale experiments are compared to one another and discussed. Then conclusions are drawn and recommendations made for future studies. To study the chemical degradation, the effect of different environmental conditions on the quality parameters of pellets is investigated. This is done by placing various types of pellets at variable environmental conditions by changing the temperature and relative humidity. These experiments are performed on a laboratory-scale.

The numerical part is carried out using the discrete element method (DEM). DEM was first proposed by Cundall in 1971 [14] in rock mechanics and later on, this type of modeling was applied in many engineering fields such as bulk materials, powder mechanics, mining processes, and agricultural processes. It uses equations of motion to track the behavior of every single particle (micro) contact by contact resulting in the bulk material (macro) behavior of a system. In this dissertation, a breakage contact model based on the so-called Timoshenko-Ehrenfest theory developed by EDEM® (Edinburgh, UK) is used to model the breakage behavior of individual pellets at different configurations of a compression test. The model is compared and validated with the experimental results obtained in the experimental part of this dissertation. The calibrated model can open up a huge world of opportunities for future investigations of the physical degradation of pellets by leading to new equipment design for transport and storage.

1.5 Outline of the Thesis

Figure 1.2 presents the outline of this dissertation. **Chapter 2** presents a comprehensive literature review on the role of feedstock properties and the specifications of the pelletization process on the quality parameters of biomass pellets. Moreover, the common methods to quantify the quality parameters are introduced and critically discussed. This enables us to have a holistic overview of the influence of various factors on the quality parameters of biomass pellets. Then, according to the visual outline, Chapters 3, 4, and 5 explain, the experimental on the mechanical degradation of pellets as follows: **chapter 3** investigates the influential

properties of biomass pellets and test conditions affecting the laboratory-scale degradation assessments. **Chapter 4** presents a pilot-scale investigation of the degradation behavior of pellets during transport by a belt conveyor and **chapter 5** presents the degradation behavior of pellets throughout large-scale transportation in a case study power plant. To address the aim of this dissertation on studying the chemical deterioration of pellets, the experimental results and analysis at different environmental conditions, i.e. temperature and relative humidity, are presented and discussed in **chapter 6**. A numerical DEM model, which is validated based on the experimental results of the pellet breakage, is presented in **chapter 7**. Finally, **chapter 8** explains the overall conclusions and recommendations.

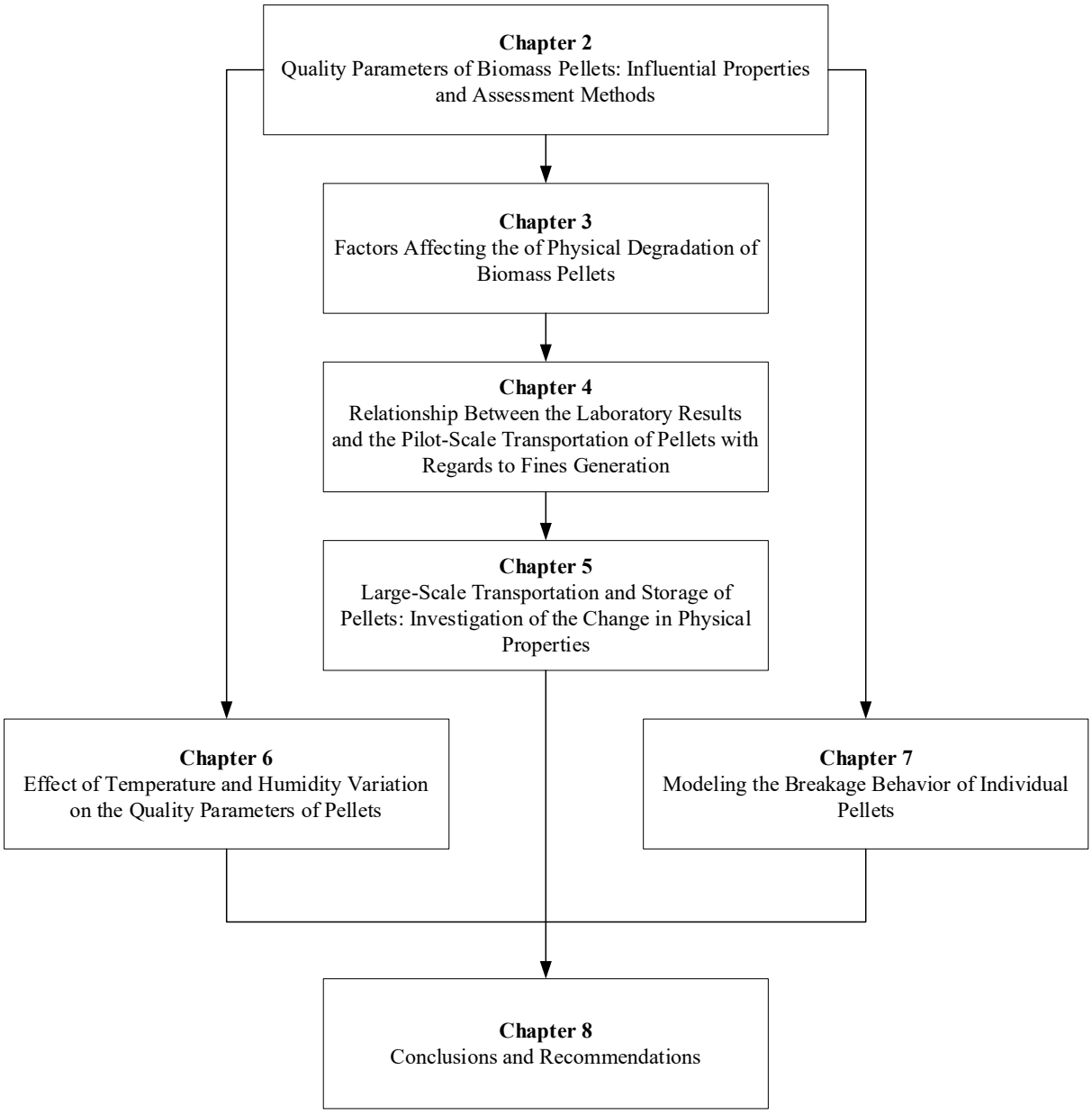

Figure 1.2: Thesis outline.

2 Quality Parameters of Biomass Pellets: Influential Properties and Assessment Methods*

As a first step to discover how different factors affect the quality parameters of biomass pellets, this chapter presents a comprehensive literature review. The review focuses on two main questions in biomass pellet degradation: (1) how do different factors affect the quality parameters of biomass pellets, and (2) how are these quality parameters assessed?

The most recent publications in this field of research were collected to conclude different aspects of quality parameters, i.e. physical and chemical properties of biomass pellets. Then, different measurement methods and techniques are discussed in detail in order to better understand the differences and their effect on the final results

*This chapter is based on Hamid Gilvari, Wiebren de Jong, and Dingena L. Schott. "Quality parameters relevant for densification of bio-materials: Measuring methods and affecting factors-A review." Biomass and Bioenergy 120 (2019): 117-134.

2.1 Introduction

Densification is the compacting process of material under specified conditions. Densification is classified into pelletization, briquetting, and extrusion [15]. According to Falk [16], the primary aim of pelletization is "the agglomeration of small particles into larger particles by means of a mechanical process in combination with moisture, heat, and pressure". Densification is widely used in biomass industries, animal feed making, and pharmaceutical industries. Generally, densification increases the bulk density, improves transportation and handling and logistics, decreases dust generation, and reduces labor costs. Depending on the application, densification may provide also other advantages, for example, easy adaptation in direct-combustion or co-firing with coal, improving the flow properties of biomass, improving feed quality for animals, and uniformity in mass and size of pharmaceutical products [4], [17]–[22].

Pellet mills, hydraulic piston presses, mechanical piston presses, tabletizers, roller presses, and screw extruders are some examples of densification systems widely used in industry [10]. Densified materials are commonly cylindrical; however, there are other shapes such as hexagons with or without a hole in the center. Although there are some standards for densified material size classification [23], there is no standard value to distinguish the pellets and briquettes by length and diameter size. According to CEN TS 14588 standard [3], the terms biofuel briquettes and biofuel pellets refer to densified biofuels made from pulverized biomass with or without pressing aids. The briquettes are cubic or cylindrical, however, pellets are cylindrical with a typical random length of 5 to 30 mm with broken ends. Regarding the literature, most researchers used the term "Pellet" when the cylinder diameter was between 3 and 27 mm with a length of 3 to 31mm [17]–[20], [24]–[31] and some other authors used the term "Briquette" when the cylinder diameter was between 18 and 55 mm and the length was between 10 and 100 mm [32]–[40]. It is clear that for a diameter between 18 and 27 mm, both terms are used in the literature. In a study on wood residue, densified cylinders of 49 mm in diameter and 50 mm in length are named "Log" [15]. Other shapes of briquettes are also reported, for example, Chou et al. [41] made cubic briquettes of rice straw with the dimensions of 40×40×35 mm. In order to avoid confusion the terms pellets, briquettes, and logs in this chapter are used in the same way as in the corresponding cited paper.

The suitability of the densification process is evaluated by measuring some of the physical properties of the final product. According to Richards [42], resistance to crushing, durability, impact resistance, and water adsorption are four crucial factors to be taken into account in developing and evaluating the densification process and quality of densified materials. He

pointed out that there is a relationship between compressive strength, impact, and abrasion resistance. According to other researchers, density along with durability are the most significant factors in determining the physical quality of densified materials [22]. Czachor et al. [43] in their study of biomass pellets found that there is a relationship between density and physical quality of the pellets. Richards [42] stated that as the compressive strength increases, the density also increases, but the reverse is not always true since higher density does not necessarily stand for stronger bonding. Larsson and Samuelsson [44], showed that the compressive strength of pellets highly depends on pellet density and durability where it can be modeled with a good fit.

Quality standards serve as a reference to provide customers with information about the quality and performance of products. Moreover, standards help to systematically assess the quality differences between the material of various origin and processes. It should be noted that the standards refer to firstly measuring methods such as using a standard tumbling device for durability measurement, and secondly, the product quality classification such as classification of pellets based on their durability.

With the advent of new densified bio-materials such as densified biomass and densified torrefied biomass in recent years, there is a concern about the performance of the existing transportation equipment in terminals and transportation units for large-scale transportation and storage. Research on biofuel demand in Northwest Europe carried out by Sikkema and Fiorese [45] shows that the import of woody biomass pellets for electricity generation may reach up to 16 Mt by 2035. The increasing biomass demand in other countries underlines the importance of transportation, handling, and storage. Presently, there are a few standards to measure the quality parameters of biomass-based materials, such as durability and density standards. In order to better understand the material behavior during transport and storage, standards to measure the compressive strength, impact resistance, and moisture adsorption are required.

Several studies have reviewed different densification systems, their energy consumption, factors affecting densification processes, strategies to increase densified biomass durability, and bonding mechanisms [4], [10], [46], [47]. However, there is no integrated approach that discusses the methods used to characterize the quality parameters of densified bio-materials. Based on an extensive literature study, the primary aim of this chapter is to survey different quality assessment methods in detail and to investigate the effect of different experimental setups on the characterizations of material quality. This will be described in section 2.2 where the state-of-the-art experimental setups, their advantages and disadvantages, and comparisons

with the existing standard methods are given. The other aim, which is outlined in section 2.3, is to investigate the effect of different factors on quality parameters of densified bio-material from integrated perspectives. Then, the results are discussed in section 2.4. The overall conclusions and outlook will be outlined in section 2.5. It is worth mentioning that this chapter is targeted at all the research and industrial units that are involved in bio-material production, handling, and logistics, i.e. producers to end-users.

2.2 Methods to measure the physical properties

Once the pellets or briquettes have been produced, they are stored and transported to the end-user location. During transportation, the materials are subjected to several forces, which may cause degradation [48]. The forces are divided into three main categories, namely compressive forces, shear forces, and impact forces [49]. Due to several limitations such as time, cost, unavailability of equipment, and on-site test difficulties it might not be possible to test the physical properties of the materials in the supply chain. Thus a number of tests, including compressive strength tests, impact tests, and abrasion tests were developed to simulate the conditions of the transportation, handling, and storage [4], [33]. Despite the existence of standard methods for measurement of a selected number of physical properties shown in Table 2.1, there are many different methods in the literature to measure the strength of pellets or briquettes against these forces, which are described in the following sections.

Table 2.1: Examples of national and international standards to measure quality parameters of different materials.

Standard Test	Quality parameter	Material
ASTM D2166-85:2008	Compressive strength	Wood
ASAE S 269.4	Density, durability, and moisture content	Cubes, pellets, and crumbles
CEN[a]/TS 15639:2010	Mechanical durability	Solid recovered fuels-Pellets
PFI[b]: Call Number: LD2668.T4 1962	Mechanical durability	Residential/commercial densified biomass
ISO 17831-1:2015	Mechanical durability	Solid Biofuels-Pellets
ISO 17831-2:2015	Mechanical durability	Solid biofuels-Briquettes
ÖNORM M 7135[c]	Mechanical durability	Wood pellets and briquettes
ASTM D 441-86	Mechanical durability	Standard test method of tumbler test for coal
ASTM D 440-86	Drop shatter test	Standard test method of drop shatter test for coal
DIN[d] 51705	Bulk Density	Solid fuels
EN 15103:2010	Bulk Density	Solid biofuels with a nominal top size of maximum 100 mm

[a] CEN: Common European Standard
[b] PFI: Pellet Fuel Institute (USA)
[c] Austrian Standard
[d] German Standard

2.2.1 Compressive Strength

Compressive strength measurements simulate the compressive forces acting on a sample during transport and storage. For example, when the bulk material is transferred via belt conveyors or chutes or discharged into the storage silos, they encounter forces from either the equipment or the bulk material. Different devices have been used in literature to characterize the compressive strength [47]–[50]. The working principle of the majority of these devices is the same. The material is normally placed between two horizontal plates or a pressure piston and a bar, which compress the sample at a constant rate until failure or breakage. Then the maximum force is recorded. Presently, there is no standard method for the compressive strength of densified bio-materials, however, according to the standard test method for compressive strength of cylindrical concrete specimens [51], a compressive axial load applies to the specimen until failure occurs. Then the compressive strength is calculated by dividing the maximum load by the cross-sectional area of the specimen. In literature, the compressive strength for densified bio-materials is defined as the maximum axial force (Figure 2.1 a) a material could withstand until failure or breakage or the maximum force during deformation [18], [19], [31], [37], [52]. If the force is applied perpendicular to the cylinder axis, it is called tensile strength (Figure 2.1

b). According to the standard test method for splitting tensile strength of cylindrical concrete specimens [53], in this test a diametrical compressive force applies along the length of the specimen until failure occurs. Then the tensile strength is calculated by:

$$T = \frac{2P}{\pi dl}, \tag{2.1}$$

where T is the splitting tensile strength (MPa), P is the maximum load (N), l is the length (mm), and d is the diameter of the specimen (mm). However, some researchers do not follow these definitions and they use these terms conversely. Normally the compressive strength is higher than the tensile strength [33].

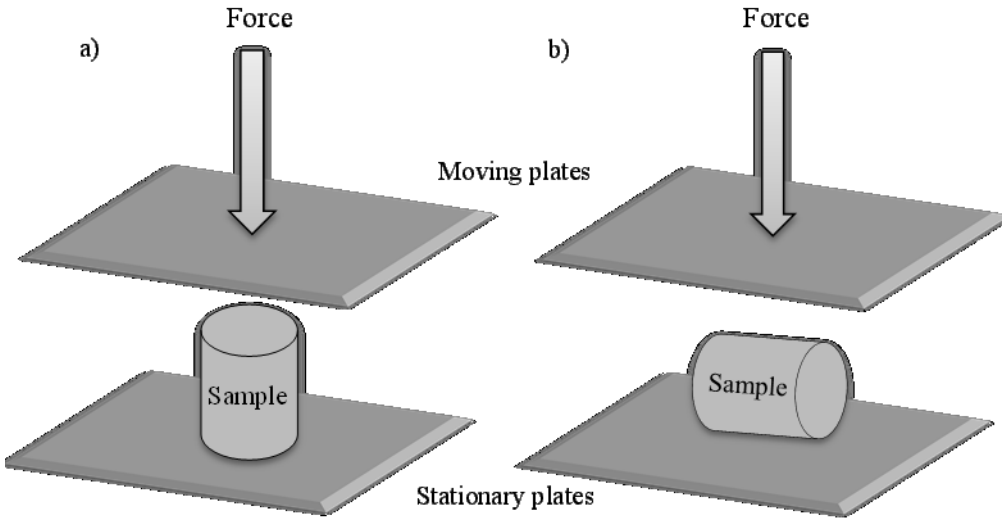

Figure 2.1: Orientation of a typical crushing experimental setup during (a) compressive and (b) tensile strength testing adapted from Ref. [33].

During transport and storage, the material encounters the forces from any direction. Therefore, some researchers argue that determining the tensile strength seems more practical than compressive strength because the tensile strength is related to the weakest orientation of the pellet or briquette [42]. Anyway, numerous researchers have only measured the compressive strength as an indication of the sample quality without giving any information about their choice argument [15], [18], [19], [27], [31], [32], [37], [39], [40], [52], [54].

Comparing the literature results enables us to obtain a good understanding of the factors affecting the material properties. Nevertheless, variation in the test procedures and equipment in the literature mostly due to a lack of standard methods make it difficult or impossible to

compare different material properties. For example, Kambo and Dutta [19] used a compression device to measure the strength of the pellets in the radial direction by applying a compression rate of 25 mm.min^{-1} and reported the compressive strength as the maximum force that breaks the pellets. Hu et al. [18] also used the same procedure as Kambo and Dutta [19], but they applied a force rate of 2 mm.min^{-1}. Yaman et al. [39] also used an Instron device to measure the compressive strength of fuel briquettes. They measured the compressive strength by dividing the maximum load to fracture the material over the cross-section area of the sample, however, the compression rate in their study was not stated.

Mitchual et al. [40] in their study of fuel briquettes used an Instron machine, which compressed the cubic shape material at a rate of 0.305 mm.min^{-1} and reported the compressive force using the equation (2.2):

$$\mathrm{CS}= \frac{3F}{l_1 + l_2 + l_3}, \tag{2.2}$$

where CS is the compressive strength, F is the maximum force (N) crushing the material, and l_1, l_2, and l_3 are the dimensions of briquettes (mm).

Abdollahi et al. [31] and Svihus et al. [55] used a texture analyzer (Figure 2.2, adapted from [56]) to measure the compressive strength of animal feed pellets. They placed the samples between a pressure piston and a bar horizontally, compressed the materials at the rate of 0.16 mm.min^{-1}, and recorded the maximum force at which the particle breaks. Then, the compressive strength was reported as the maximum force in Newton.

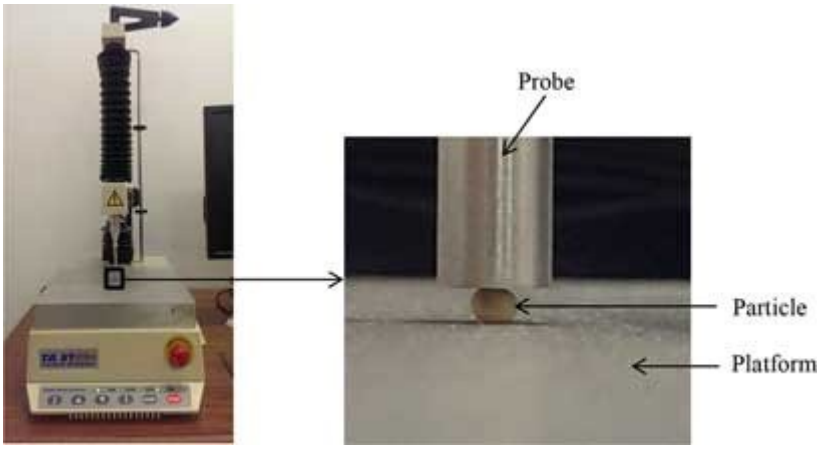

Figure 2.2: A texture analyzer device adapted from [56].

Bergström et al. [27] investigated the compressive strength by positioning the samples between two parallel horizontal plates and compressed them in the radial direction at a rate of 0.4

mm.min^{-1} until the sample was crushed. Then they reported the compressive strength according to equation (2.3):

$$\mathrm{CS}=\frac{F}{L}, \tag{2.3}$$

where CS is the compressive force, F is the force, and L is the length of pellets [mm]. They argued that by dividing the force by the pellet length, the effect of length on the compressive strength was eliminated.

In the other study of densified solid fuels, Bazargan et al. [33] compressed the material perpendicular to the cylinder axis at a rate of 30 mm.min^{-1} and measured the tensile strength using equation (2.4):

$$\sigma_T = \frac{2F}{\pi D h}, \tag{2.4}$$

where σ_T is the tensile strength, F is the force, and D and h are the pellet diameter and length, respectively. Liu et al. [57] also used the same procedure to measure the tensile strength of biomass pellets using a compression rate of 1 mm.min^{-1}.

Chin and Siddiqui [36] have invented a test to measure the shear strength of biomass briquettes. They placed a sample on a 34 mm diameter and 12 mm deep stand and tied a piece of string of 5 mm diameter around the sample while the other end of the string was tied to a spring load using a pulley. Then, the shear force, which breaks the briquette, was reported as the shear strength.

Richards [42] believes that using stress instead of compressive strength could remove the dependency of compressive strength on the shape and size of a briquette. The stress can be derived from equation (2.5):

$$\sigma = \frac{F_l}{\mathrm{A}}, \tag{2.5}$$

where σ is the stress, F_l is the load at fracture, and A is the cross-sectional area of the plane of fracture.

Meyer Hardness

Another way of expressing the material strength is to determine the material hardness. Hardness is defined as the resistance to deformation. Brinell hardness, Vickers hardness, Rockwell hardness, and Meyer hardness are different kinds of hardness tests from which the Meyer

hardness is most commonly used in literature to determine the hardness of densified bio-materials [17], [28], [58]–[62]**.** Meyer suggested the hardness should be based on the projected area of the impression rather than the surface area. Therefore, the Meyer hardness is the mean pressure between the surface of an indenter and the indentation i.e. the load divided by the projected area of the indentation [63]. Lam et al. [61] and Li et al. [28] believed that the Meyer hardness reflects the material strength during transport and storage.

The Meyer hardness is measured by placing the sample between two anvils of a press while the force is diametrical. The maximum force a sample could withstand before breaking is measured and then the Meyer hardness (H_M) is calculated from equation (2.6):

$$H_M = \frac{P}{\pi r^2}, \tag{2.6}$$

where P is the pressure and r is the indentation radius.

Tabil et al. [62] showed that the Meyer hardness could also be expressed by the indentation depth, thus the equation (2.6) could be expressed as equation (2.7):

$$H_M = \frac{P}{\pi\,(Dh - h^2)}, \tag{2.7}$$

where D is the indenter diameter and h is the indentation depth

Peng et al. [58] developed the equation (2.7) in order to determine the Meyer hardness for wood pellets. In their study, they indicated that as the surface of the wood pellets is mostly a curved shape, the cross-sectional area between the hemispherical probe and the pellet is oval-shaped. The developed equation is:

$$H_M = \frac{P}{\pi\sqrt{Dh - h^2}\sqrt{\frac{D_p^2}{4} - \left[\frac{\frac{D_p^2}{2} + \frac{D.D_p}{2} - D.h - D_p.h + h^2}{D + D_p - 2h}\right]^2}}, \tag{2.8}$$

where D is the indenter diameter, h is the indentation depth before the pellet breakage, and D_p is the pellet diameter.

Peng et al. [60] used a 6.35 mm hemispherical probe on a press machine and compressed the samples positioned vertically at a speed of 1 mm.min^{-1}, then used the above equation to characterize the Meyer hardness.

Regarding the probe shape and size and their effect on the Meyer hardness values, Tabil et al. [62] defined a number of experiments on different sizes of alfalfa cubes. Overall, they argued that the sphere-end shaped probe is more practical in Meyer hardness determination since firstly, the values obtained had a lower variance than a flat-end probe, and secondly, it results in lower values of hardness corresponding to the occurrence of cracking in the cubes.

Bending strength

A bending test is used to determine the Young's bending modulus, i.e. the displacement of a material when different force values are exerted. By studying the bending test for rigid materials, the maximum force a material can withstand in bending can be determined. The principle of the bending test is similar to the compressive strength measurements; however, the force exerted on the material is concentrated on one spot. For instance, as shown in Figure 2.3, the force is orthogonally acting on the center of a plant stem.

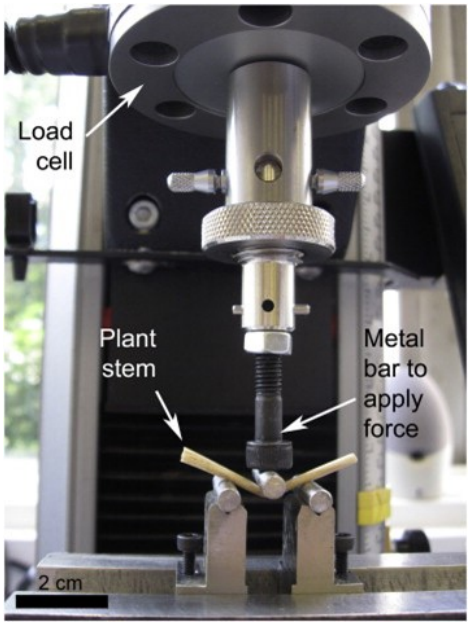

Figure 2.3: Bending test on a sample of salt marsh canopies adapted from [64].

Rupprecht et al. [64] measured the bending strength of different biomass plant stems using an Instron machine at a displacement rate of 10 $mm.min^{-1}$. To measure the bending strength of palm oil biomass pellets, Arzola et al. [65] used a Shimadzu testing machine fitted with a 50 N load cell at 20 $mm.min^{-1}$. The results of the latter study are shown in Figure 2.4.

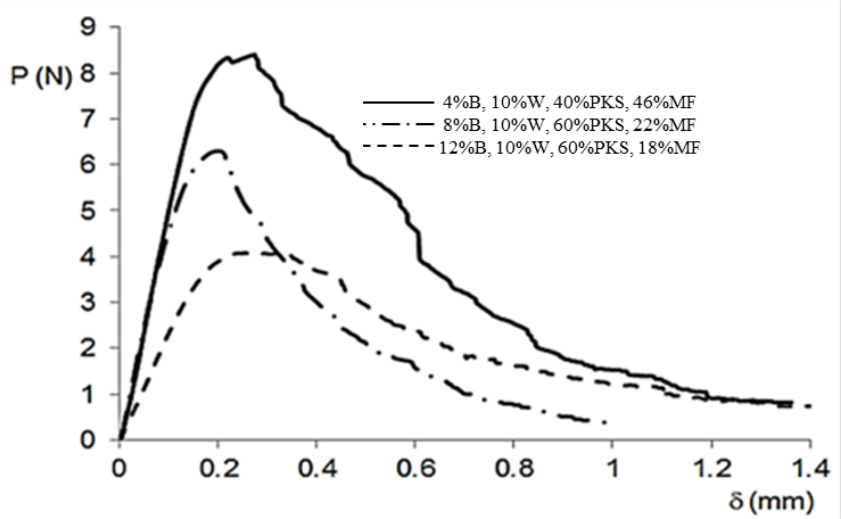

Figure 2.4: Average curve of load vs deflection for biomass blend pellets adapted from [65].

Summary

Although different researchers used various rates of compressions in their studies, the effect of compression rates on the compressive strength or tensile strength is not clear yet and no study has been found to investigate this. Future research should be directed toward studying the effect of the compression rate on the compressive and tensile strength in order to fill this gap. Furthermore, in order to reliably compare the Meyer hardness of different studies, the effect of geometrical factors such as indenter shape and size should be reported.

Some examples of compressive/tensile strength and Meyer hardness values of the above-mentioned literature are shown in Table 2.2 and Table 2.3, respectively. Although the compressive strength alone is not an indication of densified biomass strength during handling and transportation, Rahman et al. [66] believed that briquettes showing a compressive strength of at least 19.6 $N.mm^{-1}$ are suitable for handling for domestic purposes. Richards [42], suggested a minimum of 350 kPa (0.35 MPa) compressive strength is necessary for coal briquettes in order to withstand crushing in unclosed belt conveyors and normal bin storage. Nevertheless, the compressive strength test is widely used in characterizing the bio-materials strength; however, there is no dedicated standard procedure for densified bio-material. Therefore, there is an urgent need for the development of standard compressive test methods, which encounter both pellets and briquettes in any, shape and be capable of predicting material breakage during transport and handling.

Table 2.2: Compressive or tensile strength of different densified material.

Raw material		Shape and dimensions (mm)	PSD* of raw material (mm)	Binder	Densification conditions	Density (kg.m^{-3})	Strength	Ref
Pyrolysed wood	@ 650ºC	Pellet D*:20 L*: 12–20	Mean size: 0.05–0.64	Alkaline lignin	P*: 128 MPa	PD*~1100	~15 MPa	[18]
	@ 550ºC					PD~1000	~9 MPa	
Miscanthus	HTC @ 190ºC	Pellet D: 6.35	< 0.73	No binder	P: 8.6 MPa HT*: 10 s	PD: 887	~310 N	[19]
	HTC @ 225ºC					PD: 959	~275 N	
	HTC @ 260ºC					PD: 1036	~205 N	
	Torrefied @ 260ºC					PD: 820	~145 N	
Pine	Fine	Pellet D: 8	< 1	No binder	Pellet press (30 kW)	PD: 1263	61.2 N.mm^{-1}	[27]
	Reference		< 8			PD: 1259	52.4 N.mm^{-1}	
	Middle		1–2			PD: 1276	51.3 N.mm^{-1}	
	Coarse		1–4			PD: 1274	40.1 N.mm^{-1}	
Wheat-based	Animal feed-starter period	Pellet D:3 L: 3	NS	Commercial pellet binder or moisture or no binder	Steam conditioning for 30 s T*: 60ºC	NS	14.9 N with binder: 18 N with MC: 23.9 N with binder & MC: 23.4 N	[31]
					T: 90ºC		28.4 N with binder: 37.8 N 41.7 N with binder: 45.7 N	
	Animal feed-finisher period	Pellet D:3 L: 6			T: 60ºC		24.3 N with binder: 27.3 N with MC: 30.8 N with binder & MC: 29.4 N	

Raw material	Shape and dimensions (mm)	PSD* of raw material (mm)	Binder	Densification conditions	Density (kg.m^{-3})	Strength	Ref
Gasified palm kernel shell	Briquette D: 25 L: 10–14	> 3 0.7–3 03–0.7 < 0.3	Starch & water	P: 80 MPa HT: 10 s	PD~720	TS~0.027 MPa TS ~0.022 MPa TS ~0.026 MPa TS ~0.035 MPa	[33]
Sawdust Coconut fiber Palm fiber Peanut shell Rice husk	Briquette D: 30	0.3–0.85 0.1–0.5 < 0.15 0.15–0.5 0.1–0.18	Molasses & starch water	P: 10 to 100 bar	RD*: 462 RD: 157 RD: 192 RD: 547 NS	27.5–95.7 N 10–73.3 N 10–36.2 N 1.3–6.7 N 1.2–4.6 N	[36]
Biomass-Lignite blends	Briquette D: 50 L: 100	< 0.25	Biomass	P: 250 MPa	NS	Without binder @ 40.7% MC: 1.1 MPa Without binder @ 10% MC: 11.8 MPa With binder @ 10% MC: 26.6 MPa	[39]
C. Pentandra T. Scleroxylon A. Robusta T. Superba P. Africana C.Mildbreadii	Briquette D: 55.3	2–3.35	No binder	P: 50 MPa HT: 10 s	RD: 651 RD: 597 RD: 573 RD: 673 RD: 720 RD: 655	51.45 MPa 40.89 MPa 26.88 MPa 24.67 MPa 55.45 MPa 19.18 MPa	[40]
Maize cobs					RD: 541 to 659	0.12–0.54 N.mm^{-1}	
C. Pentandra	Briquette D: 55.3 L: 52.5	< 1	No binder	P: 20 to 50 MPa HT: 10 s	RD: 523 to 716	29.23–44.58 N.mm^{-1}	[54]
C. Pentandra: Maize cobs 90:10					RD: 565–742	27.29–59.22 N.mm^{-1}	
C. Pentandra: Maize cobs 70:30					RD: 584–749	16.66–33.47 N.mm^{-1}	

Raw material		Shape and dimensions (mm)	PSD* of raw material (mm)	Binder	Densification conditions	Density (kg.m^{-3})	Strength	Ref
C. Pentandra: Maize cobs	50:50	Pellet D: 13.5 L.D^{-1}: 0.9	NS	No binder	P: max 280 MPa HT: 5 s	RD: 588–774	7.72–24.04 N.mm^{-1}	[54]
Pinewood sawdust						PD: 1141	3.91 MPa	
Rice husk						PD: 1093	2.05 MPa	
Coconut fiber						PD: 984	1.51 MPa	
Coconut shell						PD: 1101	0.96 MPa	
Hydrochar of	Pinewood sawdust		< 0.15			PD: 1191	7.10 MPa	[57]
	Rice husk					PD: 1334	4.21 MPa	
	Coconut fiber					PD: 1153	7.5 MPa	
	Coconut shell					PD: 411	2.97Pa	

*PSD: Particle size distributions, D: Diameter, L: Length, P: Pressure, PD: Pellet density, HT: Holding time, T: Temperature, RD: Relaxed density, NS: Not specified

Table 2.3: Meyer hardness values of different densified material.

Raw Material	Shape and dimensions (mm)	Binder	Densification Conditions	Pellet Density ($kg.m^{-3}$)	Meyer hardness ($N.mm^{-2}$)	Ref
Chinese fir	Pellet D*: 7	Sewage sludge	P*: 83 MPa HT*: 30 s	863 with binder: 1160	3.02 with binder: 4.15	[17]
Camphor				883 with binder: 1144	2.87 with binder: 4.03	
Rice straw				1027 with binder: 1217	3.98 with binder: 4.18	
Torrefied Sawdust @ 260ºC	Pellet D: 6.5 L*: 12	Moisture	4000–6000 N HT: 30 s T*: 70ºC	~1060	~3	[28]
Torrefied Sawdust @ 270ºC				~1050	~3	
Torrefied Sawdust @ 280ºC				~1020	~4	
Torrefied Sawdust @ 290ºC				~1010	~4	
Torrefied Sawdust @ 300ºC				~1000	~3.5	

* D: Diameter, L: Length, P: Pressure, HT: Holding time, T: Temperature

2.2.2 Durability (Abrasion Resistance)

The presence of abrasive forces in the supply chain is highly likely. Hence, knowing the abrasion resistance is beneficial in order to decrease the risk of dust generation resulting in possible dust explosion, environmental risks, and waste generation.

According to standard terminology, definitions, and description of solid biofuels [3], mechanical durability is "the ability of densified biofuel units (e.g. briquettes, pellets) to remain intact during loading, unloading, feeding, and transport".

Unlike the compressive strength, which is tested using a single sample, the abrasion test is normally measured with multiple particles. Generally, a known mass of the screened pellets or briquettes is placed into the device, which enables particle-particle and particle-wall interactions in a specified time. Then the amount of fines created is determined by means of sieving and finally, the durability is calculated based on the percentage of remaining mass on the sieve divided by the initial mass. Different devices were used by researchers to determine the material durability such as the rotating drum, tumbling can, ligno tester, Holmen device, and electronic friabilator. The working principles and some examples of each test device are explained in the following.

Rotating drum

The rotating drum consists of a cylindrical chamber with baffles inside which rotates around its axial direction. A rotating drum of 101.6 mm in diameter and 95 mm in length was used by Reza et al. [29] to investigate the durability of torrefied pine pellets by using 10 pellets of the sample. Two baffles of 25.4×88.9 mm were installed perpendicular to the drum inner wall and opposite to each other and the drum rotated at 38 rpm for 3000 revolutions. After the revolutions, the sample was sieved through a 1.56 mm sieve size. In another study of mechanical properties of biomass pellets, Gil et al. [67] used a rotating drum of 130 mm diameter and 110 mm length, having two baffles of 30×110 mm perpendicular to the wall cell. They placed 40 pellets of 8 mm in diameter in the drum and rotated it for 3000 revolutions at 35 rpm. Then, they used a sieve with a 2 mm mesh size to separate the created fine particles.

Temmerman et al. [68] used a rotating drum with a diameter and depth of 598 mm and a baffle of 598×200 mm perpendicular to the walls of the cylinder for measuring the durability of briquettes (Figure 2.5). They used a rotational speed of 21 rpm and measured the durability of different briquettes for different rotational times. Then used a 40 mm sieve size to separate the fine particles created at different drum rotation numbers.

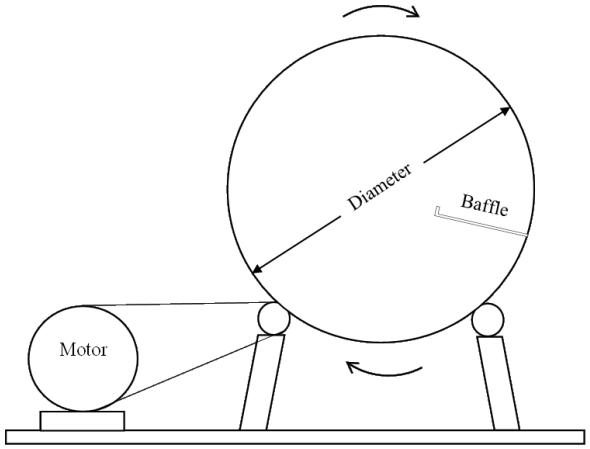

Figure 2.5: Schematic of briquette durability tester adapted from [68].

Ligno tester

To characterize the pellets' durability, Temmerman et al. [68] used a commercial ligno tester device according to the ÖNORM M 7135 [69]. As shown in Figure 2.6, the device is a four side pyramid containing 2 mm round holes on each side. The particles are swirled by means of an air stream inside the equipment, which causes the particles to collide with each other and against the walls. In their study, they used a standard air stream pressure of 70 mbar for one minute.

Bergström et al. [27] put 100 grams of pellets in a ligno tester device and rotated it twice for 30 s. The rotation velocity was not mentioned. Then the mass of abraded material was reported.

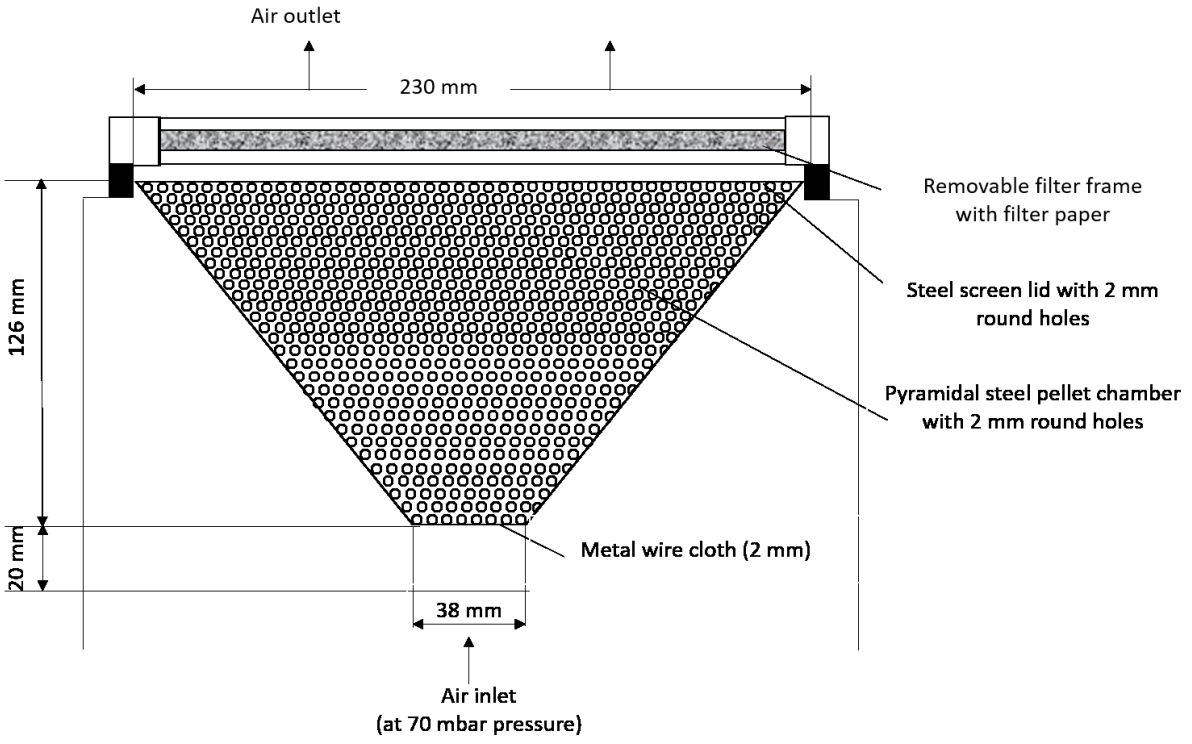

Figure 2.6: ÖNORM M 7135 apparatus for durability testing of pellets [68].

Holmen durability tester

The Holmen durability tester circulates the samples pneumatically inside the device by using an airstream in which particles collide with each other and with the equipment walls and creates fines. Normally, the test is conducted in less than two minutes. Abdollahi et al. [31] used a Holmen durability tester to measure the durability of animal feed pellets in 30 seconds of sample circulation. Then the pellet durability index (PDI) was defined as the remained mass of samples on the sieve to the initial sample mass. The sieve size to separate the fines is not indicated in their study.

Vibrating bed

Gilbert et al. [25] in the study of the durability of switchgrass pellets, used a vibrating bed working at 5 Hz frequency and amplitude of 7–8 mm for 100 min and measured the mass loss of the original pellets. The equipment is shown in Figure 2.7.

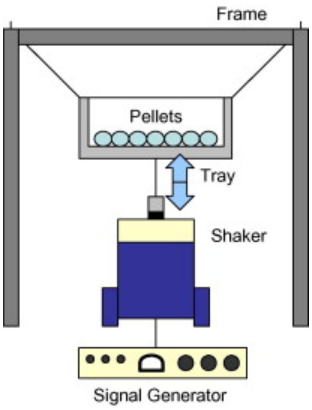

Figure 2.7: Vibrating durability tester adapted from [25].

Tumbling can

Karunanithy et al. [70] and Fasina [71] used a commercial tumbling can durability tester device (Figure 2.8) according to ASABE Standard S269.4 [72]. They placed 100 g of samples into the device, rotated it at 50 rpm for 10 minutes, and used the sieve sizes of 4.75 mm and 4 mm to separate fines, respectively. They reported the durability as the mass of particles remaining in the sieve to the initial mass of material.

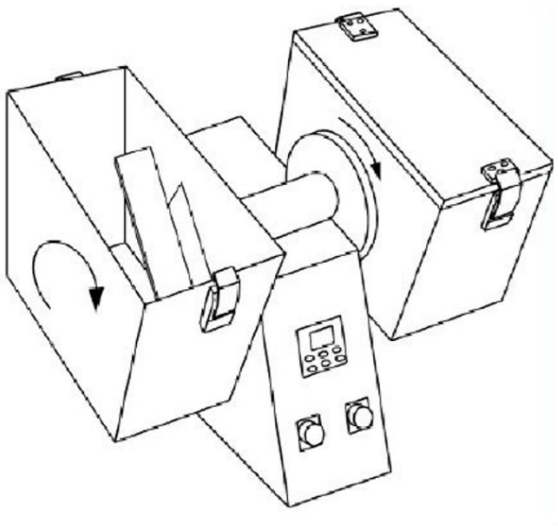

Figure 2.8: Schematic of tumbling can tester [72].

Friabilator

Friabilators form another class of durability testers. Friabilators are mostly used in the pharmaceutical industries in order to measure the durability of pharmaceutical products. A typical friabilator contains a cylinder low in depth (compared to the diameter) with a curved baffle attached between two walls of the cylinder (Figure 2.9). Zainuddin et al. [20] used a commercial friabilator to examine friability of animal feed pellets. They placed 20 pellets into the drum and rotated this for 4 minutes at 25 rpm. After 100 rotations, they measured the fines created and reported the friability by dividing the mass of the created fines by the initial mass of pellets.

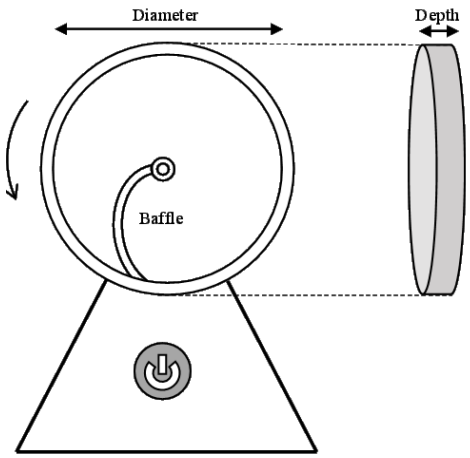

Figure 2.9: A typical friabilator.

Other durability testing methods

Li and Liu [15] used a porcelain jar to measure the abrasion resistance of logs made from wood residues. Three logs of 49 mm in diameter and 50 mm in length were put in the jar and were rotated at 60 rpm for 40 min. The mass loss of the logs indicated durability.

Sengar et al. [34] constructed a cuboid steel box with the dimensions of 30×30×45 cm and used a hollow shaft to set the frame diagonally, then rotated it for 15 min. They did not mention the other details of their set up such as the rotational frequency. They measured the durability index using equation (2.9):

$$\mathrm{DI} = 100\text{-}m_l, \tag{2.9}$$

where DI stands for durability index and m_l is the percent of mass loss of the initial sample.

Umar et al. [24] used an Erlenmeyer flask to measure the durability of animal feed pellets. They placed 100 g of pellets sieved on a 2.36 mm mesh size into an Erlenmeyer flask and tumbled on a shaker at 50 rpm for 10 min. Then they used the aforementioned sieve to separate the fines and reported the pellet durability index (PDI) according to EN15210-1 [73] as follows:

$$\mathrm{PDI} = \frac{m_a}{m_b} \times 100, \tag{2.10}$$

where m_b is the pellet mass before test and m_a is the pellet mass after the test.

Schulze [74] has explained an attrition test procedure using a ring shear test. The ring shear test is a device mostly used to measure the angle of internal friction. In a ring shear test apparatus, the material fills the shear cell and the shear cell is placed on the tester and covered by a lid. Then the sample is sheared to a pre-determined shear displacement. Shear displacement is the relative rotational displacement of the bottom ring and lid, which is measured at the mean radius of the sample. The amount of fines created by the test determines the vulnerability of samples.

Summary

Regardless of the test device type, the chosen sample volume in each test batch in the literature was less than 2% of the drum volume. None of the authors pointed out how the sample volume was chosen. It is clear that the more free space inside the drum allows particles to freely move and interact with other particles and equipment wall, and vice versa.

Considering the equipment type and sieve size used, even the standard methods are modified by some changes by the researchers. For example, to use the standard tumbling method, Reza et al. [29] used a 1.56 mm sieve size and Temmerman et al. [68] used a 40 mm sieve size while according to the standard the sieve size should be 3.15 mm. Therefore, it should be noted that the reported durability values in the literature are not comparable unless a complete standard method was used. Consequently, not all the high durability values in the literature are acceptable from the standard or practical point of view.

Some examples of the durability values of various pellets and briquettes using different raw materials and test methods are shown in Table 2.4. Besides the differences between the devices and device setup, there are still differences between the experiments. As an example, Lindley and Vossoughi [37] measured the durability of a single briquette by a tumbling can method while most of the researchers used a batch of particles in their durability test devices. It should be highlighted that when using a single briquette in the tumbling can, the method misses the abrasion forces between samples and may increase abrasion between the briquette and equipment wall, which may lead to different values of durability compared to the use of a group of particles. Another approach followed is that several researchers have reported the durability based on the amount of releasing fines while some other researchers reported that based on the mass loss of the initial sample. It appears that the former is mostly used for pellets while the latter is mostly used for briquettes. However, neither durability values nor dust generation characteristics are comparable when using these two different methods.

Table 2.4: Durability of different densified material.

Raw Material	Shape and dimensions (mm)	PSD* of raw material (mm)	Binder	Densification Conditions	Density (kg.m^{-3})	Durability (%)	Ref
Oak	Log D*: 49 L*: 50	< 50	No binder	P*: 34 to 138 MPa HT*: 0–60 s	Max*: 915	@ P 138 MPa: 98.3	[15]
Oak bran					Max: 1006	@ P 138 MPa: 97.6	
Pine					Max: 980	@ P 138 MPa: 93.2	
Cottonwood					Max: 960	@ P 138 MPa: 98.5	
Animal feed (pineapple)	Pellet D: 8 L: 30	< 1	35% Moisture	Extruder T*: 100ºC	BD*: 303 TD*: 1520	99.15	[20]
			40% Moisture		BD: 323 TD: 1514	99.09	
			45% Moisture		BD: 323 TD: 1508	98.98	
			50% Moisture		BD: 345 TD: 1503	98.78	
Pine	Fine	< 1	No binder	Pellet press (30 kW)	PD*: 1263	98.8	[27]
	Reference	< 8			PD: 1259	99.1	
	Middle	1 to 2			PD: 1276	99.1	
	Coarse	1 to 4			PD: 1274	98.4	
Torrefied loblolly pine @	Pellet D: 13 L.D^{-1}: 0.6 to 0.75	0.6 to 1.18	Moisture	P: 250 MPa HT: 30 s	PD: 1048	77.3	[29]
	250ºC				PD: 1012	78	
	275ºC				PD: 931	55.6	
	300ºC				PD: 689	9.3	
	350ºC				PD~1110	95	
	250ºC		10 wt.% HTC loblolly pine 260ºC		PD~1010	92	
	275ºC				PD~950	83	
	300ºC				PD~1120	98	
	250ºC	0.6 to 1.18	50 wt.% HTC loblolly pine 260ºC	P: 250 MPa HT: 30 s	PD~1080	99	
	275ºC						

Raw Material		Shape and dimensions (mm)	PSD* of raw material (mm)	Binder	Densification Conditions		Density (kg.m^{-3})	Durability (%)	Ref
Torrefied loblolly pine @	300ºC	Pellet D: 13 L.D^{-1}: 0.6 to 0.75	0.6 to 1.18	50 wt.% HTC loblolly pine 260ºC	P: 250 MPa HT: 30 s		PD~1050	97	[29]
	350ºC						PD~730	92	
loblolly pine HTC*@ 260ºC				No binder			PD~1430	99.8	
Wheat-based	Animal feed-starter period	Pellet D: 3 L: 3	NS*	Commercial pellet binder & moisture	Steam conditioning for 30 s	T: 60ºC	NS	56.5 with binder: 63.1 with MC: 67.2 with binder & MC: 70.2	[31]
						T: 90ºC		63.2 with binder: 69.6 92.8 with binder: 93.1	
	Animal feed-finisher period	Pellet D: 3 L: 6				T: 60ºC		74.1 with binder: 73.9 with MC: 84.7 with binder& MC: 89.7	
Malaysian mahseer		Pellet D: 3	NS	Tapioca-sago starch	P: 8 to 10 MPa		BD: 421 to 491	81 to 86.6	[24]
Switchgrass		Pellet D: 26.8 L: 20 to 31	10 to 70	No binder	P: 4.1 MPa P: 55.2 MPa	HT: 30 s	PD: 310 to 505	95 98.5	[25]
Cashew nut : Grass : Rice husk	50:25:25	Briquette	D: 22.5, L: 60.5	NS	No binder	NS	BD: 895	95	[34]
	25:50:25		D: 22.7, L: 53				BD: 1105	93	
	25:25:50		D: 22.4, L:49.8				BD: 1109	92	

Raw Material	Shape and dimensions (mm)	PSD* of raw material (mm)	Binder	Densification Conditions	Density (kg.m^{-3})	Durability (%)	Ref
Pine sawdust	Pellet D: 8	< 1	-	A commercial tablet press was used	-	~88	[67]
Chestnut sawdust						~93	
Eucalyptus sawdust						~36	
Cellulose residue						~70	
Coffee husks						~10	
Grape waste						~2	
Bituminous coal		< 0.212				~75	
Anthracite coal						~0	
Mixed wood	Briquette	-	-	Commercial briquettes	-	@ 105 rotation ~95 @ 210 rotation ~90 @ 315 rotation ~84 @ 420 rotation ~78 @ 630 rotation ~68	[68]
Mixed wood	Pellet	D: 6–8	-	-	Commercial pellets	-	99 to 99	
Softwood		D: 6–8					91 to 99	
Hardwood		D: 6					91	
Straw		D: 9–10					93 to 98	
Corn stover	Briquette D: 60	< 3.36	No binder	A commercial briquetting machine was used	-	~90	[70]
Switchgrass						~78	
Prairie cordgrass						~72	
Sawdust						~89	

Raw Material	Shape and dimensions (mm)	PSD* of raw material (mm)	Binder	Densification Conditions	Density ($kg.m^{-3}$)	Durability (%)	Ref
Pigeon pea grass						~55	
Cotton stalk						~88	

* PSD: Particle size distributions, D: Diameter, L: Length, P: Pressure, HT: Holding time, Max: Maximum, BD: Bulk density, TD: True density, T: Temperature, PD: Pellet density, NS: Not specified, HTC: Hydrothermal carbonization

2.2.3 Impact Resistance

The impact resistance, which is, also called shattering resistance or shattering test or drop test measures the resistance of samples when dropping from a known height onto a known floor material. Kambo and Dutta [19] believed that by measuring the impact resistance it is possible to investigate the forces acting on pellets when unloading from trucks to the ground surface or transferring the material from chutes into bins and also resistance during pneumatic conveying. Although many tests have been set to measure the resistance of densified material against shattering, there is no standard method for densified biomass [75]. Mostly, researchers design drop test experiments based on their knowledge or imitate other literature. Meanwhile, some researchers used another material's standard (e.g. coal and concrete) tests in their experiments.

Richards [42] has introduced the impact resistance index (IRI) for the fuel briquettes based on the drop number and number of pieces created. He dropped single briquettes three to six times from a height of 2 m onto a concrete floor until the briquettes broke down into smaller pieces. Then he recorded the average number of pieces created and defined the IRI as below:

$$\mathrm{IRI}=\frac{N_d}{N_p}\times 100, \tag{2.11}$$

where N_d and $N_p$stand for the average number of drops and pieces of briquettes, respectively. He proposed that the IRI of 50 is the minimum acceptable value for laboratory work.

Mitchual et al. [54] used the ASTM standard D440 which is a test method of drop test for mineral coal and Li and Liu [15] adapted their drop test from that standard test. The test procedure is to drop the material from a 2 m height onto a concrete floor and measuring the resistance index using the equation (11) while only the created pieces of bigger than 5% of the initial mass of material are taken into account. Demirbas and Sahin-Demirbas [76] used the standard method of coke shattering indices (ISO 616:1995). The test consists of dropping the material from the height of 1.8 m onto a steel plate, then the drop resistance is measured by determining the portion of material retained on a sieve having a 20 mm mesh size. This is repeated until the entire materials pass the aforementioned sieve. The sum of percentages is called the shatter index [39].

Sengar et al. [34] dropped the briquettes from a height of one meter onto an RCC floor and concrete floor and reported the shattering resistance (SR) by the following equations:

$$SR = 100\text{-}m_l, \tag{2.12}$$

$$m_l = \frac{(m_i - m_f)}{m_i} \times 100, \tag{2.13}$$

where m_i and m_f are the initial and final mass of briquettes, respectively.

Al-Widyan et al. [38] and Kambo and Dutta [19] measured the durability of olive cake briquettes by dropping them four times from a height of 1.85 m on a steel plate and measured the durability as the final mass retained on the briquette after falling.

Oveisi et al. [77] placed 100–5000 g biomass pellets in an enclosed bag made of synthetic material and released the bag from different heights onto a concrete floor. Weatherstone et al. [75] collected the material in bags of 300 and 2000 g after which they dropped them from a height of 7.52 m 10 times. Then, the impact resistance was reported based on the particles bigger than 3.15 mm and 3.16 mm, respectively. Moreover, the former research studied the effect of sample cushioning and concluded that by increasing the sample mass from 1000 to 5000 g, the increase in mass loss is smaller. Nonetheless, the effect of the bag cushioning was never studied.

Rotary impact device

Wu et al. [78] used a rotary impact test device (Figure 2.10) to measure the particle breakage. The material was fed between two parallel discs, which rotated at a pre-determined speed. The material shoots out and hits the steel plates inside the apparatus. The fines created during the test were determined. They used two different disc tip speeds of 6.5 and 24.3 $m.s^{-1}$ in a tangential direction to simulate a higher limit of impact in practice and then they measured the created fines by sieving the material by two sieve sizes of 2.8 and 6.3 mm. The results are showing in Table 2.5. As expected, the amount of fines created for 24.3 $m.s^{-1}$ disc tip speed tests is higher than for the tests performed at 6.5 $m.s^{-1}$.

Table 2.5: Impact resistance of different densified materials.

Raw Material		Shape and dimensions (mm)	PSD* of raw material (mm)	Binder	Densification Conditions	Density (kg.m^{-3})	Impact resistance (%)	Ref
Olive cake		Briquette D*: 25	NS*	35% Moisture	P*: 15–45 MPa	RD*: 1100–1300	75–99.25	[38]
Cashew nut : Grass: Rice husk	50:25:25	D: 22.5 L*: 60.5	NS	No binder	NS	BD*: 895	97	[34]
	25:50:25	Briquette D: 22.7 L: 53				BD: 1105	95	
	25:25:50	D: 22.4 L: 49.8				BD: 1109	94	
Miscanthus		HTC* @ 190ºC	Pellet D: 6.35	< 0.73	No binder	P: 8.6 MPa HT*: 10 s	PD: 887	[19]
		HTC @ 225ºC					PD: 959	
		HTC @ 260ºC					PD: 1036	
		Torrefied @ 260ºC					PD: 820	
Rice husk & Corn cobs blends		Briquette D: 32 L: 100	Rice < 2 Corn < 1.6	Starch	P: 19–31 MPa	NS	90	[32]
Flax Straw		Briquette D: 18 L: 50	< 6 < 25	Moisture	P: 35.2–91.4 kg.cm^{-2}	PD*: 1069	97.1	[37]
Wheat Straw					P: 58.4–84.4 kg.cm^{-2}	PD: 1056	98.8	
Sunflower					P: 31.6–98.4 kg.cm^{-2}	PD: 1432	99.2	

Raw Material	Shape and dimensions (mm)	PSD* of raw material (mm)	Binder	Densification Conditions	Density (kg.m^{-3})		Impact resistance (%)		Ref
Torrefied pellets	Pellet D: 6	NS	NS	Commercial pellets	@ 6.5 m.s^{-1}	S1[a]: 99.9 S2[b]: 99.9	@ 24.3 m.s^{-1}	S1: 97.8 S2: 93	[78]
Wood pellets	Pellet D: 6					S1: 99.8 S2: 95.8		S1: 95.9 S2: 84.1	
	Pellet D: 8					S1: 99.7 S2: 99.3		S1: 97.4 S2: 94.9	
	Pellet D: 12					S1: 99.5 S2: 98.8		S1: 96.2 S2: 91.1	

* PSD: Particle size distributions, D: Diameter, L: Length, NS: Not specified, P: Pressure, RD: Relaxed density, BD: Bulk density, HTC: Hydrothermal carbonization, HT: Holding time, PD: Pellet density

[a] S1: 2.8 mm sieve
[b] S2: 6.3 mm sieve

Figure 2.10: Rotary impact test apparatus of the University of Greenwich [78].

Summary

The impact resistance values of different materials are shown in Table 2.5. No research has been found in the literature to discuss the kinetic energy of samples and the impact force value at the impact point. However, these values depend on many factors such as sample mass, sample shape, and velocity at the impact point.

To figure out the material strength during transport, Richards [42] believed that there is a relationship between the compressive strength, impact resistance index, and abrasion resistance. He showed that briquettes with compressive strength values of higher than 375 kPa and IRI of higher than 50, usually show more than 95% abrasion resistance. Therefore, he suggested a drop test could be used as a guideline to estimate the strength of the material before conducting compression or durability tests. If the minimum acceptable quality is reached, then the other tests such as the compressive strength test or abrasion test could be investigated. Nevertheless, the test seems to be the simplest test method for evaluating the material strength in terms of facilities, laboratory work, time, and cost. However, similar to the compressive strength, the lack of a standard test method has resulted in widely differing results in the literature, which makes them incomparable.

2.2.4 Density measurements

Density can be expressed in three different ways namely granular density, particle density, and bulk density. The granular density (or true density) is the density of the material without porosity, the particle density is the density of densified material (like pellets or briquettes) considering the inner porosity, and finally, the bulk density is the density of a group of material containing the porosity between particles.

Different materials show different abilities to compress. Therefore, the degree of densification (DoD) showing the ability of the material to bond has been defined [79] as shown in equation (2.14):

$$\mathrm{DoD}=\left(\frac{\rho_d-\rho_r}{\rho_r}\right)\times 100, \tag{2.14}$$

where ρ_d is the density of the densified materials and ρ_r is the density of the raw material.

When measuring the particle and bulk densities, one should pay serious attention to the volume expansion or shrinkage of the material which might occur immediately after densification in both axial and lateral directions [17], [22], [25]. Carone et al. [22] reported up to 5% expansion in diameter of pellets having an original diameter of 6 mm and Gilbert et al. [25] observed around 10% decrease in pellet density of switchgrass one hour after densification. According to Jiang et al. [17], the volume expansion, on the one hand, creates more pores inside the densified material causing less resistance against abrasion and compression forces, and on the other hand, may produce a remarkable amount of fines before any transportation or handling activity. Moreover, the expansion creates more fines at the surface of the material causing coarser surfaces, which might inflict more fines production in the future, handling compared to smooth surfaces. Al-Widyan et al. [38] observed more than 10% shrinkage in the axial direction of briquettes made from olive cakes. They believed that the reason lies in the excessive loss of moisture content from the briquettes after densification.

In the following, different methods to determine the granular, particle, and bulk densities are discussed.

Granular density

The granular or true density is mostly measured using a "Pycnometer". The measurement is according to the pressure difference between a pre-determined reference volume and the sample cell volume. A schematic of a typical gas displacement pycnometer is shown in Figure 2.11. A sample of a known mass is placed into the volume calibrated sample cell. First, valve 1 opens to flow the inert gas into the chamber. Then valve 1 closes and one lets the chamber to reach equilibrium conditions. Once the equilibrium is reached, the pressure value is recorded. After that, valve 2 opens to allow the gas to go through the reference cell. After the whole system reaches an equilibrium condition, the pressure is recorded again. Finally, the solid sample

volume is calculated based on the pressure difference between the first and second equilibrium conditions.

Zainuddin et al. [20], Karunanithy et al. [70], and Fasina [71] used helium gas to fill the reference and sample cells. The true density (TD) was then measured based on the following equation:

$$\mathrm{TD}=\frac{m}{V_{cell}-\frac{V_{exp}}{\left(\frac{P_1}{P_2}\right)-1}}, \tag{2.15}$$

where m is the sample mass, V_{cell} is the empty volume of the sample cell, V_{exp} is the expansion volume, P_1 is the pressure before expansion, and P_2 is the pressure after expansion.

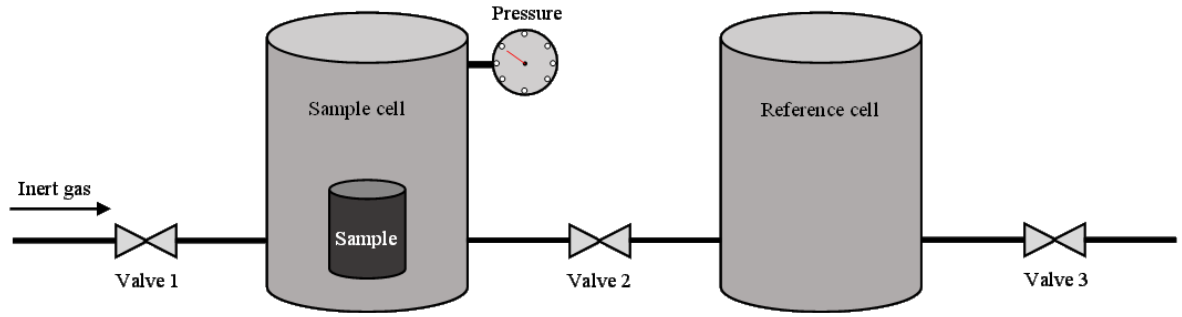

Figure 2.11: Schematic of a typical gas displacement Pycnometer.

Particle density

Particle density also is known as apparent density, intrinsic density [33], or relaxed density [38]—If measured after a certain time from the material's production—Is the ratio of mass and sample volume including pore volume [68]. Normally, densified materials are not smooth in shape, which creates measurement difficulties in practice. Therefore, several studies tried to measure the volume by applying different methods. Temmerman et al. [68] used the buoyancy method (based on the Archimedes principle) to estimate the volume of different pellets and briquettes. The sample mass is measured in air and a liquid with a known density. Then the volume of the sample can be calculated based on the liquid density. The method might create difficulties in practice since some materials disintegrate in the liquid, quickly. The other disadvantage of the method is that the liquid might go inside the pores resulting in errors in the experiments then it may rather determine the true density.

Another method is to immerse the particles in a liquid while coated with wax. Sengar et al. [34] used this method for the volume determination of biomass briquettes. First, they coated each

briquette with wax and then weighted it. Secondly, they immersed the coated sample in water and the displacement water was measured indicating the wax briquette volume. Then the volume of each briquette was calculated by the difference between coated briquette volume and coating wax volume. The volume of coating wax was obtained by dividing its mass by its density. The mass of the coating wax was also determined by subtracting the mass of wax briquette and the original briquette. Comparing the previous method, this method prevents water adsorption inside the material pores.

Several studies used an easier method to determine the particle density [19], [40], [78], [80]. They measured the mass of each pellet or briquette by using a laboratory balance and measured the material volume based on the diameter and length of the sample measured by a caliper. Then the ratio of mass to the volume was determined as the particle density. The advantage of this method is that a rough estimate of the particle density is achieved very quickly and simply, however, the disadvantage is that the method is not precise because the volume is not accurately determined. Some researchers have modified this method in order to improve the results. For example, Mitchual et al. [40] measured the diameter and length of cylindrical briquettes at three different points and calculated the particle density (PD) using the average value of the diameter (mm) and length (mm) according to equation (2.16):

$$PD = \frac{108000 \times m_p}{\pi \times (d_1 + d_2 + d_3)^2 \times (l_1 + l_2 + l_3)} \tag{2.16}$$

where m_p is the mass of the particle, and d and l are the diameter and length, respectively.

Bulk density

Bulk density is the mass ratio of a known volume of the bulk material to its volume including the voids between particles. The mass and volume are measured using a balance and a container with a known volume, respectively. The European bulk density measurement standard for solid biofuels EN 15103 [81], states that the volume of the container could be between 1 and 50 liters depending on the solid biofuels size and the quantity available. Karunanithy et al. [70] used the ASAE standard method to measure the bulk density of ground feedstocks and briquettes. They used a 2000 ml glass container and calculated the bulk density by dividing the mass of the material by the glass volume. Zainuddin et al. [20] filled a 200 ml cylinder with the pellets of 8 mm diameter and 3 cm length and tapped the container twice to obtain a uniform packing and reduce the wall effects. Wu et al. [78] used a 1 liter steel container for pellets of less than 12

mm in diameter. Jackson et al. [26] and Mani et al. [30] used a funnel above the center of the container in order to have a more homogenous filling.

Summary

Particle density is an important factor in densified material formulation and quality while bulk density is of high importance in the packaging, transport, and marketing [42]. Mainly, the bulk density depends on the particle density and the voids ratios. Nonetheless, bulk density is not an inherent property of the material and should be considered as a dynamic property rather than a static one. Regardless of the material components and densification process, bulk density depends on the test procedure and examiner accuracy [82]. Pellets or briquettes rearrangement in the container during the test, PSD, container material and surface smoothness, and container filling method are the factors affecting the bulk density. Although using different methods rather than standards may increase accuracy, it creates difficulties in comparing the results of different methods. Consequently, the bulk material values in literature are not comparable unless a unique method is used.

2.2.5 Hydrophobicity

Most of the material being densified might adsorb moisture from the environment after densification. Biomass, due to its inherent hydrophilic nature [83] is a well-known example. Increasing the biomass moisture content might degrade the material and will decrease the energy content on an as-received basis [83], [84]. Several research works have been carried out to increase the biomass hydrophobicity by means of torrefaction, steam explosion, and by increasing densification temperature [18], [19], [75]. Some methods had partially increased the hydrophobicity, however, still, the material absorbs moisture when exposed to a high humid environment (60–80%) [71].

Generally, the hydrophobicity tests could be divided into two different methods; firstly to position the sample in a humid environment (moisture adsorption), and secondly to immerse the sample in water (water resistance). The former simulates the storage and transportation condition under humid weather conditions while the latter simulates rain exposure conditions. Much research has been done in order to investigate the hydrophobicity of different biomaterials under different conditions of which some are discussed in the following.

Moisture adsorption

The moisture adsorption test methods in literature could be divided into two major groups: inside (laboratory) and outside. Mostly, humidity chambers are used in laboratory tests to

determine the amount of moisture that a sample can adsorb under constant temperature and humidity conditions. Peng et al. [85], Jiang et al. [17], and Li et al. [28] used a humid chamber at 30ºC temperature and 90% relative humidity to determine the moisture adsorption of biomass and torrefied pellets. Pellets were pre-dried at 105ºC for 24 hours. During the experiments, the sample mass was measured at sequential time intervals until reaching a constant level. The increase in the pellet mass was reported as the amount of moisture adsorption. For the saturated moisture measurements, Peng et al. [85] placed the pellets in the chamber at the temperature of 20 to 35ºC and relative humidity from 40 to 95%. Hu et al. [18], used the above-mentioned procedure while setting the humidity at 70% for pyrolyzed woody biomass. Rhén et al. [52] also followed the same procedure for Norway spruce pellets, however, before starting the moisture adsorption experiments they let the pellets equilibrate in a 30% humidity environment at 23ºC.

Kambo and Dutta [19] used a relative humidity of 48–52% and a temperature of 22–23ºC for 24 hours to determine the equilibrium moisture content (EMC) of raw and pre-treated miscanthus pellets. After the test, samples were dried at 103ºC for 16 hours. The mass difference before and after drying was expressed as the EMC.

As an example of the outside experiments, Bergström et al. [27] placed batches of pine sawdust pellets (five randomly selected pellets in each batch) outside covered with a roof for 14 days. The environmental conditions were recorded and showed the temperature between -20 and 0ºC and humidity of 74 to 100%. Then the moisture adsorption was reported based on the mass difference before and after the test. The results showed around 10% moisture adsorption for all the samples.

Comparing the laboratory environment chambers and outdoor storage, the primary advantage of the chamber is that the temperature and humidity could be set at a constant level and could be adjusted according to the atmosphere of the location. However, the fluctuations in the real atmosphere are neglected while in outdoor storage the material meets the real weather conditions. Anyway, using the chamber is more common because the experimental conditions are more controllable.

Water Resistance

The ability of a material to resist water is normally measured by the water immersion test. Similar to the moisture adsorption tests, water resistance measurements in literature can be divided into two major groups: inside (laboratory) and outside conditions. Water immersion is

used when the material does not degrade in water; otherwise, the test is disrupted. Richards [42], set an inside water immersion test which immerses a single briquette in a cool water bath for up to 30 min. The physical consistency of the materials was checked at 10 minutes intervals by finger pressure. Intact materials were weighted and the proportion of adsorbed water was determined. Then he defined the water-resistance index (WRI) as an indication of moisture adsorption and proposed a minimum value of 95 would be an acceptable value for most briquettes:

$$\mathrm{WRI} = 100 - W_a, \tag{2.17}$$

where W_a is the absorbed water after 30 minutes immersion.

Bazargan et al. [33] followed the procedure above for palm kernel shell biochars. Sengar et al. [34] measured the water adsorption of biomass briquettes by immersing them in a water height of 25 mm at 27ºC for 30 seconds and measured the resistance to water penetration using the equation (2.17).

Kambo and Dutta [19] following the method described in Pimchuai et al. [86], immersed torrefied and hydrothermally carbonized pellets in water for 2 hours. Then the pellets were removed from the water and excess water removed by using an adsorbent paper. After that, the pellets were put in a controlled environment of 48–52% relative humidity and 22–23ºC temperature for 4 hours. The moisture adsorption was determined by a change in the pellet mass.

Summary

Biomass-based materials are hydrophilic in nature; however, different techniques may improve their hydrophobicity. In some cases, even a small amount of moisture may notably decrease the quality. So far, there is no standard method to accurately measure moisture adsorption in different well-defined conditions and there is a need for that. Developing a standard method could simultaneously eliminate the concerns about the suitability of the storage place and reduce extra costs due to the overestimation of the environmental conditions.

2.3 Factors affecting the physical properties of densified material

Abdollahi et al. [47], in their review study, have determined the possible factors to manufacture animal feed pellets with high material quality. These factors include diet formulation, binder addition, manipulation of PSD, manipulation of steam in the densification process, press setting, a decrease of production rate, and manipulating cooling and drying. Stelte et al. [46], in their

review paper, pointed out the process variables affecting the densification process and products, namely: the moisture content, temperature, particle size, press channel dimensions, and pelletizing pressure. However, this section points out the recent findings in the area of densification and systematically addresses the effect of different variables from an integrated perspective.

Regardless of the material type, generally, the affecting factors on the physical properties of densified products can be classified into four major groups namely the raw material, preparation conditions, densification process, and storage conditions. The effect of these factors are discussed in detail in the following sections.

2.3.1 Raw material

Raw material composition and blends

The raw material components play a key role in determining the physical properties of densified material. The presence of lignin, proteins, and starch help to increase inter-particle bonding, increasing hardness, and durability [10].

Several studies showed that blending biomass of different raw materials could improve durability and compressive strength of densified products [10], [80], [87], [88]. Mitchual et al. [54] reported that mixing 10% corn cobs with biomass sawdust of C. Pentandra at compressive pressures of 30 to 50 MPa significantly improved the compressive strength of briquettes compared to briquettes made of only a single biomass type (see Table 2.2). The compressive strength of pure corn cobs and pure C. Pentandra was 0.54 and 44.58 $N.mm^{-1}$, respectively, while the compressive strength of the mixture was 59.22 $N.mm^{-1}$.

Moisture content

Moisture content is a key process factor in the production of densified material. Bazargan et al. [33] reported that it is not possible to make strong pellets without the presence of moisture. Abdollahi et al. [31] have studied the effect of moisture on the quality of animal feed pellets made from wheat. They concluded that at the densification temperature of 60ºC the addition of 24 $g.kg^{-1}$ moisture (i.e. 2.4 wt.%) increases both hardness and pellet durability index (see Table 2.2 and Table 2.4).

Many studies have investigated the effect of moisture content on the durability of densified biomass [20], [24], [26], [33], [62], [71], [80]. They unanimously argue that by increasing the moisture, material strength first increases and then decreases. The optimum value depends on

the biomass species. For example, for peanut hull pellets it was reported that the presence of 9.1% moisture produced the most durable pellets with a durability value of 90.3% [71]. Jackson et al. [26] made pellets with four different biomass spices: miscanthus, switchgrass, corn stover, and wheat straw and reported that the least necessary moisture value for pellet making is 20% while the most durable pellets (durability of 90%) contain 25% moisture. In the study of palm kernel shell biochar, Bazargan et al. [33] obtained the optimum moisture of 30% for the highest tensile strength of 0.035 MPa for briquettes made at 60 MPa pressure. They also found that adding 20% water along with 10% starch increased the tensile strength of palm kernel biochar more than 100 fold. Umar et al. [24] studied the physical properties of extruded aquafeed and observed the maximum durability of 86.6% at a moisture level of 40%.

Tabil et al. [62] studied the effect of moisture content on the Meyer hardness of two different alfalfa cubes having 7.1, 10.8, and 14.3% moisture and reported that regardless of the cube type and probe size, the Meyer hardness decreased by increasing the moisture.

Zainuddin et al. [20] made pellets of pineapple to use as animal feed. They made the pellets using four moisture levels of 35, 40, 45, and 50% and observed a minor difference in both bulk density and friability of pellets. However, other researchers [30], [89]–[91], reported a negative influence on bulk density by increasing the moisture content.

In addition to the above-mentioned literature results, Huang et al. [92] concluded that although the presence of moisture is vital for the densification process, the optimum amount varies depending on the material type. Moreover, they believed that the effect of moisture content might depend on the other factors such as temperature and pressure, therefore, which should not be investigated alone. More research on the effect of simultaneous factors is necessary to fully understand their influence on the final product quality.

Particle size distribution

Bazargan et al. [33] densified bio-chars of different particle sizes using 0.7, 3, and 7 mm sieve sizes. They concluded that the finer particles lead to a more smooth surface and higher tensile strength compared to coarse particles (see Table 2.2). Muazu and Stegemann [32] used a PSD of less than 2 mm in their study and reported that the lower PSD leads to less relaxation. Lindley and Vossoughi [37] in their study used particles of less than 2 mm (from 0.004 to 2 mm) and concluded that smaller particle sizes make stronger briquettes. Mani et al. [30] used PSD of between 0.075 and 3.2 mm for wheat straw, barley straw, corn stover, and switchgrass and

reported a slight increase in density for all pellets by decreasing the particle sizes, except for the wheat straw.

Gilbert et al. [25] observed more compressive strength of pellets made by cut switchgrass (10 to 70 mm length) in comparison with shredded (< 4 mm length) and torrefied switchgrass. They believed that the reason lies in the interlocking of long strands of cut switchgrass which act as an additional binding alongside the lignin effect. Mitchual et al. [40] also observed more strength for the samples made by using bigger particle sizes. They declared that their results contradict the other researchers' results. They believed that as the smaller particles show more surface area, at higher temperatures starch gelatinization occurs, making the pellet stronger. However, because they performed the experiments at room temperature the effect of starch gelatinization disappeared.

In conclusion, the effect of particle size depends on the mechanical interlocking of particles. Larger particle sizes cause increased interlocking, creating a stronger bonding. At higher temperatures, the greater surface area provided by finer particles increases the bonding opportunities as well by activating different bonding phenomena such as starch gelatinization, lignin glass transition, and protein denaturation.

2.3.2 Pretreatment Conditions

Biomass pretreatment is carried out to improve the physical and/or chemical properties of the material. Pyrolysis, torrefaction, and hydrothermal carbonization are some examples of the common pretreatment techniques for the improvement of biofuels properties [25], [29], [70]. Due to the changes in the structure and energy content of pellets, the material behavior after densification will also change. For example, torrefaction is reported to change the properties of biomass from hydrophilic to hydrophobic [93]. Here, it should be noted that the pretreatment is not always taken into consideration as an affecting factor on densified material properties because in some cases the raw material is densified without any pretreatment.

Liu et al. [57] studied the effect of hydrothermal carbonization of woody and agro-residue biomass on the physical properties of pellets and found that the compressive strength of all the samples increases notably after hydrothermal carbonization (see Table 2.2). The moisture uptake of all the materials also decreased by carbonization, an indication of changing the hydrophilic structure to hydrophobic.

Kambo and Dutta [19] made pellets from raw, torrefied, and hydrothermally carbonized miscanthus (at three different temperatures of carbonization) and found that the compressive strength of the pellets decreased by increasing the carbonization temperature while pellets made from torrefied biomass show the least compressive strength compared to hydrothermally carbonized and raw biomass (see Table 2.2). Wu et al. [94] also observed the same results and reported that hydrothermally treated cotton stalk and wood sawdust showed higher compressive strength than torrefied cotton stalk and wood sawdust. Kambo and Dutta [19] suggested that the lower compressive strength of torrefied biomass is due to the observed pores inside the material structure. Moreover, as stated by Liu et al. [57] hydrothermal carbonization increases the hydrophobicity, resistance against water immersion, and increases the grindability of pellets. Peng et al. [85] and Li et al. [28] also reported similar results as Kambo and Dutta [19] where they found torrefied material more difficult to compress into dense and strong pellets compared to non-torrefied pellets.

Hu et al. [18] made various pellets by using pyrolyzed biomass at the temperatures of 250 ºC, 350 ºC, 450 ºC, 550 ºC, and 650ºC at 128 MPa densification pressure and 35% moisture content. Considering the bulk density, first, they observed a slight decrease and then a notable increase by increasing the pyrolysis temperature. The trend for the compressive strength was similar to the bulk density. For biomass pyrolyzed at 250ºC, the compressive strength was around 5 MPa and decreased to around 4 MPa for pyrolyzed biomass at 350ºC and then sharply increased to around 15 MPa for 650ºC pyrolysis biomass temperature. They also concluded that the effect of pyrolysis temperature on the pellet properties was dominant over the moisture content.

2.3.3 Densification process

The effecting parameters on densification can be distinguished into the densification process temperature, pressure, dwell (holding) time, press shape and length, and cooling and drying. Below, a detailed explanation of the effects of each of these parameters is given.

Press temperature

The press temperature is reported to have a high influence on product density and hardness [22], [85]. The relation between die temperature and pellet hardness and density lies in the raw material components. As an example, lignin is one of the main natural binders found in the biomass species. Increasing the material temperature helps lignin to reach the glass transition temperature (around 100–140ºC) thus improves the bonding mechanism and hardness [85]. The

die temperature is normally elevated on purpose, however, it usually abruptly increases during compression due to particle-wall frictions [28].

Li et al. [28] observed an around 4.7 fold increase in hardness of untreated sawdust by increasing the die temperature from 70 to 170ºC and the Meyer hardness increased from 1.44 to 6.81 $N.mm^{-2}$.

Some researchers believed that a compression temperature higher than room temperature is crucial for making pellets with high durability [25], [37]. Carone et al. [22] believed that in order to generate highly durable olive residue pellets with the highest density, a minimum temperature of 150ºC is required. Lam et al. [61] reported that for the Douglas fir species the optimum die temperature for the hardest material is 200ºC. Peng et al. [85] stated that to obtain the same hardness as raw biomass pellets, a die temperature of at least 230ºC is required for the torrefied pellets. Verhoeff et al. [95] also reported that torrefied pellets compressed at a die temperature of 225ºC results in durability of about two times greater than the raw biomass pellets densified at 100ºC.

Considering these reports, one may conclude that the compression temperature to make the most durable pellets should exceed 150ºC, however, the high temperature might affect the raw material structure to increase the brittleness and lead to the loss of a big portion of moisture content [25]. Moreover, one should pay serious attention to the fact that in most of the aforementioned studies a single or laboratory scale densifier rather than a pilot or an industrial scale piece of equipment was used. Segerström and Larsson [96] showed that although a single pelletizer could mimic a pilot-scale densification process, the effect of die temperature on pellet density is inconsistent for single and pilot scale. In a single pelletization setup, the temperature has a positive effect on the pellet density; however, in the pilot-scale process, the pellet density has a negative correlation with the die temperature.

Pressure and residence time

Several studies investigated the effect of compression pressure on density and hardness of pellets and briquettes [15], [18], [25], [30], [32], [33], [36]–[38], [40], [52], [54], [76], [85], [97]. Figure 2.12 shows the applied pressure intervals. According to these literature sources, density increases by increasing the compression pressure, however, in some cases it was insignificant. The effect on the hardness—compressive strength or tensile strength—was complicated. At compression pressures of one to around 50 MPa, hardness increases by increasing the pressure. For example, Chin and Siddiqui [36] reported that the shear strength

increased around 3.5 to 7.3 fold by increasing the press pressure from 1 to 10 MPa for biomass briquettes of different origins. Nonetheless, there exist some exceptions, for example, Al-Widyan et al. [38] reported an optimum pressure of 35 MPa in their studies for adequate durability of olive cake briquettes. For higher pressures of up to 130 MPa, there is usually a maximum at which the material hardness shows the highest value. For instance, the reported optimum pressure for gasified palm kernel shell was 60 MPa [33], and for wood biochar 128 MPa [18]. Peng et al. [58] and Demirbas and Sahin-Demirbas [76] examined higher pressures of 125 to 249 MPa and 300 to 800 MPa, respectively, and concluded that the effect of pressure on the material hardness is very low, i.e. the hardness is less sensitive to the pressure.

Li and Liu [15] investigated the effect of residence time (also known as holding, dwell, and retention time) from 0 to 60 s and observed a 5% increase in density when increasing the holding time from 0 to 10 s. The density increased as the time increased up to 20 s and after that, no significant increase in density was observed. However, they observed no effect of holding time at high pressure of 138 MPa. Chin and Siddiqui [36] also reported dwell time between 20 and 60 s as the optimum for different biomass spices of sawdust, rice husk, peanut shell, coconut fiber, and palm fiber. For olive cake briquettes, Al-Widyan et al. [38] reported that neither durability nor density increases by applying dwell time of between 5 and 20 s, therefore dwell time should not exceed 5 s. Bazargan et al. [33] concluded that at high-pressure densification the holding time has almost no effect on the material properties.

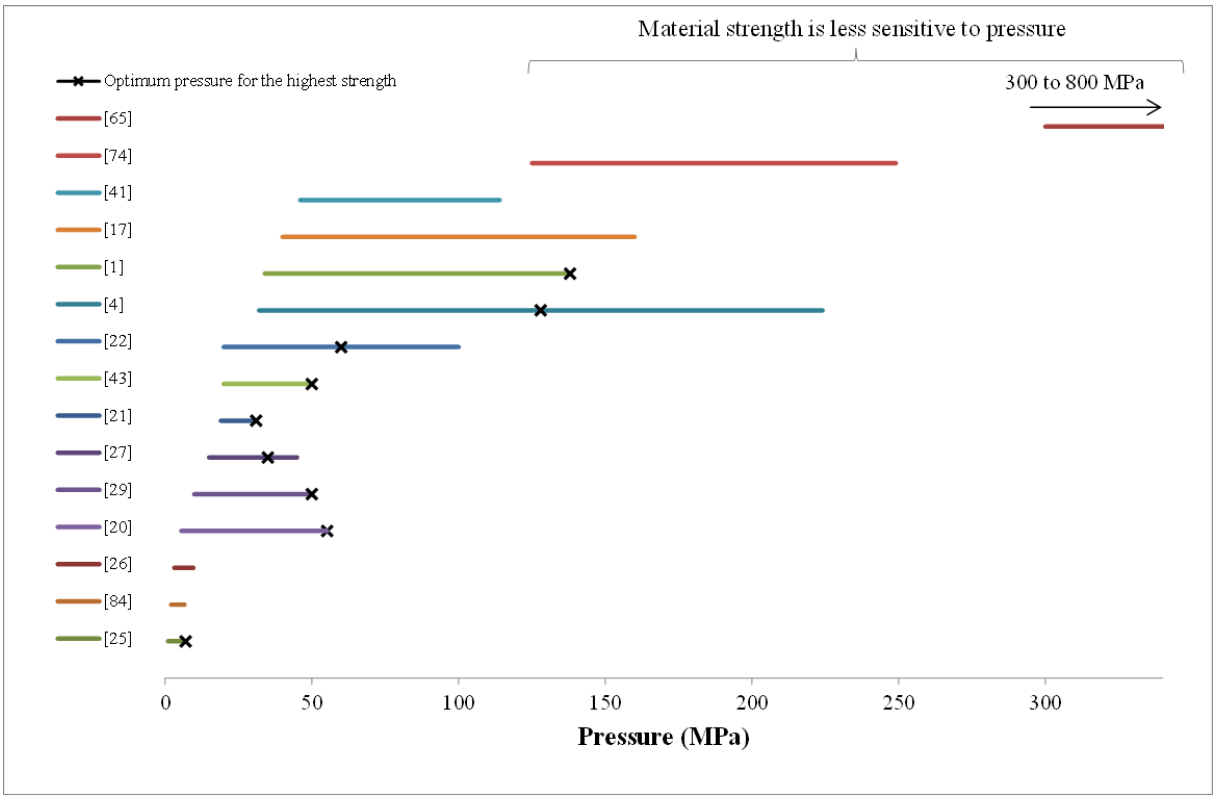

Figure 2.12: Densification pressure domain reported in the literature.

Binder

Generally, binders help stronger bonding between particles, thus increasing the hardness and durability of densified products [37], [70]. The presence of structurally incorporated binders, such as lignin and proteins improves the hardness and durability of the densified material, especially at high levels of pressure and temperature [17], [41], [98], however, high lignin content is reported to be responsible for the brittle structure of densified material [19]. In many cases, the structurally incorporated binders are not enough to make a highly durable material, thus the addition of an external binder is vital. The addition of 10% starch and 20% water as binder reported increasing the biochar pellet hardness more than 100 times [33].

The addition of a binder could be as easy and cheap as adding water [87] or it could be a kind of biomass, starch, protein, glycerin, etc. Mostly, the addition of binder increases the total cost of the process and in some cases, it may affect negatively the combustion behavior and density of densified fuels [19]. Muazu and Stegemann [32], in their study of preparing the rice husks and corn cobs briquettes used starch as a binder and found that starch inflicted the particle swelling which notably decreased the relaxed density.

Choosing the appropriate binder type and the dose is of vital importance for densified material preparation. Not surprisingly, Järvinen and Agar [59]observed lower quality when using wheat

flour as a binder to prepare pellets from torrefied pine. In general, they observed lower density, durability, hardness, and energy density, and more moisture uptake when adding wheat flour as a binder. For some animal feed pellets, Abdollahi et al. [31] also observed a slight decrease in compressive strength by the addition of a binder along with moisture compared to adding moisture alone (see Table 2.2).

Press shape and press channel length

According to Richards [42], the shape of a densified material affects the durability i.e. regardless of the other factors, materials with sharp edges show lower abrasion resistance than those with a round-shaped edge.

Thrän et al. [84] believed that pellets with a 6 mm diameter comprise the highest durability, while pellets with a diameter of 8 mm increase the production capacity. They also reported that for torrefied softwood and torrefied herbaceous biomass die aspect ratio (the ratio of diameter to length) is an affecting factor on durability. Heffner and Pfost [99] showed that durability increases as the aspect ratio increases.

In the other study, the effect of press channel length on pelletization of torrefied scot pine was investigated [100]. Three channels with the lengths of 25, 30, and 35 mm representing the aspect ratio of 3.125, 3.75, and 4.375, respectively, were used. They reported that a 35 mm channel length yielded high and fluctuated the mill motor current, thus they eliminated this channel length from the investigations. They also reported that it was not possible to pelletize the biomass torrefied at 291ºC with a channel length of 25 mm. The reason is not clearly stated in their work. However, for samples torrefied at a higher temperature of 308 and 315ºC the pellets were successfully made using the same channel length. Comparing the effect of channel length on the bulk density, they reported around 20 $kg.m^{-3}$ increase in bulk density with an increase of channel length for 1 mm.

Cooling and Drying

Normally, densified material leave the densification process at temperatures ranging from 60 to 95ºC and moisture content between 12 and 17.5 % on a wet basis while the desired temperature and moisture is normally 5 to 8ºC higher than the ambient temperature and 5 to 8%, respectively [47], [101]. If the material is not cooled and dried properly, it may lose its quality and result in heating, combustion, and caking in post transportation and storage. Cooling time is an important factor in determining the material quality. According to Maier and Bakker-Arkema [101], the cooling time may take 4–15 min, however, it should be noted that choosing

the optimum cooling time is of high importance in terms of material quality. Too quick cooling may result in cooling the outer layer while the inner layer remains warmer resulting in stresses in the material followed by the crack formation in the outer layer and a decrease of the mechanical strength. On the other hand, a too-long cooling period may result in a too dry material which increases the brittleness and reduced quality [47].

2.3.4 Storage Conditions

Storage is one of the most important parts of a supply chain [83]. The storage time and atmospheric conditions (temperature and humidity) are of crucial importance for any kind of densified bio-material.

Many authors investigated the effect of atmospheric conditions on the physical properties of densified material [17]–[19], [27], [28], [52], [58]. All researchers argued that storing in humid condition increased the moisture content of biomass-based material. Weatherstone et al. [75] stored torrefied spruce and poplar pellets outside in the stockpiles of 1 to 4 tonnes for more than 6 months and observed large moisture adsorption and degradation of the upper layer (around 10 cm). They concluded that outside-uncovered storage for a long period would deteriorate the torrefied biomass quality.

The volume of the material might expand during storage time. Jiang et al. **3** have made pellets of Chinese fir, camphor, and rice straw and observed 0.31 to 1.34% volume expansion (with or without adding binder) after two weeks of storage. The interesting point was that they reported around 1.25% fine particles separated from the pure biomass pellet surface during the storage time. The elastic recovery of the biomass particles and weak bonding were believed to cause these phenomena.

2.4 Discussion

As shown in this review, the reported quality characterization methods mostly do not follow a standard procedure. As a result, the quality values reported are hardly comparable to other literature sources making the assessment difficult or impossible. Furthermore, the use of dissimilar units makes it even harder to compare the results. For example, as presented in Table 2.2 the compressive strength values are reported in already different units of N, $N.mm^{-1}$, and MPa.

Researchers showed that even some of the existing standards are not capable of testing the quality parameters for a range of material characteristics. For example, Weatherstone et al. [75]

reported that the EN15210-1 [73] standard for the durability measurement of untreated wood pellets is not appropriate for materials with high moisture content and requires further modifications. In addition, durability testers measure fines generation when abrasive forces are encountered, however, the scale of the compressive forces applied does not match with the large-scale transportation conditions. Therefore, existing standards require development based on real conditions. The future investigations of the measurement methods of densified material quality parameters should focus on the development, preparation, and use of dedicated standards in order to unify the test procedures and make different results comparable.

Dust generation is a crucial factor in determining a densified material quality, especially from a health, safety, and the environment (HSE) perspective. Dust is detrimental from three points of view: material loss, equipment fouling issues, and environmental problems. Dust generation capability during large-scale transportation can be investigated by several laboratory-scale experiments; however, this is very difficult and requires dedicated facilities pushing the need for standards.

Regarding the existing literature, many researchers used the one-variable-at-a-time (OVAT) approach to investigate the factors affecting the quality parameters of densified bio-materials [18], [20], [25], [26], [36], [39]. In this method, the effect of each factor is individually investigated while the other factors are kept constant. Not only using OVAT increases the number of experiments and requires resources, but also it is often not reliable and may lead to incorrect results. According to Jiju [102], major problems in industrial process optimizations are mostly due to the interactions between the factors rather than the effect of individual factors. Changing only one variable at different levels might be advantageous to reach the optimum value of a specific parameter or when the other factors are less important in process optimization. However, as we showed here, there are many factors involved in bio-material densification, which play key roles in product quality. Future research in this field may focus on discovering the most affecting interactions and optimization of different parameters, simultaneously. Nevertheless, one should pay attention to the fact that the conclusions presented in section 2.3 are based on the assumption that all the quality parameters are assessed in the same way, i.e. using the same methods and devices. However, as shown in section 2.2, the quality assessment method has an extreme impact on the results of compressive strength, durability, and density.

2.5 Conclusions and Outlook

In order to measure the quality parameters of densified bio-materials, numerous devices and customized methods have been used by researchers. We showed that results reported in the literature are not comparable unless the same devices, processing conditions, and methods are applied. Although all the quality parameters shown here are of high significance in transportation, handling, and storage of densified bio-material, there exist only a few standard methods for durability and density. Therefore, there is an urgent need for developing new standard methods for compressive strength determination (including hardness and bending test), impact testing, and characterization of hydrophobicity.

Considering the existing quality standards, there is no clear relationship between the experimental results and issues of bio-solids handling under real conditions. The existing standards can classify different pellets based on their fines generations in a laboratory condition, however, they provide no information about the particle breakage or the number of fines created during the whole supply chain. A suitable standard method should mimic the real transportation and storage issues by considering the impact, compressive and abrasive forces on the materials simultaneously.

Besides experiments to assess the physical properties of densified bio-materials, computer modeling tools such as the discrete element method (DEM) can be applied to decrease the experimental cost and time. In DEM, individual particles can be modeled to represent the material behavior of a bulk solid. For example, Schott et al. [48] and Mahajan et al. [103] compared the durability of wood pellets in different conditions using DEM and found reliable results. The use of these numerical methods could accelerate the design and optimization of transportation and storage facilities. Anyway, using DEM in densified bio-material is in its initial stages of research and requires more studies.

3 Factors Affecting the Physical Degradation of Biomass Pellets*

In chapter 2, common methods to measure the quality parameters of biomass pellets were introduced. It was shown that mechanical strength is of high significance from the breakage and attrition point of view and that it is usually measured using mechanical durability testers. So far, the effect of pellet length distributions (PLD) and operational conditions of the durability testers on the mechanical durability results has not been investigated.

The goal of this chapter is to investigate the effect of the aforementioned factors on the durability of pellets using the most commonly used durability tester (tumbling can). This helps to understand the relationship between the durability results and the extent of fines generation during transport, handling, and storage. This relationship is covered in more detail in chapters 4 and 5.

*This chapter is based on Hamid Gilvari, Wiebren De Jong, and Dingena L. Schott. "The Effect of Biomass Pellet Length, Test Conditions and Torrefaction on Mechanical Durability Characteristics According to ISO Standard 17831-1." energies 13, no. 11 (2020): 3000.

3.1 Introduction

Biomass pellets show great potential as a renewable energy carrier for replacing fossil fuels in the near future. According to the Bioenergy Europe statistical report 2019 [104], the worldwide production of biomass pellets was around 32 million tonnes in 2017, of which the EU, a net consumer, used more than 24 million tonnes. Biomass pellets are mostly imported into the EU from the USA and Canada [104]. Despite the huge international pellet trade, the market faces many challenges in terms of transportation, handling, and storage, in particular, due to the high fines content and dust generation throughout the supply chain. For instance, there have been many fatal accidents caused by dust explosions [105].

The amount of fines and dust generated during transport and handling is linked to the pellet strength, which in turn depends on the material origin, pre-treatment processes, and the densification process [4]. According to ISO standard 16559 [106], mechanical durability is defined as "the ability of densified biofuels units (e.g. briquettes, pellets) to remain intact during loading, unloading, feeding, and transport". Note that mechanical durability is not the same as pellet strength: while pellet strength is an inherent property of the biomass pellet and is directly linked to the aforementioned parameters, mechanical durability depends on the test and operational handling conditions. The material origin, pre-treatment processes, and densification process specifications affect the pellet strength but once the pellets have been made, the effect of these remains constant. The amount of fines and dust generated during transport and handling is normally measured in the laboratory, for example using mechanical durability testers [68]. One such mechanical durability tester, defined by ISO 17831-1 [107], is the tumbling can method, which is commonly used for industrial and research purposes [108]–[116].

The higher the mechanical durability of the pellets, the lower the fines content and dust generation during transport and handling. National and regional standards have been introduced to classify biomass pellets based on their properties [117]–[121]. ISO standard 17225-2 [122] is an international standard for the classification of biomass pellets based on their mechanical durability values, namely DU97.5 and DU96.5, which represent mechanical durability of more than 97.5% and 96.5% respectively. However, there is yet no direct and clear link between the laboratory tests and real conditions regarding the amount of fines and dust generated during large-scale transportation, even for pellets of known mechanical durability.

Research has been carried out to correlate mechanical durability with other physical properties. Larsson and Samuelsson [44] compared the results of ISO standard 17831-1 with those of Ligno

single pellet durability and found a good correlation ($R^2 = 0.94$), although they found almost no correlation between the compressive strength of individual pellets and the mechanical durability. Temmerman et al. [68] found no correlation between mechanical durability and pellet density. Williams et al. [123] compared the mechanical durability of six different types of commercial biomass pellets with their required milling energies ($kWh.t^{-1}$) and the material grindability and found a good correlation between milling energy and mechanical durability ($R^2 > 0.92$). However, they only found a high correlation between mechanical durability and grindability for pellets with mechanical durability (based on ISO standard 17831-1 [107]) of higher than 97% ($R^2 > 0.994$).

The relationship between mechanical durability and the pellet length has been reported in two papers, to the best of the author's knowledge. Chico-Santamarta et al. [124] simultaneously studied the correlation of pellet length and storage duration on the mechanical durability of canola pellets with a length between 15 and 25 mm. They measured the length of 50 randomly chosen pellets from different batches. Because the effect of particle length was not isolated from the effect of storage duration, a correlation between the length and mechanical durability could not be established. Serrano et al. [125] measured the length of just 15 randomly chosen pellets from different batches of barley straw pellets. They found that the mechanical durability increases by increasing the average pellet length. However, the correlation has not been quantified.

As biomass pellets become increasingly popular, research into the pre-treatment processes is continuing to enhance the material properties. Torrefaction is one such process and involves roasting the material at a temperature of 200–300ºC in the absence of oxygen to reduce the moisture content and the volatile matter [126]. Torrefied biomass pellets have a higher bulk and energy density and increased hydrophobicity [127]. Due to the partial removal of the natural plasticizing agents such as lignin and hydroxyl groups during the torrefaction process, the resulting pelletized materials are however more fragile [100], [128]. Larsson et al. [129] showed that torrefaction temperature and moisture content may affect the mechanical strength of the pilot-scale produced Norway spruce. They torrefied the materials at a temperature of 270–300ºC and produced pellets by the addition of moisture at the two levels of 11 and 15%, while the die temperature was an uncontrolled variable. The resulting mechanical durability was between 80.4 and 90.3%. Rudolfsson et al. [100] concluded that the degree of torrefaction has a complex effect on pellet quality parameters such as mechanical durability for the pilot-scale

produced torrefied Scots pine. This effect is not yet fully understood and none of the above studies have addressed the relationship between mechanical durability and pellet length.

The primary goal of this chapter is to evaluate the influence of the pellet length distribution (PLD) on the mechanical durability results obtained from ISO standard 17831-1 [107]. We tested a range of materials, including white and torrefied pellets, to study the effect of torrefaction on mechanical durability. The findings contribute to a better understanding of the breakage behavior and, consequently, the mechanism of fines and dust generation during a mechanical durability test.

3.2 Materials and methods

3.2.1 Materials

Five different types of biomass pellets with varying origins and produced under different conditions were used in this study. These were torrefied mixed wood, torrefied poplar, raw and torrefied Miscanthus, and sawdust pellets. The Miscanthus was first pelletized and then torrefied at a temperature of 270ºC for 45 minutes, during which it lost around 20% of its initial mass. The poplar was torrefied at 285ºC for around 45 minutes with a mass loss of 25%. No information was disclosed about the densification processes. The lengths and diameters of the pellets were measured based on EN 16127 [130] and the moisture content was measured according to ISO 18134-2 [131]. The pellet density was calculated based on the pellet weight and volume, which were measured using a laboratory balance and a caliper, respectively, for five randomly chosen pellets. To increase the accuracy of the pellet density results, the two ends of the pellets were polished using sandpaper resulting in a cylindrical shape with a known volume. The properties of the materials are shown in Table 3.1.

Table 3.1: Properties of the materials used in this study (pellet diameter and pellet density are the means of five repetitions and the ± show the standard deviation).

Sample	Diameter (mm)	Length (mm)	$L.D^{-1*}$ ratio (-)	Moisture (%)	Pellet density ($kg.m^{-3}$)
Sawdust	12.49±0.15	10.00–46.30	0.80–3.71	7.7	1150±37
Raw miscanthus	6.10±0.03	5.00–40.00	0.82–6.56	4.5	1320±64
Torrefied miscanthus	6.00±0.08	4.00–41.70	0.64–6.95	2.9	1109±22
Torrefied poplar	8.09±0.07	5.50–65.90	0.68–8.15	7.9	1126±62
Torrefied mixed wood	6.02±0.04	4.10–47.40	0.68–7.87	9.7	1304±40

*Length to diameter ratio

3.2.2 Methods

Determination of the mechanical durability

The mechanical durability was measured using the tumbling can method, based on ISO 17831-1 [107]. According to this standard, around 500 g of the sample material should be selected using the CEN/TS standard 14778 and sieved using a round holes screen size of 3.15 mm. Then, 500±10 g of the material should be weighed and placed in the tumbling can. This is a steel box with a baffle attached diagonally to one wall of the cube. Once the material has been placed in the can, it is rotated at a speed of 50 rpm for 10 minutes in order to reach a total of 500 rotations. The sample should then be sieved using the same sieve mesh and weighed again. The mechanical durability (DU) is calculated using equation (3.1):

$$DU = \frac{m_a}{m_b} \times 100, \tag{3.1}$$

where m_{b} is the mass of sieved particles before the durability test and m_{a} is the mass of the particles remaining on the sieve after the test. Each test is duplicated using two representative test samples and the reported mechanical durability value is the mean of these results.

To study the correlation of PLD on mechanical durability, different test cases were considered to fully understand the breakage pattern and the mechanism of fines and dust generation. The test cases are defined as follows:

- Test case 1: Pellets with different length distributions
- Test case 2: Pellets under different durability test conditions
- Test case 3: Non-torrefied and torrefied pellets of the same origin

In the first test case, pellets of sawdust, torrefied mixed wood, torrefied poplar, and raw Miscanthus were classified on visual inspection according to their lengths into four different categories relating to their length distributions and then their actual lengths were characterized using the image processing tool described in section 2.2.2. Note that pellets of different size categories were directly chosen from the total batch as-received, and thus, there was no pre-processing for the pellets. The objective was to investigate the correlation of PLD on mechanical durability values. Category 1 consisted of pellets shorter than 15 mm, category 2 of pellets between 15 and 30 mm, category 3 of pellets longer than 30 mm, and category 4 consisted of a random sample of pellet lengths, as shown in Figure 3.1. This random-sized sample was taken as the reference case.

3.15 mm < Category 1 < 15 mm 15 mm < Category 2 < 30 mm Category 3 > 30 mm

Figure 3.1: Samples of different categories of torrefied mixed wood pellets.

The second test case was designed to identify the critical pellet breaking time during tumbling and the effect of tumbling time on the mechanical durability values. Here, category 3 of the torrefied mixed wood and category 2 of the raw Miscanthus and categories 1 to 3 of sawdust pellets were selected in the same way as explained in the first test case. For torrefied mixed wood, the mechanical durability test was executed every 2.5 minutes up to a total mechanical durability time of 10 minutes. For raw Miscanthus and sawdust, continuous full mechanical durability tests were performed three and four times respectively.

The third test case was executed to study the effect of torrefaction on the mechanical durability of biomass pellets with different length distributions. Due to the low availability of torrefied Miscanthus, categories 1 and 4 were examined here. In order to better understand the effect of torrefaction on the material's strength, individual compression tests were executed as well as the mechanical durability test. Pellets were subjected to uniaxial and diametrical compression tests by means of a compression device (Instron 5500R) at a constant compression rate of 1 $mm.min^{-1}$. For the uniaxial compression test, the ends of the pellets were sandpapered so that they could stand vertically on the lower plate with a uniform force distribution over the pellet ends. For diametrical compression, the pellets were placed lengthwise on the lower plate and compressed. Five pellets with different lengths were used for each test while the force and displacement were recorded. The stress-strain ($\sigma - \varepsilon$) values were calculated using equations (3.2) and (3.3) for the uniaxial compression and equations (3.4) and (3.5) for diametrical compression [123].

$$\sigma_a = \frac{F}{\pi r^2}, \tag{3.2}$$

$$\varepsilon_a = \frac{l_0 - l}{l_0}, \tag{3.3}$$

$$\sigma_d = \frac{F}{rl}, \tag{3.4}$$

$$\varepsilon_d = \frac{d_0 - d}{d_0}, \tag{3.5}$$

where F is the force (N), r is the pellet radius (mm), l_0 is the initial pellet length, l is the length displacement (mm), d_0 is the initial pellet diameter (mm) and d is the diameter displacement (mm).

Determination of the PLD

As the primary goal of this study was to investigate the influence of the length on the mechanical durability characteristics of biomass pellets, the first step is to characterize the length distributions. Previous work reported the pellet length as the average length of a limited number of pellets [124], [125], or a typical pellet length without mentioning the method and number of pellets to be tested [132], [133]. Measuring the pellet length distribution is possible to a certain extent using standard sieving methods such as ISO 17827-1 [134]. However, the method has some drawbacks. Firstly, pellets that are longer than the sieve mesh size may pass through the sieve lengthwise, which biases the results. Secondly, the results show a distribution of pellet length for each sieve mesh size, rather than the individual pellet lengths. There is therefore a need for a more accurate, quick and easy method to automatically capture the individual pellet length. Gil et al. [135] used image processing technology to capture the size of small heterogeneous milled biomass particles (particle size < 5 mm). However, there is a need for a tool to capture the length of bigger homogenous particles (biomass pellets) in a more accurate way based on the standard. For that purpose, we developed an image processing tool to capture the length of the individual pellets based on EN standard 16127 [130] using image processing codes—extrema method, shape measurement—in MATLAB (2017b) and, therefore, the length distribution of a batch of pellets. The procedure for determining the PLD is as follows. Pellets are first placed on a light panel (to remove shadows caused by the surrounding lights above the panel). The pellets are then manually repositioned to remove any overlap. An image is then taken from above the panel and used as input information for the MATLAB codes. The tool generates a horizontal line in the center of each pellet (dashed line in Figure 3.2). It then determines the end points (red circles in Figure 3.2) and draws vertical lines from every end point perpendicular to the horizontal line (solid lines in Figure 3.2). The maximum distance between these two solid lines determines the pellet length. The mass-based cumulative PLD is then calculated based on the pellet lengths and pellet density.

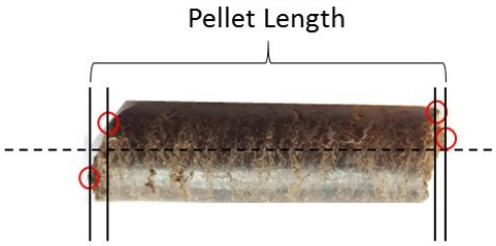

Figure 3.2: A 2D image of a typical biomass pellet under analysis using the extrema method in MATLAB.

Using this method, it is also possible to determine the number of pellets before and after each mechanical durability test. This helps to identify the breakage pattern during the mechanical durability test and can be used to understand the origin of fines and dust generation by providing information about the number of broken pellets and the amount of fines and dust.

Validation of the image processing tool

To validate the image processing tool, the lengths of 80 g of pellets (test portion size according to EN 16127 [130]) with a diameter of 6 mm were measured in two ways: manually using a digital caliper and automatically using the in-house tool. The tool was calibrated before use as the distance between the camera and the light panel has a big influence on the results. Therefore, a 20 euro cent coin (diameter= 22.25 mm) was used to calibrate the pixel sizes based on the coin size. The results of the two measurements are given in Figure 3.3. As this figure shows, the developed tool was able to measure the PLD of cylindrical pellets with a very high correlation with the experimental measurements, while also capturing the total number of pellets. The L_{20}, L_{50}, and L_{80} (L_x stands for the pellet length at which x% by weight of the pellets have a length of L or lower) from the manual measurements were 13.45, 19.99, and 24.14 respectively, and from the in-house tool 13.02, 19.48 and 25.4 respectively. The results show that the difference between the PLD measured using the tool and the manual measurements were minimal.

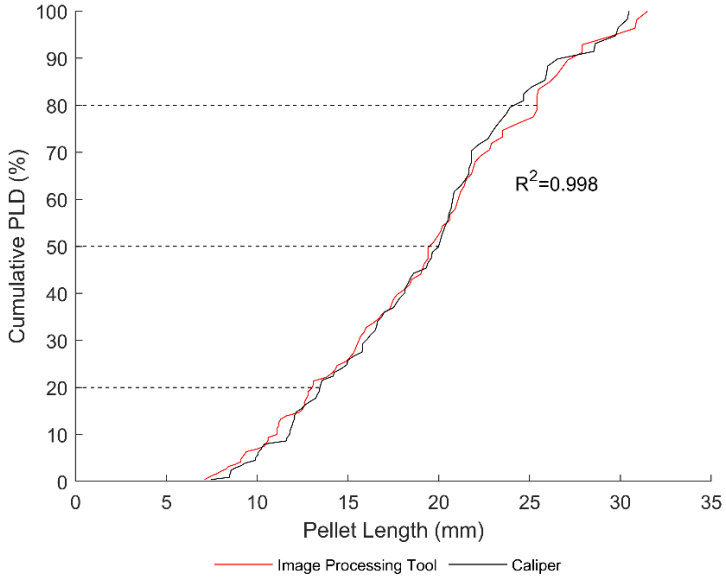

Figure 3.3: PLD measured by caliper and the in-house image processing tool.

3.3 Results

3.3.1 Test case 1: effect of pellet length

Figure 3.4 shows a sample photograph of the torrefied mixed wood pellets from category 3 before and after the mechanical durability test. The mechanical durability values of various types of biomass pellets for the four PLD categories are shown in Figure 3.5. This clearly shows that the mechanical durability results for three of the materials (torrefied mixed wood, raw Miscanthus, and torrefied poplar) highly correlate with the PLD. The mechanical durability values increase with an increase in the length of the pellets. Torrefied poplar shows the highest correlation on the PLD, with a difference of 12.8% in the mechanical durability values between categories 1 and 3, whereas for torrefied mixed wood, raw Miscanthus, and sawdust pellets the value is 5.8%, 3.9%, and 1.8%, respectively.

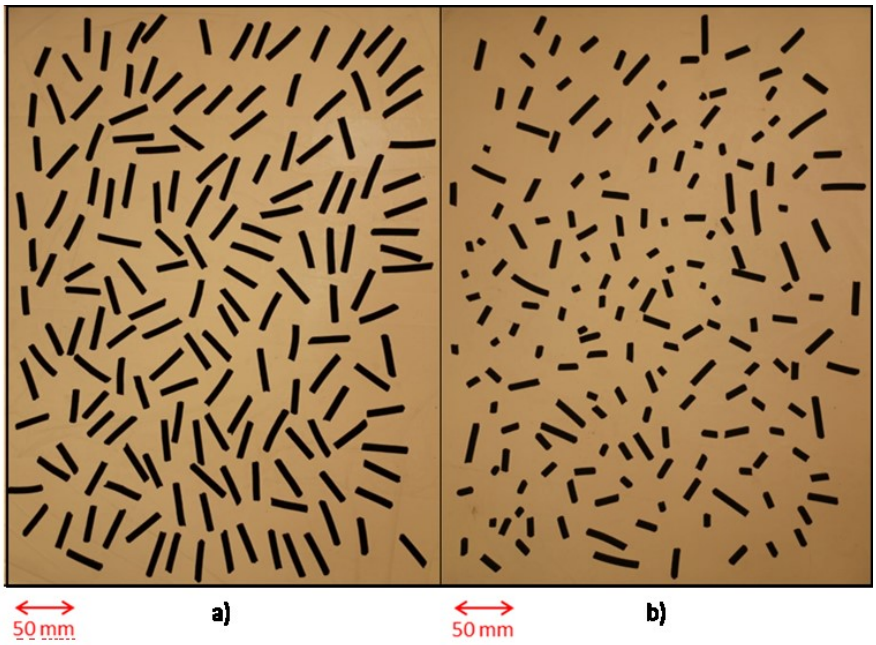

Figure 3.4: A sample image taken from the torrefied mixed wood pellets, (a) before and (b) after mechanical durability test.

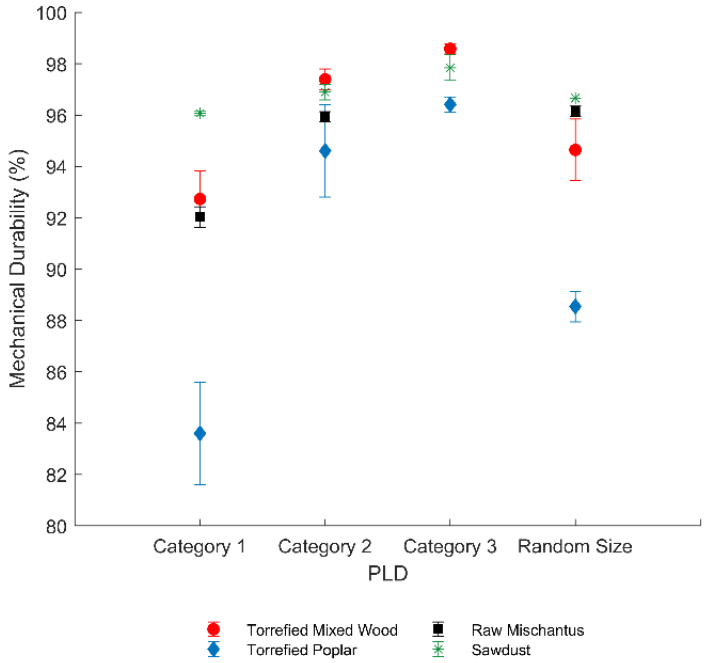

Figure 3.5: Mechanical durability results of different biomass pellets based on their pellet length distributions. Error bars show the standard deviation.

The PLDs before and after the mechanical durability tests are shown in Figure 3.6. Category 3 shows the most alteration in the PLD after the durability test, due to the fragmentation of long pellets for pellets with a diameter smaller than or equal to 8 mm. However, Figure 3.5 shows that category 3 shows the highest mechanical durability values amongst all categories.

Therefore, the shorter the pellets, the less breakage takes place, but the higher the probability of fines and dust generation.

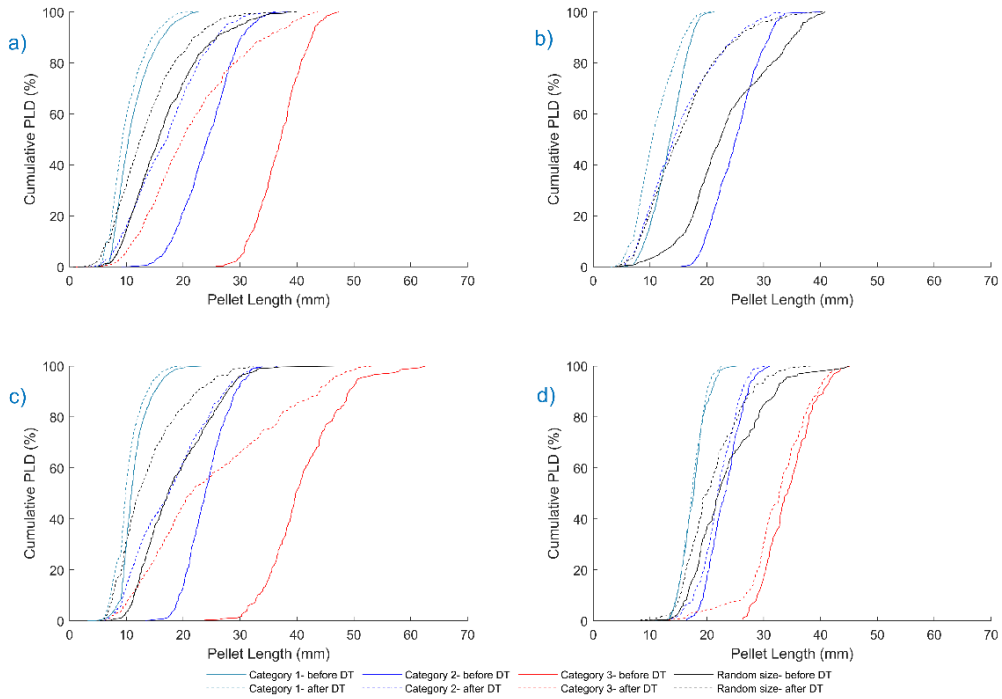

Figure 3.6: Pellet length distributions before and after mechanical durability tests for (a) torrefied mixed wood, (b) raw miscanthus, (c) torrefied poplar, and (d) sawdust pellets (DT: durability test).

The pellet diameters were also monitored by visual inspection during the experiments, and no changes were observed. A slight change in the PLD before and after the mechanical durability test for the shorter pellets (category 1) but with the same diameter values demonstrates that the fines and dust are created mostly from the edges of the pellets due to abrasive forces during the test.

Figure 3.5 shows a small difference between the mechanical durability of sawdust pellets in the different categories, but the trend is similar to the other types of pellets. A possible reason for this is the difference in the initial number of pellets, and consequently the number of pellet collisions and impacts inside the mechanical durability tester device. In the case of sawdust, there were 386 pellets in category 1 and 125 pellets in category 3 before the mechanical durability test, as shown in Table 3.2. However, there were 2241 torrefied mixed wood pellets in category 1 and 404 in category 3. Furthermore, due to the relatively large diameter of the sawdust pellets (12 mm), the length to diameter ratio was lower than for the other pellet types, resulting in a lower breakage potential during tumbling. As can be seen in Figure 3.6 a–c, pellets with a diameter of 8 mm and less are particularly susceptible to breakage if the length to

diameter ratio is high, while no pellet breakage is seen in the sawdust pellets, even for the longer pellets (Figure 3.6 d). Although pellet breakage does not necessarily result in more fines formation, pellet breakage does result in a higher number of pellets, which can intensify the generation of fines and dust.

Table 3.2: L_{50} and the number of pellets before and after the mechanical durability test.

Sample	PLD	L_{50} (mm)			Number of pellets	
		Before DT*	After DT	% of change	Before DT	After DT
Raw miscanthus	Category 1	13.5	10.2	24.4	1329	1661
	Category 2	25.1	14.1	43.8	612	1181
	Random size	22.4	14.9	33.5	721	1165
Torrefied poplar	Category 1	10.9	9.8	10.1	1553	1498
	Category 2	23.9	17.5	26.8	420	700
	Category 3	39.8	21.6	45.7	225	477
	Random size	17.2	12.1	29.6	730	955
Torrefied mixed wood	Category 1	10.4	9	13.5	2241	1785
	Category 2	24.3	17.1	29.6	658	1094
	Category 3	37.1	19.9	46.4	404	857
	Random size	15.7	12.5	20.4	1075	1498
Sawdust	Category 1	17.7	17.3	2.3	386	379
	Category 2	23.2	21.9	5.6	216	224
	Category 3	34.2	32.7	4.4	125	136
	Random size	22.1	19.6	11.3	245	244

*Mechanical durability test

Comparing the mechanical durability results of the different categories, the lowest difference is between categories 2 and 3. That means that pellets longer than 15 mm are more durable during transport and handling; in other words, they generate fewer fines and dust. To better understand the correlation of PLD on mechanical durability, additional experiments were carried out on torrefied mixed wood with a mixture of PLDs. A mixture of categories 1 and 2 and a mixture of categories 2 and 3 were selected, and the results are shown in Figure 3.7.

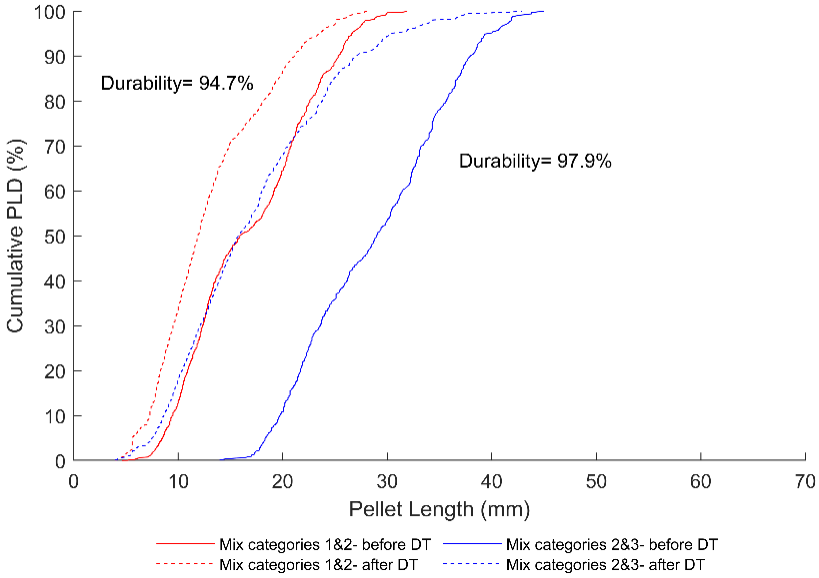

Figure 3.7: Pellet length distributions and mechanical durability values of torrefied mixed wood pellets: a combination of categories.

The mechanical durability values of the mixtures are close to the average mechanical durability of the two corresponding categories. More interestingly, a good correlation was found between the mechanical durability results and L_{50} (mean of the pellet length) with a high data fit (R^2 = 0.926), as shown in Figure 3.8. This shows that L_{50} is a good indicator of the mechanical durability of biomass pellets.

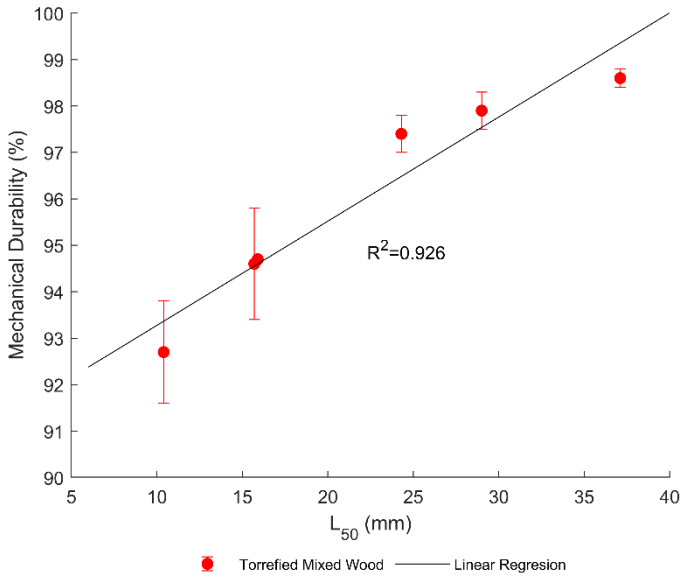

Figure 3.8: Mechanical durability values of torrefied mixed wood pellets versus the L_{50} of various length distributions. Error bars show the standard deviation.

Figure 3.9 shows the mechanical durability values versus the PLD intervals and L_{50} for each category. It shows that the mechanical durability values correlate with L_{50} for every type of biomass material.

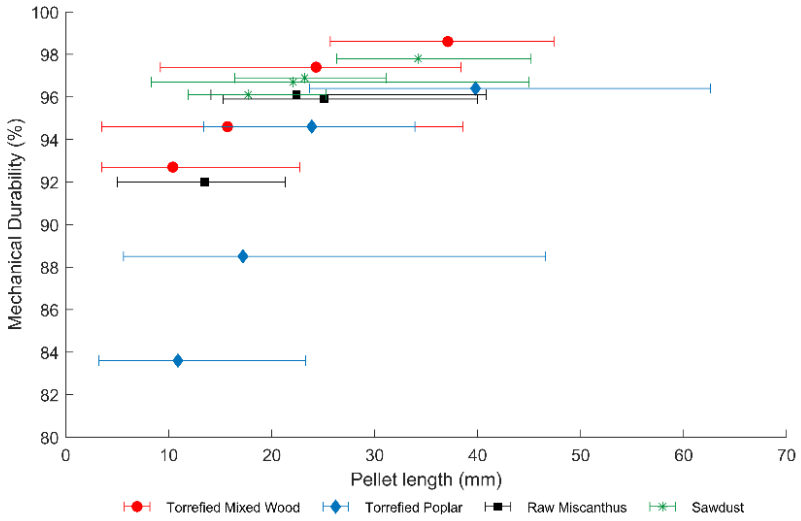

Figure 3.9: Mechanical durability value versus pellet length distribution intervals before mechanical durability test (solid markers show the L_{50}).

3.3.2 Test case 2: effect of test conditions

In this test case, the total mechanical durability test time for torrefied mixed wood pellets was divided into four equal time intervals: 2.5 minutes, 5 minutes, 7.5 minutes, and 10 minutes. For the other materials, the mechanical durability test was performed more than once. As can be seen in Figure 3.10 a, the mechanical durability value was almost the same for torrefied mixed wood in the different time intervals, with a slightly lower value in the 2.5 minutes interval, while most breakage also took place in this interval. The slightly lower mechanical durability value was probably due to the release of dust particles due to fragmentation into smaller particles.

For the raw Miscanthus and sawdust pellets, the mechanical durability value was lowest in the first test and became constant or even increased in the next tests, as shown in Figure 3.10 b and Figure 3.11. As the number of pellets was almost the same in the next tumbling steps, we conclude that the mechanical durability values stabilize over time, probably because the areas in the pellets with a high potential to generate fines and dust materials (weak points) release most of this early on during the mechanical durability test. We can also conclude that a sample that has already been used for mechanical durability testing should never be used again for the

same purpose, since the sample has already lost the areas with high potential for fines generation.

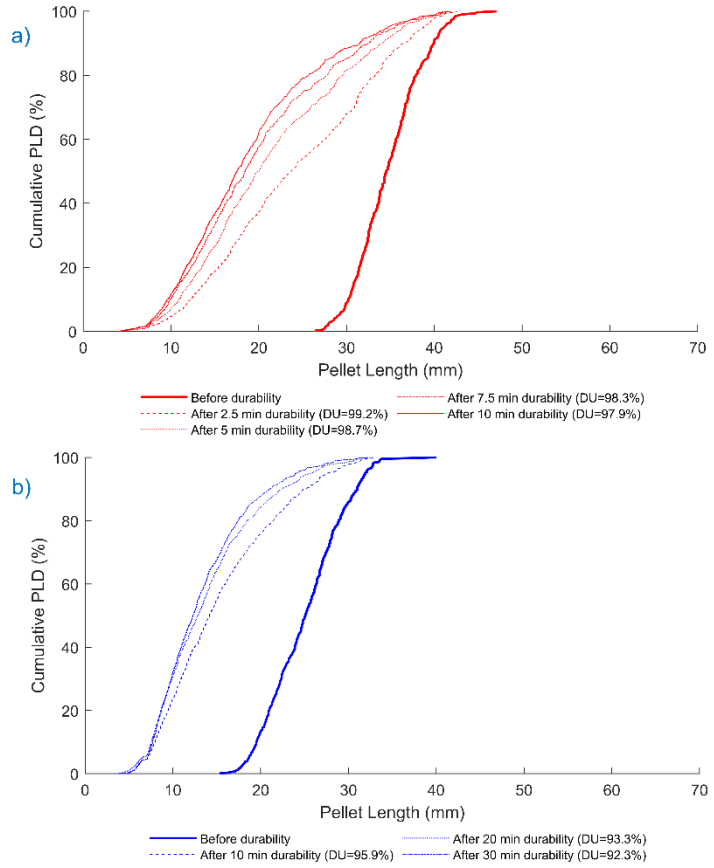

Figure 3.10: Pellet length distributions of (a) torrefied mixed wood and (b) raw miscanthus before and after different mechanical durability tests (DU: mechanical durability).

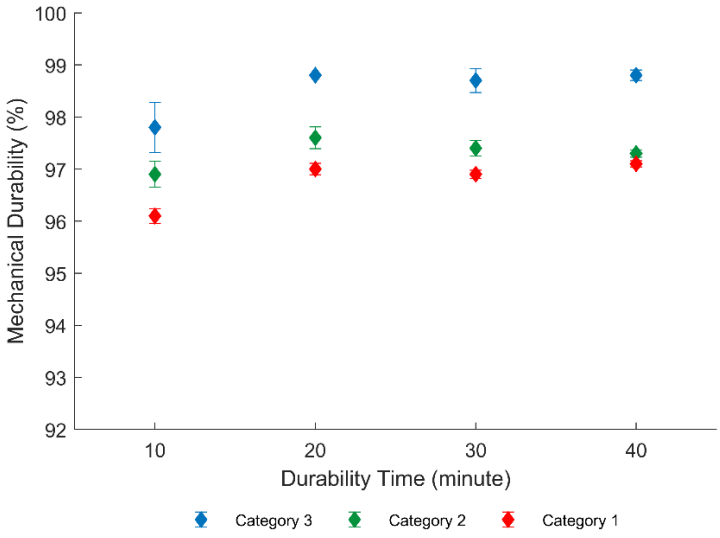

Figure 3.11: Mechanical durability values of sawdust pellets after several mechanical durability tests. Error bars show the standard deviation.

Assuming the mechanical durability test simulates the real forces acting on the pellets during large-scale transportation, fines, and dust production is highest in the first steps and additional handling steps generate fewer fines and dust. This requires additional research.

3.3.3 Test case 3: effect of torrefaction

In this test case, we studied the effect of torrefaction on the mechanical durability values of biomass pellets. Due to the limited amount of available torrefied materials, only two categories were considered for this test case. Figure 3.12 show that torrefaction in this study has a negligible effect on the mechanical durability of pelletized materials. The obtained mechanical durability values depend more on the L_{50} than the torrefaction process.

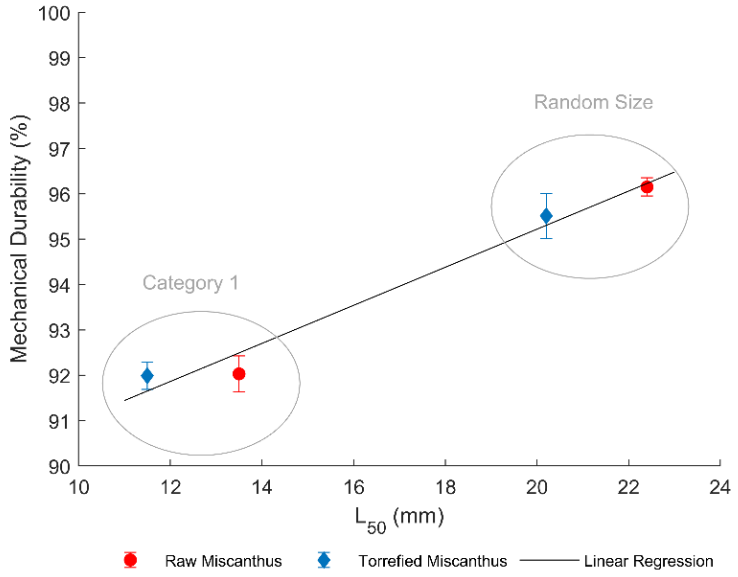

Figure 3.12: Mechanical durability values of raw and torrefied miscanthus pellets. Error bars show the standard deviation.

We would like to point out that, despite the same mechanical durability values between the torrefied and non-torrefied Miscanthus pellets, the individual pellet strength in a compression test might be different because abrasive forces play a key role in pellet degradation in a mechanical durability test and the amount of generated dust is linked to the surface properties rather than internal pellet strength. To support this statement, we tested individual pellet strengths using compression tests. The maximum stress at failure and the corresponding strain values are presented in Table 3.3. Based on the results, it is clear that the compression strengths of the raw pellets are higher than those of torrefied pellets.

Table 3.3: Maximum stress and strain at failure for uniaxial and diametrical compression tests of raw and torrefied Miscanthus.

Sample No.	Uniaxial compression				Diametrical compression			
	Raw miscanthus		Torrefied miscanthus		Raw miscanthus		Torrefied miscanthus	
	σ_a (MPa)	ε_a (-)	σ_a (MPa)	ε_a (-)	σ_d (MPa)	ε_d (-)	σ_d (MPa)	ε_d (-)
μ	17.64	0.05	13.43	0.08	16.04	0.07	9.95	0.10
Standard deviation	0.66	0.01	1.44	0.02	2.64	0.01	2.84	0.02

3.4 Discussions

According to the literature, the mechanical strength of biomass pellets depends on pellet type characterizations such as the biomass origin (composition), the pre-treatment process and densification process specifications. However, once the pellets have been made, the pellet strength remains constant unless a significant change in environmental conditions such as temperature and relative humidity occurs. On the other hand, fines generation (particles < 3.15 mm) as expressed by mechanical durability might change due to the effect of PLD, an effect that has not yet been addressed in the literature. This study shows that the mechanical durability values of biomass pellets correlates with the PLD. This correlation is maybe due to the number of pellets per unit mass, which determines the number of pellet-pellet and pellet-container collisions.

Thomas [136] showed in his study that pellet breakage occurs in two ways: through attrition and fragmentation, as shown in Figure 3.13. Therefore, in this study, fragmentation is the main breakage mechanism for longer pellets, while abrasion is more common for shorter pellets.

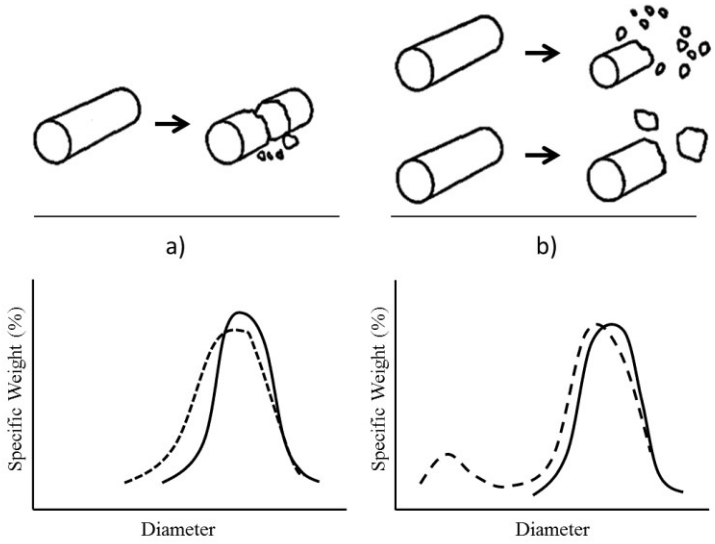

Figure 3.13: Two different breakage mechanisms of pellets. (a) fragmentation, (b) abrasion and their particle size distribution curves adapted from [136].

As well as the number of collisions affecting the mechanical durability results, the device geometry specifications may also play a role in mechanical durability results. In a tumbling can device, the shortest and longest possible travel distances for a pellet are 97 mm and 442.3 mm respectively. This means that, for a short pellet with a length of 10 mm, the lowest and highest pellet to geometry ratio is around 1:10 and 1:44, while for a longer pellet of 40 mm they are 1:2.5 and 1:11. Thus, it could be expected that the longer pellets experience fewer impacts as they pass shorter distance from one side to the other side of the device. Moreover, due to the baffle in the middle of the device, the pellet flow inside the equipment is relatively chaotic; therefore, not all the pellets pass the same route during the test. Note that the longer the pellets, the higher the mass and therefore the greater the impact, when traveling the same distance in comparison to the shorter pellets. Summarizing, calculation of the travel distances and impact forces are complex, but the device dimensions are expected to alter the mechanical durability results.

According to ISO standard 17831-1 [107], the maximum acceptable repeatability difference between the results of duplicate measurements is 2% for pellets with mechanical durability values below 97.5% and 0.4% for pellets with mechanical durability values above 97.5%. However, the results of this study show that pellets of the same type with different PLDs have substantially higher differences in mechanical durability. The effect of PLD has not yet been studied in the literature, but it seems that using the same PLD for duplicate measurements may limit the differences. Moreover, this could also be the main reason for disagreement between

the mechanical durability results tested at differing locations or by different users, such as buyers and sellers.

ISO standard 17831-1 was formulated to characterize the ability of biomass pellets to withstand mechanical forces during transport and handling. However, this standard suffers from a lack of information on the factors affecting mechanical durability values. While, according to the standard, the test samples should be selected randomly, the PLD may differ from sample to sample. There is no guideline or notice in the standard about the PLD and its possible effect on the mechanical durability results. In our previous work [137], we showed that there is an urgent need for more standards or at least modification of the existing standards for the characterization of the properties of biomass pellets. We suggest modifying ISO 17831-1 in the coming version in such a way that the PLD is reported along with the mechanical durability values.

Williams et al. [123] claimed that pellets with low mechanical durability values are not only unsuitable for transportation but also milling. In this study, we show that choosing longer pellets tends to increase the mechanical durability value. Comparing their findings [123] with the results of this study, we can also conclude that pellets less than 15 mm in length are not suitable for milling processes.

Larsson et al. [129] and Rudolfsson et al. [100] pelletized torrefied materials and Manouchehrinejad and Mani [138] and Shang et al. [139] torrefied raw pellets. Irrespective of the order of the torrefaction and palletization process, they concluded that torrefaction negatively affects the mechanical durability characteristics of different commercially produced biomass pellets. In none of the studies, the pellet length distribution data are disclosed, or used in their analysis. In this study, it was also observed that considering similar PLD for raw and torrefied pellets, torrefaction after pelletization does not influence the mechanical durability of miscanthus pellets. Likely, the difference between the mechanical durability of commercially produced torrefied and non-torrefied pellets (densified under the same conditions) is due to three factors: torrefaction severity, torrefaction process sequence, and PLD. Future studies may focus on this interdependence, i.e. the effect of torrefaction on mechanical durability before and after densification taking the PLD into consideration.

Although the correlation between the PLD and durability should be tested for other types of mechanical durability measurement methods, the same results are expected since decreasing the pellet length per unit mass increases the number of collisions. This results in a higher pellet degradation rate as demonstrated in this chapter.

3.5 Conclusions

This chapter is, to the best of our knowledge, the first to study the correlation of pellet length on the mechanical durability characteristics of biomass pellets according to ISO standard 17831-1 [107]. Using an image-processing tool, we developed a methodology to measure the individual pellet lengths of groups of particles quickly and accurately, and were able to compare the PLD before and after the tumbling can test. The conclusions of this study are as follows:

Regardless of the origin, pelletization process characteristics, and pre-treatment processes, the tendency of biomass pellets to generate fines and dust (particles passing through 3.15 mm sieve holes) strongly correlates to the pellet length.

The length to diameter ratio can affect the mechanical durability results of different PLDs. A higher length to diameter ratio decreases the difference in mechanical durability values between all PLD categories.

The observed breakage mechanism of biomass pellets is either fragmentation (breakage into smaller pellets) or abrasion. In this study, we show that most fines and dust in the tumbling can method are generated due to abrasion and not fragmentation.

In this study, the effect of torrefaction was studied using a single torrefied pellet type (torrefied Miscanthus), and the mechanical durability characteristic as compared to a white pellet (raw Miscanthus). For the torrefied Miscanthus, the torrefaction process was performed after pellet production. For this specific pellet, the torrefaction process was not an influencing factor in the mechanical durability characteristics of Miscanthus pellets. For a better understanding of this result, the role of the torrefaction process conditions such as time and temperature, the process sequence, and PLD should be further investigated by testing a wide range of raw and torrefied pellets.

Moreover to the above-mentioned conclusions, it is suspected that the number of collisions of pellets play a key role in durability value. The lower the pellet length per unit mass, the higher the number of pellets and, therefore, the more collisions in the tumbling can that result in a higher fines content and thus lower mechanical durability.

Based on the findings of this study, we highly recommend differentiating in future versions of ISO 17831-1 between the PLD categories (or the L_{50}) when reporting the mechanical durability results.

4 Relationship Between the Laboratory and the Pilot-Scale Transportation of Pellets with Regards to Fines Generation*

In chapter 3, a laboratory durability tester was studied in detail to show the influence of pellet length distribution, test conditions, and torrefaction on the durability value. However, the relationship between laboratory test results and the extent of fines and dust generation throughout a transport system remains unclear.

As stated in chapter 1, the breakage behavior of pellets can be investigated from the laboratory to large-scale systems. Therefore, after introducing the effect of different factors on the results of the laboratory tests in chapter 3, in this chapter, a pilot-scale belt conveyor is applied to show the effect of different operational conditions on the breakage behavior of biomass pellets. Moreover, the mechanical durability is measured using three different laboratory tests and the results are compared with the results of the pilot-scale transportation.

*This chapter is based on Hamid Gilvari, Coen van Battum, Richard Farnish, Yusong Pang, Wiebren de Jong, and Dingena L. Schott. "Fragmentation of fuel pellets during transport via a belt conveyor: a design of experiment study." Submitted.

4.1 Introduction

With increasing the worldwide energy demand on the one hand and increasing global warming and greenhouse emissions, on the other hand, the use of alternative energy sources to fossil fuels is becoming of vital importance. In recent years, biomass-based energy sources attracted more attention due to their low greenhouse gas (GHG) emissions and high availability [140]. In 2019, more than 9% of global energy production was supplied with biomass energy sources [2].

Raw biomass has high water content and a low bulk density. To use biomass more efficiently, it is normally subjected to drying and densification processes in which the material's quality improves in terms of energy content and bulk density. Higher bulk and energy density and lower moisture content can ensure easier and economical transport and storage. However, pellets are naturally fragile and may produce fine particulates due to breakage and attrition, which potentially challenge transport and storage. The increased number of fines—particles smaller than 3.15 mm according to ISO standard 17831-1 [107]—may increase the risk of fire, material loss, equipment fouling, and environmental issues [137], [141], [142].

The potential of pellets to produce fines depends on many factors from the feedstock to the production process and the storage conditions [4], [10]. This potential is mainly measured using laboratory-scale experiments such as durability and impact testers [137]. Nevertheless, the extent of fines generation during industrial transport and storage depends on the design specifications of the transport and storage equipment and their operational conditions

Several papers studied the effect of the operational conditions of the transport equipment and design on the extent of breakage and attrition of fuel pellets. Oveisi et al. [77] investigated the breakage of wood pellets via free fall in different scenarios and find found that for wood pellets with a durability of 97% (according to the tumbling can method), greater drop heights linearly increases the proportion of generated fines. Boac et al. [143] investigated the effect of chain conveyor and silo loading on the breakage of pellets with 13.2% moisture content and 92.9% durability (according to tumbling can) and observed an up to 32.7% increase in the number of particles< 5.6 mm. Jägers et al. [144] and Murtala et al. [145] studied the effect of pneumatic conveying on wood pellet degradation and observed that an increase in the air inlet velocity and a decrease in pellet mass flow, increases the extent of fines generation.

Belt conveyors, amongst others, are more common to be used in pellet industries due to high flow capabilities in long distances [146]. However, it is not yet clear to what extent pellets may

degrade during transfer via a belt conveyor while operating at various conditions such as different belt speeds, belt loading, belt inclinations, and the number of handling steps. Moreover, the relationship between the results of the laboratory benchmark tests such as durability testers and the generated proportion of fines during transport via a belt conveyor has not yet been studied. Therefore, the objective of this chapter is to investigate the effect of different operational conditions of a belt conveyor on the number of fines generated during transport. A design of experiment (DoE) approach based on response surface methodology (RSM) is applied to study the effect of different factors. The main contribution of this research is to correlate the strength of pellets, measured via different benchmark laboratory tests, to the proportion of fines generated via a belt conveyor in order to fill the gap between benchmark tests and belt transportation.

4.2 Materials

Fuel pellets used in this study were commercial wood pellets produced in Canada and transported to Europe via an ocean vessel for energy production purposes. The vessel contained around 30,000 metric tons pellets of which around 400 kg were randomly chosen and transported to the laboratories to perform experiments in this study. The samples contained two different types of wood pellets, hereafter referred to as white and brown pellets because of their colors, with a share of 30 to 70% for white and brown pellets, respectively. Pellets were well mixed in the whole batch (Figure 4.1). Table 4.1 shows the physical properties of the pellets. The moisture content was measured according to ISO standard 18134 [131] by placing 300 g of materials inside an oven at the temperature of 105ºC for 24 hours. The bulk density was measured using a 5 L steel cylinder according to EN standard 15210 [81]. For that purpose, the cylinder was filled with pellets using the tap method and then the mass of pellets inside the cylinder was weighted. The bulk density was measured by dividing the mass of pellets over the volume of the cylinder. The moisture content and the bulk density were measured twice based on their standards and the reported values are the mean of repetitions. The pellet lengths and diameters were measured using a digital caliper according to EN standard 16137 [130].

Figure 4.1: Wood pellets used in the experiments: a bucket of mixed pellets (left), the two different types of wood pellets in a close-up (right).

In a previous study [147], we concluded that the length of pellets can play a major role in generating fines—with shorter pellets produced more fines in a benchmark test. Therefore, for the laboratory tests in this study, the effect of pellet length distributions (PLD) was considered. For that, pellets with different length distributions were manually selected in three different intervals of between 3.15 and 15 mm, between 10 and 15 mm, and longer than 15 mm, then their lengths were measured using an in-house image processing tool using MATLAB scripts. Details of the image processing tool can be found in our previous study [147].

Table 4.1: Properties of the pellets used in this study.

Pellet properties	White	Brown
Diameter (mm)	6.6±0.1	6.7±0.1
Length distribution (mm)	5–40	
Bulk density (kg.m^{-3})	700±7.9	
Moisture content (%)	6.2±0.3	

4.3 Methods to measure fines generation

In this section, first, the benchmark test methods to measure the pellet strength, including the tumbling can and compression test, are introduced. Then, the belt conveyor setup, which was used to measure the fines generation during the transportation is presented. Finally, the applied DoE method is given.

4.3.1 Mechanical durability

The mechanical durability tester used in this study was a tumbling can operating at 50 rpm for 10 minutes based on ISO standard 17831-1 [107]. Different tests have been performed on mixed

pellets, separated pellets, and size-classified separated pellets. To execute the tests, for mixed pellets, more than 1 kg were manually sieved with a round hole screen with a mesh size of 3.15 mm, and subsequently, 500 g of that was placed into the device and tumbled. For size-classified pellets, pellets were manually classified into different groups and using the image processing tool described in [148], the PLDs were captured and then introduced to the tumbling can. For separated pellets i.e. brown and white, pellets were manually selected with mixed sizes and then placed into the tumbling can. After the tests, all samples were sieved with the same sieve (3.15 mm screen) and the mass of the remaining particles was weighed using a laboratory balance. The mechanical durability was calculated according to equation (4.1):

$$DU = \frac{m_r}{m_i} \times 100, \tag{4.1}$$

where DU is the mechanical durability, m_r is the mass of pellets after tumbling, and m_i is the mass of initial samples. All tests have been performed in two repetitions, except size-classified pellets which have been carried out once.

4.3.2 Rotary impact tester (attrition tester)

The impact tester or the attrition tester is an in-house developed device at the Wolfson center of the University of Greenwich, the UK, to study the breakage behavior of different materials at high impact velocities. This is a closed cylindrical device with a diameter of 900 mm and a height of 350 mm with a small hole at the center of the top surface. A hole is designed at the bottom surface to collect the materials after the test. Inside the device, there are two discs: one over the other with a diameter of 480 mm with 35 mm vertical separation. The upper disc has a hole with a diameter of 60 mm at the center and the lower disc is plain to enable keeping the materials on it. Around the inner discs, there are 24 plates attached to the cylinder. Upon rotation of the discs, pellets are fired from the discs and collide with these plates (Figure 4.2). In our experiments, the discs were rotating at an angular velocity of 28 Hz, giving a theoretical speed up to 25 $m.s^{-1}$ to the pellets upon impact. Pellets were gradually fed into the disk to discharge 500 g of pellets in less than two minutes. The resulting impact velocity was considered to mimic the highest impact velocity of pellets during transport and storage. A detailed working principle can be found elsewhere [78], [149]. Due to the high velocity of pellets at impact, pellets break down and produce fines. After each test, all the pellets and fragments including fines were collected for further analysis. This test has been done once for each size-category of pellets.

Figure 4.2: Rotary impact tester.

4.3.3 Compression test

Five individual pellets of each type were subjected to compression tests for the determination of their mechanical strength. This is a common test to predict the internal strength of pellets [44], [123], [150]. Due to the jagged ends, the pellet ends were manually polished using sandpaper to place the pellets vertically on the compression plate. At each run, one pellet was placed on the lower plate of the compression device. The compression tests were conducted using a Zwick compression bench equipped with a 2 kN load cell. Each test ran at a velocity of 1 mm.min^{-1} until the pellet was broken. After each test, the force-displacement data were extracted from the device, using equations (4.2) and (4.3), the stress-strain data were calculated.

$$\sigma_a = \frac{F}{\pi r^2}, \tag{4.2}$$

$$\epsilon_a = \frac{l_0 - l}{l_0}, \tag{4.3}$$

where σ_a is the stress, ϵ_a is the strain, F is the force, r is the pellet radius, l_0 is the initial pellet length, and l is the corresponding pellet length.

4.3.4 Belt conveyor setup and experiments

For this research, a pilot-scale belt conveyor setup was developed to investigate the generated number of fines when pellets are being transported. The setup, as shown in Figure 4.3, consists of a wedge-shaped hopper, a troughed (20°) belt conveyor, and a collecting bin. The size of the hopper outlet and the inclination of the belt is adjustable. The belt width is 0.4 m and its length

is 3.1 m of which 2.6 m was used for conveying the pellets in this study. To prevent material spillage, a chute is attached to the frame of the belt conveyor.

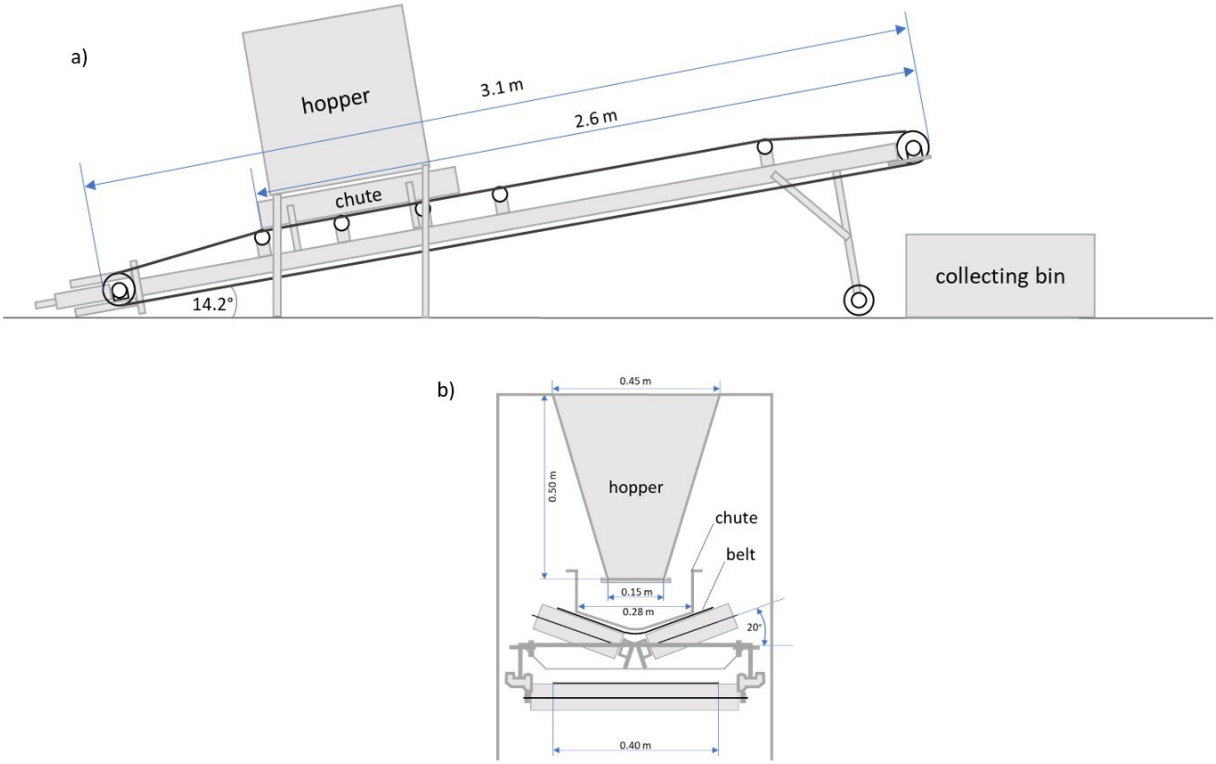

Figure 4.3: The inclined belt conveyor setup including the wedge-shaped hopper to load and a collecting bin to collect the materials, a) side view, and b) cross-sectional view.

The experimental procedure was as follows. To remove fines before starting the experiments, all pellets were manually sieved with a round-hole sieve with a screen size of 3.15 mm, according to the ISO standard 17831-1 [107]. For each experiment, 10 kg of the sieved samples were gently fed into the hopper. The speed of the belt varied from zero to 1.5 $m.s^{-1}$. The speed was manually monitored with a tachometer (DT-30LK) to confirm the target speed. At each run, after the belt was up to speed, the hopper outlet was opened rapidly to discharge pellets onto the belt. At the end of each run, pellets were collected in the collecting bin—which was covered with a Polyvinyl Chloride (PVC) sheet with approximately 1 mm thickness. This plastic sheet was used to empty the bin while preventing loss and extra degradation of pellets in collecting and recirculating the material into the hopper. After each run, pellets were manually sieved again to determine the generated number of fines. The weight percentage of generated fines (F_g) was calculated using equation (4.4):

$$F_g = \frac{m_S}{m_i} \times 100, \tag{4.4}$$

where m_i represents the particles passing through the sieve and m_B represents the mass of the initial sample.

The experiments were conducted over six days and every day the temperature and relative humidity of the laboratory were recorded with a thermocouple of National Instruments and an analog humidity gauge, respectively. This is important as it has been shown previously in [116], [132] that a prominent change in both temperature and relative humidity significantly influences the mechanical degradation of wood pellets. During our experiments, the temperature and the relative humidity were 20.1 ± 1.3ºC and 60.3 ± 3.8%, respectively. These results show that the temperature and relative humidity were approximately constant and there was no effect on the mechanical degradation of pellets.

4.3.5 Design of experiments (DoE)

The RSM with Box-Behnken experimental design [151] was used to analyze the influence of four operational factors—three continuous and one categorical factor—on the proportion of fines generation. This design was chosen because first, it enables to design experiments with four factors having three levels for three of the factors and two levels for one factor, and second, as previously shown by Ferreira et al. [152], it is more efficient than the other DoE methods such as central composite design and full factorial design. In this type of design, three factors with three levels at different blocks are being studied, therefore, enabling the estimation of the parameters of the quadratic model.

Four operational factors suspecting to influence the pellet breakage were investigated in this study. These factors include three operational conditions of the belt conveyor including the belt speed (X_1), level of loading on the belt (X_2), the drop height from the belt conveyor (X_3), and the number of handling steps (X_4) as the independent variable. X_1, X_2, and X_4 were chosen as continuous factors and X_3 was chosen as a categorical factor.

In this study, the belt speed (X_1) could be varied between 0 to 1.6 m.s^{-1}; therefore, the chosen speed range was between 0.5 to 1.5 m.s^{-1}.

The level of loading (X_2) was a percentage of the nominal belt load that can be fed to the belt without causing spillage (see Figure 4.4). The nominal load can be calculated based on equation (4.5):

$$C_N = \frac{1}{4}(\tan(\gamma) + \tan(\beta)) \cdot W^2 \cdot v_{belt}, \tag{4.5}$$

where C_N is the nominal capacity or load of the belt, γ is the surcharge angle of the material, β is the trough angle of the belt, W is the width of the loading chute, and v_{belt} is the speed of the belt, as shown in Figure 4.4. From our experiments, the maximum loading factor without materials spillage is 50% of the nominal load. Therefore, here we considered 50, 40, and 30% of the nominal load for the variation of the belt load.

The categorical factor (X_3) is a combination of the inclination of the belt and the drop height of the material at the discharge point of the belt; however, as the inclination angle itself has a negligible effect on the number of generated fines, this factor is hereafter called as the drop height. At the inclination of 0°, the drop height was 51 cm and at the inclination of 14.2°, it was 72 cm.

The number of handling steps represents the number of transfer points for pellets in which belt conveyors are used. This depends on the transport journey that pellets take (from the production site to the end-user location) and the design specifications across a transport chain. Here, each transport loop from loading the belt to discharge into the collecting bin is considered as one handling step. According to Boac et al. [143] and Oveisi et al. [77], pellets may drop approximately 10 times during their transport journey; therefore, a maximum of nine steps is considered here.

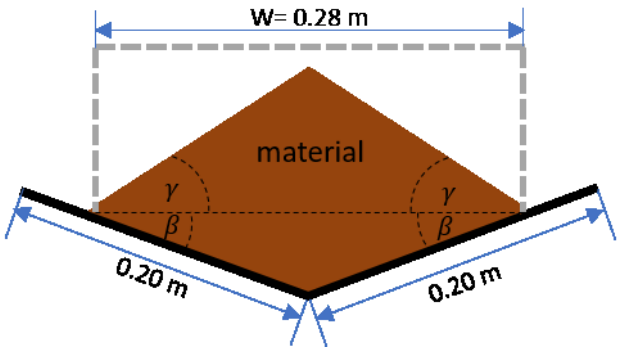

Figure 4.4: Cross-section of the belt conveyor behind the chute. The chute is represented in grey dashed line and the belt in black solid line. Angle γ represents the surcharge angle of the material, angle β represents the trough angle of the belt, W is the width of the loading chute.

A multiple regression analysis using a polynomial quadratic equation for the number of fines was performed using Minitab®18.1 software [153], as shown in equation (4.6):

$$Y = c_0 + \sum c_i X_i + \sum c_{ii} X_i^2 + \sum c_{ij} X_i X_j + \epsilon, \quad (4.6)$$

where Y is the measured response, c_0 is the intercept coefficient, c_i, c_{ii}, and c_{ij} are the regression coefficients, X_i and X_j are the factors used in the regression analysis, and ϵ is the error of the model.

For the continuous independent variables, i.e. X_1, X_2, and X_4, a range of interest is established based on preliminary tests and corresponds to three discrete levels: minimum (−1), medium (0), and maximum (+1). The independent factors and their corresponding levels are shown in Table 4.2. The categorical independent factor (X_3), which is the drop height of the pellets consists of two levels (−1 and +1). An experimental design was created in Minitab® 18.1 consisting of 30 experiments (Table A. 1). For each of the experiments, one replication was performed.

Analysis of variance (ANOVA) and regression analysis was performed to investigate the statistical significance of the regression coefficients at a confidence level of 95%. Only statistically significant terms have been included in the result of the multiple regression analysis. The model accuracy was evaluated using the coefficient of determination (R^2 value).

Table 4.2: Factors and their corresponding levels used in the design of experiments.

Factor	Low level (-1)	Medium level (0)	Low level (1)
X_1: Belt speed (m.s^{-1})	0.5	1.0	1.5
X_2: Level of loading (%)	30	40	50
X_3: Inclination of the belt conveyor (degree)	0	-	14.2
X_4: Number of handling steps	1	5	9

4.4 Results and discussion

The PLD of the samples used in the tumbling can show that the PLD of the classified samples is roughly similar except for the medium-sized pellets, which show a small deviation (Figure 4.5 a and b). In general, the proportion of generated fines in the rotary impact tester is higher than the tumbling test. This is due to the high impact velocity of pellets in the rotary impact tester. Moreover, as previously reported by other researchers such as Murtala et al. [145], in the tumbling method pellets are usually subjected to attrition forces while in the rotary impact tester the impact forces play a major role in the breakage of pellets.

The durability of brown and white pellets measured with the tumbling can was 96.8% and 98.2%, respectively, with the standard deviation of 0.05 for brown and 0.1 for white pellets. Similar to this, the durability of brown pellets in all the PLDs was lower than that of the white

pellets (Figure 4.5). This is also confirmed with the results of the compression tests (Figure 4.6) where the average maximum stress at failure for the brown pellets was 3.65 MPa (standard deviation= 0.75) and for the white pellets was 11.60 MPa (standard deviation= 4.03), although Larsson et al. [44] observed weak correlations between the mechanical strength of individual pellets and durability of a bulk of pellets.

In addition to the type and size-classified pellets, two other tests have been conducted using randomly chosen mixed pellets from the initial 400 kg samples with the tumbling can. The results show 96.5% durability (fines= 3.5%), with a standard deviation of 0.05. Therefore, the durability value of the mixed pellets in the tumbling can is lower than the durability of each pellet type in each category i.e. long, medium, and small pellets. This is probably due to the existence of the particles smaller than 7 mm and bigger than 3.15 mm in the randomly chosen mixed pellets. As shown in the subplot of Figure 4.5, the pellets used in the tumbling method were bigger than 7 mm, therefore, the number of particles in the test was lower, and consequently, this resulted in fewer interactions between the pellets. However, in the mixed pellet sample, the presence of particles with a size between 3.15 and 7 mm increases the number of particles in the sample and therefore, increases the number of collisions between particles resulting in a higher generation of fines.

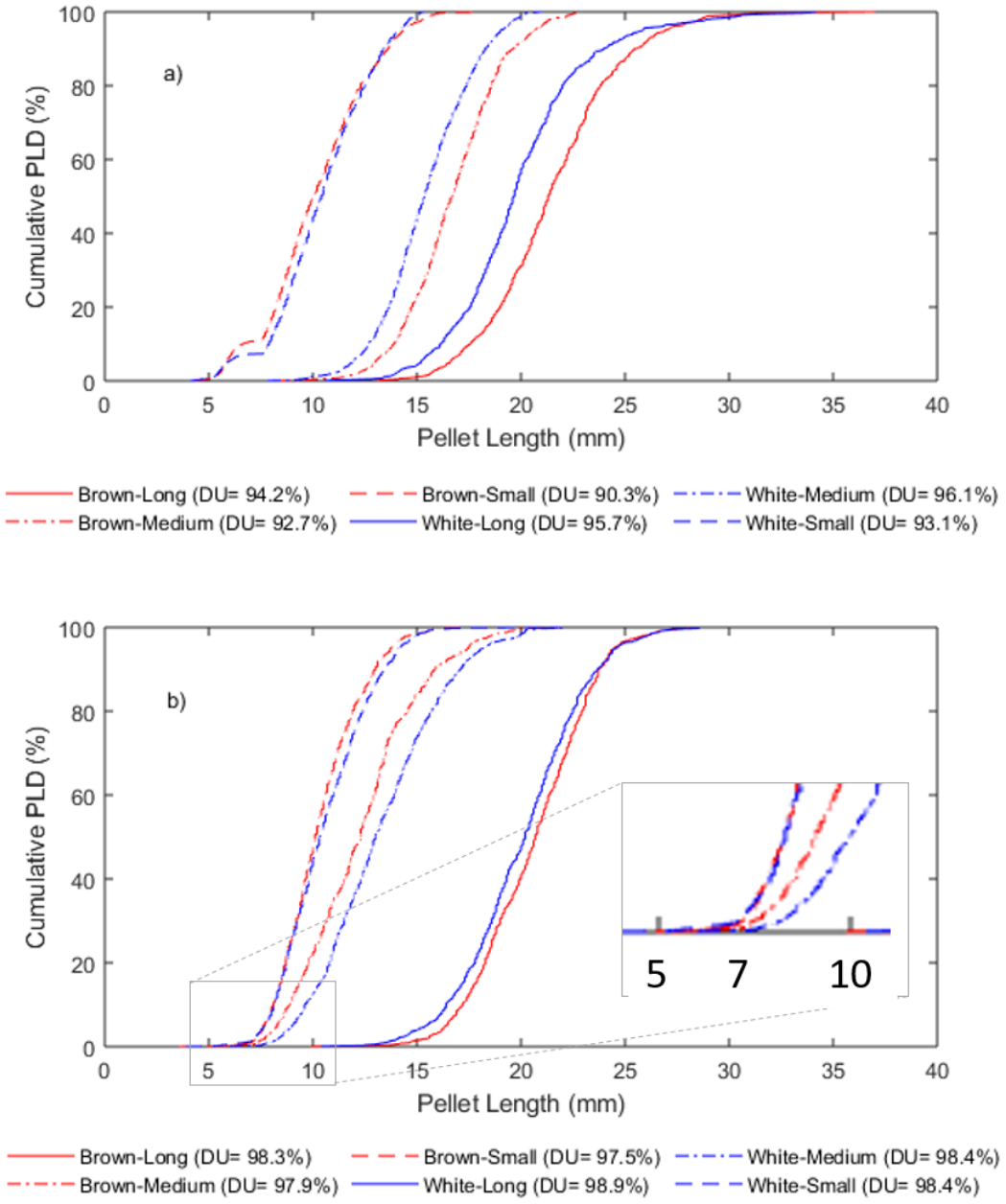

Figure 4.5: Pellet length distributions of samples tested in a) impact tester and b) tumbling can. (DU= Durability value).

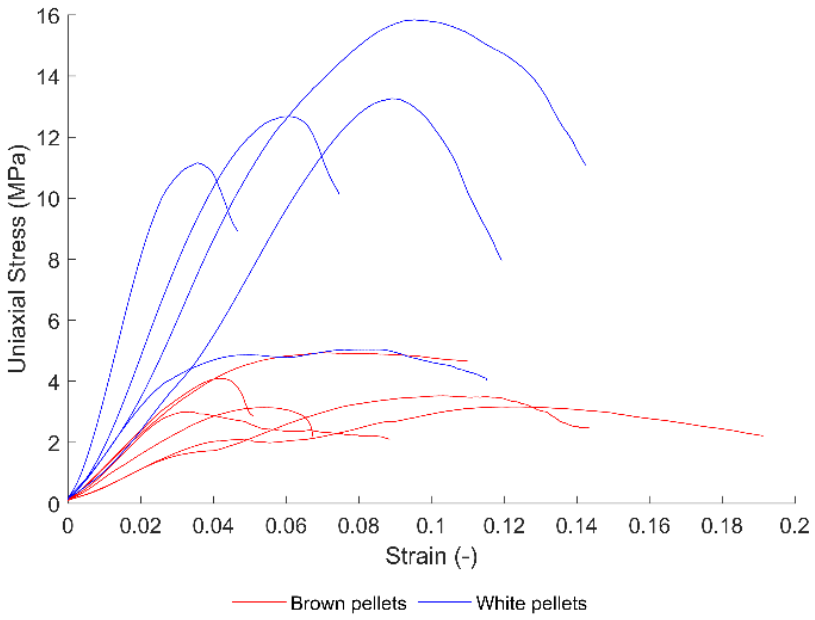

Figure 4.6: Compression test results.

The results of the belt conveyor experiments based on the Box-Behnken experimental design and those of the benchmark tests are shown in Figure 4.7. The maximum proportion of generated fine particulates via the belt conveyor was 3.6% and it was observed at the maximum number of handling steps (nine steps), drop height of 72 cm 50% level of loading, and a belt speed of 1 $m.s^{-1}$. Comparing this proportion of generated fines with the results of the benchmark tests showing in Figure 4.7, it is concluded that the result of the tumbling can testing is closer to the belt conveyor experiments consisted of several handling steps. Moreover, it is shown that the higher drop heights generate a higher number of fine particulates.

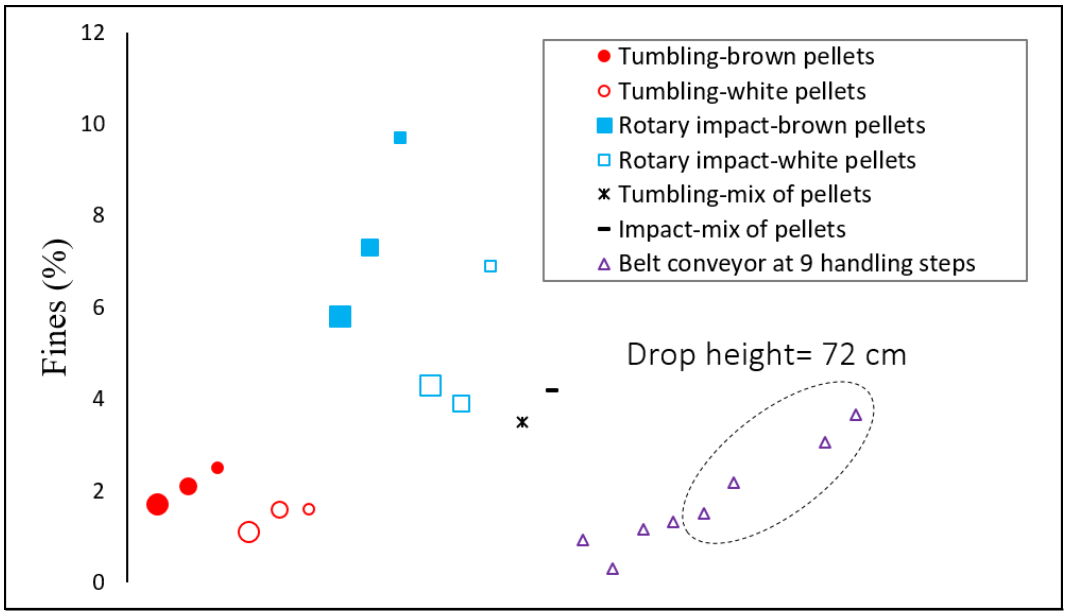

Figure 4.7: Proportion of fines in laboratory experiments and transport via the belt conveyor. The size of the round and square markers represent the PLD: the bigger the size, the longer the PLD is.

Figure 4.8 shows the absolute values of the standardized effects of the (in)dependent factors on the generated fines from high to low including a reference line (dashed line) to indicate the statistical significance. The Pareto chart shows that the inclination of the belt conveyor (X_3), the number of handling steps (X_4), the level of loading squared (X_2^2), and the interaction between the number of handling steps and the inclination (X_4*X_4) are statistically significant. With multiple regression analysis, relations between the factors and the response were found, as given in the equation (4.7):

$$\begin{cases} F_f = 0.0691 - 0.00476X_3 - 0.00055X_4 + 0.000047X_2^2 + 0.000632X_3X_4 & X_3 = 51\ cm \\ F_f = 0.0691 + 0.00476X_3 - 0.00055X_4 + 0.000047X_2^2 + 0.000632X_3X_4 & X_3 = 72\ cm \end{cases} \quad (4.7)$$

where F_f represents the fines fraction in the batch of pellets. The R^2 value for this regression analysis is 0.852, which is considered an acceptable value for such a regression in engineering fields [154].

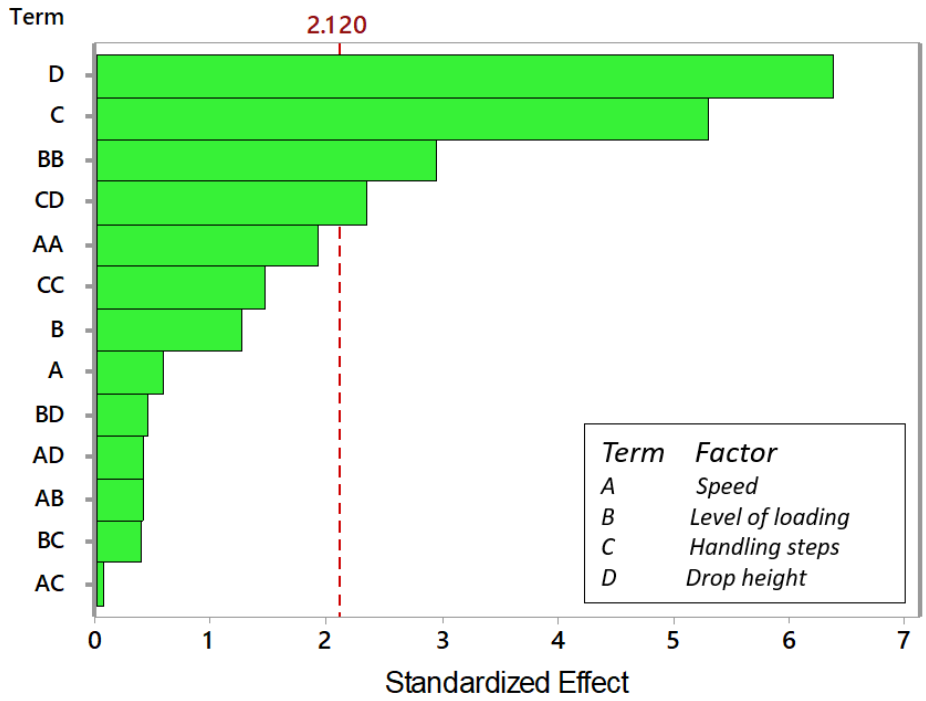

Figure 4.8: Pareto chart of the standardized effect (α= 0.05). Any term with a value more than the reference absolute value (2.120) is considered significant.

With a normal distribution of the residuals, the assumption that the data are normally distributed was checked using the method described by Antony [155]. The histogram and the normality plot shown in Figure 4.9 confirm that the residuals are normally distributed and we can see that the experimental data points are closely aligned to the reference line.

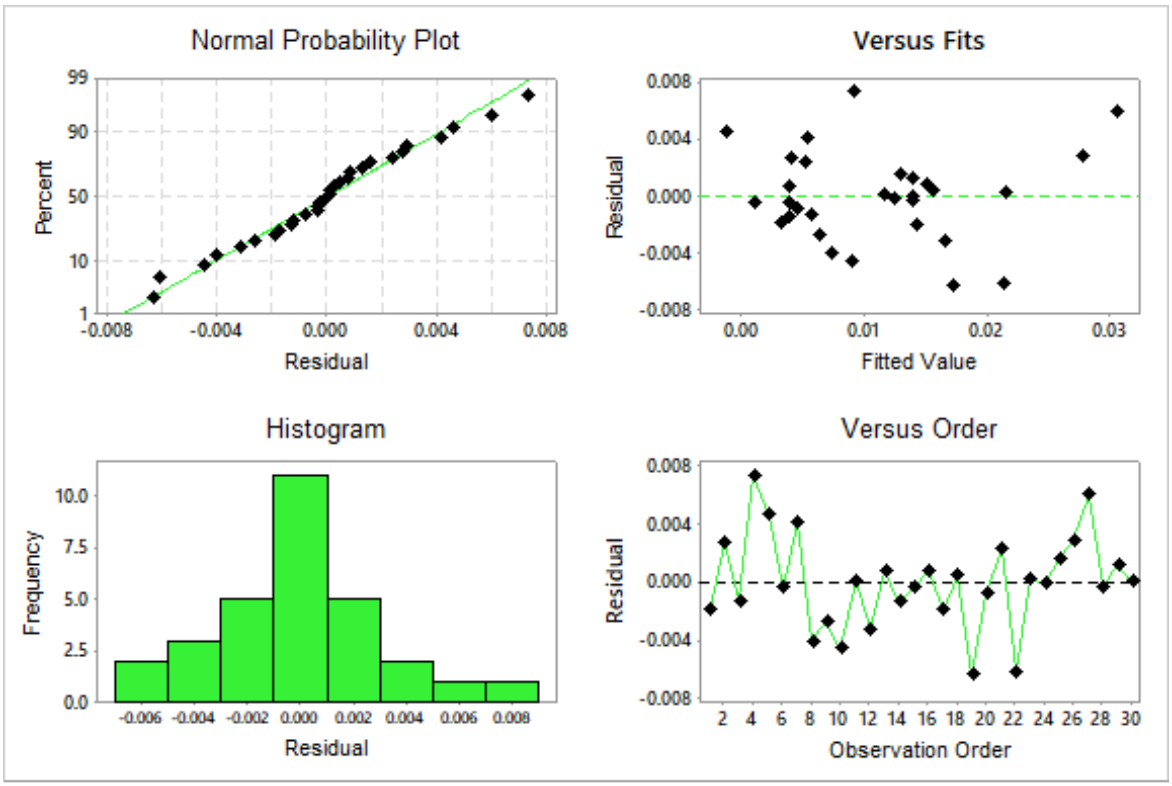

Figure 4.9: Residual plot for fines generated in the experiments of the conveyor belt.

Comparing surface plots a, b, and c (drop height of 51 cm) with the plots in d, e, and f (drop height of 72 cm) in Figure 4.10, the drop height significantly influences the proportion of generated fines. Oveisi et al. [77] found that a greater drop height induces more pellet breakage resulting in more fines generation. Our results are in accordance with their findings. However, in our study, the inclination angle is varied too. Because we did not observe a change in the drop height due to the shooting of pellets from the belt at the discharge point at the inclination of 14.2°, we consider that the effect of inclination angle is negligible. Nonetheless, future studies can focus on the effect of discharge trajectory and angle of impact on the number of the generated fines.

It is already proven that a higher impact velocity increases the impact forces on pellets [156]. Although an increased falling height (0.21 meter) increases the speed of the pellets upon impact and so increases the impact velocity, a belt speed in the range of 0.5 and 1.5 $m.s^{-1}$ does not seem to play a significant role in the generation of fines. Jäger et al. [144] found that higher pellet velocities (7.5–15.7 $m.s^{-1}$) induce progressive particle size reduction of wood pellets when transported by pneumatic conveying. However, our findings are in contrast with this, as the speed of the belt in a range between 0.5 and 1.5 $m.s^{-1}$ does not significantly influence the number of generated fines.

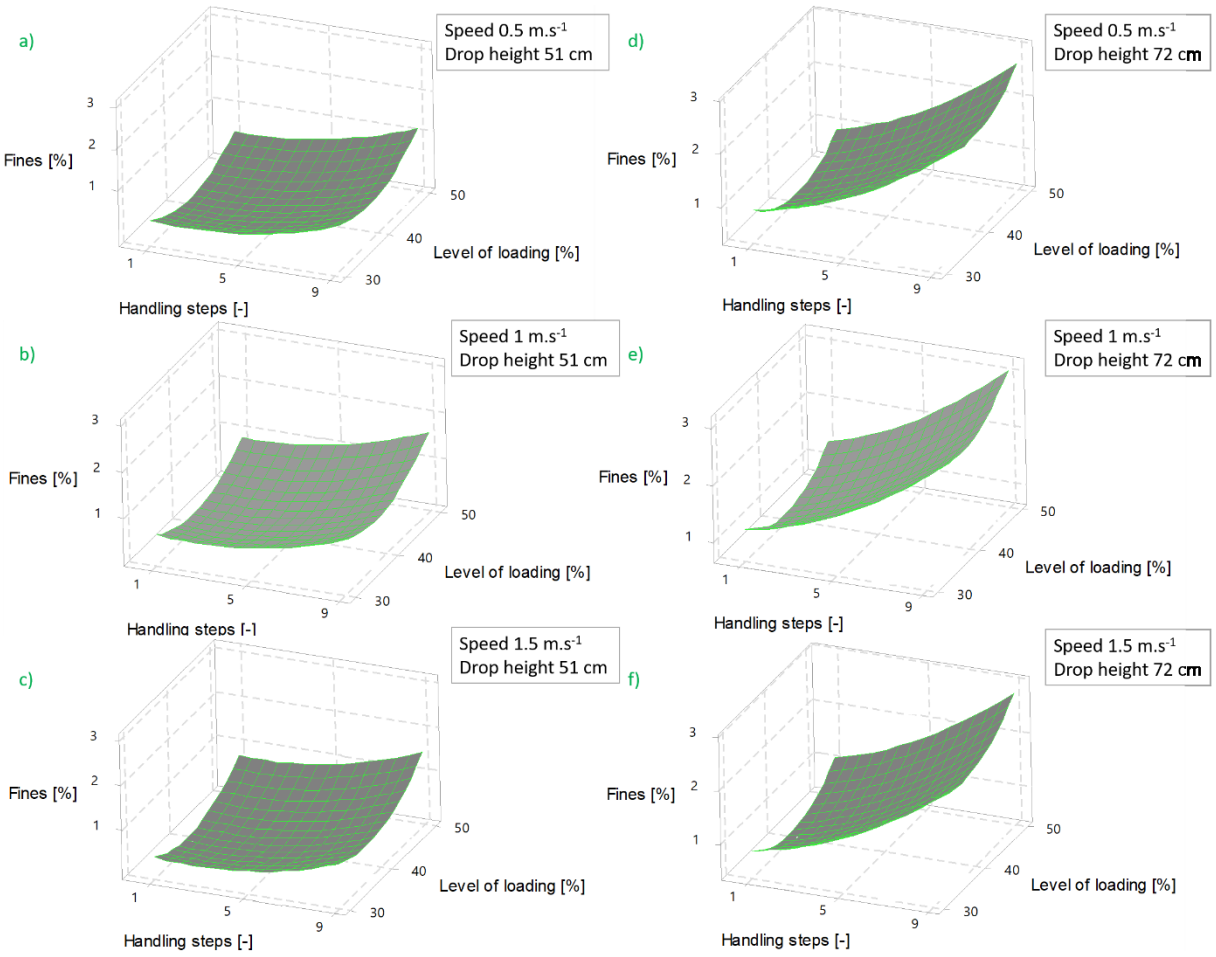

Figure 4.10: Surface plot of the proportion of fines at different operational conditions of the belt.

According to the study by Oveisi et al. [77], the number of generated fines depends on the bedding material. When pellets impact a bed covered by pellets (not the bottom surface of the collecting equipment), the number of generated fines is lower. Jägers et al. [144], also found a larger pellet mass flow (a higher level of loading) reduces the comminution effects. In contrast, in this study, the Pareto chart analysis (Figure 4.8) shows that, together with the number of handling steps and the drop height, the level of loading squared is statistically significant for the number of generated fines.

The number of handling steps significantly influences the number of generated fines. This can be found in any of the surface plots shown in Figure 4.10. These results are following the findings of Oveisi et al. [77] who concluded that the pellets become increasingly weaker after repeated impact. Cracks and tears upon the next impact can evolve into breakage of the pellets resulting in a higher number of generated fines.

Looking at Table A. 1, the proportion of produced fines at the drop height of 72 cm and nine handling steps is 2.2–3.6%, which is close to the generated proportion of fines of the randomly chosen sample in the tumbling method (3.5%), and a slightly different from that of rotary impact tester (4.2%), as shown in Figure 4.7. Therefore, the tumbling can method could successfully predict the proportion of fines in a gentle transport system of pellets with several handling steps and a low drop height. The rotary impact tester, however, can probably predict the fines at higher impact velocities. Although Murtala et al. [145] concluded that for the predictions of the number of fines particulate in transferring pellets via pneumatic conveying system a combination of both tumbling can and rotary impact tester should be used, our observations show that the tumbling box is capable of predicting the fines generation in gentle transport (a low-speed and small drop height) with several transfer points.

4.5 Conclusions

Using a Box-Behnken response surface design, the number of fines generated during the transport of fuel pellets by a pilot-scale belt conveyor was studied. It was shown that the number of handling steps and the drop height are the most influential parameters on the generation of fines; however, the level of loading and the speed of the belt in a range between 0.5 and 1.5 $m.s^{-1}$ were not affecting the fines generation. Moreover, using a regression model, a polynomial quadratic model (R^2= 0.852) to predict the number of fines generation via a belt conveyor was introduced. It is concluded that for gentle transport of pellets, the falling height and the number of handling steps should be carefully considered. It is also concluded that the tumbling box method can predict the proportion of generated fines with high accuracy for the pellets that are transported and discharged via a belt conveyor nine times.

5 Large-Scale Transportation and Storage of Wood Pellets: Investigation of the Change in Physical Properties*

In chapters 3 and 4, we investigated the breakage behavior of pellets in the laboratory and pilot-scales. This chapter presents results of breakage behavior and the generated number of fines and dust in an industrial-level transportation and storage system. Moreover, the effect of transportation on the other properties of pellets such as moisture content, bulk density, and mechanical durability is investigated.

A measurement campaign was performed on a 450 ton.h^{-1} transportation and storage system of biomass pellets in the port of Rotterdam. Critical transfer points with a high potential to impact pellet properties were determined and sampled. The analysis includes the changes in pellet size, mechanical durability, moisture content, and bulk density.

*This chapter is based on Hamid Gilvari, Coen van Battum, Simon van Dijk, Wiebren de Jong, and Dingena L. Schott. " Large-Scale Transportation and Storage of Wood Pellets: Investigation of the Change in Physical Properties." Accepted in Particuology.

5.1 Introduction

Worldwide use of wood pellets as a renewable energy carrier has increased sharply, from ~12 million metric tons in 2008 to 56 million metric tons in 2018 [104]. More than 27 million metric tons of wood pellets were consumed in Europe in 2018, more than 45% of them for industrial purposes. However, not all pellets consumed in Europe are produced by European countries. Approximately one-third are imported from the United States and Canada [104].

Due to its inherently high moisture content and its low bulk and energy densities, biomass is usually densified to improve these properties, which is advantageous for transportation and handling steps [10]. Pellets are normally produced under high temperature and pressure conditions in a so-called pelletization process, which involves the elastic and plastic deformation of particles and the softening of natural binders such as starch, protein, lignin, fat, and fibers to help agglomerate particles [4], [30], [98], [157].

The fragile nature of pellets causes their attrition and breakage throughout the entire logistic chain [77]. As a result, average pellet length may decrease and the amount of generated small particles can increase [143]. This has consequences for pellet transportation, handling, and storage, such as an elevated risk of dust explosion, fire, segregation, arching and equipment fouling, health issues for people inhaling the dust, and losing a notable portion of the material [141], [142], [158]. Moreover, pellet breakage and the generation of small particles undermine the pelletization effort by decreasing the bulk density [159].

The ability of biomass pellets to remain intact during loading, unloading, feeding, and transport is called “mechanical durability” [106]. From the definition itself, the mechanical durability can indicate the extent to which the material can keep its initial shape. In practice, however, durability is characterized by measuring the amount of pre-defined small-size particles created in laboratory tests. This small size may be different in some of the literature, but a size between 3 and 5 mm is usually considered [107], [133]. According to the literature, mechanical durability depends on the characteristics of the raw material; specifically, factors such as particle size and moisture content, pelletization process parameters, and storage conditions [46], [137], [160], [161].

Undoubtedly, the extent of pellet breakage and attrition very much depends on the type of pellet; the higher the pellet’s strength, the lower its breakage and attrition rates are. However, pellets may undergo mechanical degradation due to high impacts and compression forces caused by,

for instance, long drops, poor equipment design, increased number of handling steps [141], [142].

Different breakage mechanisms have been proposed for biomass pellets during transport and handling, namely breakage into two or more pellets while practically keeping the cylindrical shapes, attrition of pellet surfaces and ends, and crushing of the whole pellet [136], [143].

In industry, various equipment is used for the transportation, handling, and storage of pellets. Of these, grabs, belt conveyors, pneumatic conveyors, pipe conveyors, hoppers, transfer chutes, silos, and bins are the most common [162], [163]. Each of these types of equipment may degrade the pellets mechanically, due to attrition, compression, or impact. Recently, research has been underway to characterize the breakage and attrition of pellets [143], [145], [150], [164]. For instance, research on pneumatic conveyors has shown that pellet attrition increases with the increase in particle velocity, which is induced by increasing the air inlet velocity and decreasing the mass flow of pellets. Moreover, a shorter bend radius increases the breakage of pellets [144], [158].

It is known from previous studies that the magnitude of impact force, number of handling steps, and amount of bulk material directly influence the breakage and attrition of pellets [77], [143], [165]. Oveisi et al. [77] investigated the effect of drop height, pellet mass, and repeated handling steps on the degradation of wood pellets during free fall while they placed the pellets in a bag made of synthetic materials. They also studied the effect of pellet mass per bag and of repeated handling steps, concluding that greater drop heights and an elevated number of handling steps increase the amount of fines. Moreover, pellet mass shows a linear correlation with the generated mass of fines as long as the initial mass is kept lower than 1 kg.

Looking at corn-based animal feed pellets, Boac et al. [143] studied the effect of the number of handling steps on the number of broken pellets (particles passing a sieve with a 5.6 mm mesh) and dust particles (< 0.125 mm) generated. The feed pellets contained 13.2% moisture and had a nominal diameter of 6.4 mm and a durability of 92.9%, according to the tumbling box method. Their test setup included a bucket elevator with a height of 54.9 m, which cycled the pellets from the bottom of storage bins to their top and from a first bin to a second one, then vice versa, with an average flow rate of 59.4 metric tons per hour. They repeated the discharge and loading of the bins eight times and observed a notable increase in the proportion of particles < 5.6 mm, from 17.5% to 50.2%. The average dust generation was 0.069% per transfer.

As shown above, existing literature regarding the mechanical strength, breakage behavior, and generation of fines and dust of biomass pellets is limited mainly to laboratory or pilot-scale studies. The objective of this paper, therefore, is to quantify small particles at different positions in a large-scale "real world" transportation system (~450 ton.h^{-1}). This should allow us to determine the major transport steps in which pellet breakage and attrition occur and one can use it as a benchmark for investigating the changes in pellet properties in any other pellet transport system. In addition, the changes in other pellet properties—such as mechanical durability, bulk density, and moisture content—due to multiple transportation steps are studied. For that purpose, a pellet-fired power plant in the Netherlands was chosen as a case study to investigate the breakage and attrition of wood pellets. The transportation system in this power plant consists of a grab unloading system, belt conveyors, and storage in a silo.

5.2 Materials and methods

The material for this case study originated with an anonymous company in the USA. A wide range of woody feedstock was used to produce the pellets, including both soft and hard woods. No information about the densification process was disclosed. After their production and local storage in the USA, the pellets were transported in bulk to a local port and loaded into an ocean-going vessel with a capacity of 28,000 metric tons, then shipped across the Atlantic Ocean to the port of Antwerp, Belgium. Here they were transshipped to barges holding ~2.500 metric tons each. Twelve barges were thus required for the entire transatlantic cargo. No information was disclosed regarding changes to the particle size distribution of the pellets up to this stage. The twelve barges proceeded to the port of Rotterdam, where they berthed next to the end user's plant at a rate of one barge per day. The cargo comprised a mixture of seven different types of wood pellets, which differed by color, diameter, and length as shown in Table 5.1.

Physical properties of the pellets, including their moisture content, bulk density, diameter, length, and mechanical durability, were measured as follows. Moisture content was measured according to EN standard 14774-2 [166], using 300 g of pellets that were placed in an oven at 105ºC for 24 h. The moisture content was then calculated based on the difference between the mass of the pellets before and after the test. Bulk density was measured according to EN standard 15103 [81] using a 5 L steel cylinder using the tap method. The bulk density was calculated from the mass of pellets divided by the volume of the cylinder. Pellet diameters were measured according to EN standard 16127 [130] using a digital caliper. Twenty-eight pellets were measured in this way: four per pellet type, chosen at random (Table 5.1). Pellet length

distributions were measured according to EN standard 16127 [130], using an in-house image processing tool; details of this can be found in our previous publication [147]. Mechanical durability was measured according to ISO standard 17831-1 [107], which is a common global method for durability measurement of biomass pellets and is used extensively by researchers in this field [44], [46], [84], [115], [116], [167]. The mechanical durability was determined by placing 500±10 g of sieved pellets (round-holed sieve with a screen size of 3.15 mm) in a tumbling can. This was rotated at a speed of 50 rpm for 10 minutes. After the test, the sample was sieved again using the same sieve, and then, weighed. Its mechanical durability was calculated by dividing the mass of the material remaining in the sieve by the mass of the initial sample multiplied by 100. The moisture content, bulk density, and mechanical durability experiments were repeated twice; the reported values are thus the mean values of duplicate measurements.

Table 5.1: Different types of wood pellets shipped from the USA to the port of Rotterdam.

Row	Type 1	Type 2	Type 3	Type 4	Type 5	Type 6	Type 7
1							
2							
3							
4							

To determine the change in particle size distributions of the samples, three different sieves with screen sizes of 5.6 mm (square holes), 3.15 mm (round holes), and 1 mm (square holes) were used. The sieve with the smallest screen size determined the amount of dust (< 1 mm), the medium one determined the amount of fines (1mm < fines < 3.15 mm), and the largest one was chosen to determine the amount of lumps (3.15 mm < lumps < 5.6 mm). All particles longer

than 5.6 mm were considered "whole pellets". Hereafter, all particles smaller than 3.15 mm are referred to as "fines and dust", and all those smaller than 5.6 mm as "small particles".

To characterize the classified particles, every sample was first weighed and then sieved manually using the three screen sizes. The masses of dust, fines, and lumps were then weighed and recorded. The percentage of each category was calculated using equation (5.1):

$$P_i = \frac{m_j}{m_t} \times 100\%, \tag{5.1}$$

where P_i is the percentage of category i in a sample, m_j is the mass of category j in the sample, and m_t is the total mass of the sample. The percentage of "whole pellets" was calculated by subtracting the percentage of small particles (< 5.6 mm) from 100.

5.3 Sampling locations and methods

Once the pellets had arrived in Rotterdam, they were unloaded by a clamshell grab into a hopper (see Figure 5.1). This fed the incoming material onto a covered belt conveyor (hereafter referred to as the first conveyor). The grab's capacity is 10 metric tons and the height of the hopper is 4 m. A dust filter is installed just after the hopper to collect airborne dust before the material is loaded onto the first conveyor. This transported the pellets on an upward incline to the top of a transfer tower with a height of 24.0 m, at a speed of 1.7 $m.s^{-1}$. The length and width of the first conveyor are 150.0 and 1.4 m, respectively. It, therefore, has an angle of inclination of 9.2°. At the top of the transfer tower, the pellets were dropped from the first conveyor onto a second one by means of a free fall with a vertical drop of 7.8 m. Between these two conveyors is a chain bucket sampler, which collected samples at a consistent cross-section of the material's stream during its free fall. This is an automatic sampler, already installed in the system for on-site sampling purposes. The samples it took were transferred to a small dosing conveyor (length 3.0 m, width 0.2 m), which in turn fed a rotary tube divider as shown in Figure 5.2. The role of the rotary tube divider was to divide a small portion of the samples by rotating the materials in such a way that, eventually, 2 kg of samples were collected every 11 minutes.

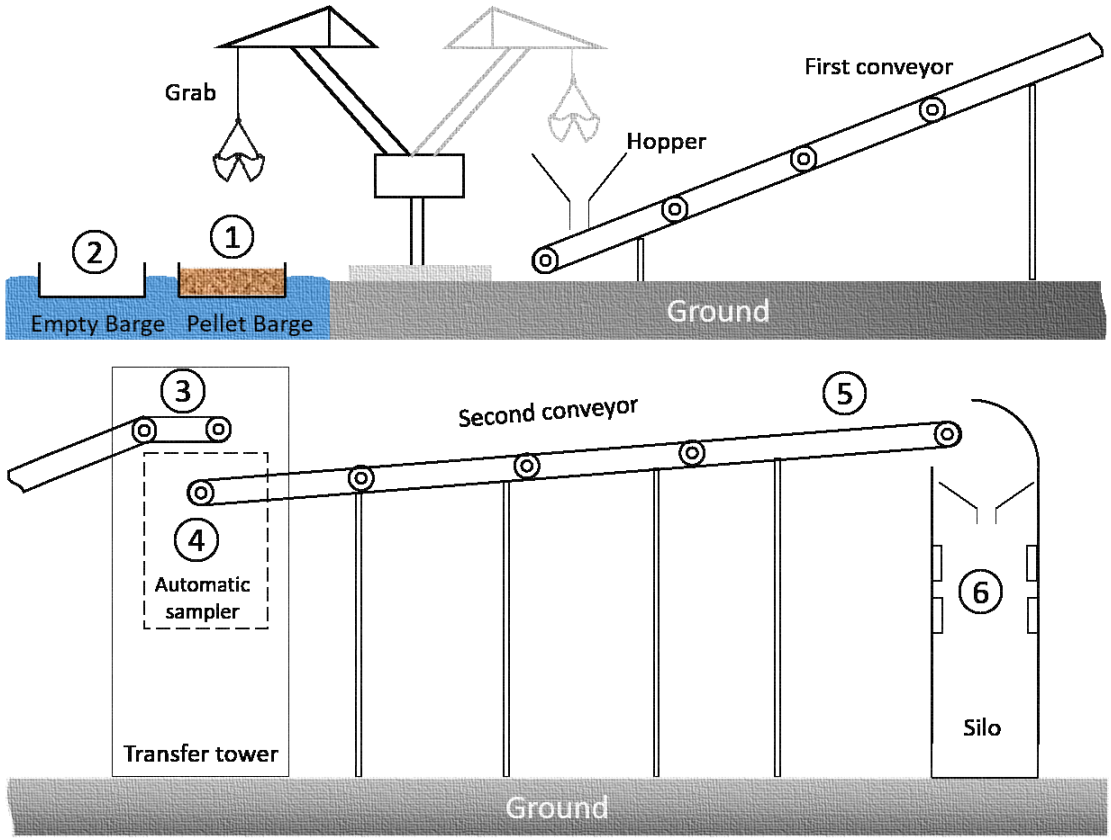

Figure 5.1: A 2-dimensional overview of the transportation system. The numbers show the sampling locations. A detailed overview of the automatic sampler is shown in Figure 5.2. The size of the equipment may not represent the real case.

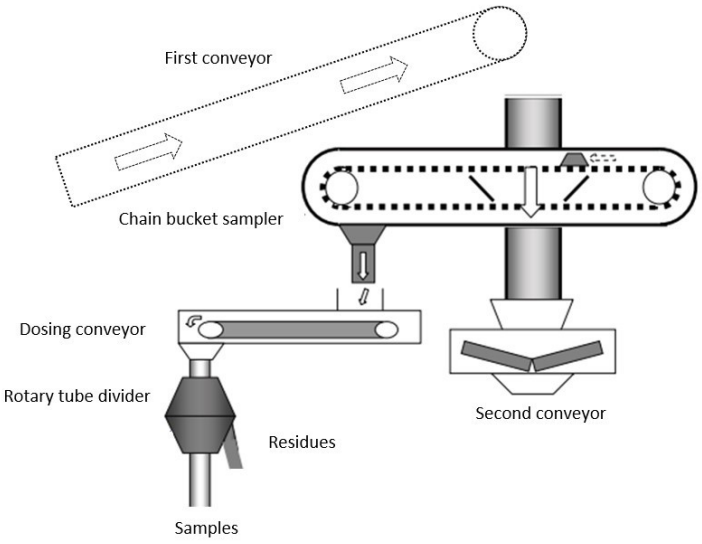

Figure 5.2: Detailed overview of the automatic mechanical sampler system in the transfer tower.

The second conveyor has a length of 500 m and transferred the pellets at a speed of 2.6 $m.s^{-1}$ to the top of the silo, into which they were dropped via a free fall. Whenever required, pellets are discharged from the bottom of the silo for further processing. The samples for this study were taken on three consecutive non-rainy days in the winter of 2019. Every day, a barge carrying 2500 metric tons of pellets was unloaded into the system. Six different locations throughout the entire transportation system, from the barge to the silo, were identified for the sampling used in this study. Samples were taken at different increments from different sampling locations, and all were analyzed in terms of particle size distribution, mechanical durability, bulk density, and moisture content. A summary of the sampling locations, days of sampling, and number of samples taken at each location is given in Table 5.2. In total, 77 samples were collected for this study. All were placed in sealed plastic bags to prevent moisture uptake and any further changes to pellet properties due to varying environmental conditions. The samples were then transported carefully to a laboratory at the Delft University of Technology for further analysis. The sampling locations are explained in detail below and they are shown in Figure 5.1.

Table 5.2: Summary of sampling locations, days of sampling, and the number of increments per location.

Sampling location	Location number	Day of sampling	Number of increments
Barge	1	1	8
		2	9
Second barge	2	1	5
First conveyor	3	1	8
		2	9
Rotary divider	4	3	17
Second conveyor	5	1	8
		2	9
Silo	6	3	4
Total	-	-	77

Sampling location 1 was situated inside the barge. Samples were collected from the upper surface of the pellet cargo at different time intervals. At this location, the physical properties of the wood pellets just before they enter the end user's transportation system can be characterized. As mentioned before, the pellets were unloaded from the barge using a clamshell grab with a capacity of 10 metric tons. Each grab cycle took approximately one minute, so emptying the entire barge (~2500 metric tons) took more than 4 h. To ensure that the samples represent the

pellet properties at different layers inside the barge, samples were taken every 30 minutes. Nine were collected on the first day and eight on the second, using a plastic scoop to gather approximately 6 kg of material per sample.

Sampling location 2 was situated in an extra empty barge (hereafter referred to as the second barge) positioned next to the pellet-loaded barge. Note that no such second barge is used in normal plant operations. However, this sampling location was introduced to investigate the effect on the pellet properties of the mechanical forces exerted during grabbing. At this location, one grab of the material was discharged every hour to collect five individual grabs in total. To obtain a representative sample from every discharged grab, the grab contents were dumped onto a flat surface in the second barge, creating a pile of wood pellets. Sampling was then performed according to EN/TS standard 14778-1 [168] by taking nine samples of approximately 0.5 kg each from different locations within the pile (Figure 5.3), using a plastic scoop. These nine samples were collected from the top (one sample), middle (three samples), and bottom of the pile (five samples), and were combined to create one single sample. Samplings at this location was undertaken only on the first day.

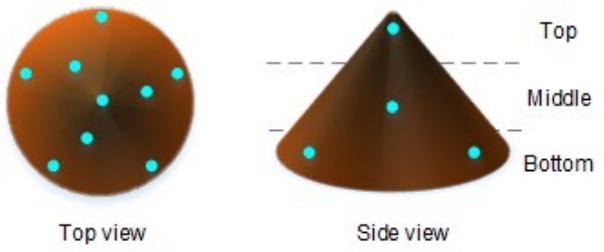

Figure 5.3: Schematic representation of the pile of pellets in the second barge and of the samples taken it (cyan markers). Note that the real pile deviated from a perfect cone shape.

Sampling location 3 was situated inside the transfer tower at the end of the first conveyor, which brings the pellets from the hopper to the transfer tower. This sampling location is situated just before the pellets were discharged onto the second conveyor (see Figure 5.1). This location was used to estimate the effect on the material's properties of grabbing and of a vertical free fall of 4 m (the hopper's height). Note that in each grabbing cycle, the pellets were dumped at the center of the hopper, and so the effect on them of hopper wall impacts can be considered negligible. This sampling location is useful as a benchmark to check the reliability of the properties of the samples divided by the automatic sampler at location 4. At this location, samples were taken using the stopped-belt method provided for in EN/TS standard 14778-1 [168]. In other words, the entire transportation system was halted at the sampling times and the

samples were taken from the belt conveyor after being isolated from the other material on it by means of two steel plates (Figure 5.4). Consequently, all the material on a cross-section of the conveyor belt was collected and labeled as coming from sampling location 3 at the relevant time. Each sample contained approximately 6 kg of material. As with location 1, sampling at this location was performed on days one and two. Moreover, all the samples here were collected at the same time as those from location 1 (the barge). In all, 17 samples were thus collected at this location.

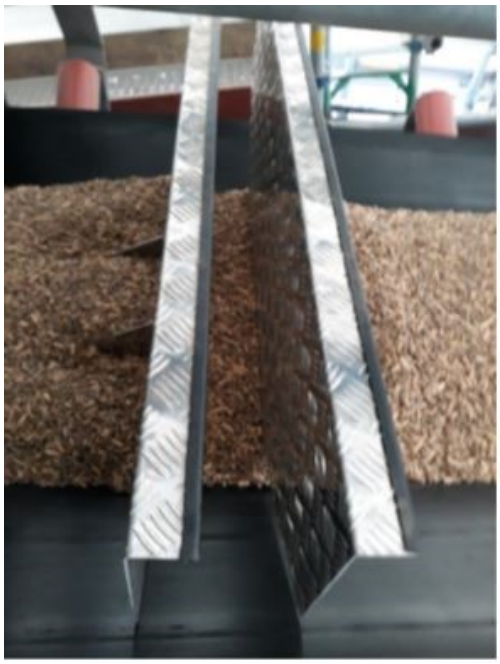

Figure 5.4: Isolation of the samples on the conveyor using the stopped-belt method.

Sampling location 4 was a part of the automatic mechanical sampler within the transfer tower. Samples taken at this location can be used to investigate the reliability of the material properties provided by the rotary divider with regard to the other locations in the transportation system, e.g. at the end of the first conveyor. Each sample was collected automatically, filling a plastic bag with approximately 2 kg of material within 11 minutes. Samples were only taken at this location on the third day, in 17 increments.

Sampling location 5 was situated at the end of the second conveyor, just before the material was discharged into the silo. Samplings at this location can demonstrate the effect of a 7.8 m vertical free fall (between the two conveyors) on pellet properties. The effect of the conveyor's vibrations on the pellet properties was assumed negligible. The stopped-belt method with the same type of steel-plate isolators as at sampling location 3 (Figure 5.4) was used here, too. Samples were taken at this location on days one and two only, each weighing approximately 6

kg. On average, these were collected three minutes after each of those at location 3, since that was how long it took for the pellets to be transferred from there to location 5 on the second conveyor.

Sampling location 6 was situated at the storage silo (with a height of 31 m and a diameter of 9 m) and was used on the third day. Four samples have been collected from the four hatches installed at the wall because sampling inside the silo was impossible at the time of the experiments. These hatches were located at two levels, and two samples were taken at each level (see Figure 5.5).

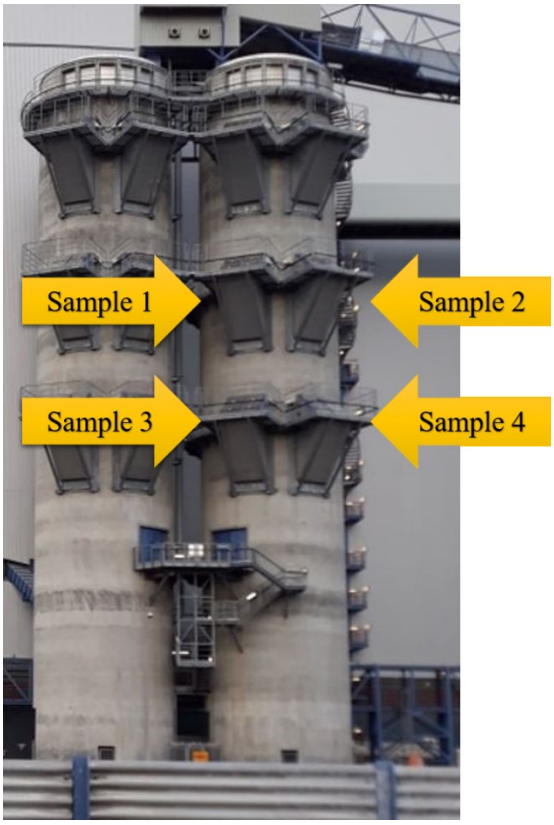

Figure 5.5: The silo and sampling ports.

5.4 Results and discussion

5.4.1 Mechanical durability, bulk density, and moisture content

Figure 5.6 shows the pellet properties with regard to the sampling locations and days. Analysis of variance (ANOVA) of all 77 samples revealed that there was no bias in the results for pellet properties at different locations or on different days ($\alpha = 0.05$, i.e. 95% confidence interval). From Figure 6, it can be seen that mechanical durability, bulk density, and moisture content are independent of the day of sampling and of the sampling location. Moreover, there was no

correlation between bulk density and moisture content. However, the mechanical durability varied between 90.8% and 98.7% in all locations, and this exceeded the 2% repeatability limit set by the standard [107]. The average values of pellet properties measured at different locations on three different days of sampling can be found in Table 5.3. This table implies that although a large deviation in durability, only a few samples widely diverge from the average value and that the average durability can be considered as reliable data in our study.

Table 5.3: Pellet properties at different locations on different days of sampling. Numbers in parentheses show the standard deviations.

Property	Location	Day of sampling	Average value
Moisture content (%)	All	All	5.9 (0.3)
Bulk density ($kg.m^{-3}$)	All	All	640 (25)
Mechanical durability (%)	All	All	97.6 (1.3)
Diameter (mm)	3, 4	2, 3	7.11 (0.59)
Length distribution* (mm)	1, 3, 4	1, 2, 3	50% < 13.40 99% < 32.70 100% < 42.10

*Based on the pellet length distributions of samples shown in Figure 5.7

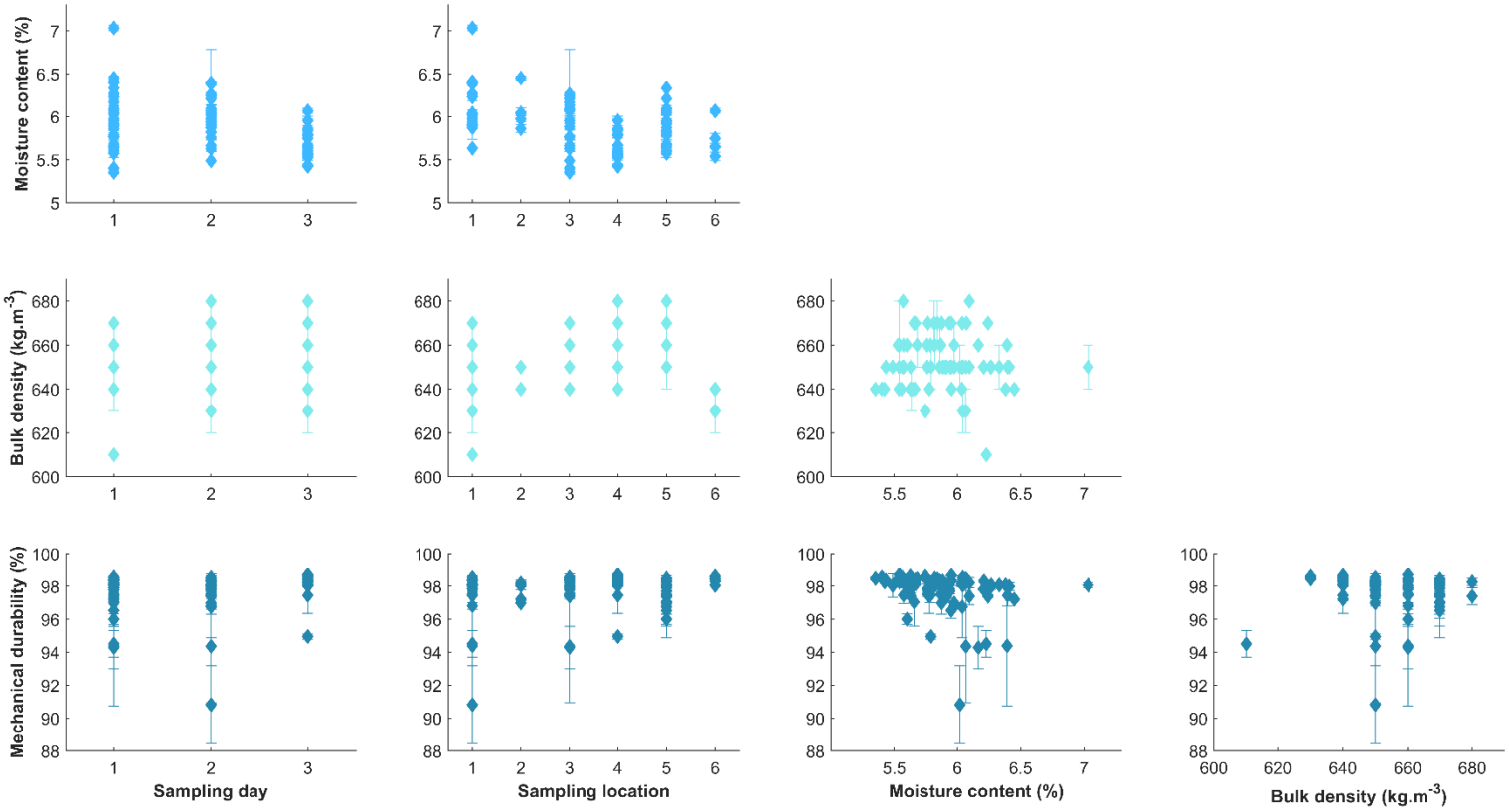

Figure 5.6: Pellet properties measured at different sampling locations and on different sampling days. The error bars show the standard deviations.

No correlation was found between the mechanical durability of the pellets and the number of handling steps they underwent. Nevertheless, there are two explanations for the variation we found in mechanical durability. First, in our previous study [147] we showed that pellet length distributions (PLDs) can be a contributing factor in the measured mechanical durability value, which increases with greater pellet lengths. To study this effect, the PLDs of ten samples (five out of 77 samples, with two replications each) were determined before durability tests (Figure 5.7) using our self-developed in-house image processing tool [147]. As can be seen in Figure 5.7, a sample containing the highest quantity of small particles (< 5.6 mm) showed the lowest mechanical durability value. Take, for example, samples 2-3-2-1 and 2-3-2-2 in Figure 5.7. These samples were two randomly selected 500 g from the initial 6 kg sample that was taken on day 2 at location 3 as the third increment. However, their durability values differ by 4.7%. This relatively high deviation can confirm the effect of length distributions. Second, as the share of each pellet type in each sample was not counted here, it is suspected that other factors such as the share of pellet type may cause a bias in the results.

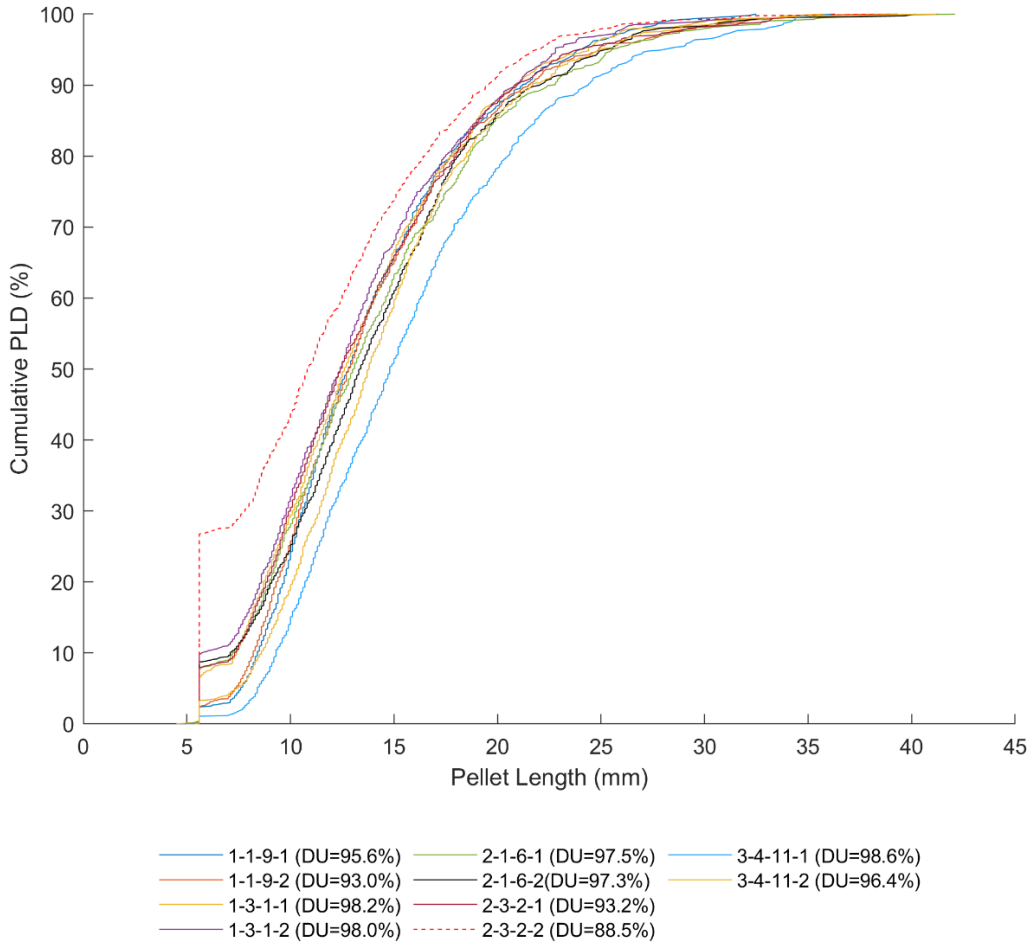

Figure 5.7: Pellet length distributions of different batches of pellets used for mechanical durability (DU) test (legend: digits from left to right = sampling day, sampling location, number of increment, and repetition number).

5.4.2 Particle size distributions

Figure 5.8 shows a sample image of the classified particles. In this, it can be seen that all particles longer than 5.6 mm are whole pellets retaining their cylindrical shape.

As explained in section 5.3, samples at locations 1 and 3 were collected at the same time and each discrete sample at location 5 was collected on average three minutes after each collection at locations 1 and 3. Therefore, it is likely that all corresponding samples originated from the same location in the barge. Hence, the effect on the particle size distributions at these locations of different transportation units can be investigated concerning their original particle size.

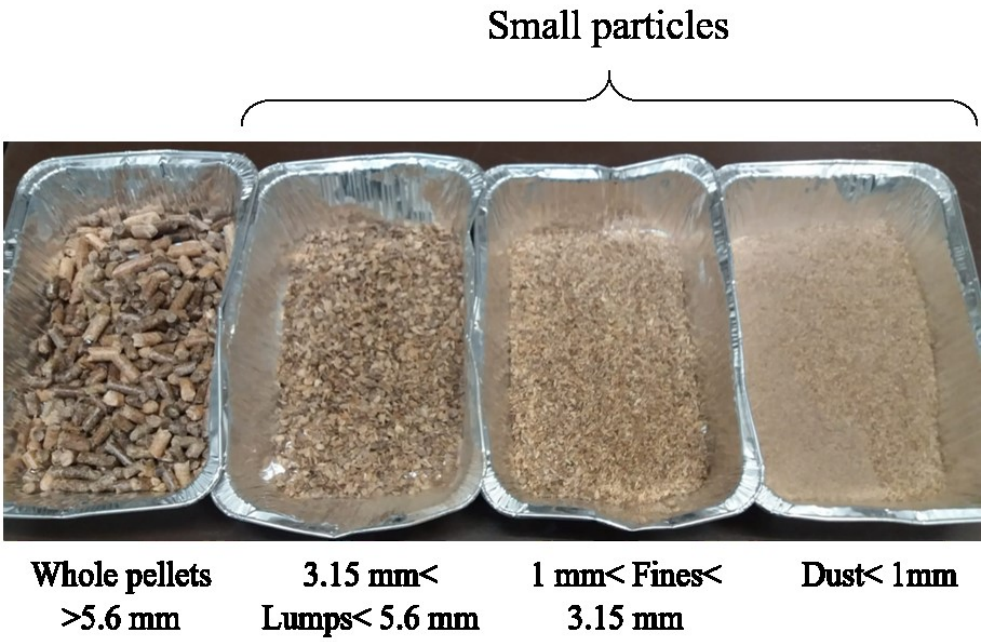

Figure 5.8: Size-classified particles after sieving.

Figure 5.9 shows the results of sieving analysis at locations 1, 3, and 5 (the main transportation stream) on the first and second days of sampling. According to these results, on each day the barges contain a notable amount of small particles at different sampling times before unloading. This also shows that different layers of the barge's cargo (from top to bottom) contain different particle size distributions. However, no evidence was found regarding the accumulation of small particles in one specific layer or at one specific location in the barge. The results (Table 5.4) show that, on average, the share of each size category on day one is consistent with the results on day two.

The statistical analysis shows a significant difference between the amount of fines and dust in the samples collected at different locations ($\alpha = 0.05$, i.e. 95% confidence interval). The *p*-value for one-way ANOVA analysis between the sampling locations and the amount of fines and dust (< 3.15 mm) was zero, which means that there was a significant difference in the average values. On average, the proportion of fines and dust was 6.02% at location 1 (first barge), 4.82% at location 3 (end of the first conveyor), and 9.01% at location 5 (end of the second conveyor) on the first and second days.

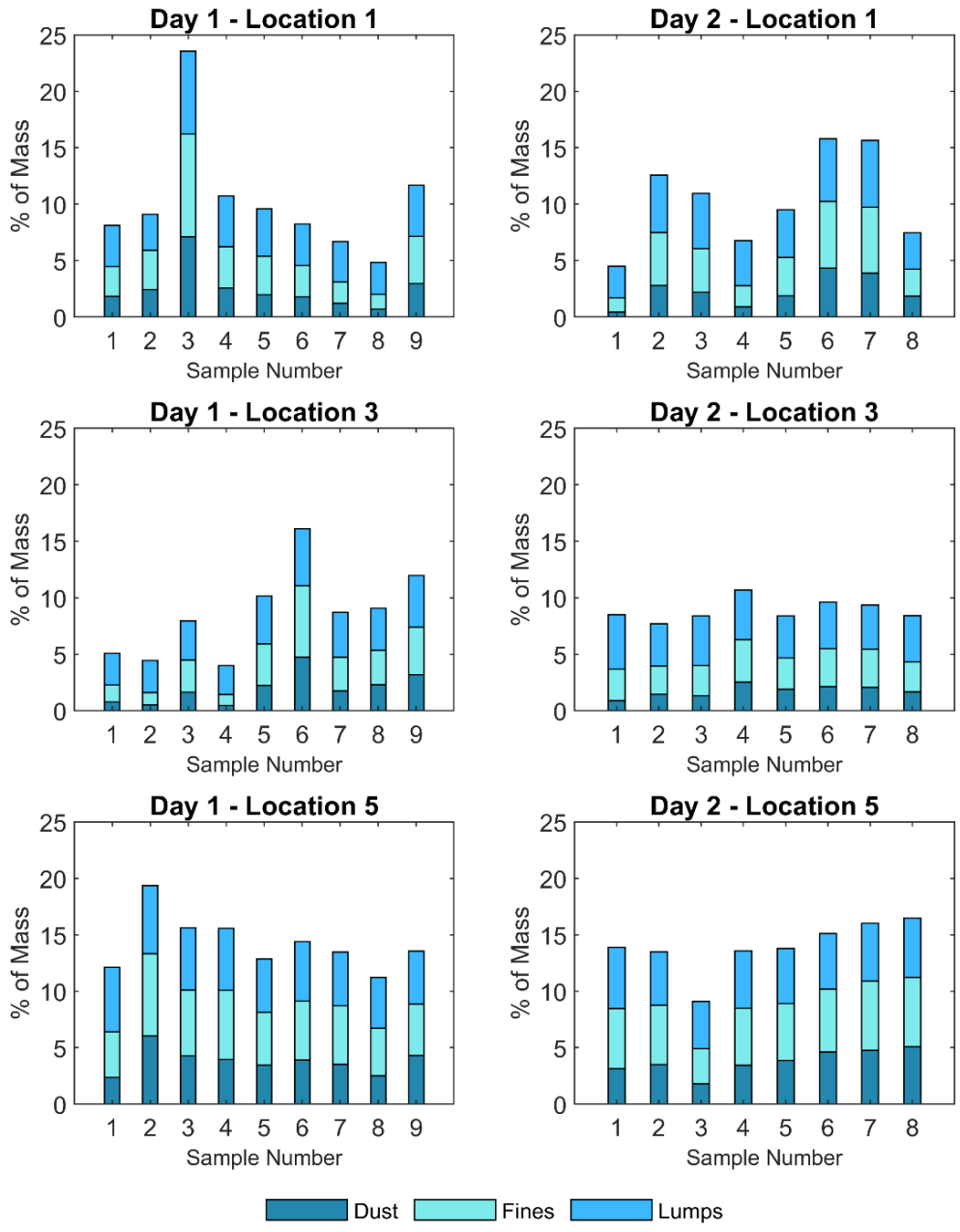

Figure 5.9: Sieving analysis at locations 1 (first barge), 3 (end of the first conveyor), and 5 (end of the second conveyor). The sample numbers correspond to the sampling order.

Table 5.4: Average share of categorized particles at locations 1, 3, and 5 on the first and second days of sampling (%). Numbers in parentheses show the standard deviations.

Location	Sampling day	Particles < 5.6 mm	3.15 <particles< 5.6 mm	Particles < 3.15 mm	Particles < 1 mm
1 (first barge)	1	10.28 (5.08)	4.17 (1.24)	6.11 (3.87)	2.50 (1.75)
	2	10.40 (3.86)	4.47 (1.09)	5.93 (2.89)	2.27 (1.26)
3 (end of first conveyor)	1	8.61 (3.68)	3.70 (0.81)	4.91 (2.89)	1.95 (1.31)
	2	8.87 (0.89)	4.14 (0.36)	4.73 (0.87)	1.74 (0.49)
5 (end of second conveyor)	1	14.24 (2.28)	5.19 (0.51)	9.05 (1.94)	3.81 (1.03)
	2	13.93 (2.12)	4.95 (0.35)	8.98 (1.85)	3.77 (0.99)

A similar trend to that for fines and dust (< 3.15 mm) is observed for all small particles (< 5.6 mm) as well, since the ANOVA analysis shows significant differences between the percentages of these by sampling location. The average proportion of small particles (< 5.6 mm) on days one and two was 10.33% at location 1 (first barge), 8.73% at location 3 (end of the first conveyor), and 14.09% at location 5 (end of the second conveyor). This indicates that a significant quantity of small particles (< 5.6 mm) is generated at least after the first sampling point in the system.

One interesting result is the reduction in the number of small particles (< 5.6 mm) after the pellets are grabbed and discharged onto the first conveyor, i.e. between locations 1 and 3 (Table 5.4). The proportion of small particles decreased relatively between these two locations by up to 16.24% on the first day and 14.71% on the second day. There are two explanations for this. Firstly, a number of small particles escaped from the grab into the air while the grab was loading in the barge and shifting upwards towards the hopper. Secondly, the dust filters at the beginning of the first conveyor removed some dust; however, the accumulated dust in those filters was not measured in this study. On the other hand, by comparison with location 3 (end of the first conveyor), the average proportion of small particles (< 5.6 mm) at location 5 (end of the second conveyor) increased from 8.61% to 14.24% on the first day and from 8.87% to 13.93% on the second day, showing a relative increase of 65.74% and 57.04%, respectively. Assuming that the effect of conveyor vibrations on the generation of small particles (< 5.6 mm) is negligible, all of these extra ones must have been generated due to the vertical free fall of 7.8 m at the transfer point between the two conveyors. Boac et al. [143] observed an average increase of 3.83% in the number of particles smaller than 5.6 mm in one transportation cycle of feed pellets

in a bucket elevator and silo feeding system for pellets with the durability of 92.9% and a nominal pellet diameter of 6.4 mm. In this study, however, an average 5.36% increase in the number of particles smaller than 5.6 mm was observed solely due to a free fall of 7.8 m. This is probably related to the compression and impact forces associated with the amount of material being transported, which was around 450 ton.h^{-1} in the present study and 54.9 ton.h^{-1} in [143].

The results show that the average proportion of small particles at location 2 (second barge) was 6.56%, with a 1.51% standard deviation. This was lower than the figure for location 1 (10.34%). During grabbing from the first barge to the second one, it was observed that a portion of small particles was released from the grab due to leakage. Because of this, the measured small particles are not representative for the whole particles and the effect of grabbing on the generation of small particles remains unclear.

Figure 5.10 shows the percentage of small particles at location 4 (automatic sampler) on the third day: 6.05%, with a standard deviation of 2.04%. As discussed earlier in this section, the results from the first two days show high repeatability in terms of generating small particles at each sampling location. Therefore, the share of small particles at each location on days one and two can be postulated to be similar to that on the third day. Based on this assumption, the results for the first and second days at location 3 (end of the first conveyor) can be compared to the results for the third day at location 4 (automatic sampler). The average proportion of small particles at location 3 on the first and second days was 8.73%, while at location 4 it was 6.05%. Thus, on average, the number of small particles decreased between these two locations by 2.68%, showing that the automatic sampler (location 4) does not produce similar particle size distributions when compared to location 3. A possible reason for this is the segregation of bigger particles due to the rotation of particles in the rotary divider, which separates larger particles from the smaller ones in such a way that the latter are rejected as residues (see Figure 5.2).

The average percentage of small particles (< 5.6 mm) at location 6 (silo) is shown in Figure 5.10. On average, these made up 4.00% of the samples taken from the silo hatches. Comparing the proportion of small particles here with that at location 5 (end of the second conveyor), it can be concluded that the whole pellets accumulated at the silo walls. This can be explained by percolation segregation, whereby the smaller particles are captured in the voids and bigger ones move down the slope towards the walls [74].

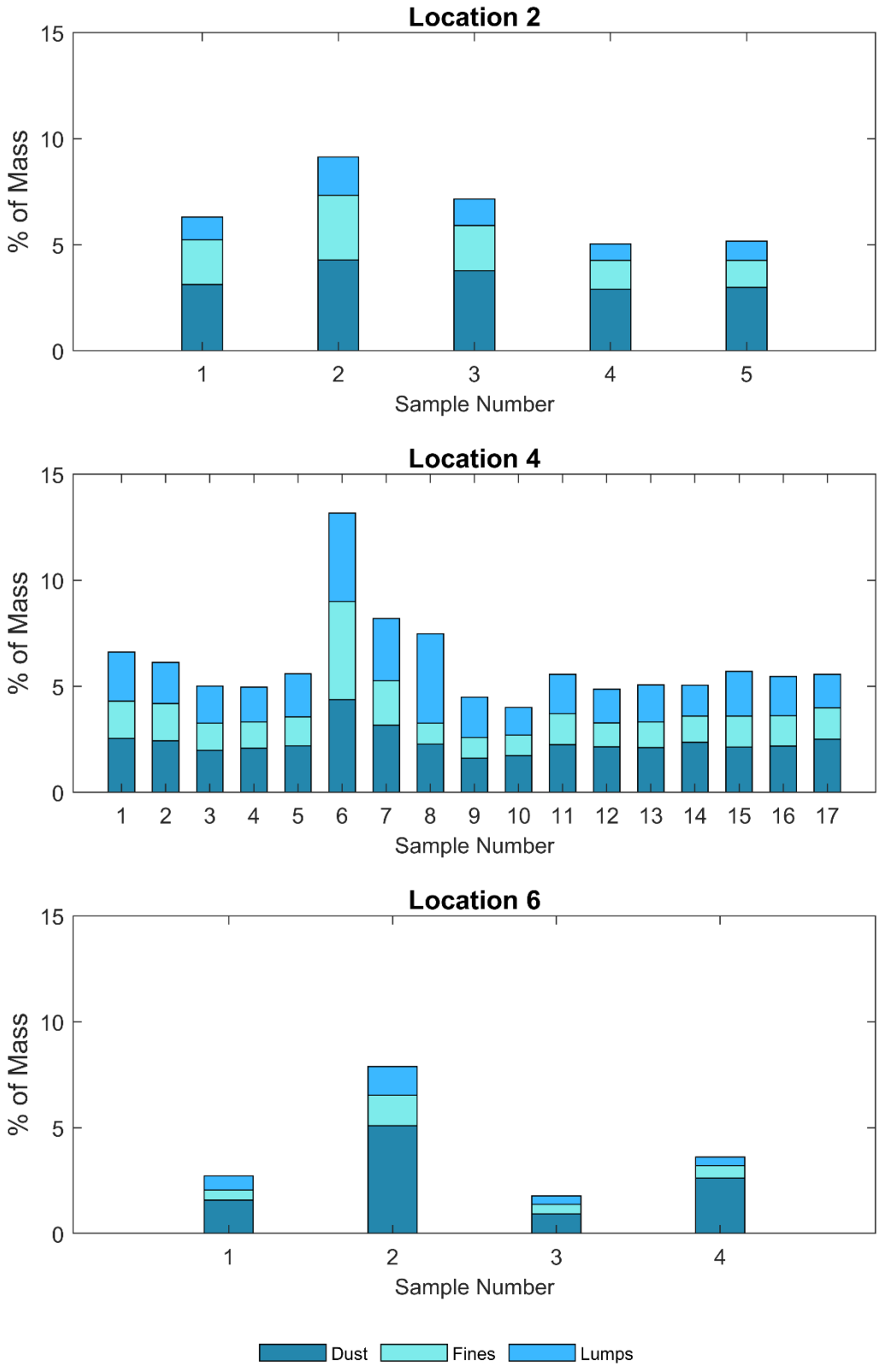

Figure 5.10: Share of small particles at locations 2, 4, and 6.

Thomas [136] showed that pellet fragmentation and attrition are the two major mechanisms for the physical degradation of pellets. Figure 5.11 shows the share of lumps, fines, and dust in all the samples taken from different locations and includes a surface fit that is the best least square fit plane for all the samples. Although the breakage mechanism was not studied in this work, Figure 5.11 shows that the shares of dust, fines, and lumps at different locations and on different sampling days are correlated to one another while the share of dust can be obtained via equation (5.2) with an R^2 value of 0.829. In other words, in all samples, the quantity of dust particle was increased by increasing the proportion of lumps and fines.

$$d = 1.44 - 0.6017\ (f) + 1.029\ (l), \tag{5.2}$$

where d, f, and l, represent the percent of dust, fines, and lumps, respectively.

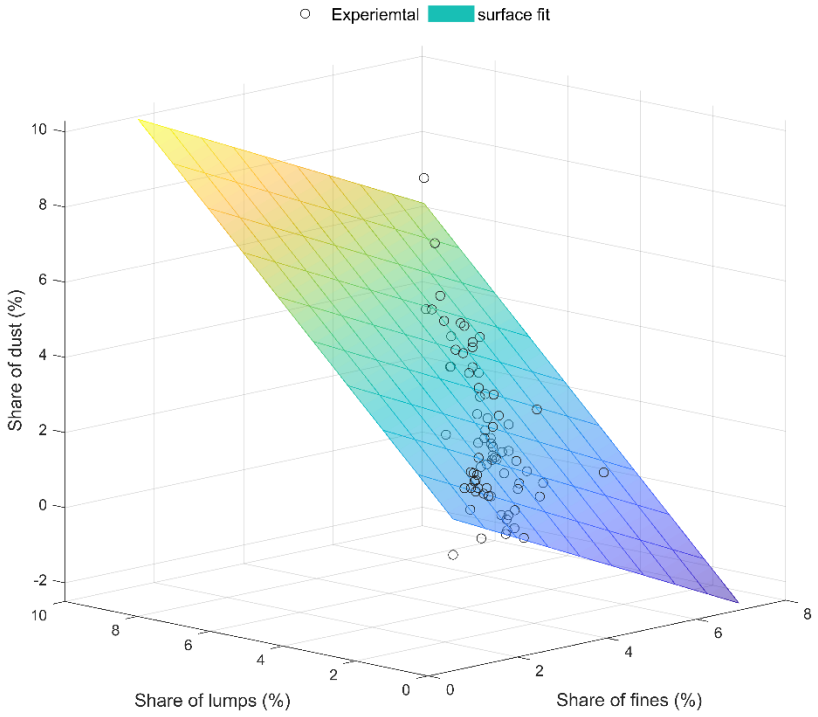

Figure 5.11: Correlations between classified small particles.

5.5 Conclusions

In this study, we have investigated the change in the physical properties of commercial wood pellets with a focus on breakage and attrition behavior during large-scale (~450 ton.h^{-1}) transport and storage in a pellet-fired power plant in the Netherlands. Our main conclusion is that transferring the wood pellets with average mechanical durability of 97.6% (based on ISO standard 17831-1) via a free fall from a height of 7.8 m (the transfer point between two conveyors) increases the proportion of small particles (< 5.6 mm) from 8.74% to 14.09%, on average, and the amount of fines and dust

from 4.82% to 9.01%. This emphasizes the importance of equipment design and operation with respect to material degradation. The mechanical durability of the samples taken at different locations differed by up to 7.9%, while no correlation was observed between moisture content, bulk density, sampling location, or day of sampling and mechanical durability. This suggests that other properties—most probably pellet length distribution—play a significant role in the measured mechanical durability value.

6 Effect of Temperature and Humidity Variation on the Quality Parameters of Pellets*

In the previous chapters, we focused on the physical degradation of pellets. In this chapter, however, the goal is to assess the effect of the most influencing factors on the chemical properties of pellets. The literature reflected in chapter 2 indicated that moisture content and temperature are the most influencing factors on the quality parameters of pellets.

In this chapter, we investigate the effect of varying temperature and relative humidity on the properties of pellets with a focus on moisture uptake and energy content. Three types of biomass pellets were placed in various environmental conditions from -19 to 40ºC and 50 to 85% relative humidity to represent different environmental conditions in different regions and seasons.

*This chapter is based on Hamid Gilvari, Luis Cutz, Urša Tiringer, Arjan Mol, Wiebren de Jong, and Dingena L. Schott. "The Effect of Environmental Conditions on the Degradation Behavior of Biomass Pellets." polymers 12, no. 4 (2020): 970.

6.1 Introduction

Biomass has shown a great potential to meet a significant share of the energy demand in the near future, as one of the main sources of renewable energy [169]. In 2018, up to 10% of the total world energy demand was provided by biomass [2], while it has been estimated that up to 18% of the world's primary energy demand can be provided only by woody biomass in 2050 [169]. The huge increase in the use of biomass, in particular solid biomass, has raised concerns regarding its transport, storage, and handling due to the inherent low bulk and energy density and high moisture content [141]. The combination of torrefaction and densification is proved to increase the bulk and energy density and decrease the moisture content of raw biomass [137]. Torrefaction is a thermochemical treatment process in which biomass is heated at a temperature of 200–300°C in an oxygen-free environment and results in partial decomposition of biomass and removes different types of volatiles such as carbon dioxide, carbon monoxide, methane, steam, etc. [170], [171]. Pelletization is a type of densification process in which biomass is compressed into cylindrical holes and it produces pellets with a typical diameter of 3–27 mm and length of 3–31 mm [137]. The global production of biomass pellets has increased more than threefold during the last decade and reached 55.7 million tons, in 2018 [104]. The main intercontinental trading of pellets takes place between America and Europe. Up to 7.6 million tons of biomass pellets were traded from the USA and Canada to Europe for bioenergy purposes in 2018 [104]. The UK, Denmark, and Italy play a key role in the European biomass pellet import [104].

Large-scale transportation of pellets is mostly performed in bulk. For instance, pellets that are imported from North America to Europe are shipped using large-scale vessels over the Atlantic ocean [172]. This journey may take a few weeks or a couple of months, depending on the origin, final destination, and terminal time plans [173]. Furthermore, pellets could be stored over weeks before their final use at the end-user storage facilities. In all steps, transport, storage, and handling, pellets are exposed to several mechanical forces (compression, tension, and impact) and drastic changes in temperature and relative humidity (RH), which result in pellet breakage and dust generation, moisture uptake or release, and changes in the calorific value [124], [132], [174], [175].

On the other hand, raw biomass is prone to adsorb and absorb moisture from the environment [175] due to the nature of its fibrous structure and presence of hydroxyl groups in the polysaccharides [173], [175]. Hereafter, the moisture adsorption and absorption processes will be referred to as moisture uptake. Regained moisture content reduces the mechanical strength

of the pellets and affects the heating value [176]. Additionally, pellets with high moisture content tend to produce more fines and dust during transport, storage, and handling activities [175], which in turn increases the risk of self-ignition, results in loss of a notable portion of bulk and may cause equipment blockages [141], [174]. Moreover, this also creates health problems for people exposed to these conditions [142]. However, the quality parameters of pellets may change due to variations in environmental conditions. The most relevant quality parameters of biomass pellets in terms of handling, storage, and combustion are the heating value, moisture content, volatile matter, ash content, bulk density, the amount of fines and dust, and mechanical strength [10]. The term “fines and dust” refers to the small particles which are generated either immediately after production or during transport, handling, and storage. The size of the fines and dust may be different in literature, however, the particle size of smaller than 3.15 mm is a global standard based on ISO standard 17831-1 [107] for determination of mechanical durability, which is the most common way to determine the mechanical strength of bulk of pellets. According to ISO standard 16559 [106], mechanical durability is defined as "the ability of densified biofuels units (e.g. briquettes, pellets) to remain intact during loading, unloading, feeding, and transport". The mechanical durability may be measured using different methods; however, it is usually defined as the mass of fines and dust generated during the experiments to the initial mass of pellets multiplied by 100. The heating value refers to the released energy of the material after combustion. Table 6.1 presents the effect of storage conditions on some quality parameters of interest of biomass pellets in different storage conditions as published in prior literature.

Table 6.1: Literature review of the quality parameters of biomass pellets after storage.

Type of pellets	Quality parameter	Assessment method	Storage conditions	Storage time	Key results	Ref
Pellets from sawdust, logging residues, and bark	Mechanical durability, Moisture, LHV [a]	6 kg of pellets in an octagonal tumbler, fines were sieved using a 3 mm sieve	20ºC and RH of 85–90%	5 months	• 11% increase in moisture uptake • Lower mechanical durability value • No change in the heating values	[174]
White and steam exploded pellets made of softwood and hardwood chips	Mechanical durability	100 g of pellets tumbled in a Dural (II) tester; fines were sieved using a 4.75 mm sieve	Outdoor uncovered or outdoor with covered roof	20 months	• 82% drop in the mechanical durability of steam-exploded pellets stored outdoor and 3% drop for white pellets stored indoor	[132]
Untreated and thermally treated birch and spruce pellets	Mechanical durability	ISO standard 17831-1	Outdoor under cover and uncovered	5 months	• High moisture uptake tendency for pellets stored uncovered • Mechanical durability decreased highly in uncovered storage conditions for up to 26% for torrefied pellets and up to 6% for steam explosion pellets • Untreated pellets were totally disintegrated after uncovered storage	[175]

Type of pellets	Quality parameter	Assessment method	Storage conditions	Storage time	Key results	Ref
Canola pellets	Mechanical durability	ISO standard 17831-1	Enclosed shed	48 weeks	• Small changes in the mechanical durability	[124]
Wood pellets	LHV	NA*	15–25ºC	180 days	• Increase in calorific value due to a decreased moisture content	[176]
Softwood pellets	EMC [b]	Weight difference	Up to 93% RH 22ºC	10 days	• Linear correlation between the EMC and RH between 15 and 80%	[177]
Spruce, Pine, and mixed biomass pellets	EMC	Weight difference	20–90% RH 15 to 25ºC	4-8 days	• Temperature has a negligible effect on EMC • -EMC at high RH depends on pellet type	[178]
Biomass, Cotton stalk, and woody saw mill	EMC	Weight difference	20–80% RH	-	• No difference in EMC of different biomass types at storage up to 70% RH	[179]
Latin species [c]	EMC	Weight difference	40–85% RH	-	• RH and EMC relationships were similar for all biomass samples	[180]
Torrefied wood pellets	EMC	Weight difference	90% RH 30ºC	25 h	• The higher the torrefaction degree, the lower the moisture uptake	[85]

Type of pellets	Quality parameter	Assessment method	Storage conditions	Storage time	Key results	Ref
Softwood pellets Torrefied mixed wood Steam exploded pellets	Mechanical durability	100 g of pellets tumbled in a Dural (II) tester, fines were sieved using a 4.75 mm sieve	Various RH and Temperatures	Up to 18 days	• Decreased mechanical durability up to 14% for steam exploded pellets and 70% for white pellets at 90%RH and 30ºC	[133]
8 different biomass pellets	Mechanical durability	ISO standard 17831-1	-28ºC	5 days	• Change in mechanical durability was negligible for pellets with high durability, while for pellets with a lower durability, there was a notable decrease in mechanical durability	[115]
Cedar wood pellets	Hardness	Meyer hardness	30–90% RH 30–70ºC	5 days	• Hardness decreased by increasing the RH and temperature	[181]
Wood and torrefied biomass	Dry matter loss	NA	95% RH 22ºC	20 days	• White wood is more prone to biological degradation in compare to torrefied pellets	[84]
	Mechanical durability, EMC	ISO standard 17831-1	Outdoor	1 year	• Torrefied pellets show less tendency to uptake moisture than wood pellets • Outdoor storage is unsuitable for torrefied pellets	

Type of pellets	Quality parameter	Assessment method	Storage conditions	Storage time	Key results	Ref
Pine and recycle wood	Mechanical strength	Three-point bending test	20–95% RH 30ºC	4 days	• Linear relationship between EMC and RH • Bulk density and flexural stress decreased with an increased RH	[182]
	EMC	10 g of a sample heated at 105ºC for 25 minutes				
	Bulk density	Using a standard 1 L container				

[a] Lower heating value
[b] Equilibrium moisture content
[c] Sorghum stalk, corn stover, wheat straw, and big bluestem
[*] Not avaiable

Although it is known from previous studies (Table 6.1) that uncovered open storage (with direct rain exposure and sunshine) degrades the pellets significantly, [84], [132], [174], there is not yet a clear guideline for the effect of covered environmental conditions (without a direct rain exposure) on the pellet quality. As shown in Table 6.1, there are limited sources in the literature addressing the changes in mechanical durability of biomass pellets using the ISO standard 17831-1 [107] as a global baseline and heating values in various controlled temperature and RH conditions. This chapter studies the influence of a wide range of controlled storage conditions (temperature, RH, and storage time) on the EMC, higher heating values (HHV), and mechanical durability of raw wood and torrefied biomass pellets in bulk. Different storage conditions were designed and executed to mimic various local weather conditions in North America and the European region as the main biomass pellet trade happens between these two regions. The main novelty of the present work is to evaluate the effect of sudden changes in the temperature and RH on the pellet properties. This was done by the immediate change in the temperature and RH of the storage conditions from freezing temperature to high temperature and RH and vice versa.

6.2 Materials and Methods

6.2.1 Materials and measurements

Two types of commercially produced wood pellets and one type of torrefied pellets were studied in this work. The wood pellets were provided from local shops in the Netherlands where their main application was residential heating. Both types of wood pellets were bought in sealed plastic bags of 10 kg. The sealed bags prevented any moisture uptake to the pellets before starting the experiments. Since the wood pellets were different in color (brown and white), hereafter, we refer to them as brown pellets and white pellets. The brown pellets were made of softwood residues from the wood industry and certified ENplus A1 [183]. The white pellets were also made of sawdust from the wood industry, but their origin was not disclosed. The torrefied pellets were produced in the UK in a pilot-scale production facility. No information about the densification or torrefaction process for the tested pellets was disclosed.

The proximate analysis of the samples is shown in Table 6.2. Proximate analysis was determined using a thermogravimetric analyzer (TGA, Thermal Advantage SDT Q600) for determination of fixed carbon and a muffle furnace (Nabertherm L3/12, USA) for determination of moisture and ash content. Ash and moisture determinations were performed according to the standards EN 14775 [184] and ISO 18134-2 [131], respectively. Fixed carbon content was

determined by the difference between the final residual mass of the TGA experiments and the ash content. Finally, the volatile content was determined by the difference of 100 from the sum of moisture, ash, and fixed carbon. For the TGA runs, 15 mg of samples were placed in an alumina cup in the apparatus and the purge flow rate was set at 50 mL.min^{-1}. Experimental runs were performed in an inert nitrogen atmosphere. The TGA runs were executed at a heating rate of 20ºC.min^{-1} up to 900ºC.

The pellet diameter was measured using a digital caliper according to EN standard 16127 [130]. To measure the pellet density, the ends of pellets were sanded to have a uniform surface. Then the pellet length was measured using a digital caliper. The volume of each pellet was calculated based on diameter and length. The weight of each pellet was measured by using a laboratory balance (Model: Mettler Toledo (model PG 1003-S),±0.001 g precision). Finally, the pellet density was calculated by the division of pellet weight to its volume. The pellet density measurement was repeated five times for each pellet type. The bulk density was measured according to the EN standard 15103 [81], using a 5 L cylindrical container.

Before starting the experiments, pellets were kept at laboratory conditions of 20±1°C and RH of 60±4%. Temperature and RH were monitored at different time intervals between one day and one week. We characterized the degradation of pellets by the change in the moisture content, HHV, and mechanical durability.

The moisture content before storage and the EMC after storage for each pellet type at each storage condition was measured according to EN 14774 [166], by placing 300 g of the sample pellets into an oven at 105°C for 24 hours. The EMC ratio (EMC_{ratio}) was calculated using equation (6.1):

$$EMC_{ratio} = \frac{EMC_{AS}}{\mathrm{MC_{AR}}}, \tag{6.1}$$

where EMC_{AS} is the equilibrium moisture content of pellets after each storage condition and $\mathrm{MC_{AR}}$ is the as-received moisture content of pellets.

The HHV was measured using a bomb calorimeter (Parr 6772, Parr Instrument Company, USA), using 1 g of the sample pellets following the BS 1016-5 standard [185]. The measurements of moisture content and HHV were repeated twice and the reported value is the average of the two replications. Table 6.2 summarizes the properties of the pellets studied in the present work before storage, i.e. “as-received”.

The mechanical durability was measured according to ISO standard 17831-1 [107], using a tumbling can. First, a random sample of materials was sieved with a round hole sieve size of 3.15 mm, and 500±10 g was weighed and placed into the tumbling can. The device was then rotated at a rotational speed of 50 rpm, for 10 minutes to reach a total of 500 rotations. Finally, the materials were sieved again, using the same sieve to remove the fines and dust from the sample. The mechanical durability (DU) was calculated using equation (6.2):

$$DU = \frac{m_a}{m_b} \times 100, \tag{6.2}$$

where m_b is the mass of the sieved samples before executing the mechanical durability test and m_a is the mass of the sieved samples after the mechanical durability test. The reported mechanical durability results are the mean value of duplicate measurements according to ISO standard 17831-1 [107]. The as-received mechanical durability of the pellets studied in this work is given in Table 6.2.

Table 6.2: As-received properties of pellets used in this study.

Pellet properties	Brown pellets	White pellets	Torrefied pellets
Diameter (mm)	6.1±0.1	6.4±0.1	6.0±0.0
Density (kg.m^{-3})	1209±60	1169±32	1304±40
Bulk Density (kg.m^{-3})	660	600	660
HHV (MJ.kg^{-1})	21.2	20.5	17.8
Mechanical durability (%)	98.6	96.9	92.7
Proximate analysis			
Moisture content (%)	7.2	8	9.3
Ash content (%)	0.7	0.7	16.7
Fixed carbon (%)	17.7	17.9	16.0
Volatile matters (%)	74.4	73.0	58.0

6.2.2 Storage conditions

Pellets were placed in different storage facilities: four climate rooms, one industrial climate chamber, and one home application freezer. A summary of the storage conditions is provided in Table 6.3. We defined a storage identification code to indicate the temperature and RH in each of the storage facilities. For example, in the storage code “T-19_RH90”, the number next to “T” denotes the temperature (°C) set at the storage facility, while the number after “RH”

indicates the relative humidity (%) set for each storage experiment. The conditions in the storage facilities were set to simulate different weather conditions, from freezing temperature to high temperature and high RH. The maximum temperature and RH chosen for this study were 40°C and 85%, respectively, since higher temperature and humidity values may cause significant off-gassing [186] and physical disintegration to the pellets [177].

Table 6.3: Summary of the temperature and RH of the climate chambers.

Storage code	Storage type	Temperature (°C)	RH* (%)	Example countries
T-19_RH90	Freezer	-19	90	Sweden, Norway, Finland, Canada
T5_RH86	Climate room	5	86	The Netherlands, Germany, France
T20_RH50	Climate room	20	50	
T20_RH65	Climate room	20	65	Italy, Portugal, Poland, the UK
T20_RH80	Climate room	20	80	
T40_RH85	Climate chamber	40	85	Spain, USA, Brazil

*Relative humidity

Temperature and RH of the climate rooms were controlled every 2 minutes to ensure a constant temperature and RH. The climate chamber (Model: C+10/600-CTS, Germany) was used only for 40°C and 85% RH storage conditions. A freezer (Whirlpool, USA) was used for the storage under freezing conditions. The temperature and RH inside the freezer were monitored once a week using a digital thermometer and an analog humidity gauge, respectively. All the storage conditions were kept constant except the RH in one of the climate rooms (T5_RH86) where it was arbitrary varied between 72 to 100% (data is shown in Figure B. 1). Therefore, to refer to this storage condition, we use the average RH between the minimum and maximum value, which is 86.

Besides, the effect of storage time was studied for two storage durations, 7 and 30 days, respectively. The maximum storage time was chosen to mimic the duration of travel from the most common pellet exporter ports (e.g. port of Vancouver) to the EU region (e.g. port of Rotterdam). Storage time was calculated based on the average speed of bulk carriers and the distance between ports. According to Magelli et al. [172], the average speed of bulk carriers is 10 miles.h^{-1}. Considering that the distance between the port of Vancouver and the port of Rotterdam is 7170 miles, the whole journey takes around 30 days. On the other hand, 7 days of

storage is set to mimic the shorter storage periods, such as storage at the processing plants after production or at the end user's location.

Inside each storage facility, two batches of 500 g pellets from each pellet type were placed in an aluminum tray without cover (Figure 6.1). This has been done for each storage time. In total, 76 batches of pellets (38 kg) were stored at different storage facilities.

Figure 6.1: Pellets on aluminum trays in the climate chamber. This figure is an example showing the pellets on aluminum trays. The same trays were used for the other storage conditions.

Two approaches were taken to study the effect of sudden changes in temperature and RH on the properties of the pellets, defrosting, and frosting. First, defrosting was studied by storing the pellets in a freezer (T-19_RH90) for 30 days. Then, pellets were transferred (within 30 minutes) to the climate chamber at 40°C and 85% RH (T40_RH85) to be stored for another 30 days. Vice versa, for the frosting experiment, we first stored the pellets in the climate chamber at T40_RH85 and then, in the freezer (T-19_RH90). Therefore, the total storage time for either defrosting or frosting conditions was 60 days.

6.3 Results and discussion

6.3.1 Moisture uptake

Figure 6.2 presents the EMC ratio of different types of pellets stored for 7 days and 30 days, at different storage conditions. Results for the EMC ratio indicate that all pellets are already saturated after 7 days, except for T5_RH86 for all pellets, T20_RH65 in the cases of brown pellets, and T40_RH85 in the case of white pellets. In the case of T5_RH86, as showed in section 6.2.2, the RH varied between 72 and 100%, varying RH seems to be the main reason for non-uniform EMC after 7 days. For the other two cases, the reason has to be further studied; however, the difference in both cases is 0.11% in the EMC ratio.

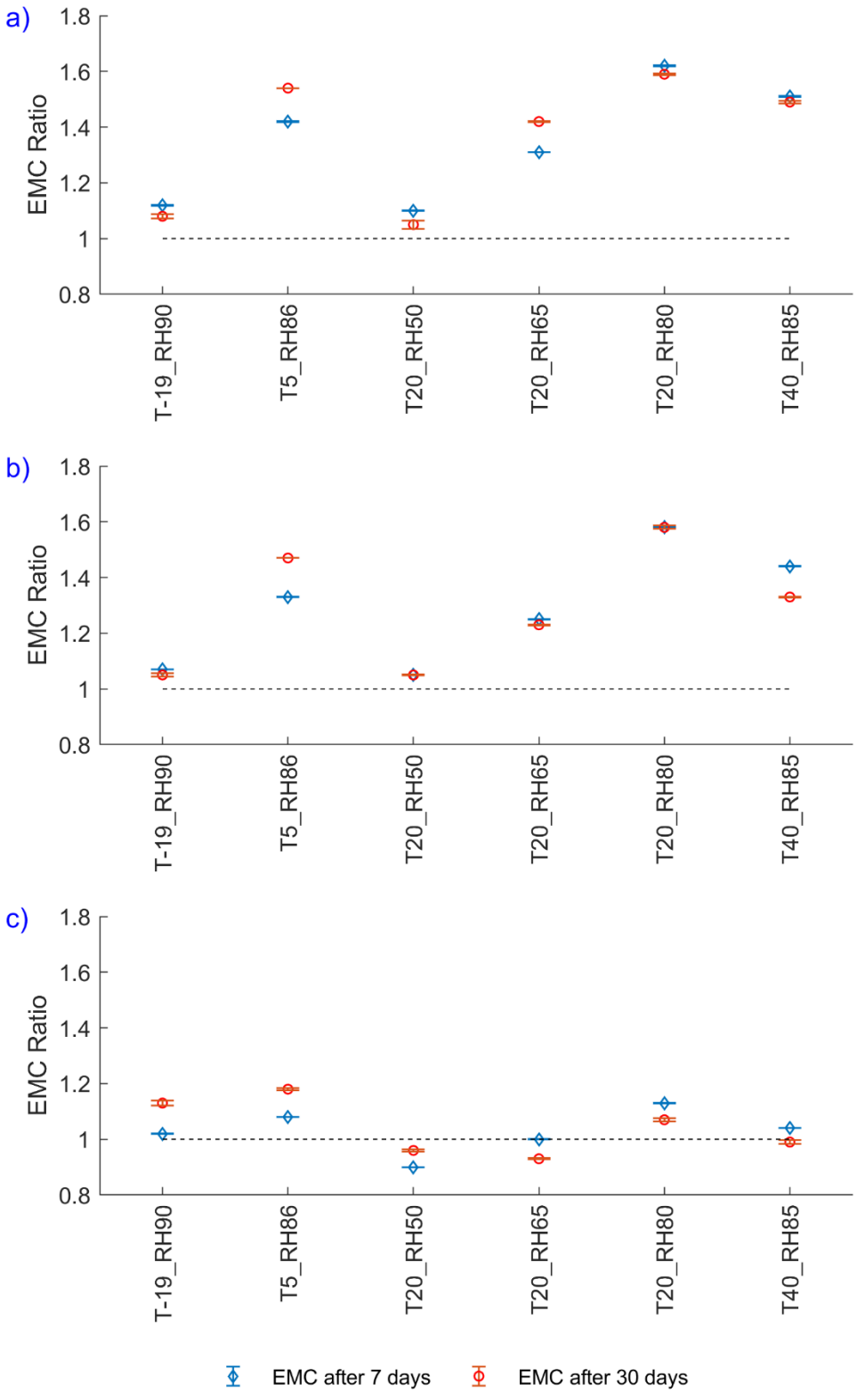

Figure 6.2: EMC ratio of pellets after 7 and 30 days of storage for (a) brown, (b) white, and (c) torrefied pellets. The error bars show the standard deviation and the dashed lines show the EMC for as-received pellets.

Lee et al. [176] reported that the EMC is reached after 20 days for wood pellets at temperatures of 25, 35, and 45°C and Peng et al. [85] reported that the saturated moisture uptake is reached after 10 h for regular and torrefied pellets at a temperature of 30°C and RH of 90%. Although it is challenging to compare the saturation time of different types of pellets due to variations in biomass origins, from the results of this study, it can be concluded that the EMC may remain constant at least after 7 days of storage. The EMC results show that torrefied pellets are more hydrophobic than wood pellets. Similar results have been reported before [124], [132], [133], [174], [175]. Moreover, we observed a clear relationship between the EMC of wood pellets and RH at a constant temperature of 20°C. The experimental data at 20°C were modeled with the Oswin model (equation (6.3)), which is shown to be an accurate model for the sorption isotherms of biomass pellets [178]:

$$MC = a.\left(\frac{\frac{RH}{100}}{1-\frac{RH}{100}}\right)^{b}, \tag{6.3}$$

where MC is the moisture content, RH is the relative humidity, and a and b are the model constants. The results show a high correlation between the EMC and RH of pellets at 20°C with R^2= 0.900 for brown pellets and R^2= 0.997 for white pellets (Figure B. 2). Herein, for wood pellets at T20_RH80 and T40_RH85, we observed that an increase in both temperature and humidity decreases the EMC of brown pellets up to 0.71 % and white pellets up to 1.96% with regard to the as-received moisture content. On the contrary, increasing the temperature from 5 to 20°C results in a slight increase in the EMC of brown and white pellets up to 0.38% and 0.87%, respectively. This suggests a threshold in the temperature for the highest moisture adsorption phenomena (here at 20°C), however, more data is required to confirm this. Furthermore, when wood pellets are stored at lower temperatures compared to ambient conditions, for example at T-19_RH90 and T20_RH50, the moisture uptake is very low. This can be explained as a combination of low relative humidity (T20_RH50) and decreased movement of water molecules at low temperatures (T-19_RH90) [187]. These findings are consistent with observations made by He et al. [187].

The EMC ratio after defrosting and frosting in the storage conditions was higher as compared to the EMC in the single storage conditions. EMC ratio increased up to 1.75 for brown and 1.69 for white pellets after defrosting and 1.77 for brown and 1.74 for white pellets after frosting.

Considering the stable EMC ratios after 7 days, it is concluded that the higher EMC at defrosting and frosting conditions might be due to a change in the pellet structure which we noticed by visual observations indicating an increased number of cracks at the surface of pellets rather than due to the long storage time. Moreover, Graham et al. [132] observed the increased number of surface cracks generated and surface propagation in pellets after six months of outdoor storage.

The fluctuations in the standard deviations of the EMC (Figure 6.2) suggest that other parameters may also play a role in the results. For example, Whittaker and Shield [160] stated that the main moisture adsorption occurs at the ends of the pellets because, in the pelletization process, the outer layer faces the highest heating rate resulting in plasticizing and binding of materials to create a polished surface, which in turn preserve the pellet to uptake moisture from the environment. Obviously, the higher the number of particles per batch implies the higher the number of pellet ends. Therefore, the moisture uptake capacity may change due to the number of pellets in a batch. Moreover, existing cracks in the as-received materials may increase the moisture uptake capacity. This requires further studies. Although the number of pellets in each batch was not counted in this study, it may explain the fluctuations in EMC results.

6.3.2 Higher heating values (as-received)

Figure 6.3 shows the HHV values of three types of pellets after storage at different storage conditions after 30 days of storage. Note that the HHV was not measured after 7 days of storage.

Before storage, the HHV values for brown, white, and torrefied pellets were 21.2, 20.5, and 17.8 $MJ.kg^{-1}$, respectively. Note that the HHV of torrefied pellets is lower than the HHV of wood pellets due to the presence of a high amount of ash in the torrefied pellets (Table 6.2). Results from Figure 6.3 show that HHV decreased after 30 days of storage regardless of the storage conditions tested in this study. This may not be only due to the moisture uptake, but also due to potential oxidation of unsaturated fatty acids, as stated by Wang et al. [181]. However, the amount of fatty acids in this work has not been measured. Considering all the storage conditions, the reduction in the HHV for brown pellets was between 5.1 to 10.5% (on average 6.0%), for white pellets between 2.2 and 5.3% (on average 3.5%), and torrefied pellets between 1.6 and 5.9% (on average 3.5%) after 30 days of storage.

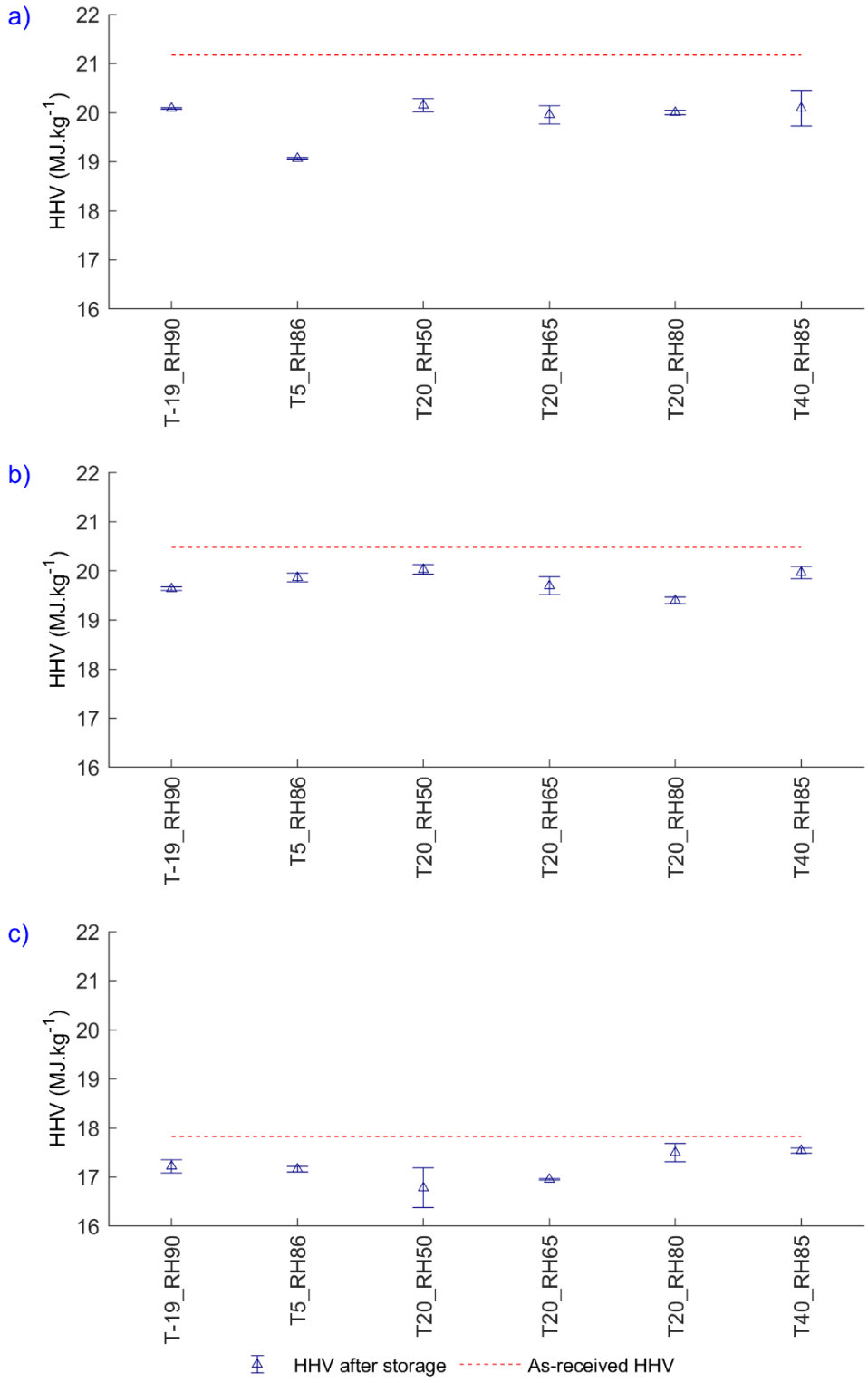

Figure 6.3: HHV of (a) brown, (b) white, and (c) torrefied pellets at different storage conditions after 30 days of storage.

Figure 6.4 shows the HHV values with respect to the EMC values for all pellets at different storage conditions including defrosting and frosting conditions. The reduction of the HHV after defrosting was up to 5.7% for brown and 5.3% for white pellets. Meanwhile, for frosting conditions, the HHV decreased up to 4.9% for brown and 6.1% for white pellets. Therefore, defrosting or frosting conditions did not result in a higher reduction of HHV compared to storage at one controlled temperature and RH. Besides, no correlation between the EMC and the HHV was found for all pellets.

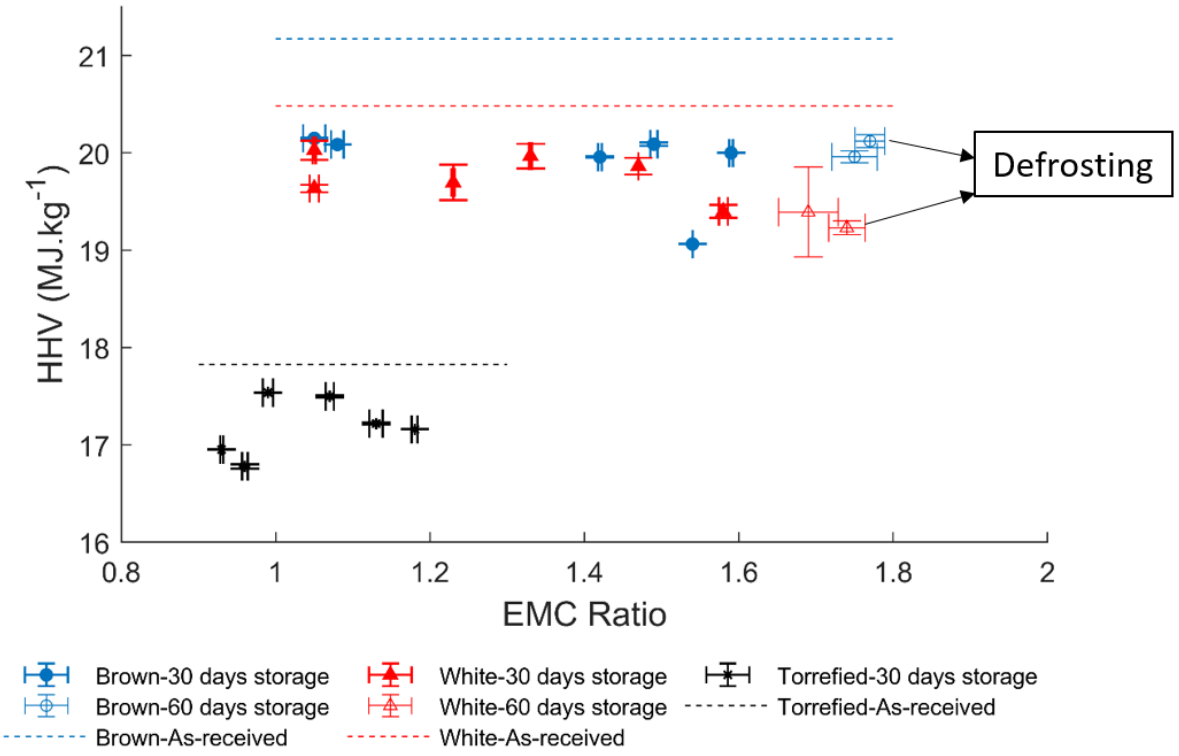

Figure 6.4: HHV versus EMC of pellets after 30 and 60 days of storage at different storage conditions.

6.3.3 Mechanical durability

The results of the mechanical durability tests at different storage conditions are shown in Figure 6.5. The solid lines show the as-received mechanical durability values including the error bars at the ends of the lines showing the standard deviations and the dashed-lines show the repeatability limit, which will be defined and explained later in this section. As shown in Figure 6.5, the as-received mechanical durability for both wood pellets show negligible standard deviations while for torrefied pellets the standard deviation is 1.1%. This might be attributed to the wide heterogeneity in the structure of torrefied pellets, which may result in different

amounts of fines generated. Even if pellets of the same type are produced under the same conditions, the structure of pellets may significantly differ (Williams et al. [123]).

For white and brown pellets, mechanical durability was affected mostly when the RH was equal or higher than 80% at a temperature above 20°C (Figure 6.5). This occurs due to extended storage and breakage of local bonds in the pellet structure at elevated temperature and RH. By increasing the temperature, water molecule mobility increases [187], so they can diffuse freely within the pellet destroying the pellet structure. The maximum reduction in mechanical durability was up to 1.2% for brown, 2.0% for white, and 1.3% for torrefied pellets after 30 days of storage.

Defrosting and frosting experiments result in a higher reduction of the mechanical durability of wood pellets. According to the results presented in Figure 6.5, defrosting the pellets at 40°C and 85% RH decreased the mechanical durability values up to 2.5% for brown and 4.3% for white pellets. On the other hand, frosting the wood pellets (pellets moved from storage at 40°C and 85% RH to -19°C and 90% RH) changes the mechanical durability values up to 1.3% for brown and 3.8% for white pellets. Therefore, defrosting the pellets proves more detrimental for the mechanical durability of wood pellets in comparison with frosting. Moreover, these results can also confirm the results presented in section 3.1 where the change in pellet structure due to crack generation and propagation at the surface of pellets was observed and reported by visual inspection.

In this study, the mechanical durability was measured using the ISO standard 17831-1 [107]. According to the standard, the repeatability limit is 0.4% for pellets with a mechanical durability value higher than 97.5% and it is 2.0% for pellets with a mechanical durability value lower than 97.5%. Considering the repeatability limits in the mechanical durability results after storage (Figure 6.5), it is concluded that for brown pellets (mechanical durability> 97.5%) storage at RH higher than 80% results in a significant reduction in mechanical durability value. For white pellets, the mechanical durability changes significantly only if it undergoes defrosting or frosting conditions. For torrefied pellets, although the change in mechanical durability after the storage is 1.3%, this change can be considered insignificant because all mechanical durability results overlap with the standard deviation of the reference value.

Looking at the changes in mechanical durability, it can be concluded that either the pellet quality was changed or remained constant based on the standard classifications. For instance,

the brown pellets, which initially met the ENplus A1 certificate, may still meet the standard requirement in terms of mechanical durability. However, as the mechanical durability is not the only standard parameter to be considered for the pellet's quality, it cannot be concluded whether the pellets keep or meet the standard quality after storage at different conditions. The effect of storage conditions on pellet quality based on the standards requires further research.

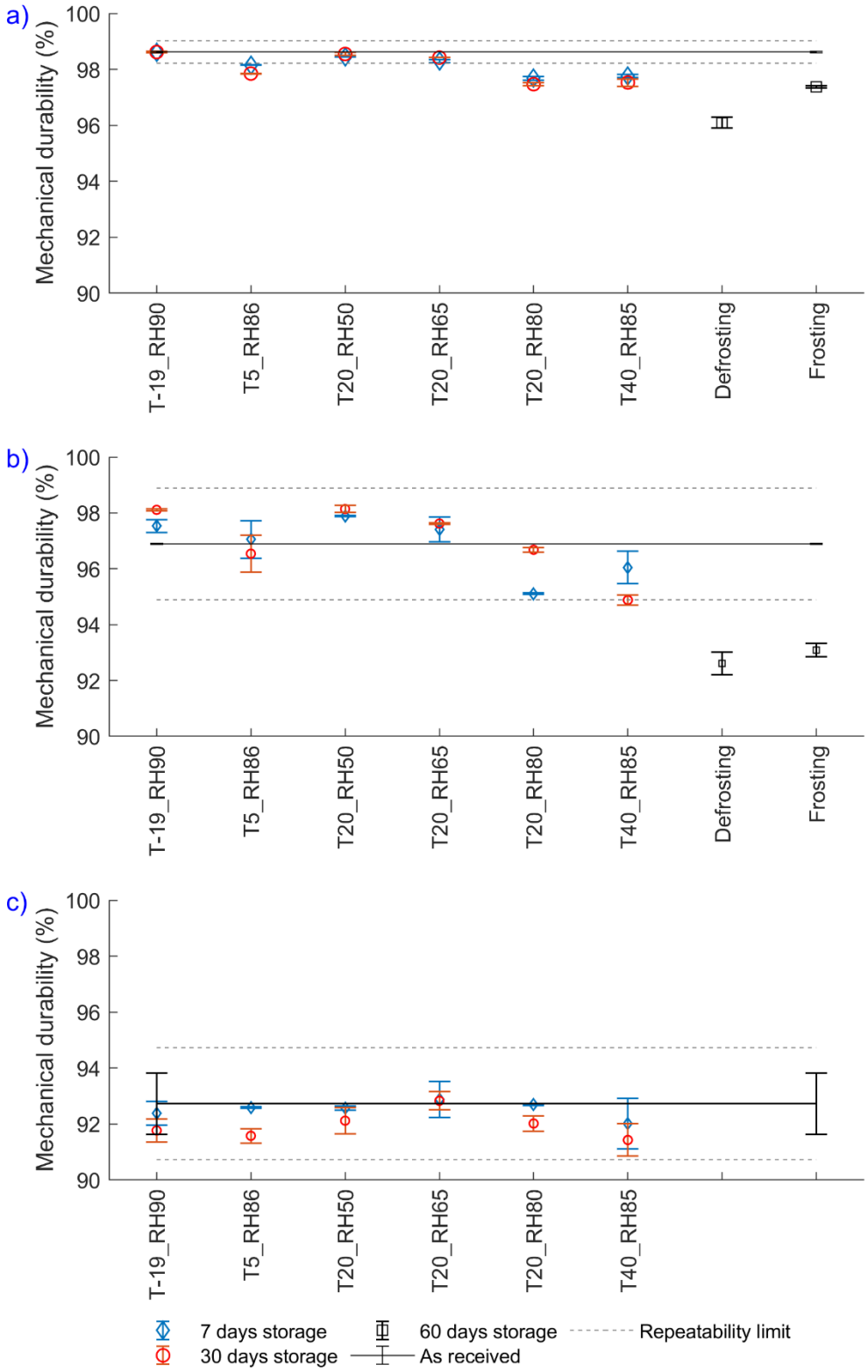

Figure 6.5: Mechanical durability values of different pellets after storage for (a) brown, (b) white, and (c) torrefied pellets. The error bars show the standard deviations and the solid lines show the as-received mechanical durability.

6.4 Conclusions

The effect of various storage conditions on the properties of two types of untreated wood pellets and one type of torrefied pellets was studied. Results indicate that regardless of the storage temperature and RH, all pellets were already saturated after 7 days of storage at constant temperature and RH conditions. Moreover, we found that the EMC ratio depends on the storage conditions and the type of pellets since the EMC ratio was obtained between 1.05 and 1.59 for wood pellets and 0.93 and 1.18 for torrefied pellets. Regardless of the storage conditions, the HHV of all the pellets decreased on average by 6.0% for brown pellets and 3.5% for white and torrefied pellets after 30 days of storage at controlled temperature and humidity conditions, which is expected to have great implications in terms of thermal efficiency and economics of pellet conversion. This highlights the importance of storage conditions for biomass-based pellets. On the other hand, the mechanical durability of pellets was not significantly affected after 30 days of storage, according to ISO standard 17831-1. However, this does not mean that a reduction in mechanical durability is of low importance because the decrease of mechanical strength, especially at large-scale applications, may have a significant impact on dust and fines generation, which in turn may increase the risk of fire. Furthermore, defrosting and frosting conditions (from freezing temperature to 40°C and 80% RH and vice versa for 60 days) decrease the mechanical durability of the tested wood pellets up to 4.3% and up to 3.8%, respectively. Moreover, defrosting or frosting conditions resulted in increased EMC and relatively similar HHV compared to 30 days of storage at constant temperature and relative humidity. To sum up, if possible, a change in the storage conditions should be avoided to keep the mechanical durability as high as possible.

7 Modeling the Breakage Behavior of Individual Pellets*

Series of experiments were conducted in chapters 3, 4, and 5 to investigate the breakage behavior of pellets during transport and storage. However, due to the broad variety of types of equipment and pellets, studying pellet-pellet and pellet-equipment interactions via experiments is difficult. One interesting approach to investigating the breakage behavior of biomass pellets is using numerical methods. Simulation-based models enable us to assess the properties of materials under different conditions and may also contribute to design evaluation and optimization of the transport chain equipment to decrease fines generation.

This chapter introduces a numerical model based on the discrete element method (DEM). The model is capable of representing the breakage behavior of individual pellets under the compression test. Pellets from different origins are subjected to compression tests. The model shows good potential for future studies on the degradation of pellets using DEM.

*This chapter is based on Hamid Gilvari, Wiebren de Jong, and Dingena L. Schott. "Breakage behavior of biomass pellets: an experimental and numerical study." Computational Particle Mechanics (2020): 1-14.

7.1 Introduction

The fragmentation of biomass pellets and the generation of fines and dust during transport and storage has inflicted several problems in handling steps and operational units [105]. Equipment fouling, increased risk of fire, dust inhalation problems, and environmental issues are the consequences of existing fines and dust inside the bulk materials [137]. Biomass pellets are mostly transported on a large scale (ten thousand tons per hour) resulting in high impact forces during transport and handling [77]. The potential of fines and dust generation is highly linked to the mechanical strength of materials. The mechanical strength of biomass pellets could be measured individually or in bulk [44].

The individual mechanical strength assessment methods are conducted either by compression or impact tests. In a typical compression test, a single pellet is placed between two anvils of a compression device that compress the pellet while recording the force-displacement data. Then the stress-strain curve and the modulus of elasticity are calculated from the data. In a typical impact test, a single pellet is dropped from a known height to a plate of known material and the number of fines and the number of pieces split from the original pellet is recorded. The bulk strength is typically measured using durability testers such as tumbling can, ligno tester, and Holmen durability tester. These devices enable pellets to collide with each other and with the walls to mimic the transportation and handling conditions by use of an air stream or rotating the device.

Research on handling and storage properties of biomass pellets has been recently taken into consideration by some researchers [116], [141], [142], [147], [188]. They highlighted the effect of transportation and handling systems on the number of generating fines. Bradley [188], pointed out that the transfer chutes are the main cause of the pellet breakage and fines generation during the handling process. Ilic et al. [141] claimed there are up to 25 wt.% fines particles smaller than 3.15 mm in the biomass pellet plants while the expected amount in the equipment design process is around 5–8 wt.%.

Recently, the use of numerical methods to predict the bulk flow materials has attracted attention [189]. Discrete Element Method (DEM) is proven as a powerful tool with the capabilities of monitoring the behavior of individual particles inside a system resulting in understanding the bulk material behavior. Recently, researchers applied DEM to study the flow properties of cylindrical pellets [190], mixing and transportation of wood pellets [191], and durability characteristics of biomass pellets [48], however, fragmentation of biomass pellets have been

scarcely investigated by modeling and simulations. A recent study addresses the modeling of deformation and breakage behavior of biofuels wood pellets [13] using the finite element method (FEM). However, due to the inherent nature of FEM, the particle-particle contacts which are crucial in breakage behavior and fines generation is missing in the model.

The objective of this chapter is first to characterize the individual pellet strength of different types of biomass under uniaxial and diametrical compressions and second, to present a calibrated DEM model capable of predicting biomass breakage patterns during compression tests capable of tracking the behavior of each particle. The model can be used for future research on pellet fragmentation, equipment design, and to set new standards for transportation, storage, and handling of biomass pellets.

7.2 Materials

Two different non-torrefied and five different torrefied biomass pellets were used in this study. The origin, ultimate, and proximate analysis of the samples are given in Table 7.1. The moisture content and ash content of the torrefied mixed wood pellets were determined according to EN standard 14774-2 [166] and EN standard 14775 [184], respectively. The volatile matter of torrefied mixed wood pellets was measured using the method described in [192]. The proximate analysis of the rest of the samples was taken from [193]. The amount of fixed carbon was calculated by the difference of one hundred to the summation of ash, moisture, and volatile matters. There is no information about the densification processes of the pellets; however, it is known that all Ashwood and all Spruce pellets were densified in similar densification processes.

Table 7.1: Production properties and the proximate analysis of pellets.

Sample Code	Sample Origin	Torr* Temp (°C)	Torr Time (min)	MC* (%)	A* (%)	VM* (%)	FC* (%)
TMW	Torrefied Mixed Wood	NA*	NA	9.3	18.4	69.5	12.1
RA	Raw Ash	-	-	4.6	0.5	79.3	20.2
TA250	Torrefied Ash	250	30	5.7	0.5	72.5	27.0
TA265	Torrefied Ash	265	30	5.8	1.0	68.6	30.4
RS	Raw Spruce	-	-	5.9	0.3	82.2	17.5
TS260	Torrefied Spruce	260	30	5.4	0.3	74.5	25.2
TS280	Torrefied Spruce	280	30	4.8	0.4	73.5	26.1

*Torr:Torrefaction, MC: Moisture content (as-received), A: Ash Content, VM: Volatile Matter, FC: Fixed Carbon, NA: Not Available

7.3 Methods

7.3.1 Experimental

Pellet density

The pellet densities were measured based on the volume and the mass of individual pellets. To get the most accurate volume, pellets were polished in both ends using sandpaper. Then the pellet length and diameter were measured according to the EN standard 16127 [130]. Mass of each pellet was measured using a laboratory balance with readability down to 0.001 g. The pellet density measurement was repeated five times per sample, and then, the mean values and the standard deviations were reported.

Compression tests

The biomass pellet strength under compression is mostly measured in two different configurations including the unconfined uniaxial and diametrical compressions [33]. The diametrical compression test is also known as Brazilian tensile strength. All the experiments in this study were carried out using an Instron compression device (Instron 5500R) using a 10 kN load cell. Pellets were placed on the lower plate of the device, which gradually compressed upward with a compression rate of 1 $mm.min^{-1}$.

For the uniaxial tests, each pellet was polished in both ends using sandpaper to vertically stand on the plate and to ensure that the compressive force applies evenly to both end surfaces of the pellet. For diametrical compressions, pellets were placed on the lower plate lengthwise. Five pellets were tested for each test per sample. The force-displacement data was recorded for each test from the beginning until a 20% drop in the force value after failure. The stress and strain values were calculated using equations (7.1) and (7.2) for uniaxial compression and equations (7.3) and (7.4) for diametrical compressions, respectively:

$$\sigma_a = \frac{F}{\pi r^2}, \tag{7.1}$$

$$\varepsilon_a = \frac{l_0 - l}{l_0}, \tag{7.2}$$

$$\sigma_d = \frac{F}{rl}, \tag{7.3}$$

$$\varepsilon_d = \frac{d_0 - d}{d_0}, \tag{7.4}$$

where F is the force, r is the pellet radius, l_0 and d_0 are the initial pellet length and diameter, and l and d are the pellet length and diameter at the corresponding time, respectively. In addition, Young's modulus (E_p) derived from the linear part of the stress-strain curve is reported.

7.3.2 Numerical method

The Discrete Element Method (DEM) is proven as a powerful numerical method for modeling the granular material flow regimes [194]–[197], bulk material characterization [198][199], breakage models [200]–[204], etc. In DEM, individual interactions of the particles are monitored contact by contact and the particle motion is modeled particle by particle [205]. Therefore, the properties of the particles are individually determined using the equations of motion, equations (7.5) and (7.6), while the objective is to represent the macroscopic behavior of the bulk material:

$$m_i \frac{dv_i}{dt} = \sum \left(F_{ij}^n + F_{ij}^t\right) + m_i g \,, \tag{7.5}$$

$$I_i \frac{d\omega_i}{dt} = \sum \left(R_i \times F_{ij}^t - \tau_{ij}^r\right) , \tag{7.6}$$

where m_i,v_i, ω_i, and I_i, are the mass, translational velocity, rotational velocity, and moment of inertia of particle i, respectively. g is the gravity vector and F_{ij}^n and F_{ij}^t are the normal and tangential forces caused by the interaction between particles i and j at time-step t. τ_{ij}^r is the torque between particles i and j and R_i is the vector connecting the center of particle i to the location where F_{ij}^t is applied as shown in Figure 7.1.

The material breakage in DEM could be modeled using various models such as the Particle Replacement Method (PRM), Bonded Particle Method (BPM) [206], and fast-breakage model [207]. Recently, the so-called Timoshenko beam theory (also called Timoshenko-Ehrenfest beam theory [208]) model based on Timoshenko-Ehrenfest's theory [209] was developed and validated by Brown [210] using EDEM® software provided by DEM Solutions Ltd., Edinburgh, Scotland, UK. The model is called the Edinburgh Bonded Particle Model (EBPM) [210]. The main advantage of the EBPM model is the model capabilities of representing the normal, shear, bending, and torsion movements in a bond that has not been implemented in any other breakage model in DEM.

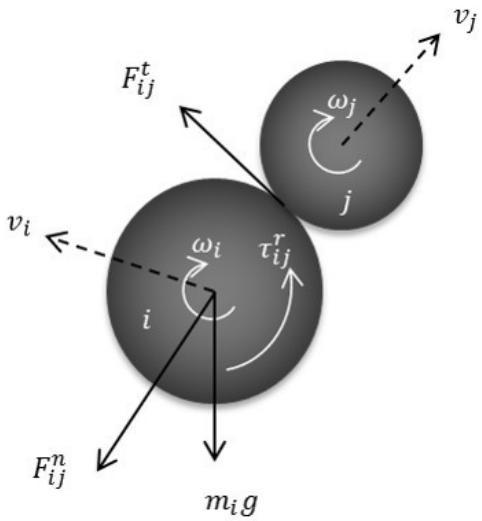

Figure 7.1: Two particles interacting with each other in DEM.

Plant-based biomass consists of lignocellulosic materials such as cellulose, hemicellulose, and lignin. In densification processes, lignin or supplementary binding agents act as glue to bond the celluloses and hemicellulose particles. To numerically investigate the breakage behavior of densified biomass materials, a model containing particle bonding is required. In DEM, the lignocellulosic material could be represented by individual particles while the binding agents can be represented using bonds or beams.

Implementation of Timoshenko-Ehrenfest theory in DEM

The EBPM consists of two different contact models: Timoshenko-Ehrenfest beam theory, and the Hertz-Mindlin model. The former applies for bonded contacts and the latter applies for the non-bonded contacts. The model considers a cylindrical beam between the centers of every two neighboring particles at a user-defined time-step and bonds them in such a way that each bond breaks only if the applied force exceeds the maximum strength in compression, tension, or shear direction. Generally, each bond shares 6 degrees of freedom at each end, which allows compression, tension, and shear forces and torques as illustrated in Figure 7.2. The domain of the neighboring particles is determined using a contact radius multiplier (CRM) which could be any number above 1. This number multiplies the particle radius and creates a virtual radius so that the model creates a bond between every two particles if their virtual radii overlap as shown in Figure 7.3. Only one bond can exist between every two particles and once a bond breaks it will never regenerate. The existence of the bonds is checked at each time-step and once there is no bond anymore between every two neighboring particles the contact between them follows the Hertz-Mindlin model. The Hertz-Mindlin contact model is widely used in the

literature due to its accurate calculations and computational efficiency [211], [212]. Detailed information about the Hertz-Mindlin contact model can be found elsewhere [212].

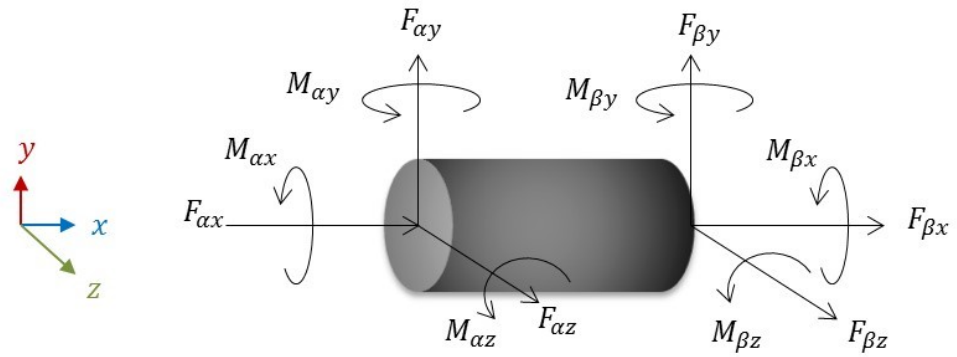

Figure 7.2: Schematic of a bond in the Timoshenko beam theory model. Each bond shares six degrees of freedom at each end.

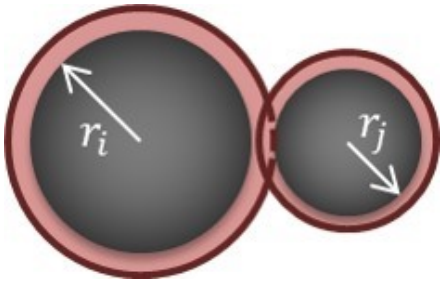

Figure 7.3: Illustration of two spheres and their virtual radii in DEM.

The calculation of the force and momentum for bonded particles is based on the Timoshenko beam theory and is calculated at each time-step according to equation (7.7):

$$\{\Delta F\} = [K].\{\Delta u\}, \tag{7.7}$$

where ΔF is the force vector and Δu is the displacement vector and [K] is the stiffness matrix as shown in equations (7.8) to (7.10):

$$\{\Delta F\} = \{\Delta F_{\alpha x}\, \Delta F_{\alpha y}\, \Delta F_{\alpha z}\, \Delta M_{\alpha x}\, \Delta M_{\alpha y}\, \Delta M_{\alpha z} \Delta F_{\beta x}\, \Delta F_{\beta y}\, \Delta F_{\beta z}\, \Delta M_{\beta x}\, \Delta M_{\beta y}\, \Delta M_{\beta z}\}^T, \tag{7.8}$$

$$\{\Delta u\} = \{\Delta d_{\alpha x}\, \Delta d_{\alpha y}\, \Delta d_{\alpha z}\, \Delta \theta_{\alpha x}\, \Delta \theta_{\alpha y}\, \Delta \theta_{\alpha z} \Delta d_{\beta x}\, \Delta d_{\beta y}\, \Delta d_{\beta z}\, \Delta \theta_{\beta x}\, \Delta \theta_{\beta y}\, \Delta \theta_{\beta z}\}^T, \tag{7.9}$$

$$\mathrm{K} = \begin{bmatrix} K_1 & -K_2 & -K_1 & -K_2 \\ K_2 & K_3 & -K_2 & K_4 \\ -K_1 & K_2 & K_1 & K_2 \\ K_2 & K_4 & -K_2 & K_3 \end{bmatrix}, \tag{7.10}$$

where

$$[K_1] = \begin{bmatrix} \frac{E_b A_b}{L_b} & 0 & 0 \\ 0 & \frac{12k}{L_b{}^2(1+\Phi)} & 0 \\ 0 & 0 & \frac{12k}{L_b{}^2(1+\Phi)} \end{bmatrix}, \tag{7.11}$$

$$[K_2] = \begin{bmatrix} 0 & 0 & 0 \\ 0 & 0 & \frac{-6k}{L_b(1+\Phi)} \\ 0 & \frac{6k}{L_b(1+\Phi)} & 0 \end{bmatrix}, \tag{7.12}$$

$$[K_3] = \begin{bmatrix} \frac{k}{(1+v_b)} & 0 & 0 \\ 0 & \frac{k(4+\Phi)}{(1+\Phi)} & 0 \\ 0 & 0 & \frac{k(4+\Phi)}{(1+\Phi)} \end{bmatrix}, \tag{7.13}$$

$$[K_4] = \begin{bmatrix} \frac{-k}{(1+v_b)} & 0 & 0 \\ 0 & \frac{k(2-\Phi)}{(1+\Phi)} & 0 \\ 0 & 0 & \frac{k(2-\Phi)}{(1+\Phi)} \end{bmatrix}, \tag{7.14}$$

where E_b, v_b, A_b, L_b, Φ, are the bond Young's modulus, Poisson ratio, bond's cross-section area, bond length, and the Timoshenko bond coefficient, respectively, and k is calculated from equation (7.15):

$$k = \frac{E_b I_b}{L_b}, \tag{7.15}$$

where I_b is the second moment of the area of the bond and is calculated from equation (7.16):

$$I_b = \frac{r_b^4 \pi}{4}, \tag{7.16}$$

The radius of every bond is equal to the radius of the smaller sphere's radius. Every bond is assigned a compressive (σ_C), tensile (σ_T), and shear stress (τ) limit which defines the maximum stress a bond can withstand before failure. The stress limits are calculated by equations (7.17) to (7.19):

$$\sigma_C = S_C.\left((\varsigma_C.N) + 1\right), \quad (7.17)$$

$$\sigma_T = S_T.\left((\varsigma_T.N) + 1\right), \quad (7.18)$$

$$\tau = S_S.\left((\varsigma_S.N) + 1\right), \quad (7.19)$$

where S_C, S_T, and S_S are the user-defined mean bond compressive, tensile, and shear strengths, respectively. ς_C, ς_T, and ς_S are the coefficient of variations of compressive, tensile, and shear strengths, respectively, which are defined by the user and can be any number from zero to one. N is a random number derived from a normal distribution with a mean of zero and a standard deviation of one. Therefore, in a multi sphere packing, depending on the value of the coefficient of variations of the bond strength (equations (7.17) to (7.19)), a value between zero and twice the mean bond strength can be assigned for each bond stress limit.

Generation of pellet packing

Rigid spherical particles are considered in the model for simplicity, which means that the individual spherical particles do not crush or degrade. However, the bonds may break and separate the particles. The pellet configurations were created in GiD software [213] using multi-sphere particles. All the packing were created using the "Radius Expansion" algorithm with a delta radius factor of 0.2 and minimum and maximum radius factor of 0.7 and 1.3, respectively with a maximum of 900 iterations. To investigate the effect of pellet packing resolution on the breakage behavior, different pellet configurations with a varying number of spheres and different radii were created using GiD software. The particle size distributions of the packing are shown in Figure 7.4. All the created cylindrical pellets were 6 mm in diameter and 20 mm in length while both ends were kept evenly smooth. Five different pellet configurations including 961, 2202, 3134, 5689, and 7965 spheres were created. There were three main assumptions for the selection of these configurations:

- Maximum sphere radius equal to 0.5 mm with various spheres radii to represent similar particle size distribution of biomass materials before the densification process.
- Maximum 8000 spheres in a configuration due to limitations in the computational time.
- No overlap between particles to allow particles to move freely when they face forces.

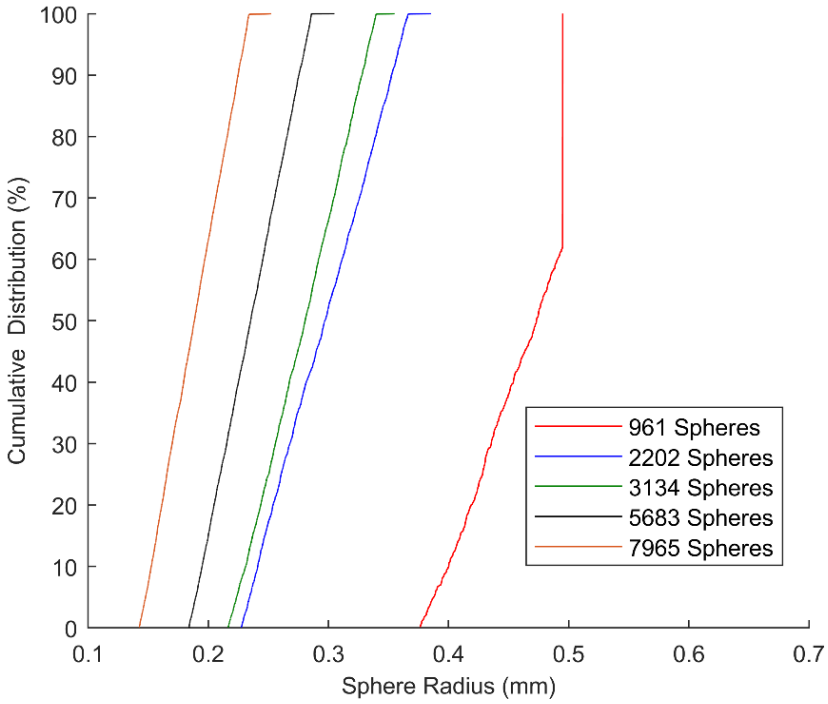

Figure 7.4: Cumulative mass-based distribution of the spheres used in different pellet packing.

Calibration procedure

The numerical part aimed to simulate the compression tests of individual biomass pellets. Here, the model is calibrated only for the torrefied mixed wood pellets. The model was calibrated considering three key performance indicators (KPI) namely the stress at failure (σ), strain at failure (ϵ), and Modulus of Elasticity (E_p) for both uniaxial and diametrical compressions of torrefied mixed wood pellets. Due to heterogeneity in the real pellet structure [123] different stress-strain curves are obtained. In the calibration procedure, the mean of the stress, strain, and Modulus of Elasticity from the experimental results were taken into account. The first step was to screen the most influential parameters. For that, a series of simulations on different input parameters that are listed in Table 7.2 were carried out. The particle and bond Young's modulus, the bond strength parameters, and CRM were found to be the most influential parameters. This is consistent with the other literature findings as the system is quasi-static [210]. Therefore, the particle-particle and particle-geometry parameters were found to be of less importance and the values used were chosen to represent a static condition.

Parker [214], characterized different properties of various types of wood species. According to him, Young's modulus of wood lumbers is in the range of 5.5 to 11 GPa. Considering the densification process of wood pellets, which makes the materials stiffer than raw wood, Young's modulus of 15 GPa for the spheres was considered in this study. There is no information about

the maximum stress limits and the modulus of elasticity of the biomass bonds in the literature. However, the bond properties were calibrated to acquire the same stress-strain taking into consideration that most breakage mechanisms should be tensile [215].

Model inputs

The compression tests in the numerical method were executed using two parallel plates, which positioned on two sides of the pellet for each compression test as shown in Figure 7.5. The compression rate of the plates was set to 10 $mm.s^{-1}$ because lower compression rates were computationally impossible [216]. The model input parameters are shown in Table 7.2. Similar inputs are considered for the entire five pellet packing, however, as the particle radius distributions vary, the particle densities are selected differently as given in Table 7.3. In EDEM® software, material density is defined as the density of the particles. For simulated pellets to represent the real pellet mass, density for each configuration should be calculated based on the number of spheres and the porosity between them. Here, the goal of the numerical part was to model the breakage behavior of torrefied mixed wood. Therefore, the total mass of each pellet configuration with 6 mm diameter and 20 mm length and density of 1304 $kg.m^{-3}$ should be 0.737 g. It should be noted that gravity was not considered in the simulations.

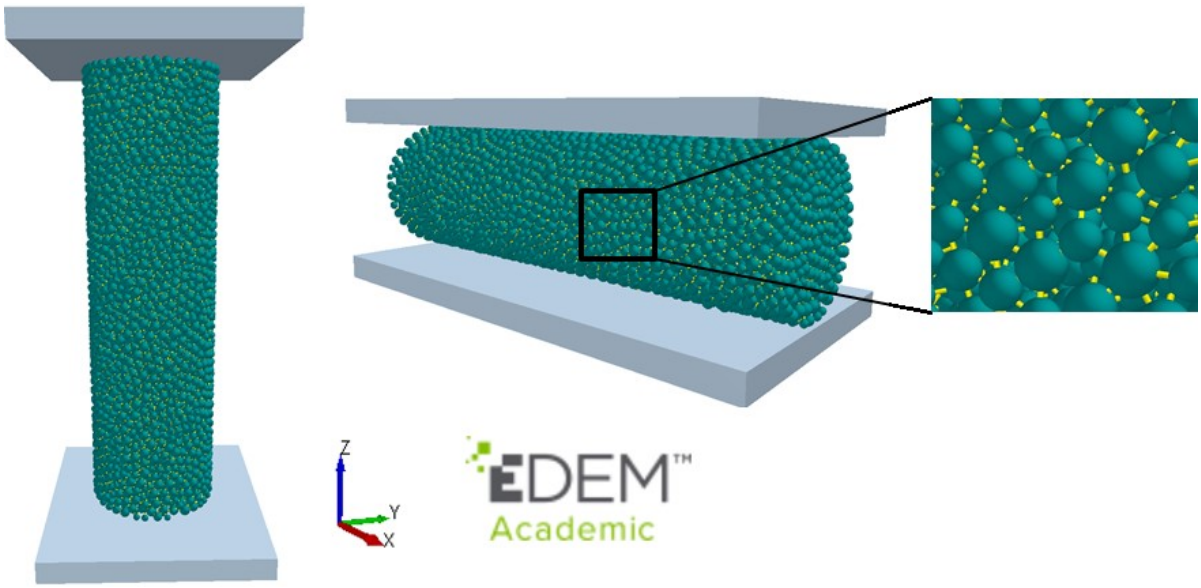

Figure 7.5: Simulated pellets under uniaxial and diametrical compressions (yellow lines between the spheres show the bonds).

Table 7.2: Model input parameters.

Parameter	Parameter	Value	Unit
Particle Inputs			
Young's Modulus	E_p	15	GPa
Poisson's Ratio	ν_p	0.25	-
Particle-Particle Static Friction	$\mu_{s,\,p\text{-}p}$	0.5	-
Particle-Particle Rolling Friction	$\mu_{r,\,p\text{-}p}$	0.5	-
Particle-Particle Restitution Coefficient	$C_{R,\,p}$	0.5	-
CRM	-	Variable	-
Geometry Inputs			
Density	ρ_w	7850	$kg.m^{-3}$
Young's Modulus	E_w	7.6	GPa
Particle-Geometry Inputs			
Particle-Geometry Static Friction	$\mu_{s,\,p\text{-}w}$	1	-
Particle-Geometry Rolling Friction	$\mu_{r,\,p\text{-}w}$	0	-
Particle-Geometry Restitution Coefficient	$C_{R,\,w}$	0.0001	-
Bond Parameters Inputs			
Young's modulus	E_b	0.55	GPa
Poisson's Ratio	ν_b	0.3	-
Radius Multiplier	-	1	-
Mean Compressive Strength	S_C	70	MPa
Mean Tensile Strength	S_T	35	MPa
Mean Shear Strength	S_S	15	MPa
Compressive Strength Coefficient of Variation	ς_C	0.8	-
Tensile Strength Coefficient of Variation	ς_T	0.8	-
Shear Strength Coefficient of Variation	ς_S	0.8	-

The simulation time-step determines the minimum required time for a stable collision to happen. As the model contains two different contact models i.e. the Timoshenko-Ehrenfest beam theory and the Hertz-Mindlin, the selected time-step should be the minimum required amongst the two contact models to ensure a stable simulation. The time-step for the Hertz-Mindlin contact model can be calculated as [216]:

$$\Delta t_{HM\ crit} = \frac{\pi\ r_p(\frac{\rho_p}{G_p})^{0.5}}{(0.1631\upsilon_p + 0.8766)}, \tag{7.20}$$

where ρ_p is the particle density, G_p is the particle shear modulus, υ_p is the Poisson's ratio, and r_p is the smallest particle radius. The shear modulus can be obtained from equation (7.21) using Young's modulus and the Poisson's ratio:

$$G_p = \frac{E_p}{2(1+\upsilon_p)}, \tag{7.21}$$

For the bonded contact, the time-step is determined based on the smallest particle mass ($m_{p\ min}$) and the largest bond stiffness component ($K_{b\ max}$) [216]:

$$\Delta t_{b\ crit} = 2\sqrt{\frac{m_{p\ min}}{K_{b\ max}}}, \tag{7.22}$$

As shown in the equations above, the minimum particle radius highly affects the minimum time-step. Consequently, the time-step for the simulations depends on the pellet configurations. The time-steps used in this study were between 0.045 and 0.75 µs.

As mentioned in section 3.2.3, CRM was found as an important variable affecting the results of simulation because it affected the coordination number. The coordination number is defined as the total number of initial bonds over the total number of particles in the packing at time zero. In this study, two approaches were considered for the coordination numbers, a constant CRM, and a constant coordination number for all the pellet configurations. For the first approach, a CRM of 1.2 was considered and for the second approach, the CRM was adjusted to reach different coordination numbers between 3.49 and 4.72 for the pellet configurations.

Table 7.3: Input parameters for different pellet packing.

Number of Spheres	Min Radius (mm)	Max Radius (mm)	Porosity (%)	Particle Density (kg.m^{-3})
961	0.33	0.44	50.7	2645
2202	0.23	0.38	54.9	2890
3134	0.22	0.35	46.8	2450
5683	0.18	0.30	42.7	2580
7965	0.14	0.25	58.2	3121

Data analysis

The simulations have been continued until a 20% drop in the forces on the compression plates after failure. Then, the stress-strain curves were drawn in the same manner as for the experiments. The force-displacements were achieved from the simulations as follows. The total force at every time-step was calculated as the mean value of the forces on the two plates. This is because of the minor deviations in the forces of the plates due to simulation errors. The displacement in axial and diametrical compressions was calculated based on the actual length or diameter of pellets at each time-step in comparison with the initial pellet length or diameter, respectively. To extract the exact pellet length or diameter at each time-step, the maximum overlap between the particles and plates was added to the distance of the plates. Then using the equations (1) to (4), the stress-strain data were calculated for uniaxial and diametrical compressions. The Young's modulus of each pellet was then calculated from the linear part of the stress-strain curve.

7.4 Results and discussion

The results of the experimental compression tests, as well as the pellet densities, are shown in Table 7.4 and a typical stress-strain curve for uniaxial and diametrical compressions of torrefied mixed wood pellets is depicted in Figure 7.6, as an example. As the standard deviations show, there is a large variation between the experimental results of the maximum stress values even for one type of pellet in different test repetitions. It was also observed that for some pellets, for instance, TA265, the value of Young’s modulus differs significantly in axial and diametrical directions. Although it was not further studied in this work, it may be explained due to the heterogeneity in the pellet structure such as differences in porosity and the number and orientation of micro cracks. Similar results were previously reported by other researchers [123]. Nevertheless, a deeper look at the pellets after compression tests shows that they mostly fail in shear as shown in Figure 7.7.

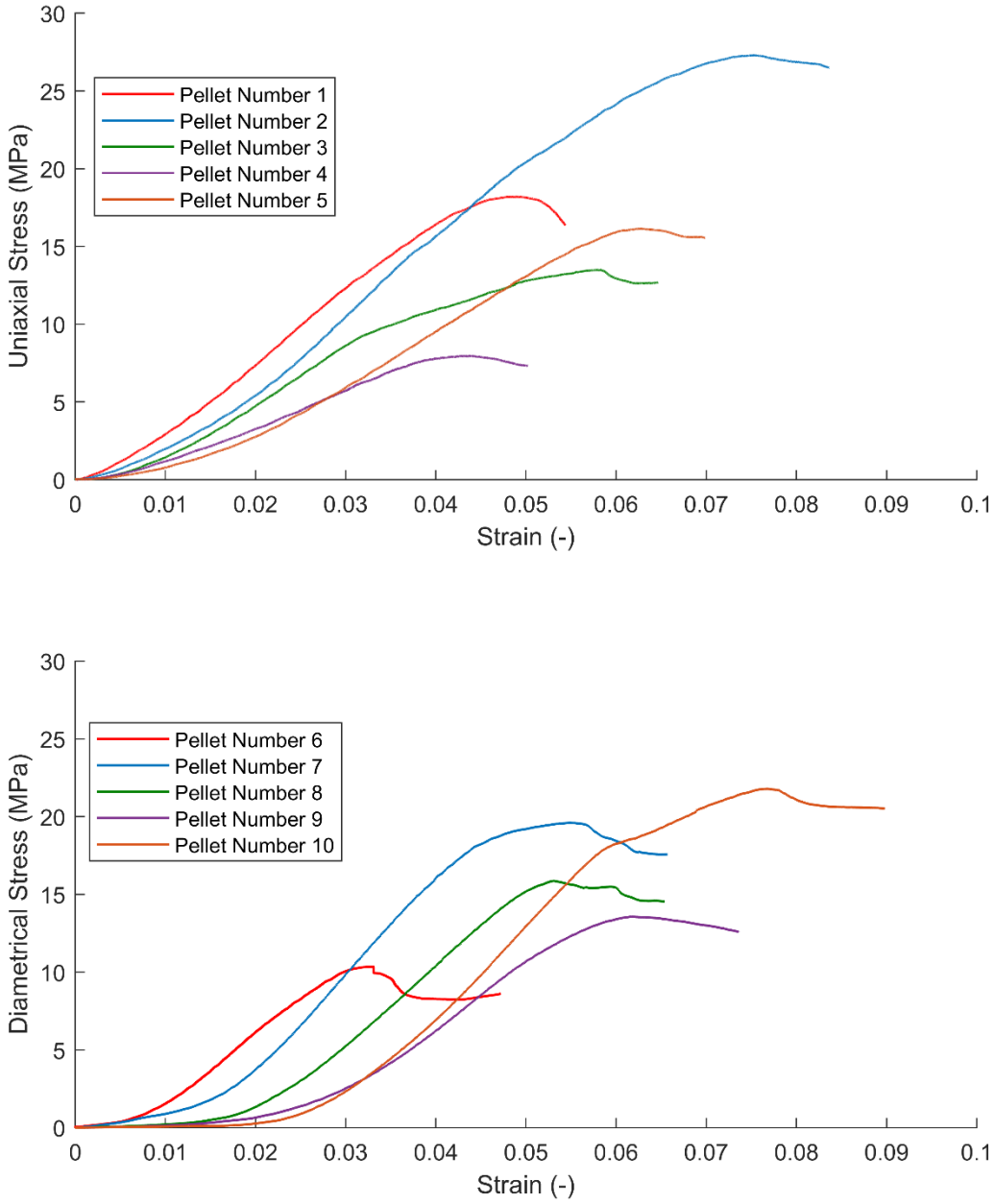

Figure 7.6: Typical experimental stress-strain curves for torrefied mixed wood pellets.

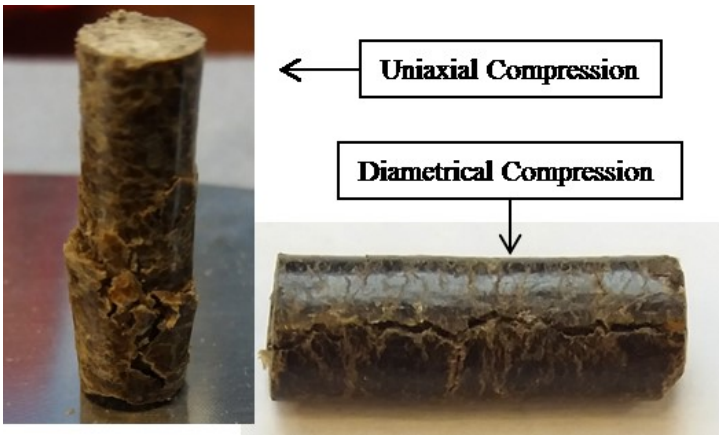

Figure 7.7: Pellets after experimental compression tests.

Table 7.4: Experimental results and standard deviations.

Sample code	Uniaxial compression			Diametrical compression			Pellet density ($kg.m^{-3}$)
	Stress (MPa)	Strain (-)	Young's modulus (MPa)	Stress (MPa)	Strain (-)	Young's modulus (MPa)	
TMW	16.62±6.35	0.06±0.01	324±86	15.4±4.4	0.061±0.02	324±82	1304±40
RA	32.34±12.48	0.09±0.03	425±157	23.56±4.4	0.07±0.02	421±72	1164±25
TA250	20.17±6.26	0.08±0.01	298±72	16.65±5.03	0.08±0.05	229±85	1069±29
TA265	18.83±4.25	0.06±0.01	357±63	14.14±0.94	0.06±0.02	160±75	1107±95
RS	15.77±2.35	0.18±0.05	105±26	14.77±5.34	0.09±0.03	195±19	1186±51
TS260	8.27±1.32	0.07±0.03	117±30	11.62±1.26	0.12±0.05	113±60	1119±56
TS280	8.31±1.35	0.08±0.04	130±61	11.0±1.88	0.08±0.03	179±53	1107±110

Table 7.5 shows the stress-strain simulation results at failure for different pellet configurations with CRM equal to 1.2. The stress-strain curves are depicted in Figure 7.8 together with the experimental results. As can be seen, the results of the simulations are consistent with the experimental results where different pellet packing result in different values for the stress and strain at failure. The simulated pellet containing 5683 spheres shows the highest stress at failure for both uniaxial and diametrical compressions, while the pellet with 7965 spheres shows the lowest values for both compressions tests. The results reveal that there is a high linear correlation between the coordination numbers and the maximum stress at failure for all the simulated pellets. The results of the second approach where CRMs were adjusted to obtain uniform coordination numbers are shown in Figure 7.9. The higher the coordination number,

the higher the number of bonds in a system, thus, the higher the stress value at failure. Therefore, different material behavior can be reasonably reached by manipulating the coordination number. Detail information on the strain-stress data for different coordination numbers is given in Figure C. 1.

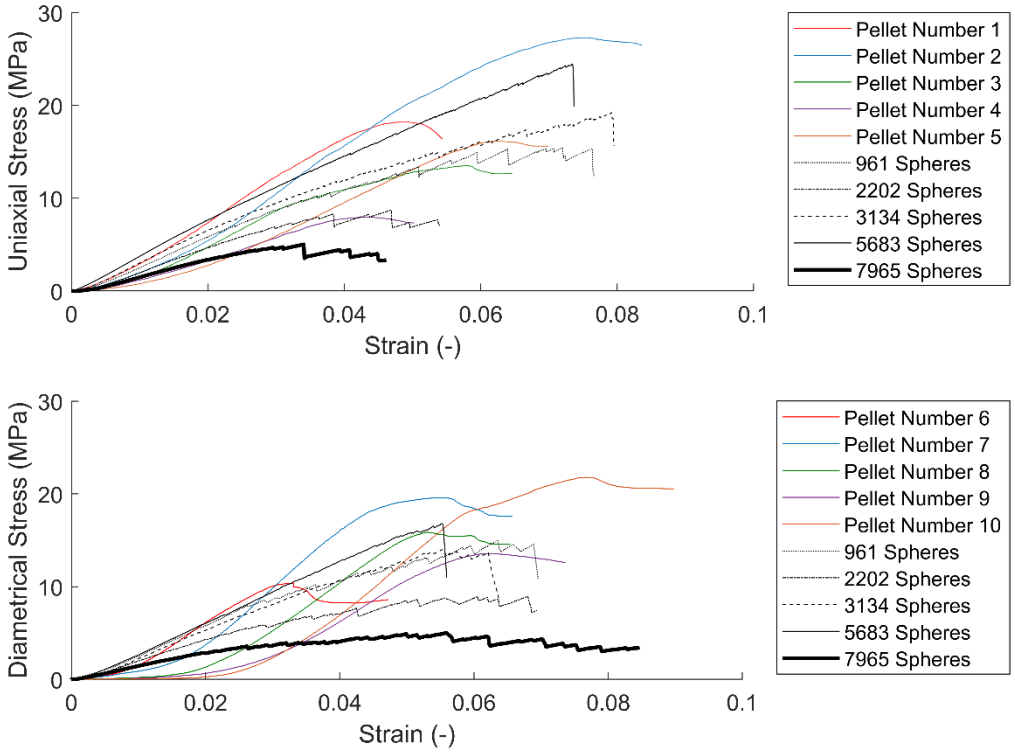

Figure 7.8: stress-strain results for the uniaxial and diametrical compressions. Experimental versus simulations at CRM of 1.2.

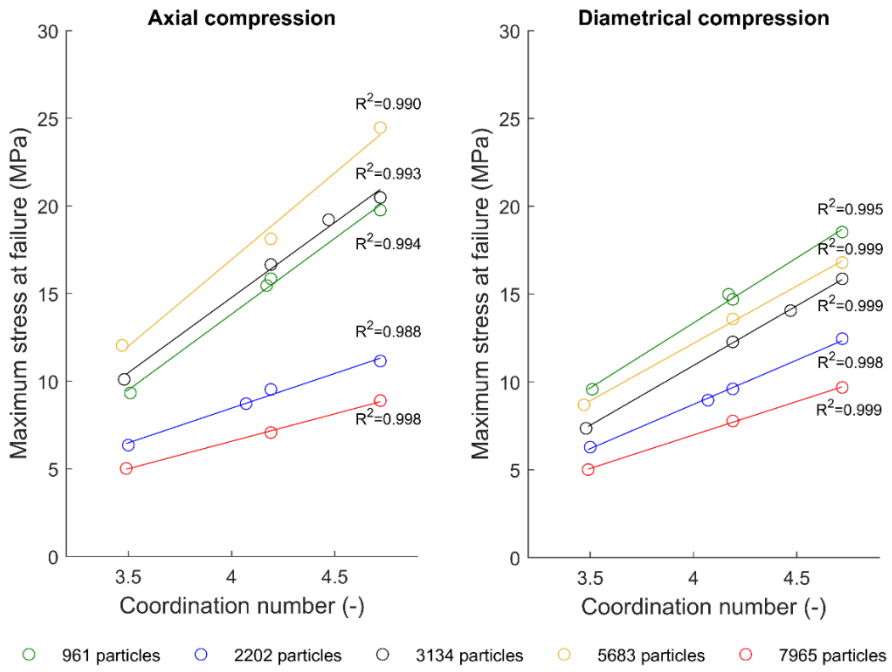

Figure 7.9: Stress at failure versus coordination numbers for all the packing.

Figure 7.10 shows maximum stress at failure versus porosity for both axial and diametrical compressions. It is seen that the stress at failure depends highly on porosity for axial compression, however, for diametrical compression, the correlation is less evident. Looking at Figure 7.9, the pellet configuration made with 961 particles predicts the highest stress at failure in diametrical compression amongst all pellet packing. This is different from the results of axial compression where this packing is in the third order in terms of stress value at failure amongst all packing. This is clearer in Figure 7.10 where 961 particles show the highest stress at failure. Figure 7.11 shows the stress at failure versus porosity for diametrical compression excluding the results of 961 particles. From Figure 7.11, it is concluded that the stress at failure correlates highly with porosity for diametrical compressions as well. Therefore, the packing with 961 particles is an exception. The possible cause of this high stress value is probably the particle size in the packing. It was previously reported that there should be a sufficient number of particles along the width of a specimen to achieve a calibration [217]. In the packing with 961 particles, due to the bigger size of the particles in comparison to the other packing, there is a low number of particles in a row in the lengthwise direction, which affects the results of the compression test.

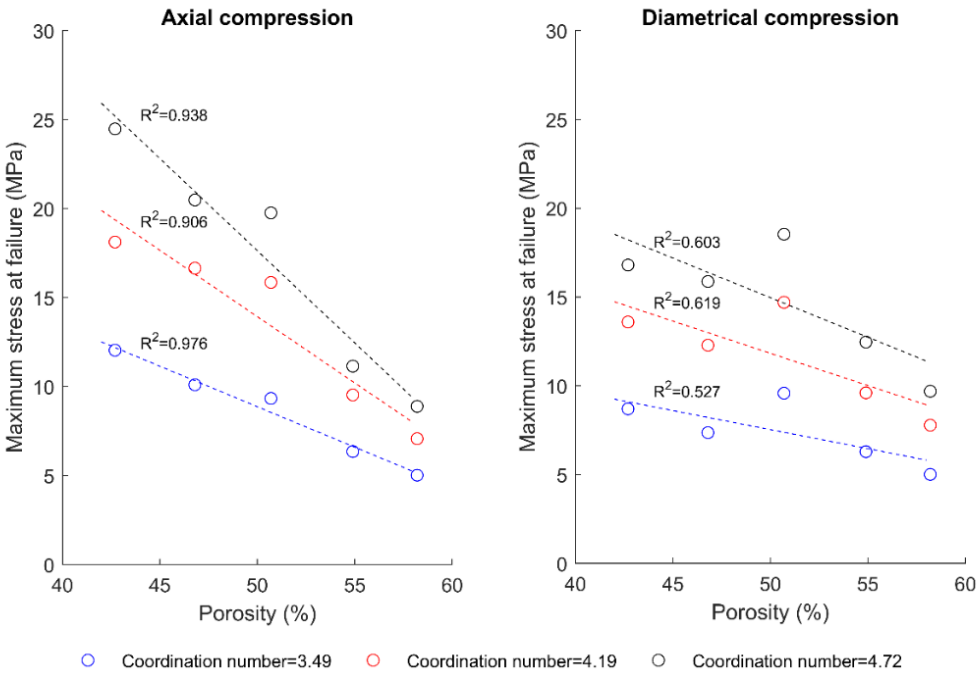

Figure 7.10: Stress at failure versus porosity for all the packing.

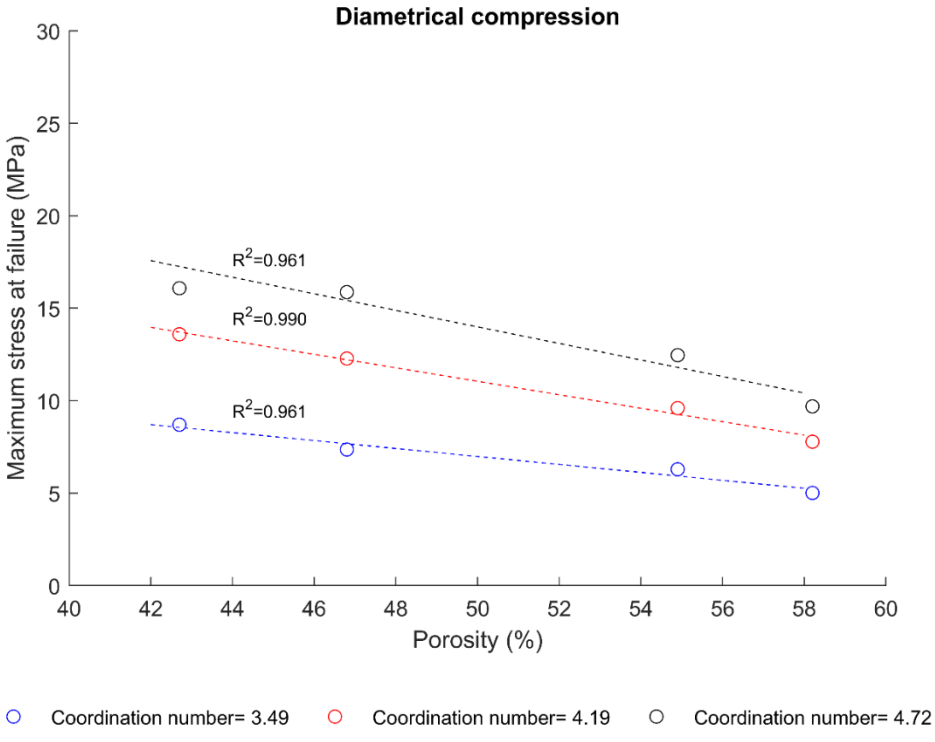

Figure 7.11: Stress at failure versus porosity excluding the packing with 961 particles.

Comparing the experimental and numerical results in Figure 7.8, the experimental results show more ductile behavior, progressive loading, and gradual collapse, however, the simulated pellets show more brittle behavior. In other words, in the experiments, the initial stress build-

up is very small despite a relatively large displacement. There are at least two reasons for that. The first reason lies in the difference between the compression rates. As mentioned before, in this study the compression rate was 1 $mm.min^{-1}$ in the experiments and 10 $mm.s^{-1}$ in the simulations. At high compression rates, the materials show more rigid behavior [123], and therefore, the stress curve increases more straight than progressive. Second, this can be explained by the differences in the pellet structures. As real pellets mostly contain surface or internal cracks, the progressive loading is possibly due to the closures of the cracks at the start of compression [218].

Looking at literature in the field of rock cutting, Kemeny [215] claimed that although there is a complicated mechanism behind the crack growth under compression, it can be approximated by the crack with a central load point where the origins of the point loads are small regions of tension that develop in the same direction of the least principal stress. Considering his findings, the major bond breakage mechanism should be tension in a compression test. Figure 7.12 shows the total proportion of broken bonds at failure for every pellet configurations and share of each breakage mechanism at CRM of 1.2 and a coordination number of 4.19. As shown, the bond breakage due to tension is the major failure mechanism for all the pellet configurations. Similar results were observed for coordination numbers of 3.49 and 4.72. It should be noted that the total number of broken bonds may not be similar to the summation of the number of broken bonds due to compression, tension, and shear because in some cases a single bond may break due to multiple mechanisms at one time-step.

Table 7.5: Simulation results of stress-strain at failure and Young's modulus for different pellet configurations.

No. of Spheres in Packing	Uniaxial Compression			Diametrical Compression		
	Maximum Stress (MPa)	Strain at Failure (-)	Young's modulus (MPa)	Maximum Stress (MPa)	Strain at Failure (-)	Young's modulus (MPa)
961	15.46	0.07	236	14.99	0.06	330
2202	8.72	0.05	212	8.96	0.07	222
3134	19.21	0.08	253	14.06	0.06	307
5683	24.47	0.07	330	16.08	0.06	334
7965	5.02	0.03	201	5.01	0.05	154

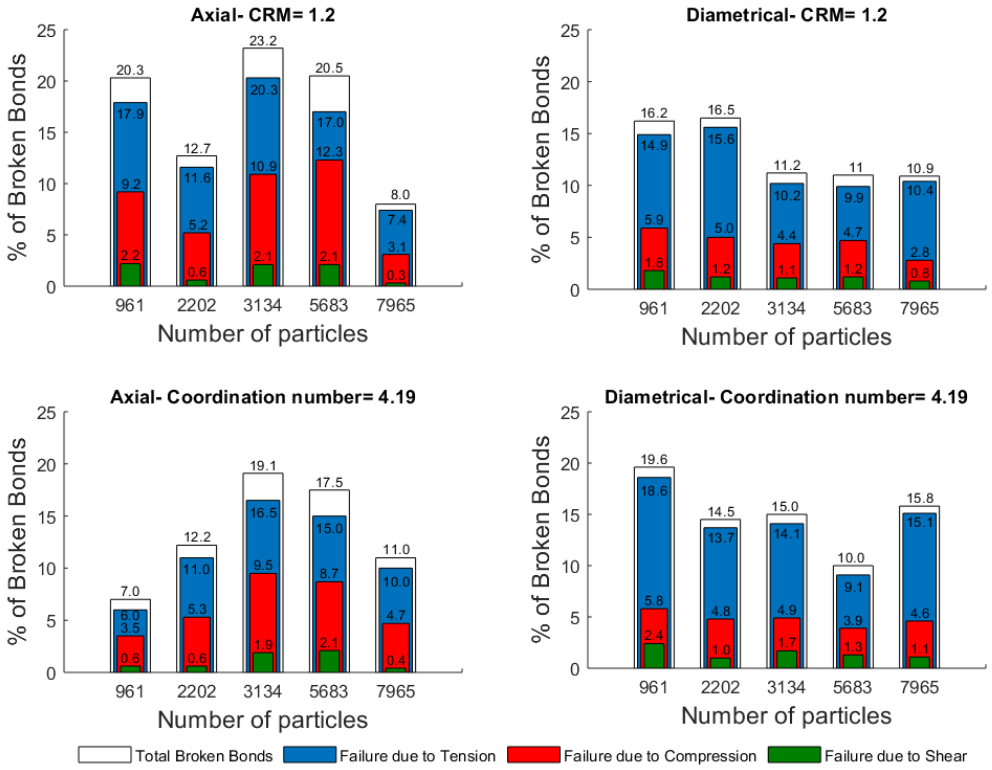

Figure 7.12: Fractions of the total broken bonds at failure and the bond failure due to tension, compression, and shear.

Table C. 1 and Table C. 2 show the breakage behavior of pellets after failure in simulations for CRM of 1.2. Comparing the breakage behavior in the experiments with those of the simulations, it is obvious that the breakage behavior is the same where pellets fail mainly due to shear albeit the main bond breakage failure mechanism is tension. This could be observed for all the simulated pellets except for the higher number of spheres, which increases the resolution and the notch formation. This is consistent with the previous research on bonded particle models [202]. The other difference between the uniaxial simulation results is the failure location in a pellet that is assumed to be related to the initiation of the micro-cracks inside pellets, which is probably a result of porosity distribution in a packing. This is a very complicated mechanism and requires further research. Nevertheless, for the diametrical compressions, the breakage happens at the top of the pellets for all the simulations. This is consistent with the experimental results, which were shown in Figure 7.7.

It is worth mentioning that in this study, the amount and size of the particles released from the pellets during compression tests were not recorded and therefore that was not compared with the simulation results. As different pellet packing include different sphere's radius distributions, some of the packings in this study may not represent the same particle size distribution of the

released fines and dust. This requires more research to determine whether any of the used packings in this study could represent the breakage behavior of different pellet types. Nonetheless, for using the calibrated model in a bulk material, it is recommended to use a combination of these packing to represent the breakage behavior of different pellets.

Although the model was calibrated based on the experimental results of the torrefied mixed wood pellets, our study shows that the model could easily represent the breakage behavior of other types of pellets by changing the coordination numbers and/or by re-calibrating the values of the bond parameters.

7.5 Conclusions

Seven different types of biomass pellets were experimentally studied for the breakage behavior under uniaxial and diametrical compression tests. From the experimental results, it can be concluded that various pellet types show different stress-strain results due to different origins, pretreatment processes, and densification processes. The differences in results were also observed for pellets from the same type due to heterogeneity in the pellet structure. The heterogeneity might be due to the differences in the particle size distribution of the raw materials, heterogeneous porosity, existence of micro-cracks, etc. However, the maximum stress at failure for the tested pellets is in the range of 8.31 to 32.34 MPa.

The numerical results show that biomass pellets could be modeled using a multi-spherical approach where a different number of spheres can be applied to represent the mechanical strength of various types of pellets. In our simulations, it was observed that the higher the coordination number and the lower the porosity, the higher the maximum stress at failure.

The breakage behavior of biomass pellets under uniaxial and diametrical compressions was successfully simulated for torrefied mixed wood pellets using discrete element method. The model was based on the Timoshenko-Ehrenfest beam theory for bonded contacts and the Hertz-Mindlin theory for non-bonded contacts. The calibrated model can predict the stress-strain curves and the modulus of elasticity of the biomass pellets. This can pave the way for future numerical studies for biomass pellet production, transportation, and handling.

8 Conclusions and Future Outlook

8.1 Conclusions

In this dissertation, we aimed to answer the following research question: *"How do biomass pellets degrade during transport and storage?"*

To answer this question, we defined six sub-questions to investigate different aspects of biomass degradation step by step. Here, the main conclusions are explained following each sub-question.

1. **What are the existing methods to assess the degradation behavior of biomass pellets? In addition, which factors affect the quality parameters of pellets prior to and post pelletization process?**

In literature, quality assessment methods are mainly based on experiments performed using small-scale equipment, which may not necessarily indicate the pellet quality in industrial-scale transport and storage systems. Considering the mechanical durability, the extent of fines generation due to attrition can be obtained via the tumbling box or the Holmen durability tester; however, both methods lack the presence of other breakage mechanisms—e.g. fragmentation due to high impact forces—actually occurring in industrial transport and storage systems. Moreover, using different methods to assess a quality parameter may lead to different results, and therefore, the results in the literature are not comparable with one another unless exactly similar methods have been used. To overcome this problem, developing other quality assessment methods considering the real pellet-equipment interactions is required.

The production of pellets with high quality is a complex process that involves too many parameters, which can be categorized into four main groups: (1) feedstock properties, (2) specifications of the pretreatment processes, (3) specifications of the pelletization process conditions, and (4) storage properties. Although lessons—such as optimum moisture content, feedstock particle size, and pelletization temperature and pressure—can be learned from previous research, to produce a pellet with high quality, the influence of all affecting factors should be systematically investigated.

2. **What are the effects of pellet length, test conditions, and torrefaction on the degradation of pellets?**

From our observations described in chapter 3, mechanical durability depends on the **length distribution of pellets**; the longer the pellet lengths, the higher the mechanical durability is. It was also observed that although longer pellets break more than shorter pellets in a durability

test, their durability value is higher. This is because the longer the pellets, the lower the number of pellets per unit mass, and consequently, there is a lower collision probability inside the durability tester, and hence, lower fines generation is observed. Analyzing the effect of operating **test conditions** reveals that due to the heterogeneous nature of pellets, some areas of the pellet structure (like cracks and extreme ends) hold a high probability to break up and produce fine particles due to attrition. Once these areas break up or release fines, they are less prone to generate fines afterward, and hence, we conclude that a given sample should not be tested more than one time for the durability measurements. Regarding the **torrefaction** effect, we observed no difference between the durability of torrefied (post pelletization) and non-torrefied pellets made of similar feedstock origin.

3. **To what extent does the physical degradation of pellets in pilot-scale transportation correlate with the durability results?**

The breakage and attrition of commercial wood pellets during transport via a pilot-scale belt conveyor showed that the amount of generated fines is a function of the number of handling steps and the drop height and neither the belt velocity (up to 1.5 $m.s^{-1}$) nor the belt loading (up to 50% of its full capacity) affects the results. The longer the height of drop, the higher the number of fines. Moreover, by increasing the number of handling steps, the accumulated energy to fracture the pellets increases, and then pellets are more prone to break.

Considering the relationship between the results of the benchmark experiments—tumbling box and rotary impact test—and the results of the belt conveyor, the durability of the tumbling box is closer to the number of generated fines in the belt conveyor experiments when repeating the handling steps for several times. However, the rotary impact test operating at relatively high velocity (25 $m.s^{-1}$) overestimates the proportion of generated fines.

4. **To what extent do pellets degrade during large-scale transport, handling, and storage, and what is the relationship between their physical degradation and durability results?**

We experimentally quantified the breakage behavior of a mixture of commercial wood pellets with average durability of 97.6%, based on ISO standard 17831-1. The experiments were conducted in a large-scale transportation system with a capacity of 450 $ton.h^{-1}$. On average, the proportion of small particles< 5.6 mm increased up to 5% at the transfer point between two belt conveyors with a vertical drop fall of 7.8 m. The average proportion of fines< 3.15 mm also

increased up to 4% in that drop fall. Considering tens of handling steps in typical transportation systems, the proportion of fines may even increase. In our case-study power-plant, the average proportion of small particles< 5.6 mm was up to 14%, and the average proportion of fines< 3.15 mm was up to 9%, in the last sampling point. Because the presence of fines decreases the flowability of the materials and may create major problems in the transport and storage, we concluded that pellets should be transferred in a more gentle way to decrease the breakage and attrition, for instance, by minimizing the drop heights in the transfer points.

5. **What is the effect of temperature and humidity variation on the degradation behavior of pellets during storage?**

In chapter 6, we showed that three types of pellets tested (two types of wood pellets and one type of torrefied pellets) were affected in their physical structure and energy contents when placing at different storage conditions. Pellets got saturated after seven days at almost any of the imitated environmental condition scenarios; however, the equilibrium moisture content depended on temperature and relative humidity and may increase up to 1.6 times at 40ºC temperature and 85% relative humidity conditions. After 30 days of storage, all pellets lost a portion of their heating values between 1.6 and 10%, depending on the type of pellets and the storage conditions. Moreover, frosting and defrosting of pellets at high temperature (40ºC) and relative humidity (85%) decreased mechanical durability up to 4%. Although the reduced durability cannot be easily related to the amount of fines generation in large-scale transportation, it is clear that a 4% reduction in durability leads to a sharp decline in the quality of pellets regarding many local and global standards and guidelines.

6. **To what extent can the degradation behavior of biomass pellets be simulated using DEM?**

As we showed in Chapter 7, the axial and diametrical compressions of biomass pellets can successfully be modeled by the discrete element method (DEM) using the so-called Timoshenko-Ehrenfest breakage model. The model developed uses a bonding approach between the different number of spheres resembling the structures of different types of pellets; therefore, by changing the number of spheres, different structures are obtained. The model showed high fidelity to predict the breakage behavior of individual pellets under compression. It was shown for a wide range of pellets, stress, strain, and Young's modulus under compression can accurately be modeled. This paves the way for future research toward the applications of

DEM concerning the degradation behavior of biomass pellets during transport and storage, although the high computational costs remain a challenge.

8.2 Recommendations for future research

Currently, the physical degradation of pellets during large-scale transport and storage is an uncontrollable phenomenon. To overcome this problem, new methods of quality control and testing standards considering the large-scale transport and storage conditions are required. Besides, to decrease physical degradation, the transportation systems should be carefully designed to reduce the impact forces exerting on pellets. Moreover, to better understand the effect of material-equipment interactions affecting the degradation behavior of pellets, testing other types of pellets and transport equipment that have not been studied in this dissertation is crucial.

The length distributions of pellets crucially affect physical degradation. Pellet producers are, therefore, recommended to produce longer pellets (longer than 30 mm). Besides, setting strict guidelines and standards for pellet quality can guarantee the lower fines generated during large-scale transport and storage.

Modeling the flow and breakage behavior of pellets can contribute to better equipment design for the highest efficiency and lowest fines and dust generation throughout the transport chain. Future research can extend the application of DEM to the bulk of pellets; however, it should be able to handle the wide variety of properties between individual pellets. Moreover, using non-spherical particles to simulate the elongated and flaky nature of biomass particles can be of interest. Considering the high computational costs of the developed model in this study, investigating the physical degradation of the bulk of pellets requires high-performance computers. Another approach to use DEM in the bulk of pellets is by applying new breakage models with higher computational efficiencies, such as the model developed by Tavares and King [219]. Using such a model, one can track and record the mass loss of pellets during multiple handling steps and use it for design optimization of industrial equipment.

The latest trend in biomass-related research shows an increased interest in non-woody biomass pellets such as agricultural residues, food processing wastes, and animal residues. Therefore, the future biomass market is expected to rely on the use of non-woody biomass. Because the composition and the structure of non-woody biomass are different from woody-biomass, future research can study the degradation behavior of non-woody biomass pellets.

Bibliography

[1] United Nations framework convention on climate change- the Paris agreement, "UNFCC," 2015, [Online]. Available: https://unfccc.int/process-and-meetings/the-paris-agreement/the-paris-agreement (2015).

[2] Enerdata, "Global Energy Statistical Yearbook 2020," 2020. https://yearbook.enerdata.net/total-energy/world-consumption-statistics.html (accessed Aug. 04, 2020).

[3] C. 14588:2004, "Solid Biofuels. Terminology- Definitions and Descriptions."

[4] N. Kaliyan and R. Vance Morey, "Factors affecting strength and durability of densified biomass products," *Biomass and Bioenergy*, vol. 33, no. 3, pp. 337–359, 2009.

[5] J. H. A. Kiel, "Torrefaction to improve biomass logistics (and end-use)," *Mini Symp. Biomass Dev. ports. Delft Univ. Technol. Netherlands*, 2012, [Online]. Available: https://publicaties.ecn.nl/PdfFetch.aspx?nr=ECN-L--12-082.

[6] G. Gauthier, I. Avagianos, C. Calderón, and B. Vaskyte, "Bioenergy Europe Statistical Report 2020," 2020. [Online]. Available: https://bioenergyeurope.org/statistical-report.html.

[7] J. S. Forrester, "Dryer Fire Reported at Pinnacle Pellet Plant," 2020. https://www.powderbulksolids.com/industrial-fires-explosions/dryer-fire-reported-pinnacle-pellet-plant (accessed Sep. 30, 2020).

[8] NBC, "Fire chief: Dust caused pellet company explosion," 2013. https://turnto10.com/archive/fire-reported-at-east-providence-wood-pellet-company (accessed Nov. 03, 2020).

[9] L. Cutz, U. Tiringer, H. Gilvari, D. Schott, A. Mol, and W. de Jong, "Microstructural degradation during the storage of biomass pellets," *Commun. Mater.*, vol. 2, no. 1, p. 2, 2021.

[10] J. S. Tumuluru, C. T. Wright, J. R. Hess, and K. L. Kenney, "A review of biomass densification systems to develop uniform feedstock commodities for bioenergy application," *Biofuels, Bioprod. Biorefining*, vol. 5, no. 6, pp. 683–707, 2011.

[11] P. Pradhan, S. M. Mahajani, and A. Arora, "Production and utilization of fuel pellets from biomass: A review," *Fuel Process. Technol.*, vol. 181, pp. 215–232, 2018.

[12] L. Visser, R. Hoefnagels, and M. Junginger, "Wood pellet supply chain costs – A review and cost optimization analysis," *Renew. Sustain. Energy Rev.*, vol. 118, no. June 2019, p. 109506, 2020.

[13] A. Russell *et al.*, "Deformation and breakage of biofuel wood pellets," *Chem. Eng. Res. Des.*, vol. 153, pp. 419–426, 2020.

[14] P. A. Cundall, "A computer model for simulating progressive, large-scale movement in blocky rock system," 1971.

[15] Y. Li and H. Liu, "High-pressure densification of wood residues to form an upgraded fuel," *Biomass and Bioenergy*, vol. 19, no. 3, pp. 177–186, 2000.

[16] D. Falk, "Feed manufacturing technology III," *Am. Feed Ind. Assoc. Arlingt.*, 1985.

[17] L. Jiang *et al.*, "A comparative study of biomass pellet and biomass-sludge mixed pellet: Energy input and pellet properties," *Energy Convers. Manag.*, vol. 126, pp. 509–515, 2016.

[18] Q. Hu *et al.*, "The densification of bio-char: Effect of pyrolysis temperature on the qualities of pellets," *Bioresour. Technol.*, vol. 200, pp. 521–527, 2016.

[19] H. S. Kambo and A. Dutta, "Strength, storage, and combustion characteristics of densified lignocellulosic biomass produced via torrefaction and hydrothermal carbonization," *Appl. Energy*, vol. 135, pp. 182–191, 2014.

[20] M. F. Zainuddin, S. Rosnah, M. M. Noriznan, and I. Dahlan, "Effect of moisture content on physical properties of animal feed pellets from pineapple plant waste," *Agric. Agric. Sci. Procedia*, vol. 2, pp. 224–230, 2014.

[21] L. S. Jensen, "Influence of pelleting on the nutritional needs of poultry.," *Asian-Australasian J. Anim. Sci.*, vol. 13, no. Special iss., pp. 35–46, 2000.

[22] M. T. Carone, A. Pantaleo, and A. Pellerano, "Influence of process parameters and biomass characteristics on the durability of pellets from the pruning residues of Olea europaea L.," *Biomass and bioenergy*, vol. 35, no. 1, pp. 402–410, 2011.

[23] A. García-Maraver, V. Popov, and M. Zamorano, "A review of European standards for pellet quality," *Renew. Energy*, vol. 36, no. 12, pp. 3537–3540, 2011.

[24] S. Umar, M. S. Kamarudin, and E. Ramezani-Fard, "Physical properties of extruded aquafeed with a combination of sago and tapioca starches at different moisture contents," *Anim. Feed Sci. Technol.*, vol. 183, no. 1–2, pp. 51–55, 2013.

[25] P. Gilbert, C. Ryu, V. Sharifi, and J. Swithenbank, "Effect of process parameters on pelletisation of herbaceous crops," *Fuel*, vol. 88, no. 8, pp. 1491–1497, 2009.

[26] J. Jackson, A. Turner, T. Mark, and M. Montross, "Densification of biomass using a pilot scale flat ring roller pellet mill," *Fuel Process. Technol.*, vol. 148, pp. 43–49, 2016.

[27] D. Bergström *et al.*, "Effects of raw material particle size distribution on the characteristics of Scots pine sawdust fuel pellets," *Fuel Process. Technol.*, vol. 89, no. 12, pp. 1324–1329, 2008.

[28] H. Li, X. Liu, R. Legros, X. T. Bi, C. J. Lim, and S. Sokhansanj, "Pelletization of torrefied sawdust and properties of torrefied pellets," *Appl. Energy*, vol. 93, pp. 680–685, 2012.

[29] M. T. Reza, M. H. Uddin, J. G. Lynam, and C. J. Coronella, "Engineered pellets from dry torrefied and HTC biochar blends," *Biomass and Bioenergy*, vol. 63, pp. 229–238, 2014.

[30] S. Mani, L. G. Tabil, and S. Sokhansanj, "Effects of compressive force, particle size and moisture content on mechanical properties of biomass pellets from grasses," *Biomass and Bioenergy*, vol. 30, pp. 648–654, 2008.

[31] M. R. Abdollahi, V. Ravindran, T. J. Wester, G. Ravindran, and D. V. Thomas, "Effect

of improved pellet quality from the addition of a pellet binder and/or moisture to a wheat-based diet conditioned at two different temperatures on performance, apparent metabolisable energy and ileal digestibility of starch and nitrogen in broilers," *Anim. Feed Sci. Technol.*, vol. 175, no. 3–4, pp. 150–157, 2012.

[32] R. I. Muazu and J. A. Stegemann, "Effects of operating variables on durability of fuel briquettes from rice husks and corn cobs," *Fuel Process. Technol.*, vol. 133, pp. 137–145, 2015.

[33] A. Bazargan, S. L. Rough, and G. McKay, "Compaction of palm kernel shell biochars for application as solid fuel," *Biomass and Bioenergy*, vol. 70, pp. 489–497, 2014.

[34] S. H. Sengar, A. G. Mohod, Y. P. Khandetod, S. S. Patil, and A. D. Chendake, "Performance of Briquetting Machine for Briquette Fuel," *Int. J. Energy Eng.*, vol. 2, no. 1, pp. 28–34, 2012.

[35] L. Wamukonya and B. Jenkins, "Wheat-Straw Briquettes As Possible Fuels for," *Biomass and Bioenergy*, vol. 8, no. 3, pp. 175–179, 1995.

[36] O. C. Chin and K. M. Siddiqui, "Characteristics of some biomass briquettes prepared under modest die pressures," *Biomass and Bioenergy*, vol. 18, no. 3, pp. 223–228, 2000.

[37] J. A. Lindley and M. Vossoughi, "Physical properties of biomass briquets," *Trans. Am. Soc. Agric. Eng.*, vol. 32, no. 2, pp. 361–366, 1989.

[38] M. I. Al-Widyan, H. F. Al-Jalil, M. M. Abu-Zreig, and N. H. Abu-Hamdeh, "Physical durability and stability of olive cake briquettes," *Can. Biosyst. Eng. / Le Genie des Biosyst. au Canada*, vol. 44, pp. 41–45, 2002.

[39] S. Yaman, M. Şahan, H. Haykiri-Açma, K. Şeşen, and S. Küçükbayrak, "Fuel briquettes from biomass-lignite blends," *Fuel Process. Technol.*, vol. 72, no. 1, pp. 1–8, 2001.

[40] S. J. Mitchual, K. Frimpong-Mensah, and N. A. Darkwa, "Effect of species, particle size and compacting pressure on relaxed density and compressive strength of fuel briquettes," *Int. J. Energy Environ. Eng.*, vol. 4, no. 1, pp. 1–6, 2013.

[41] C. S. Chou, S. H. Lin, C. C. Peng, and W. C. Lu, "The optimum conditions for preparing solid fuel briquette of rice straw by a piston-mold process using the Taguchi method," *Fuel Process. Technol.*, vol. 90, no. 7–8, pp. 1041–1046, 2009.

[42] S. R. Richards, "Physical testing of fuel briquettes," *Fuel Process. Technol.*, vol. 25, no. 2, pp. 89–100, 1990.

[43] G. Czachor, J. Bohdziewicz, and K. Kawa, "Shear Strength of the Selected Types of Pellets," *Agric. Eng.*, vol. 20, no. 3, pp. 35–42, 2016.

[44] S. H. Larsson and R. Samuelsson, "Prediction of ISO 17831-1: 2015 mechanical biofuel pellet durability from single pellet characterization," *Fuel Process. Technol.*, vol. 163, pp. 8–15, 2017.

[45] R. Sikkema and G. Fiorese, "Use of forest based biomass for bioenergy in EU-28," *Res. Rural Dev.*, vol. 2, pp. 7–13, 2014.

[46] W. Stelte, A. R. Sanadi, L. Shang, J. K. Holm, J. Ahrenfeldt, and U. B. Henriksen,

"Recent developments in biomass pelletization – a review," *BioResources*, vol. 7, no. 2011, pp. 4451–4490, 2012.

[47] M. R. Abdollahi, V. Ravindran, and B. Svihus, "Pelleting of broiler diets: An overview with emphasis on pellet quality and nutritional value," *Anim. Feed Sci. Technol.*, vol. 179, no. 1–4, pp. 1–23, 2013.

[48] D. L. Schott, R. Tans, I. Dafnomilis, V. Hancock, and G. Lodewijks, "Assessing a durability test for wood pellets by discrete element simulation," *FME Trans.*, vol. 44, no. 3, pp. 279–284, 2016.

[49] L. R. Young, "Mechanical durability of feed pellets," 1962.

[50] S. L. Graham, "Degradation of biomass fuels during long term storage in indoor and outdoor environments." University of Nottingham, 2015.

[51] C. ASTM, "Standard test method for compressive strength of cylindrical concrete specimens," *Chủ biên*, 2012.

[52] C. Rhén, R. Gref, M. Sjöström, and I. Wästerlund, "Effects of raw material moisture content, densification pressure and temperature on some properties of Norway spruce pellets," *Fuel Process. Technol.*, vol. 87, no. 1, pp. 11–16, 2005.

[53] C. ASTM, "Standard test method for splitting tensile strength of cylindrical concrete specimens," *C496/C496M-11*. 2011.

[54] S. J. Mitchual, K. Frimpong-Mensah, N. A. Darkwa, and J. O. Akowuah, "Briquettes from maize cobs and Ceiba pentandra at room temperature and low compacting pressure without a binder," *Int. J. Energy Environ. Eng.*, vol. 4, no. 1, p. 38, 2013.

[55] B. Svihus *et al.*, "Physical and nutritional effects of pelleting of broiler chicken diets made from wheat ground to different coarsenesses by the use of roller mill and hammer mill," *Anim. Feed Sci. Technol.*, vol. 117, no. 3–4, pp. 281–293, 2004.

[56] D. Singh, D. McGlinchey, and M. Crapper, "Breakage functions of particles of four different materials subjected to uniaxial compression," *Part. Sci. Technol.*, vol. 34, no. 4, pp. 494–501, 2016.

[57] Z. Liu, A. Quek, and R. Balasubramanian, "Preparation and characterization of fuel pellets from woody biomass, agro-residues and their corresponding hydrochars," *Appl. Energy*, vol. 113, pp. 1315–1322, 2014.

[58] J. H. Peng, X. T. Bi, S. Sokhansanj, and C. J. Lim, "Torrefaction and densification of different species of softwood residues," *Fuel*, vol. 111, pp. 411–421, 2013.

[59] T. Järvinen and D. Agar, "Experimentally determined storage and handling properties of fuel pellets made from torrefied whole-tree pine chips, logging residues and beech stem wood," *Fuel*, vol. 129, pp. 330–339, 2014.

[60] J. Peng *et al.*, "Effects of thermal treatment on energy density and hardness of torrefied wood pellets," *Fuel Process. Technol.*, vol. 129, pp. 168–173, 2015.

[61] P. S. Lam, P. Y. Lam, S. Sokhansanj, X. T. Bi, and C. J. Lim, "Mechanical and compositional characteristics of steam-treated Douglas fir (Pseudotsuga menziesii L.)

during pelletization," *Biomass and Bioenergy*, vol. 56, pp. 116–126, 2013.

[62] L. G. Tabil, S. Sokhansanj, W. J. Crerar, R. T. Patil, M. H. Khoshtaghaza, and A. Opoku, "Physical characterization of alfalfa cubes: I. Hardness," *Can. Biosyst. Eng. / Le Genie des Biosyst. au Canada*, vol. 44, 2002.

[63] G. E. Dieter and D. J. Bacon, *Mechanical metallurgy*, vol. 3. McGraw-hill New York, 1986.

[64] F. Rupprecht, I. Möller, B. Evans, T. Spencer, and K. Jensen, "Biophysical properties of salt marsh canopies - Quantifying plant stem flexibility and above ground biomass," *Coast. Eng.*, vol. 100, pp. 48–57, 2015.

[65] N. Arzola, A. Gomez, and S. Rincon, "Experimental study of the mechanical and thermal behavior of pellets produced from oil palm biomass blends," *Glob. NEST J.*, vol. 16, no. 1, pp. 179–187, 2014.

[66] A. N. E. Rahman, M. Aziz Masood, C. S. N. Prasad, and M. Venkatesham, "Influence of size and shape on the strength of briquettes," *Fuel Process. Technol.*, 1989.

[67] M. V. Gil, P. Oulego, M. D. Casal, C. Pevida, J. J. Pis, and F. Rubiera, "Mechanical durability and combustion characteristics of pellets from biomass blends," *Bioresour. Technol.*, vol. 101, no. 22, pp. 8859–8867, 2010.

[68] M. Temmerman, F. Rabier, P. D. Jensen, H. Hartmann, and T. Böhm, "Comparative study of durability test methods for pellets and briquettes," *Biomass and Bioenergy*, vol. 30, no. 11, pp. 964–972, 2006.

[69] M. ÖNORM, "7135 Presslinge aus naturbelassenem Holz und naturbelassener Rinde," *Pellets und Briket.*, 2002.

[70] C. Karunanithy, Y. Wang, K. Muthukumarappan, and S. Pugalendhi, "Physiochemical Characterization of Briquettes Made from Different Feedstocks," *Biotechnol. Res. Int.*, vol. 2012, pp. 1–12, 2012.

[71] O. O. Fasina, "Physical properties of peanut hull pellets," *Bioresour. Technol.*, vol. 99, no. 5, pp. 1259–1266, 2008.

[72] A. Standard, "S269. 4,'Cubes, pellets, and crumbles-definitions and methods for determining density, durability, and moisture content,' American Society of Agricultural and Biological Engineers, St," *Joseph, MI*, 2002.

[73] E. N. DIN, "15210–1: Solid biofuels-Determination of mechanical durability of pellets and briquettes-Part 1: Pellets," *Ger. version EN*, pp. 15210–15211, 2009.

[74] D. Schulze, "Powders and bulk solids," *Behav. Charact. Storage Flow. Springer*, vol. 22, 2008.

[75] S. Weatherstone, N. Simonsson, G. Karlsson, N. Padban, A. A. i Arnuelos, and P. Abelha, "Final report on bulk tests in existing storage and handling facilities," *Sect. Deliv. D*, vol. 6, p. 7, 2015.

[76] K. Demirbas and A. Sahin-Demirbas, "Compacting of biomass for energy densification," *Energy Sources, Part A Recover. Util. Environ. Eff.*, vol. 31, no. 12, pp. 1063–1068,

2009.

[77] E. Oveisi *et al.*, "Breakage behavior of wood pellets due to free fall," *Powder Technol.*, vol. 235, pp. 493–499, 2013.

[78] M. R. Wu, D. L. Schott, and G. Lodewijks, "Physical properties of solid biomass," *Biomass and bioenergy*, vol. 35, no. 5, pp. 2093–2105, 2011.

[79] S. S. Ghorpade and A. P. Moule, "Performance evaluation of deoiled cashew shell waste for fuel properties in bri-quetted form. B. Tech." Thesis (unpub.), Dapoli 15, 2006.

[80] P. Pradhan, A. Arora, and S. M. Mahajani, "Pilot scale evaluation of fuel pellets production from garden waste biomass," *Energy Sustain. Dev.*, vol. 43, pp. 1–14, 2018.

[81] EN 15103, "Solid biofuels - Determination of bulk density. European Committee for Standardization," 2010.

[82] M. Gil, D. Schott, I. Arauzo, and E. Teruel, "Handling behavior of two milled biomass: SRF poplar and corn stover," *Fuel Process. Technol.*, vol. 112, pp. 76–85, 2013.

[83] M. Kymäläinen, M. Havimo, S. Keriö, M. Kemell, and J. Solio, "Biological degradation of torrefied wood and charcoal," *Biomass and Bioenergy*, vol. 71, pp. 170–177, 2014.

[84] D. Thrän *et al.*, "Moving torrefaction towards market introduction – Technical improvements and economic-environmental assessment along the overall torrefaction supply chain through the SECTOR project," *Biomass and Bioenergy*, vol. 89, pp. 184–200, 2016.

[85] J. H. Peng, H. T. Bi, C. J. Lim, and S. Sokhansanj, "Study on density, hardness, and moisture uptake of torrefied wood pellets," *Energy & Fuels*, vol. 27, no. 2, pp. 967–974, 2013.

[86] A. Pimchuai, A. Dutta, and P. Basu, "Torrefaction of agriculture residue to enhance combustible properties," *Energy & Fuels*, vol. 24, no. 9, pp. 4638–4645, 2010.

[87] N. Kaliyan and R. V. Morey, "Natural binders and solid bridge type binding mechanisms in briquettes and pellets made from corn stover and switchgrass," *Bioresour. Technol.*, vol. 101, no. 3, pp. 1082–1090, 2010.

[88] R. Picchio *et al.*, "Pellet production from woody and non-woody feedstocks: A review on biomass quality evaluation," *Energies*, vol. 13, no. 11, p. 2937, 2020.

[89] M. Puig-Arnavat, L. Shang, Z. Sárossy, J. Ahrenfeldt, and U. B. Henriksen, "From a single pellet press to a bench scale pellet mill—Pelletizing six different biomass feedstocks," *Fuel Process. Technol.*, vol. 142, pp. 27–33, 2016.

[90] E. Zvicevičius, A. Raila, A. Čiplienė, Ž. Černiauskienė, Ž. Kadžiulienė, and V. Tilvikienė, "Effects of moisture and pressure on densification process of raw material from Artemisia dubia Wall.," *Renew. energy*, vol. 119, pp. 185–192, 2018.

[91] G. Zając, "Impact of diameter of pressing channels and moisture on parameters of pelleting process of virginia mallow biomass," *Agric. Eng.*, vol. 19, 2015.

[92] Y. Huang *et al.*, "Biofuel pellets made at low moisture content – Influence of water in the binding mechanism of densified biomass," *Biomass and Bioenergy*, vol. 98, pp. 8–

14, 2017.

[93] M. Gray, M. G. Johnson, M. I. Dragila, and M. Kleber, "Water uptake in biochars: The roles of porosity and hydrophobicity," *Biomass and Bioenergy*, vol. 61, pp. 196–205, 2014.

[94] S. Wu, S. Zhang, C. Wang, C. Mu, and X. Huang, "High-strength charcoal briquette preparation from hydrothermal pretreated biomass wastes," *Fuel Process. Technol.*, vol. 171, no. November 2017, pp. 293–300, 2018.

[95] F. Verhoeff *et al.*, "Torrefaction Technology for the production of solid bioenergy carriers from biomass and waste," *Energy Res. Cent. Netherlands*, vol. 75, 2011.

[96] M. Segerström and S. H. Larsson, "Clarifying sub-processes in continuous ring die pelletizing through die temperature control," *Fuel Process. Technol.*, vol. 123, pp. 122–126, 2014.

[97] J. T. Oladeji and C. C. Enweremadu, "The Effects of Some Processing Parameters on Physical and Densification Characteristics of Corncob Briquettes," *Int. J. Energy Eng.*, vol. 2, no. 1, pp. 22–27, 2012.

[98] P. Nanou, W. J. J. Huijgen, M. C. Carbo, and J. H. A. Kiel, "The role of lignin in the densification of torrefied wood in relation to the final product properties," *Biomass and Bioenergy*, vol. 111, pp. 248–262, 2018.

[99] L. E. Heffner and H. B. Pfost, "[Gelatinization during pelleting].[Italian]," *Tec. Molit.*, 1975.

[100] M. Rudolfsson, E. Borén, L. Pommer, A. Nordin, and T. A. Lestander, "Combined effects of torrefaction and pelletization parameters on the quality of pellets produced from torrefied biomass," *Appl. Energy*, vol. 191, pp. 414–424, 2017.

[101] D. E. Maier and F. W. Bakker-Arkema, "The counterflow cooling of feed pellets," *J. Agric. Eng. Res.*, vol. 53, pp. 305–319, 1992.

[102] A. De Jiju, "Design of Experiments for Engineers and Scientists." Elsevier, Amsterdam, 2003.

[103] A. Mahajan, I. Dafnomilis, V. Hancock, G. Lodewijks, and D. Schott, "Assessing the representativeness of durability tests for wood pellets by DEM Simulation - Comparing conditions in a durability test with transfer chutes," *EPJ Web Conf.*, vol. 140, pp. 1–4, 2017.

[104] C. Calderón, G. Gauthier, and J.-M. Jossart, "Bioenergy Europe Statistical Report 2019-Key Finding," 2019. [Online]. Available: https://bioenergyeurope.org/statistical-report-2018/.

[105] F. H. Hedlund, J. Astad, and J. Nichols, "Inherent hazards, poor reporting and limited learning in the solid biomass energy sector: A case study of a wheel loader igniting wood dust, leading to fatal explosion at wood pellet manufacturer," *Biomass and Bioenergy*, vol. 66, pp. 450–459, 2014.

[106] ISO 16559, "Solid biofuels- Terminology, definitions and descriptions," 2014.

[107] ISO 17831-1, "Solid biofuels- Determination of mechanical durability of pellets and briquettes- Part 1: Pellets," 2015.

[108] L. Riva, G. R. Surup, T. V. Buø, and H. K. Nielsen, "A study of densified biochar as carbon source in the silicon and ferrosilicon production," *Energy*, vol. 181, pp. 985–996, 2019.

[109] H. Fernández-Puratich, D. Hernández, and V. L. Arce, "Characterization and cost savings of pellets fabricated from Zea mays waste from corn mills combined with Pinus radiata," *Renew. energy*, vol. 114, pp. 448–454, 2017.

[110] M. T. Miranda, F. J. Sepúlveda, J. I. Arranz, I. Montero, and C. V Rojas, "Analysis of pelletizing from corn cob waste," *J. Environ. Manage.*, vol. 228, pp. 303–311, 2018.

[111] Y. Tang, R. P. Chandra, S. Sokhansanj, and J. N. Saddler, "The Role of Biomass Composition and Steam Treatment on Durability of Pellets," *Bioenergy Res.*, vol. 11, no. 2, pp. 341–350, 2018.

[112] M. Hossein *et al.*, "Effect of different types and levels of fat addition and pellet binders on physical pellet quality of broiler feeds," *Poult. Sci.*, vol. 98, no. 10, pp. 4745–4754, 2019.

[113] P. Kri, Ľ. Š, and J. Beniak, "The effect of papermaking sludge as an additive to biomass pellets on the final quality of the fuel," vol. 219, no. November 2017, pp. 196–204, 2018.

[114] J. S. Tumuluru, "Pelleting of Pine and Switchgrass Blends : Effect of Process Variables and Blend Ratio on the Pellet Quality and Energy Consumption," *Energies*, vol. 12, no. 7, p. 1198, 2019.

[115] A. Dyjakon and T. Noszczyk, "The influence of freezing temperature storage on the mechanical durability of commercial pellets from biomass," *Energies*, vol. 12, no. 13, p. 2627, 2019.

[116] H. Gilvari, L. Cutz, U. Tiringer, A. Mol, W. de Jong, and D. L. Schott, "The Effect of Environmental Conditions on the Degradation Behavior of Biomass Pellets," *Polymers (Basel).*, vol. 12, no. 4, p. 970, 2020.

[117] SS 187120, "Biofuels and peat- fuel Pellets.Classification- Swedish Standards Institution, Stockholm, Sweden (1998)."

[118] DIN 51731, "Testing of solid fuels. Compressed untreated wood. Requirements and testing- Deutsches Institut für Normung, Berlin, Germany." German National Standard, 1996.

[119] DIN EN 15270, "Pellet burners for small heating boilers. Definitions, requirements, testing, marking." Deutsches Institut für Normung, Berlin, Germany, 2007.

[120] CTI – R 04/5, "Recommendation: solid biofuels. Pellet characterization for energetic purposes (2004)."

[121] M. ÖNORM, "7135: compressed wood or compressed bark in natural state, pellets and briquettes, requirements and test specifications," *Vienna: Österreichisches Normungsinstitut*, 2000.

[122] ISO 17225-2:2014, "Solid biofuels- Fuel specifications and classes- Part 2: Graded wood pellets."

[123] O. Williams, S. Taylor, E. Lester, S. Kingman, D. Giddings, and C. Eastwick, "Applicability of mechanical tests for biomass pellet characterisation for bioenergy applications," *Materials (Basel).*, vol. 11, no. 8, p. 1329, 2018.

[124] L. Chico-Santamarta, K. Chaney, R. J. Godwin, D. R. White, and A. C. Humphries, "Physical quality changes during the storage of canola (Brassica napus L.) straw pellets," *Appl. Energy*, vol. 95, pp. 220–226, 2012.

[125] C. Serrano, E. Monedero, M. Lapuerta, and H. Portero, "Effect of moisture content, particle size and pine addition on quality parameters of barley straw pellets," *Fuel Process. Technol.*, vol. 92, no. 3, pp. 699–706, 2011.

[126] J. P. Bourgeois and J. Doat, "Torrefied wood from temperate and tropical species. Advantages and prospects.," in *Bioenergy 84. Proceedings of Conference 15-21 June 1984, Goteborg, Sweden. Volume III. Biomass Conversion*, 1984, pp. 153–159.

[127] B. Arias, C. Pevida, J. Fermoso, M. G. Plaza, F. Rubiera, and J. J. Pis, "Influence of torrefaction on the grindability and reactivity of woody biomass," *Fuel Process. Technol.*, vol. 89, no. 2, pp. 169–175, 2008.

[128] W. Stelte *et al.*, "Pelletizing properties of torrefied spruce," *Biomass and Bioenergy*, vol. 35, no. 11, pp. 4690–4698, 2011.

[129] S. H. Larsson, M. Rudolfsson, M. Nordwaeger, I. Olofsson, and R. Samuelsson, "Effects of moisture content, torrefaction temperature, and die temperature in pilot scale pelletizing of torrefied Norway spruce," *Appl. Energy*, vol. 102, pp. 827–832, 2013.

[130] EN 16127, "Solid Biofuels - Determination of length and diameter of pellets. European Committee for Standardization.," 2012.

[131] ISO 18134-2:2017, "Solid biofuels - Determination of moisture content- oven dry method- part 2: total moisture- simplified method."

[132] S. Graham, C. Eastwick, C. Snape, and W. Quick, "Mechanical degradation of biomass wood pellets during long term stockpile storage," *Fuel Process. Technol.*, vol. 160, pp. 143–151, 2017.

[133] S. Graham *et al.*, "Changes in mechanical properties of wood pellets during artificial degradation in a laboratory environment," *Fuel Process. Technol.*, 2016.

[134] ISO 17827-1:2016, "Solid biofuels- Determination of particle size distribution for uncompressed fuels- part : Oscillating screen method using sieves with apertures of 3,15 mm and above."

[135] M. Gil, E. Teruel, and I. Arauzo, "Analysis of standard sieving method for milled biomass through image processing. Effects of particle shape and size for poplar and corn stover," *Fuel*, vol. 116, pp. 328–340, 2014.

[136] M. Thomas, *Physical quality of pelleted feed: a feed model study*. Thomas, 1998.

[137] H. Gilvari, W. de Jong, and D. L. Schott, "Quality parameters relevant for densification

of bio-materials: Measuring methods and affecting factors - A review," *Biomass and Bioenergy*, vol. 120, pp. 117–134, 2019.

[138] M. Manouchehrinejad and S. Mani, "Torrefaction after pelletization (TAP): Analysis of torrefied pellet quality and co-products," *Biomass and Bioenergy*, vol. 118, no. August, pp. 93–104, 2018.

[139] L. Shang *et al.*, "Quality effects caused by torrefaction of pellets made from Scots pine," *Fuel Process. Technol.*, vol. 101, pp. 23–28, 2012.

[140] L. Gustavsson, P. Börjesson, B. Johansson, and P. Svenningsson, "Reducing CO2 emissions by substituting biomass for fossil fuels," *Energy*, vol. 20, no. 11, pp. 1097–1113, 1995.

[141] D. Ilic, K. Williams, R. Farnish, E. Webb, and G. Liu, "On the challenges facing the handling of solid biomass feedstocks," *Biofuels, Bioprod. Biorefining*, vol. 12, no. 2, pp. 187–202, 2018.

[142] Á. Ramírez-Gómez, "Research needs on biomass characterization to prevent handling problems and hazards in industry," *Part. Sci. Technol.*, vol. 34, no. 4, pp. 432–441, 2016.

[143] J. M. Boac, M. E. Casada, and R. G. Maghirang, "Feed pellet and corn durability and breakage during repeated elevator handling," *Appl. Eng. Agric.*, vol. 24, no. 3 mm, pp. 637–644, 2008.

[144] J. Jägers, S. Wirtz, V. Scherer, and M. Behr, "Experimental analysis of wood pellet degradation during pneumatic conveying processes," *Powder Technol.*, vol. 359, pp. 282–291, 2020.

[145] M. A. Murtala, S. Zigan, S. A. B. Michael, and A. L. Torbjörn, "Fuel pellet breakage in pneumatic transport and durability tests," *Renew. Energy*, vol. 157, pp. 911–919, 2020.

[146] R. García Fernández, C. Pizarro García, A. Gutiérrez Lavín, J. L. Bueno de las Heras, and J. J. Pis, "Influence of physical properties of solid biomass fuels on the design and cost of storage installations," *Waste Manag.*, 2013.

[147] H. Gilvari, W. de Jong, and D. L. Schott, "The Effect of Biomass Pellet Length, Test Conditions and Torrefaction on Mechanical Durability Characteristics According to ISO Standard 17831-1," *energies*, vol. 13, no. 11, p. 3000, 2020.

[148] H. Gilvari, W. de Jong, and D. Schott, "The Effect of Pellet Length on Mechanical Durability and Breakage Behaviour of Torrefied Biomass," 2019, [Online]. Available: https://pure.tudelft.nl/portal/en/publications/the-effect-of-pellet-length-on-mechanical-durability-and-breakage-behaviour-of-torrefied-biomass(6b9ec0b9-ebfc-4fcd-b3a8-0aeda3de5a9d).html.

[149] M. M. Abdulmumini, M. Bradley, and S. Zigan, "Prediction of Wood Pellets Degradation in a Pressurised Tanker Truck Delivery System Using Bench Scale Testers," 2016.

[150] H. Gilvari, W. de Jong, and D. L. Schott, "Breakage behavior of biomass pellets: an experimental and numerical study," *Comp. Part. Mech.*, 2020.

[151] Minitab 18, "Regression equation for Analyze Response Surface Design," 2019.

https://support.minitab.com/en-us/minitab/18/help-and-how-to/modeling-statistics/doe/how-to/response-surface/analyze-response-surface-design/interpret-the-results/all-statistics-and-graphs/regression-equation/ (accessed Dec. 10, 2020).

[152] S. L. C. Ferreira *et al.*, "Box-Behnken design: An alternative for the optimization of analytical methods," *Anal. Chim. Acta*, vol. 597, no. 2, pp. 179–186, 2007.

[153] Minitab 18 Statistical Software, "Minitab, Inc., State College, PA (2010)," *www.minitab.com*, [Online]. Available: www.minitab.com.

[154] S. W. Lommen, "Virtual prototyping of grabs: Co-simulations of discrete element and rigid body models," *PhD Diss. Delft Univ. Technol.*, 2016.

[155] J. Antony, *Design of experiments for engineers and scientists*. Elsevier, 2014.

[156] A. P. Grima and P. W. Wypych, "Investigation into calibration of discrete element model parameters for scale-up and validation of particle–structure interactions under impact conditions," *Powder Technol.*, vol. 212, no. 1, pp. 198–209, 2011.

[157] H. J. P. L. de Souza *et al.*, "Pelletization of eucalyptus wood and coffee growing wastes: Strategies for biomass valorization and sustainable bioenergy production," *Renew. Energy*, vol. 149, pp. 128–140, 2020.

[158] K. A. Aarseth, "Attrition of Feed Pellets during Pneumatic Conveying : the Influence of Velocity and Bend Radius," *Biosyst. Eng.*, vol. 89, pp. 197–213, 2004.

[159] J. Sjöström and P. Blomqvist, "Direct measurements of thermal properties of wood pellets: Elevated temperatures, fine fractions and moisture content," *Fuel*, vol. 134, pp. 460–466, 2014.

[160] C. Whittaker and I. Shield, "Factors affecting wood, energy grass and straw pellet durability – A review," *Renew. Sustain. Energy Rev.*, vol. 71, pp. 1–11, 2017.

[161] T. Shui, V. Khatri, M. Chae, S. Sokhansanj, P. Choi, and D. C. Bressler, "Development of a torrefied wood pellet binder from the cross-linking between specified risk materials-derived peptides and epoxidized poly (vinyl alcohol)," *Renew. Energy*, vol. 162, pp. 71–80, 2020.

[162] I. Dafnomilis, G. Lodewijks, M. Junginger, and D. L. Schott, "Evaluation of wood pellet handling in import terminals," *Biomass and Bioenergy*, vol. 117, no. March, pp. 10–23, 2018.

[163] S. H. Larsson, T. A. Lestander, D. Crompton, S. Melin, and S. Sokhansanj, "Temperature patterns in large scale wood pellet silo storage," *Appl. Energy*, vol. 92, pp. 322–327, 2012.

[164] O. Ochkin-König, S. Heinrich, and M. Dosta, "Investigation of breakage and attrition behavior of wood pellets," 2018.

[165] B. Kotzur, R. Berry, M. Bradley, G. C. Dias, and A. C. Silva, "Influence of pellet length on breakage by impact," 2016.

[166] EN 14774-2, "Solid Biofuels - Determination of Moisture Content - Oven Dry Method - Part 2: Total Moisture - Simplified Method, European Committee for Standardization,"

2009.

[167] A. Brunerová, M. Müller, V. Šleger, H. Ambarita, and P. Valášek, "Bio-Pellet Fuel from Oil Palm Empty Fruit Bunches (EFB): Using European Standards for Quality Testing," *Sustainability*, vol. 10, no. 12, p. 4443, 2018.

[168] EN/TS 14778-1, "Solid Biofuels - Sampling - Part 1: Methods for sampling, European Committee for Standardization," 2005.

[169] P. Lauri, P. Havlík, G. Kindermann, N. Forsell, H. Böttcher, and M. Obersteiner, "Woody biomass energy potential in 2050," *Energy Policy*, vol. 66, pp. 19–31, 2014.

[170] L. J. R. Nunes, J. C. O. Matias, and J. P. S. Catalão, "A review on torrefied biomass pellets as a sustainable alternative to coal in power generation," *Renew. Sustain. Energy Rev.*, vol. 40, pp. 153–160, 2014.

[171] M. J. C. Van Der Stelt, H. Gerhauser, J. H. A. Kiel, and K. J. Ptasinski, "Biomass upgrading by torrefaction for the production of biofuels : A review," *Biomass and Bioenergy*, vol. 35, no. 9, pp. 3748–3762, 2011.

[172] F. Magelli, K. Boucher, H. T. Bi, S. Melin, and A. Bonoli, "An environmental impact assessment of exported wood pellets from Canada to Europe," *Biomass and Bioenergy*, vol. 33, no. 3, pp. 434–441, 2009.

[173] E. Alakoski, M. Jämsén, D. Agar, E. Tampio, and M. Wihersaari, "From wood pellets to wood chips, risks of degradation and emissions from the storage of woody biomass - A short review," *Renew. Sustain. Energy Rev.*, vol. 54, pp. 376–383, 2016.

[174] P. Lehtikangas, "Storage effects on pelletised sawdust, logging residues and bark," *Biomass and Bioenergy*, vol. 19, no. 5, pp. 287–293, 2000.

[175] M. Kymäläinen, M. R. Mäkelä, K. Hildén, and J. Kukkonen, "Fungal colonisation and moisture uptake of torrefied wood, charcoal, and thermally treated pellets during storage," *Eur. J. wood wood Prod.*, vol. 73, no. 6, pp. 709–717, 2015.

[176] J. S. Lee *et al.*, "The effects of storage on the net calorific value of wood pellets," *Can. Biosyst. Eng. / Le Genie des Biosyst. au Canada*, vol. 57, pp. 8.5-8.12, 2015.

[177] I. D. Hartley and L. J. Wood, "Hygroscopic properties of densified softwood pellets," *Biomass and Bioenergy*, vol. 32, no. 1, pp. 90–93, 2008.

[178] L. Bennamoun, N. Y. Harun, and M. T. Afzal, "Effect of Storage Conditions on Moisture Sorption of Mixed Biomass Pellets," *Arab. J. Sci. Eng.*, vol. 43, no. 3, pp. 1195–1203, 2018.

[179] R. N. Singh, "Equilibrium moisture content of biomass briquettes," *Biomass and Bioenergy*, vol. 26, no. 3, pp. 251–253, 2004.

[180] K. Theerarattananoon *et al.*, "Physical properties of pellets made from sorghum stalk, corn stover, wheat straw, and big bluestem," *Ind. Crops Prod.*, vol. 33, no. 2, pp. 325–332, 2011.

[181] S. Wang *et al.*, "Variation in the physical properties of wood pellets and emission of aldehyde/ketone under different storage conditions," *Fuel*, vol. 183, pp. 314–321, 2016.

[182] T. Deng, A. M. Alzahrani, and M. S. Bradley, "Influences of environmental humidity on physical properties and attrition of wood pellets," *Fuel Process. Technol.*, vol. 185, pp. 126–138, 2019.

[183] EN 14961-1:2010, "Solid biofuels- Fuels specifications and classes- Part 2: wood pellets for non-industrial use."

[184] EN 14775:2004, "Solid Biofuels - Determination of Ash Content, European Committee for Standardization," 2004.

[185] BS 1016-5:1967, "Methods for analysis and testing of coal and coke. Gross calorific value of coal and coke."

[186] F. Yazdanpanah *et al.*, "Measurement of off-gases in wood pellet storage," *Adv. Gas Chromatogr*, pp. 1–33, 2014.

[187] X. He *et al.*, "Moisture sorption isotherms and drying characteristics of aspen (Populus tremuloides)," *Biomass and Bioenergy*, vol. 57, pp. 161–167, 2013.

[188] M. S. A. Bradley, "Biomass fuel transport and handling," in *Fuel Flexible Energy Generation*, Elsevier, 2016, pp. 99–120.

[189] C. J. Coetzee, "Calibration of the discrete element method," *Powder Technol.*, vol. 310, pp. 104–142, 2017.

[190] J. Rozbroj, J. Zegzulka, J. Necas, and L. Jezerska, "Discrete element method model optimization of cylindrical pellet size," *Processes*, vol. 7, no. 2, p. 101, 2019.

[191] H. Kruggel-Emden and R. Kačianauskas, "Discrete element analysis of experiments on mixing and bulk transport of wood pellets on a forward acting grate in discontinuous operation," *Chem. Eng. Sci.*, vol. 92, pp. 105–117, 2013.

[192] G.-A. Tsalidis, K. Voulgaris, K. Anastasakis, W. De Jong, and J. H. A. Kiel, "Influence of torrefaction pretreatment on reactivity and permanent gas formation during devolatilization of spruce," *Energy & Fuels*, vol. 29, no. 9, pp. 5825–5834, 2015.

[193] G. A. Tsalidis, "To gasify or not to gasify torrefied wood?," *PhD Diss. Delft Univ. Technol.*, 2017.

[194] C. González-Montellano, A. Ramirez, E. Gallego, and F. Ayuga, "Validation and experimental calibration of 3D discrete element models for the simulation of the discharge flow in silos," *Chem. Eng. Sci.*, vol. 66, no. 21, pp. 5116–5126, 2011.

[195] H. R. Norouzi, R. Zarghami, and N. Mostoufi, "Insights into the granular flow in rotating drums," *Chem. Eng. Res. Des.*, vol. 102, pp. 12–25, 2015.

[196] M. Rackl, F. Top, C. P. Molhoek, and D. L. Schott, "Feeding system for wood chips: A DEM study to improve equipment performance," *Biomass and Bioenergy*, vol. 98, pp. 43–52, 2017.

[197] J. Pachón-Morales, H. Do, J. Colin, F. Puel, P. Perré, and D. Schott, "DEM modelling for flow of cohesive lignocellulosic biomass powders: Model calibration using bulk tests," *Adv. Powder Technol.*, vol. 30, no. 4, pp. 732–750, 2019.

[198] Y. C. Zhou, B. H. Xu, A.-B. Yu, and P. Zulli, "An experimental and numerical study of

the angle of repose of coarse spheres," *Powder Technol.*, vol. 125, no. 1, pp. 45–54, 2002.

[199] Z. Yan, S. K. Wilkinson, E. H. Stitt, and M. Marigo, "Discrete element modelling (DEM) input parameters: understanding their impact on model predictions using statistical analysis," *Comput. Part. Mech.*, vol. 2, no. 3, pp. 283–299, 2015.

[200] R. Ge, L. Wang, and Z. Zhou, "DEM analysis of compression breakage of 3D printed agglomerates with different structures," *Powder Technol.*, 2019.

[201] M. A. Chaudry and P. Wriggers, "On the computational aspects of comminution in discrete element method," *Comput. Part. Mech.*, vol. 5, no. 2, pp. 175–189, 2018.

[202] D. O. Potyondy and P. A. Cundall, "A bonded-particle model for rock," *Int. J. rock Mech. Min. Sci.*, vol. 41, no. 8, pp. 1329–1364, 2004.

[203] R. Moreno, M. Ghadiri, and S. J. Antony, "Effect of the impact angle on the breakage of agglomerates: a numerical study using DEM," *Powder Technol.*, vol. 130, no. 1–3, pp. 132–137, 2003.

[204] O. Jou, M. A. Celigueta, S. Latorre, F. Arrufat, and E. Oñate, "A bonded discrete element method for modeling ship–ice interactions in broken and unbroken sea ice fields," *Comput. Part. Mech.*, vol. 6, no. 4, pp. 739–765, 2019.

[205] P. A. Cundall and O. D. L. Strack, "A discrete numerical model for granular assemblies," *Geotechnique*, vol. 29, no. 1, pp. 47–65, 1979.

[206] H. Gilvari, W. de Jong, and D. Schott, "Biomass Pellet Breakage: A Numerical Comparison Between Contact Models," 2019, [Online]. Available: https://pure.tudelft.nl/portal/en/publications/biomass-pellet-breakage(f1f1c652-dfa4-45bc-bc9f-5fe4f41c3033).html.

[207] N. Jiménez-Herrera, G. K. P. Barrios, and L. M. Tavares, "Comparison of breakage models in DEM in simulating impact on particle beds," *Adv. Powder Technol.*, vol. 29, no. 3, pp. 692–706, 2018.

[208] I. Elishakoff, "Who developed the so-called Timoshenko beam theory?," *Math. Mech. Solids*, pp. 1–20, 2019.

[209] S. P. Timoshenko, "X. On the transverse vibrations of bars of uniform cross-section," *London, Edinburgh, Dublin Philos. Mag. J. Sci.*, vol. 43, no. 253, pp. 125–131, 1922.

[210] N. J. Brown, "Discrete element modelling of cementitious materials," *PhD Diss. Univ. Edinburgh*, 2013.

[211] J. Horabik and M. Molenda, "Parameters and contact models for DEM simulations of agricultural granular materials: A review," *Biosyst. Eng.*, vol. 147, pp. 206–225, 2016.

[212] DEM Solutions Ltd., "EDEM 2017 User Guide. Copyright © 2016."

[213] A. Coll *et al.*, "GiD v.14 user manual," 2018. www.gidhome.com (accessed May 25, 2020).

[214] E. R. Parker, *Materials Data Book. For Engineers and Scientists.* McGraw-Hill, New York (NY), 1967.

[215] J. M. Kemeny, “A model for non-linear rock deformation under compression due to sub-critical crack growth,” in *International journal of rock mechanics and mining sciences & geomechanics abstracts*, 1991, vol. 28, no. 6, pp. 459–467.

[216] N. J. Brown, J.-F. Chen, and J. Y. Ooi, “A bond model for DEM simulation of cementitious materials and deformable structures,” *Granul. Matter*, vol. 16, no. 3, pp. 299–311, 2014.

[217] N. B. Yenigül and M. A. Grima, “Discrete element modeling of low strength rock,” *Numer. Methods Geotech. Eng.*, pp. 207–212, 2010.

[218] L. N. Schaefer, J. E. Kendrick, T. Oommen, Y. Lavallée, and G. Chigna, “Geomechanical rock properties of a basaltic volcano,” *Front. Earth Sci.*, vol. 3, p. 29, 2015.

[219] L. M. Tavares and R. P. King, “Modeling of particle fracture by repeated impacts using continuum damage mechanics,” *Powder Technol.*, vol. 123, no. 2–3, pp. 138–146, 2002.

Appendix A

Details of the design of experiments for the belt conveyor tests in chapter 4

Table A. 1: Experimental design in coded units resulting from the implementation of the Box-Behnken response surface design in Minitab® 18.1.

Run	X_1^* (m.s^{-1})	X_2^* (%)	X_3^* (degree)	X_4^* (-)	Generated fines (wt.%)
1	−1	−1	−1	0	0.12
2	+1	−1	−1	0	0.67
3	−1	+1	−1	0	0.42
4	+1	+1	−1	0	1.63
5	−1	0	−1	−1	0.31
6	+1	0	−1	−1	0.06
7	−1	0	−1	+1	0.93
8	+1	0	−1	+1	0.31
9	0	−1	−1	−1	0.36
10	0	+1	−1	−1	0.43
11	0	−1	−1	+1	1.16
12	0	+1	−1	+1	1.32
13	0	0	−1	0	0.45
14	0	0	−1	0	0.24
15	0	0	−1	0	0.33
16	−1	−1	+1	0	1.58
17	+1	−1	+1	0	1.22
18	−1	+1	+1	0	1.59
19	+1	+1	+1	0	1.08
20	−1	0	+1	−1	0.37
21	+1	0	+1	−1	0.75
22	−1	0	+1	+1	1.51
23	+1	0	+1	+1	2.17
24	0	−1	+1	−1	1.22
25	0	+1	+1	−1	1.44
26	0	−1	+1	+1	3.05
27	0	+1	+1	+1	3.65
28	0	0	+1	0	1.35
29	0	0	+1	0	1.50
30	0	0	+1	0	1.39

*X_1: belt speed, X_2:belt loading, X_3: drop height, X_4: number of handling steps

Appendix B

Details of experimental conditions and modeling the moisture uptake in chapter 6

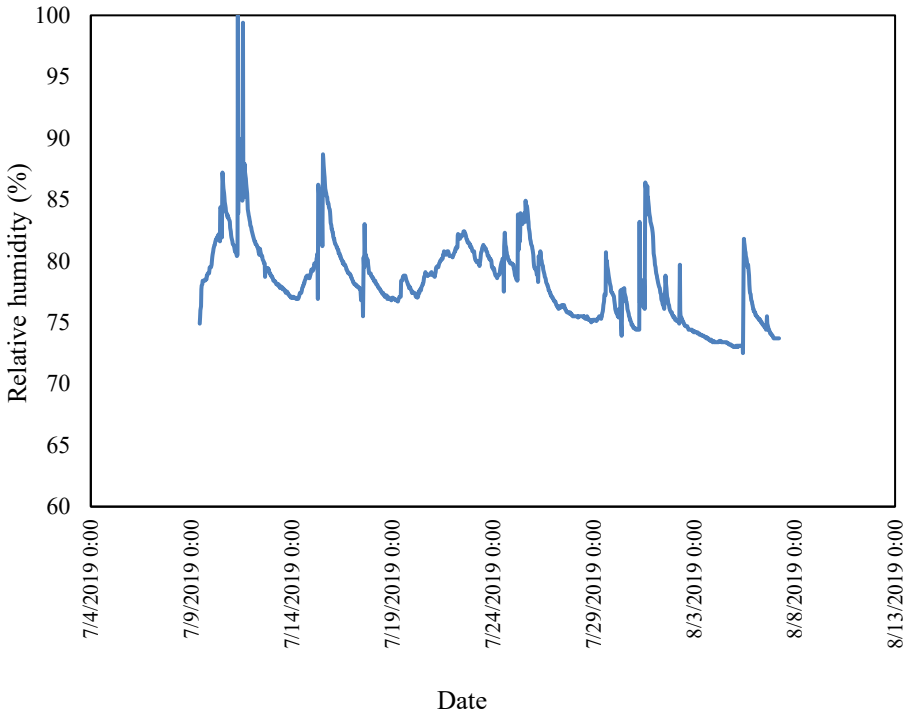

Figure B. 1: RH data at the T5_RH86.

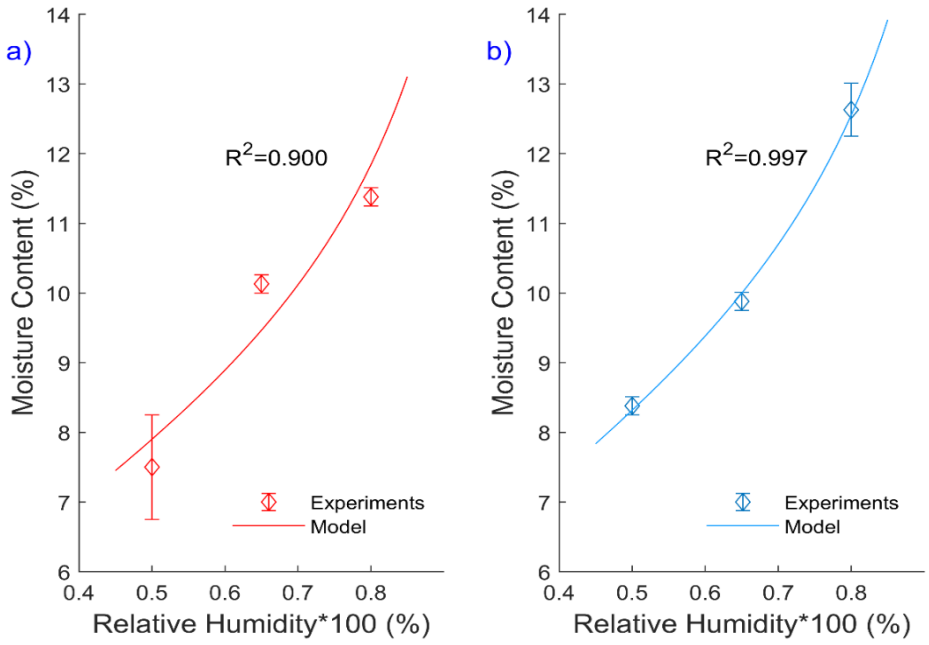

Figure B. 2: Moisture uptake at 20°C. Experimental results versus Oswin model for (a) brown and (b) white pellets.

Appendix C

Details of pellet breakage in DEM

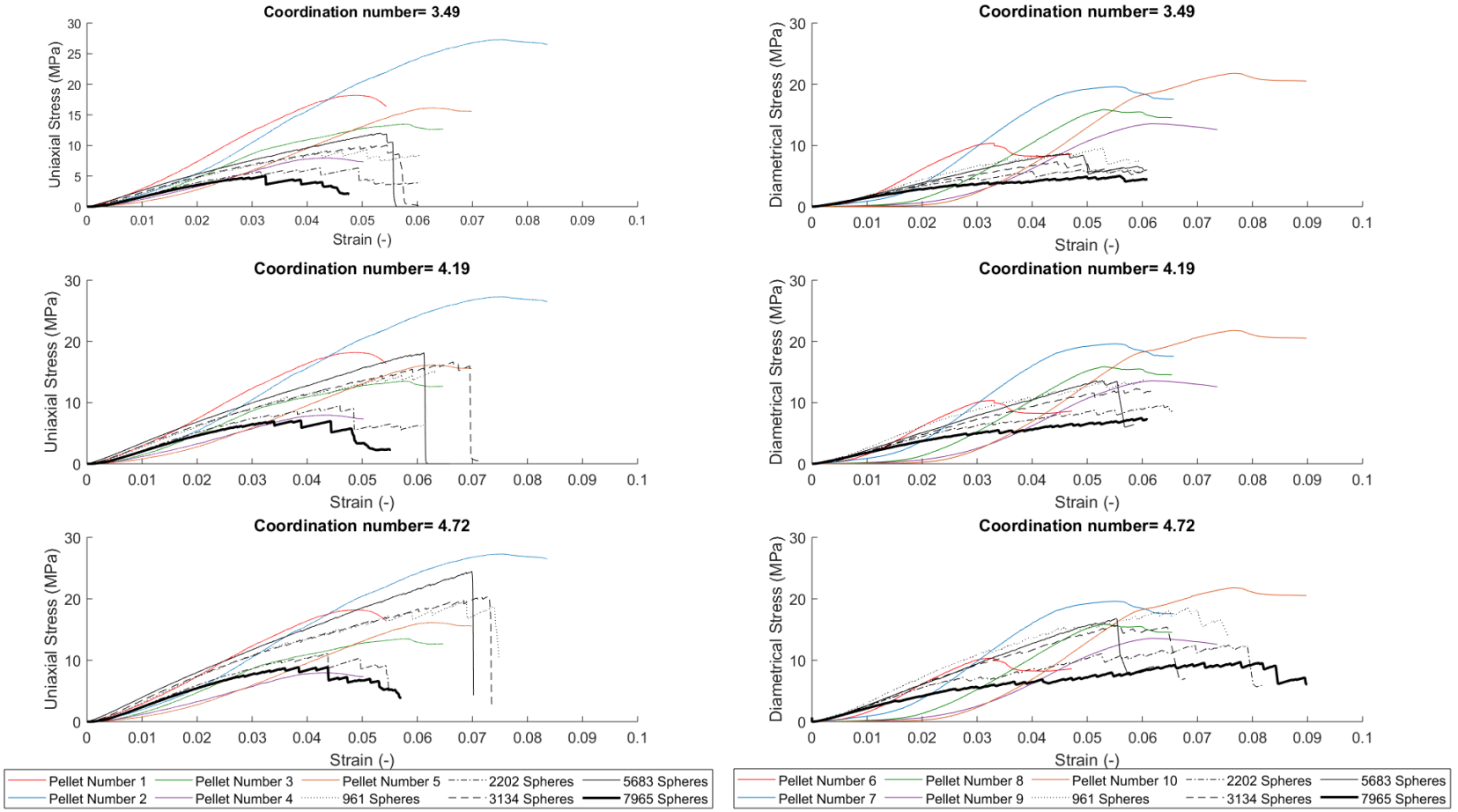

Figure C. 1: Stress-strain results for pellet packing with different coordination numbers.

Table C. 1: Breakage pattern of the simulated pellets under uniaxial compression.

Number of Spheres	At time Zero	At Failure Time	After Failure
961	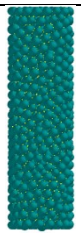	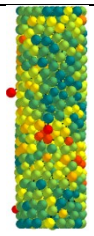	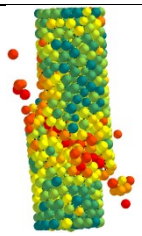
2202		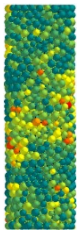	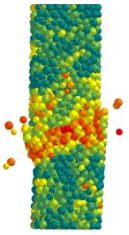
3134	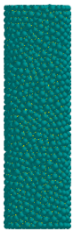	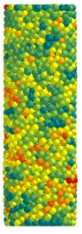	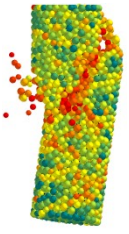
5683	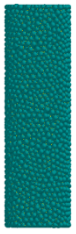	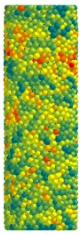	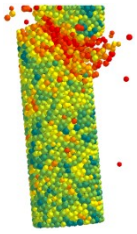
7965		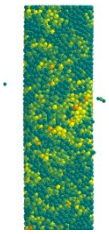	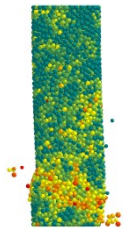

$$Damage = \frac{Number\ of\ broken\ bonds}{Initial\ number\ of\ bonds}$$

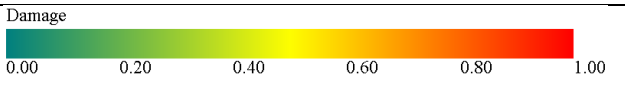

Table C. 2: Breakage pattern of the simulated pellets under diametrical compression.

Number of Spheres	At time Zero	At Failure Time	After Failure
961	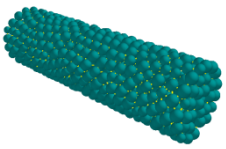	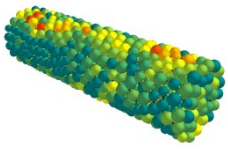	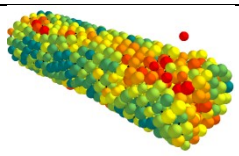
2202	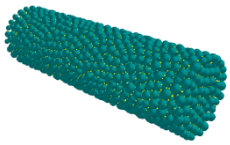	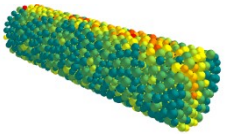	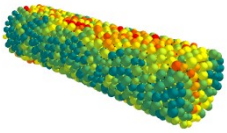
3134	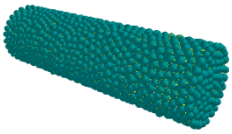	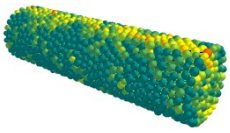	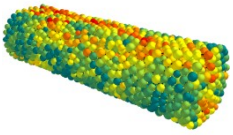
5683	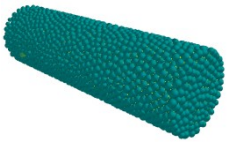	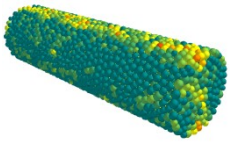	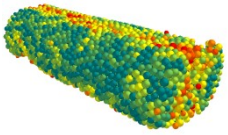
7965		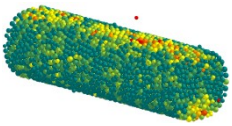	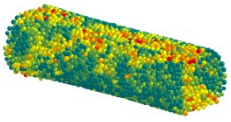
$Damage = \frac{Number\ of\ broken\ bonds}{Initial\ number\ of\ bonds}$		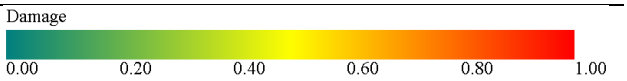	

Acknowledgment

When you start thinking about writing an acknowledgment for your thesis, it means that you are so close to the end of the journey. For me, the PhD journey was an endowment to learn, explore, observe, and feel the world around me. All of these would not have been possible without the intimate accompanying of great people who helped me to reach my goal.

First, I would like to thank Dr.ir. Dingena Schott and Prof.dr.ir. Wiebren de Jong for their invariably and utmost support and supervision. That was my pleasure to work with such eminent scholars whose way of supervision and scientific attitude always inspired me. Dingena, thanks for your trust in me, your patience, your helpful guide, and your ceaseless effort to let me focus only on my project and leave all the extras for yourself. Your insightful feedback always pushed me to sharpen my thinking and brought my work to a higher level. I never forget our weekly meetings on Thursday mornings half in English and half in Dutch! Wiebren, thanks for being my promoter and teaching me how to look at the bigger picture and also for your prompt replies whenever needed, and thanks for letting me continue my academic adventure in your group as a postdoctoral researcher.

Working in a friendly environment is a key to refresh and obtain energy to perform the best. It was always nice and joyful to meet my kind colleagues at the M&TT department and talk with them during the coffee break time, which made me relaxed and gave me hope and energy and pushed me forward. Thanks to my colleagues at the BulChaM group (Javad, Marc, Raïsa, Jovana, Yunpeng, Jeseung, Ana, and Dingena) for the coffee meetings, joyful cycling and online games during pandemic, where we had friendly chats. Thanks to Prof.ir Hans Hopman, the head of the M&TT department, for providing financial support to let me participate in the ICBMH 2019 conference in Australia. Special thanks to Dineke, Gracia, Patty, Anouk, Monique, and Pauline, the managers and the secretaries of the M&TT department, for all their supports and organizing group activities within the department especially for the day out in the summer at Hoek van Holland and Christmas events. Thanks my colleagues at the LSE group for the bi-weekly meetings and friendly chats.

I would like to thank internal and external colleagues, scholars, and experts who helped me in performing experiments and simulations. I would like to thank Prof.dr.ir Arjan Mol, Dr. Luis Cutz, Dr. Urša Tiringer, and Dr. Yusong Pang from TU Delft for their collaborations. I would also like to thank Mr. Richard Farnish and Dr. Hamid Salehi and their colleagues at the Wolfson Centre for Bulk Solids Handling Technology of the University of Greenwich to host me during

my academic visit to England. Simon van Dijk from Uniper Benelux and Eovar van Dijk from Peterson Rotterdam and their colleagues are acknowledged for their cooperation and sharing their knowledge with me.

It was enjoyable to work with bachelor and master students who I had the chance to supervise and work with them during my PhD research: Coen, Otto, Kadir, Baris, Kasper, Thom, Maarten, Dirk, Niek, Geertje, Nina, Wouter, and Rink. Special thanks to Coen for accompanying me during my visit to the University of Greenwich and his contribution to the TKI-BBE project.

Special thanks to Reyhaneh (rihannadesign) to design the thesis cover and Raïsa Roeplal and Coen van Battum for editing the Dutch summary.

Doing a PhD is difficult without having fun times after work and during holidays. I always had a chance to have a very nice time with my friends who their kindness always surprised me and helped me go forward. I would like to thank all of them for being my friends and making good memories for me.

Finally, I would like to thank my family. Thank you, Mom and Dad, Hadi, Eli, Mohammad, Mahnaz, Hossein, and my lovely niece Mehrsa for your supports and sacrifices and love to raise me, care about me, and helping me reach my goals. Although I am living far from you, I am thinking of you every moment. I hope that I can make you happy by dedicating this dissertation to you. Thanks to my wife's parents and Reyhaneh (my sister-in-law) for their supports and for encouraging me to pursue my goals.

Last but not least, thanks to my lovely wife, Hengameh for your startling sacrifices, unlimited patience, constructive help, conscious guidance, utmost peace, and sincere love that you always gave to me. I love you!

April 2021, Delft

List of publications

Journals:

1. Gilvari, H., van Battum, C., Farnish, R., Pang, Y., de Jong, W., & Schott, D. L. Fragmentation of fuel pellets during transport via a belt conveyor: a design of experiment study. (Submitted).
2. Gilvari, H., van Battum, C. H., van Dijk, S. A., de Jong, W., & Schott, D. L. (2021). Large-scale transportation and storage of wood pellets: Investigation of the change in physical properties. Particuology, 57, 146-156.
3. Cutz, L., Tiringer, U., Gilvari, H., Schott, D. L., Mol, A., & de Jong, W. (2021). Microstructural degradation during the storage of biomass pellets. Communications Materials 2, 2.
4. Gilvari, H., de Jong, W., & Schott, D. L. (2020). Breakage behavior of biomass pellets: an experimental and numerical study. Computational Particle Mechanics, 1-14
5. Gilvari, H., Cutz, L., Tiringer, U., Mol, A., de Jong, W., & Schott, D. L. (2020). The Effect of Environmental Conditions on the Degradation Behavior of Biomass Pellets. Polymers, 12(4), 970.
6. Gilvari, H., De Jong, W., & Schott, D. L. (2020). The Effect of Biomass Pellet Length, Test Conditions and Torrefaction on Mechanical Durability Characteristics According to ISO Standard 17831-1. Energies, 13(11), 3000.
7. Gilvari, H., de Jong, W., & Schott, D. L. (2019). Quality parameters relevant for densification of bio-materials: Measuring methods and affecting factors-A review. Biomass and Bioenergy, 120, 117-134.
8. Khayati, G., Daghbandan, A., Gilvari, H., & Pheyz-Sani, N. (2011). Liquid-liquid equilibria of aqueous two-phase systems containing polyethylene glycol 4000 and two different salts of ammonium. Research Journal of Applied Sciences, Engineering and Technology, 3(2), 96-98.

Conferences:

1. Gilvari, H., de Jong, W., & Schott, D. L. (2019). The effect of pellet length on mechanical durability and breakage behavior of torrefied biomass. In 13th International Conference on Bulk Materials Storage, Handling and Transportation (ICBMH, 2019) (p. 385). Gold coast, Australia.
2. Gilvari, H., de Jong, W., & Schott, D. (2019). Biomass pellet breakage: a numerical comparison between contact models. In Proceedings of the 8th international conference on discrete element methods (DEM8). Enschede, The Netherlands.
3. Gilvari, H., Karaca, K., de Jong, W., & Schott, D. L. (2018). Influential Properties on Mechanical Degradation of Densified Torrefied Biomass in Large Scale Transportation and Storage. In 26th European Biomass Conference & Exhibition. Copenhagen, Denmark.

Curriculum Vitae

Hamid Gilvari was born in 1987 in Tehran, Iran. He obtained his bachelor degree in Chemical Engineering with a minor study in food technology at the Guilan University, Iran. Then, he moved to Finland to pursue his education in master studies of Chemical and Process Engineering with a major study in sustainable process technology at the Lappeenranta University of Technology. After obtaining his M.Sc. degree, in 2017, he started his PhD research at the Delft University of Technology in the Netherlands working on the "degradation behavior of biomass pellets during transport and storage" at the section of Transport Engineering and Logistics (TEL) of the Maritime and Transport Technology (M&TT) department at the faculty of Mechanical, Maritime, and Materials Engineering (3mE). He is currently working as a post-doctoral researcher on the gasification of waste plastics under the project "Towards improved circularity of polyolefin-based packaging" at the Large-Scale Energy storage group (LSE) at the 3mE faculty of the Delft University of Technology. Apart from his career, Hamid is interested in psychology, economy, and history. As a hobby, he likes reading, mountain climbing, camping, and cooking.

He can be contacted using the following email addresses:

h.gilvari@tudelft.nl

hamid.gilvari@yahoo.com